

# Northumbria Research Link

Citation: Bowerbank, Samantha (2021) Liquid chromatography-mass spectrometry analysis of compounds from complex matrices. Doctoral thesis, Northumbria University.

This version was downloaded from Northumbria Research Link:  
<http://nrl.northumbria.ac.uk/id/eprint/49082/>

Northumbria University has developed Northumbria Research Link (NRL) to enable users to access the University's research output. Copyright © and moral rights for items on NRL are retained by the individual author(s) and/or other copyright owners. Single copies of full items can be reproduced, displayed or performed, and given to third parties in any format or medium for personal research or study, educational, or not-for-profit purposes without prior permission or charge, provided the authors, title and full bibliographic details are given, as well as a hyperlink and/or URL to the original metadata page. The content must not be changed in any way. Full items must not be sold commercially in any format or medium without formal permission of the copyright holder. The full policy is available online: <http://nrl.northumbria.ac.uk/policies.html>



**Northumbria  
University**  
NEWCASTLE



**UniversityLibrary**

**LIQUID CHROMATOGRAPHY-MASS  
SPECTROMETRY ANALYSIS OF  
COMPOUNDS FROM COMPLEX  
MATRICES**

**SAMANTHA LOUISE BOWERBANK**

PhD

2021

# **LIQUID CHROMATOGRAPHY-MASS SPECTROMETRY ANALYSIS OF COMPOUNDS FROM COMPLEX MATRICES**

**SAMANTHA LOUISE BOWERBANK**

A thesis submitted in partial fulfilment of  
the requirements of the University of  
Northumbria at Newcastle for the degree  
of Doctor of Philosophy

Research undertaken in the Faculty of  
Health and Life Sciences

June 2021

## Abstract

The aim of the work was to establish two methods for the analysis of 4 thyroid hormones and 18 plant toxins by liquid chromatography-tandem mass spectrometry (LC-MS/MS) using electrospray ionisation (ESI). The developed and validated methods were then applied to samples, with a range of complex matrices, namely serum, simulated gastro-intestinal fluid, tablet formulation and plants, with sample preparation methods developed and validated for each.

Thyroid disorders, hypothyroidism and hyperthyroidism, are a common medical condition with diagnosis obtained via the analysis of thyroid hormones present within serum samples. Currently within the NHS analysis is performed using electrochemiluminescence to measure thyroid stimulating hormone, thyroxine and triiodothyronine. However, these methods have limited sensitivity and inaccuracies of 30% at the limit of detection. Therefore, diagnosis of hypothyroidism can often be missed with multiple medical visits being required. The developed method allows for the detection and qualification of 4 thyroid hormones, thyroxine, triiodothyronine, reverse triiodothyronine and diiodothyronine, using low resolution and high resolution mass spectrometry. The developed method showed significant improvements over the current NHS method with LOQs of <math><5.9\text{ pmol/L}</math>,  $r^2$  of >0.990 and precision of <math><3.8\%</math>. A direct comparison between the development method and the current clinical method showed that the result obtained were comparable in terms of thyroid hormone levels detected. Allowing for LC-MS/MS to be a suitable, more reliable alternative for the detection and quantification of thyroid hormones.

Plant toxins are a common cause of accidental poisoning with a range of symptoms including burns, nausea, convulsions, paralysis and even death. Many of the plants analysed in this study can be purchased from garden centres and online nurseries with little to no safety information provided. A method was developed for the analysis of 18 plant toxins, atropine, aconitine, capsaicin, cathinone, colchicine, coumarin, digitoxin, digoxin, hellebrin, 5-methoxypsoralen, 8-methoxypsoralen, psoralen, salvinorin A, scopolamine, solanine, strychnine, thujone and veratridine, based upon the plant availability. The developed method showed good linearity,  $r^2 > 0.9952$  and precision of <math><10.7\%</math>. The analysis of the

plant materials showed toxins consistent with information obtained from the head gardener at Alnwick Gardens, which holds the largest poison garden in the UK. A risk assessment for ingestion and dermal exposure was compared with the LD<sub>50</sub> and it was found that *Colchicum autumnale* posed the greatest risk via ingestion with *Atropa belladonna* also posing significant risk via ingestion. The dermal risk was minimal; however, care should be taken in the case of dermal contact due to the presence of phototoxins present in plant such as *Heracleum mantegazzianum*.

## Contents

Chapter 1: Introduction .....	1
1. Introduction.....	2
1.1. The changing face of analytical chemistry .....	2
1.2. Liquid Chromatography-Mass Spectrometry .....	8
1.2.1. Liquid chromatography .....	8
1.2.2. Column chemistry .....	13
1.2.3. Detectors .....	16
1.2.3.1. Ultraviolet/visible detector.....	16
1.2.3.2. Fluorescence .....	17
1.2.3.3. Refractive index.....	18
1.2.3.4. Mass Spectrometry.....	19
1.2.3.4.1. Ionisation mechanisms for Mass spectrometry.....	20
1.2.3.4.1.1. Electrospray ionisation .....	20
1.2.3.4.1.2. Atmospheric Pressure Chemical Ionisation.....	22
1.2.3.4.2. Mass spectrometer analysers.....	23
1.2.3.4.2.1. Single quadrupole .....	24
1.2.3.4.2.2. Triple quadrupole .....	26
1.2.3.4.2.3. Time of flight.....	27
1.2.3.4.2.4. Ion Trap.....	27
1.2.3.4.2.5. Orbitrap .....	29
1.2.3.4.3. Mass spectrometry detectors.....	30
1.2.3.4.3.1. Electron multiplier.....	30
1.3. Method development and validation.....	33
Chapter 2: Complex matrices.....	35
2. Complex matrices.....	36
2.1. Thyroid hormones .....	36
2.1.1. Thyrotropin releasing hormone, Thyroid Stimulating Hormone and Thyroglobulin .....	36
2.1.2. Thyroid hormones.....	40
2.1.3. Physiological effects .....	45
2.1.4. Thyroid disorders .....	47
2.1.5. Current methods of analysis .....	51
2.1.5.1. Electrochemiluminescence immunoassay (ECLIA) .....	51
2.1.5.2. Enzyme linked immunoassay (ELISA).....	53
2.2. Plant toxins .....	54

2.2.1.	Aconitine .....	55
2.2.2.	Atropine and scopolamine .....	59
2.2.3.	Capsaicin .....	62
2.2.4.	Cathinone .....	65
2.2.5.	Colchicine .....	68
2.2.6.	Coumarins .....	71
2.2.7.	Digitoxin and Digoxin .....	74
2.2.8.	Hellebrin.....	76
2.2.9.	Salvinorin A.....	78
2.2.10.	Solanine.....	80
2.2.11.	Strychnine.....	82
2.2.12.	Thujone.....	83
2.2.13.	Veratridine .....	87
3.	Aims .....	90
Chapter 4: Experimental .....		92
4.	Experimental .....	93
4.1.	Sample preparation.....	93
4.2.	LC-UV .....	93
4.3.	LC-MS.....	93
4.4.	Prep-LC.....	94
4.5.	NMR.....	95
4.6.	Materials .....	97
4.6.1.	Thyroid hormone analysis.....	97
4.6.2.	Plant toxin analysis .....	98
4.7.	Preparation of standard solutions, samples and reagents. ....	98
4.7.1.	Thyroid hormone analysis.....	98
4.7.2.	Plant toxin analysis .....	100
4.8.	Data Analysis .....	101
Chapter 5: Thyroid hormone results and discussion .....		102
5.	Thyroid hormone results and discussion .....	103
5.1.	Method development.....	103
5.1.1.	Evaluation of columns and mobile phase.....	103
5.1.2.	Optimisation of MS parameters .....	104
5.1.4.	Tablet sample method development.....	106
5.1.5.	Serum sample method development .....	112
5.2.	Method Validation .....	116
5.2.1.	Selectivity.....	116

5.2.2.	Linearity .....	116
5.2.3.	Precision .....	119
5.2.4.	Limits of detection and quantification .....	120
5.2.5.	Standard stability .....	120
5.3.	Tablet Analysis.....	125
5.3.1.	Method.....	125
5.3.2.	Results and discussion .....	125
5.4.	Dissolution .....	126
5.4.1.	Method.....	126
5.4.2.	Results and discussion .....	128
5.5.	Serum Analysis .....	130
5.5.1.	Method.....	130
5.5.2.	Results and discussion .....	131
5.6.	Conclusion .....	132
	Chapter 6: Plant toxins results and discussion .....	135
6.	Plant toxins results and discussion.....	136
6.1.	Method development.....	136
6.1.1.	Evaluation of mobile phase .....	136
6.1.2.	Optimisation of MS parameters .....	137
6.1.3.	Use of internal standard.....	166
6.1.4.	Sample extraction .....	166
6.2.	Method Validation .....	168
6.2.1.	Selectivity.....	168
6.2.2.	Linearity .....	168
6.2.3.	Precision .....	171
6.2.4.	Limits of detection and quantification .....	171
6.3.	Standard Stability.....	171
6.4.	Targeted plant analysis .....	174
6.4.1.	Method.....	174
6.4.2.	Results and discussion .....	174
6.5.	Helleborous root extract and determination .....	186
6.5.1.	Method.....	186
6.5.2.	Results and discussion .....	186
6.6.	Conclusion .....	191
	Chapter 7: Conclusion and further work.....	193
7.	Conclusion and further work.....	194
7.1.	Conclusion .....	194

7.2. Further work.....	196
8. References.....	198

## List of Tables

Title	Page
Table 2.1: Thyroid hormone levels indicative of thyroid function	48
Table 2.2: Compound properties	56
Table 4.1: Instrument parameters	95
Table 4.2: Collision energies for LC-MS/MS	96
Table 4.3: Preparative LC gradient profile	97
Table 5.1: Comparison of existing methods for the analysis of thyroid hormones	107
Table 5.2: Fragmentation parameters and ions observed	108
Table 5.3: Solvent recoveries for tablet extraction development	111
Table 5.4: C18 SPE solvent recovery comparison	116
Table 5.5: % recoveries for spiked serum dilutions	119
Table 5.6: Linearity and LOQ/LOD results for the analytical techniques	121
Table 5.7: Individual %CV results	122
Table 5.8: Impact of freeze-thaw cycles on standard solutions	123
Table 5.9: Impact of freeze-thaw cycles on spiked serum samples	123
Table 5.10: Tablet results	126
Table 6.1: Comparison of existing methods for the analysis of plant toxins	139
Table 6.2: LC-MS buffer suitability	143
Table 6.3: Resolution of neighbouring peaks	143
Table 6.4: Fragmentation ions observed	148
Table 6.5: Breakdown of MS/MS method	147
Table 6.6: Solvent extraction study results for sonication	170
Table 6.7: Linearity and LOQ/LOD results	172
Table 6.8: Types of plants and compounds present	175
Table 6.9: Concentration of toxins found in plants sampled	182
Table 6.10: Numerical values used in risk factor calculations	185
Table 6.11: Preparative LC gradient profile	198
Table 6.12: Tentative compound identification	190

## List of Figure

Title	Page
Figure 1.1: Examples of complex sample treatment	5
Figure 1.2: Soxhlet extraction set up	6
Figure 1.3: Schematic of LLE	6
Figure 1.4: Schematic of SPE modes	7
Figure 1.5: Stages in the analytical process for complex samples	9
Figure 1.6: Schematic of HPLC system	9
Figure 1.7: Schematic of a) binary pump and b) quaternary pump	10
Figure 1.8: Example van Deemter curve	12
Figure 1.9: Column packing materials	13
Figure 1.10: Types of silanol groups and pore shapes where a) cylindrical, b) inkbottle shaped and c) funnel shaped	14
Figure 1.11: Structure of stationary phase for a) F5 column and b) C18 column	15
Figure 1.12: Schematic of a) variable wavelength detector and b) photo diode array detector	17
Figure 1.13: Schematic of fluorescence detector	18
Figure 1.14: Schematic of refractive index detector	19
Figure 1.15: Ionisation techniques relative to analyte physiochemical properties	21
Figure 1.16 Schematic of ESI operation in positive mode	22
Figure 1.17: Schematic of APCI source	23
Figure 1.18: Schematic of PQD process	24
Figure 1.19: Schematic of quadrupole mass analyser	25
Figure 1.19: Mathieu stability diagram for ion motion in an electrical field	25
Figure 1.20: Ion stability as function of U and V	26
Figure 1.21: Schematic of triple quadrupole mass analyser	26
Figure 1.22: Schematic of time-of-flight mass analyser	27
Figure 1.23: Ion trap mass analyser	28
Figure 1.24: WideBand Activation™	29
Figure 1.25: Schematic of a) LTQ orbitrap, b) Q Exactive orbitrap and c) ID-X orbitrap mass analysers	31
Figure 1.26: Orbitrap mass analyser	32

Figure 1.27: Schematic of a) discrete dynode and b) continuous dynode electron multiplier	32
Figure 2.1: Structure of TRH	37
Figure 2.2: Hierarchic regulation of endocrine system	38
Figure 2.3: Hypothalamus and pituitary gland location within the brain	38
Figure 2.4: Structure of Thyroglobulin	40
Figure 2.5: Structures of thyroxine and 3,3',5-triiodothyronine	41
Figure 2.6: Location and shape of thyroid gland	41
Figure 2.7: Biosynthesis of thyroid hormones	43
Figure 2.8: Suggested mechanism for the coupling of thyroid hormones	44
Figure 2.9: Metabolism of thyroid hormones	46
Figure 2.10: Graphical representation and image of a goitre	50
Figure 2.11: Schematic of ECLIA reaction	52
Figure 2.12: Types of ELISA	53
Figure 2.13: Example of a plant from each family analysed	57
Figure 2.14: Biosynthesis of aconitine	60
Figure 2.15: Biosynthesis of hyoscyamine (atropine) and scopolamine	62
Figure 2.16: Biosynthesis of capsaicin	64
Figure 2.17: Biosynthesis of cathinone	66
Figure 2.18: Comparison of cathinone with similar monoamine alkaloids	67
Figure 2.19: Conversion of cathinone to norephedrine and norpseudoephedrine	67
Figure 2.20: Biosynthesis of colchicine	70
Figure 2.21: Structure of linear and non-linear furocoumarins	71
Figure 2.22: Biosynthesis of coumarin and coumarin related compounds	73
Figure 2.23: Formation of adduct between psoralen and a thymine base	73
Figure 2.24: Biosynthesis of digitoxin and digoxin	75
Figure 2.25: Biosynthesis of hellebrin	77
Figure 2.26: Biosynthesis of salvinorin A	79
Figure 2.27: Biosynthesis of $\alpha$ -solanine	82
Figure 2.28: Biosynthesis of strychnine	84
Figure 2.29: Biosynthesis of $\alpha$ and $\beta$ -thujone	85
Figure 2.30: Biosynthesis of veratridine	88
Figure 5.1: HPLC-UV chromatogram of a) T3 and b) rT3 with acetonitrile as organic modifier	104

Figure 5.2: Chromatogram of T4, T3, rT3 and T2 by low resolution LC-MS/MS	105
Figure 5.3: Mass spectrum for a) T2, b) T3, c) rT3 and d) T4	109
Figure 5.4: Mass spectrum fragments for a) T2, b) T3, c) rT3 and d) T4	110
Figure 5.5: Comparison of sonication times on % recoveries	111
Figure 5.6: Method development of SPE using HPLC-PDA. a) Strata-SDB-L™, b) Strata-X™ and c) C18	114
Figure 5.7: Comparison of standard in mobile phase and serum by LR-MS-MS/MS. a) T2, b) rT3, c) T3 and d) T4	117
Figure 5.8: Comparison of standard in mobile phase and serum by HR-MS-MS/MS. a) T2, b) T3, c) rT3 and d) T4	118
Figure 5.9: Stock solution stability for solutions stored at a) -20 °C and b) 2-8 °C	124
Figure 5.10: Analysis of Cytomel™ tablet	127
Figure 5.11: Combined calibration graph for all dissolutions. a) T3 (n=8) and b) T4 (n=2)	129
Figure 5.12: Dissolution profile of 4 batches of thyroid supplements	129
Figure 5.13: Kinetic profile of the dissolution of T3 and T4	130
Figure 5.14: Measurement Agreement plots for a) T4 by ELISA or ECLIA versus LC-MS and b) T3 by ELISA or ECLIA versus LC-MS.	133
Figure 6.1: Standard chromatograms for a) water:acetonitrile and b) buffer:methanol using the gradient in Table 4.1	138
Figure 6.2: Standard extracted ion chromatograms for a) 5- and 8-methoxypsoralen, b) aconitine, c) atropine, d) capsaicin, e) cathinone and f) colchicine	144
Figure 6.3: Standard extracted ion chromatograms for a) coumarin, b) digitoxin, c) digoxin, d) hellebrin, e) psoralen and f) salvinorin A	145
Figure 6.4: Standard extracted ion chromatograms for a) scopolamine, b) solanine, c) strychnine, d) thujone and e) veratridine	146
Figure 6.5: Full scan MS/MS spectrum for a) 5-methoxypsoralen, b) 8-methoxypsoralen and c) compound fragmentation	149
Figure 6.6: Full scan MS/MS for a) aconitine and b) compound fragmentation	150
Figure 6.7: Full scan MS/MS for a) atropine and b) compound fragmentation	151

Figure 6.8: Full scan MS/MS for a) capsaicin and b) compound fragmentation	152
Figure 6.9: Full scan MS/MS for a) cathinone and b) compound fragmentation	153
Figure 6.10: Full scan MS/MS for a) colchicine and b) compound fragmentation	154
Figure 6.11: Full scan MS/MS for a) coumarin and b) compound fragmentation	155
Figure 6.12: Full scan MS/MS spectrum for a) digitoxin and b) compound fragmentation	156
Figure 6.13: Full scan MS/MS spectrum for a) digoxin and b) compound fragmentation	157
Figure 6.14: Full scan MS/MS spectrum for a) hellebrin and b) compound fragmentation	158
Figure 6.15: Full scan MS/MS spectrum for a) psoralen and b) compound fragmentation	159
Figure 6.16: Full scan MS/MS spectrum for a) salvinorin A and b) compound fragmentation	160
Figure 6.17: Full scan MS/MS spectrum for a) scopolamine and b) compound fragmentation	161
Figure 6.18: Full scan MS/MS spectrum for a) $\alpha$ -solanine and b) compound fragmentation	162
Figure 6.19: Full scan MS/MS spectrum for a) strychnine and b) compound fragmentation	163
Figure 6.20: Full scan MS/MS spectrum for a) $\alpha$ -thujone and b) compound fragmentation	164
Figure 6.21: Full scan MS/MS spectrum for a) veratridine and b) compound fragmentation	165
Figure 6.22: Unspiked matrix chromatogram following ASE	167
Figure 6.23: Comparison of sonication time with compound recoveries	169
Figure 6.24: Standard stability at 2-8 °C	173
Figure 6.25: Example extracted positive ion ESI SRM chromatogram of a) aconitine from <i>Aconitum lycoctonum</i> stem and b) Atropine and scopolamine from <i>Brugmansia suaveolens</i> petal	176

Figure 6.26: Example extracted positive ion ESI SRM chromatogram of a) capsaicin from <i>Capsicum chinense</i> chilli, b) cathinone from <i>Catha edulis</i> leaf, c) colchicine from <i>Colchicum autumnale</i> bulb and d) coumarin from <i>Daphne laureola</i> leaf	177
Figure 6.27: Example extracted positive ion ESI SRM chromatogram of a) digitoxin and digoxin from <i>Digitalis ferruginea</i> flower and d) hellebrin from <i>Helleborus cyclophyllus</i> root c) psoralen, 5- and 8-methoxypsoralen from <i>Ruta graveolens</i> foliage and d) salvinorin A from <i>Salvia divinorum</i>	178
Figure 6.28: Example extracted positive ion ESI SRM chromatogram of a) solanine from <i>Solanum tuberosum</i> , b) thujone from <i>Artemisia absinthium</i> leaf and c) veratridine from <i>Veratrum album</i> flower	179
Figure 6.29: Correlation graphs for hellebrin in a) root and flower concentration, b) root and foliage concentration and c) flower and foliage concentration	181
Figure 6.30: Chromatogram of preparative HPLC for a) hellebrin standard and b) plant extract	187
Figure 6.31: Preparative HPLC chromatogram following gradient adjustment	188
Figure 6.32: Example a) proton, b) carbon and c) HSQC NMR spectrum obtained from hellebrin root fractions	190

## **Appendix**

Appendix 1: Ingestion exposure risk factors

Appendix 2: Number of day exposure required for ingestion risk to hit LD50

Appendix 3: Dermal absorption exposure factor

Appendix 4: Number of years exposure required for dermal risk to hit LD50

## List of abbreviations

APCI: Atmospheric pressure chemical ionisation

ASE: Accelerated solvent extraction

ATP: Adenosine triphosphate

BMR: Basal metabolic rate

cAMP: Cyclic adenosine monophosphate

CDS: Chromatography data system

CID: Collision induced dissociation

CL: Chemiluminescence

CoA: Co enzyme A

CYP750B1: (+)-sabinene hydroxylase

CYP76AA25: (+)-sabinene hydroxylase

CYP90B27: Cholesterol 22-hydroxylase

CYP90G1: 22-hydroxy-26-aminocholesterol 22-oxidase

CYP94N1: 22-hydroxycholesterol 26-hydroxylase/oxidase

DA: Diterpene alkaloid

DIT: Diiodothyrosyl

DNA: Deoxyribonucleic acid

DPS: dioxygenase for potato solanidine synthesis

ECLIA: Electrochemiluminescence immunoassay

ECL: Electrochemiluminescence

ELISA: Enzyme linked immunosorbent assay

EMA: European Medicines Agency

EPA: Environmental Protection Agency

ESI: Electrospray ionisation

F5: Pentafluorophenyl

FaSSGF: Fasted state gastric fluid

FaSSIF: Fasted state small intestinal fluid

FTICR: Fourier transform ion cyclotron resonance

GABA<sub>A</sub>:  $\gamma$ -aminobutyric acid A

GABAT1: 22-hydroxycholesterol-22-as transaminase

GC: Gas chromatography  
GPCR: G-protein coupled receptors  
HILIC: Hydrophilic interaction liquid chromatography  
HPLC: High performance liquid chromatography  
HSQC: Heteronuclear single quantum coherence  
ICH: The International Council for Harmonisation  
ITDI: Iodothyrosine deiodinase  
KPS: Kolavenyl diphosphate synthase  
LC: Liquid chromatography  
LC-MS: liquid chromatography-mass spectrometry  
LC-MS/MS: Liquid chromatography-tandem mass spectrometry  
LD<sub>50</sub>: Median lethal dose  
LED: Light emitting diode  
LLE: Liquid-liquid extraction  
LOD: Limit of detection  
LogP: Logarithm of Partition coefficient  
LOQ: limit of quantification  
M1: Muscarinic acetylcholine receptor 1  
M2: Muscarinic acetylcholine receptor 2  
M3: Muscarinic acetylcholine receptor 3  
M4: Muscarinic acetylcholine receptor 4  
M5: Muscarinic acetylcholine receptor 5  
MAPK: Mitogen-activated protein kinase  
MIT: Monodothyrosyl  
NADPH: Nicotinamide adenine dinucleotide phosphate  
NIS: Sodium iodide symporter  
NMR: Nuclear magnetic resonance  
NP: Normal phase  
P: Pendrin  
PI3K: Phosphoinositide 3-kinase  
PQD: Pulse Q collision induced dissociation  
PUVA: Photo Ultra-violet A

RI: Refractive index  
RP: Reversed phase  
rT3: Reverse T3  
SEC: Size exclusion  
SFC: Supercritical fluid chromatography  
SGT1: solanidine galactosyltransferase 1  
SGT2: solanidine glucosyltransferase 2  
SGT3:  $\beta$ -solanidine rhamnosyltransferase  
SLE: Solid-liquid extraction  
SPE: Solid phase extraction  
SRM: Selected reaction monitoring  
T3: Triiodothyronine  
T4: Thyroxine/tetraiodothyronine  
TG: Thyroglobulin  
TO: Thyroid oxidase  
TOF: Time of flight  
TPO: Thyroid peroxidase  
TRH: Thyrotropin releasing hormone  
TRHR: TRH receptor  
TRPV1: Transient receptor potential vanilloid 1  
TSH: Thyroid stimulating hormone  
TSI: Thyroid stimulating immunoglobulin  
UCP-1: Uncoupling protein 1  
UCP-2: Uncoupling protein 2  
UCP-3: Uncoupling protein 3  
UV: Ultra-violet  
UV/vis: Ultra-violet/visible

## List of accompanying material

Journal article 1: SL. Bowerbank, MG. Carlin and JR. Dean, "A direct comparison of liquid chromatography-mass spectrometry with clinical routine testing immunoassay methods for the detection and quantification of thyroid hormones in blood serum", *Analytical and Bioanalytical Chemistry*, 2019, 13, 2839-2853.

Journal article 2: SL. Bowerbank, MG. Carlin and JR. Dean, "Dissolution Testing of Single- and Dual-Component Thyroid Hormone Supplements", *Separations*, 2019, 6, 18-24.

## **Acknowledgements**

I would like to acknowledge and thank my supervisory team, Prof. John Dean and Dr Michelle Carlin for their guidance and support throughout this project and my progression panel, Prof. Steven Stanforth and Dr Renli Ma for the valuable insight and unique perspective on the project. I would also like to thank Dr Jonathan Knowles for his assistance and guidance in the preparation of NMR samples and reviewing of NMR data. In addition, I would also like to thank the technical manager, Dave Wealleans, for allowing the funding and allocation of time to complete this project and to the members of the technical team who have supported and guided me with various aspect of this project.

A special thank you is due to Mark Brassell, Trevor Jones and Robert Ternent of Alnwick Gardens for allowing me authorisation to collect and analyse plants from the garden and for their knowledge in relation to the plants. Without which a large portion of this project could not have taken place.

A very big thank you to my friends and colleagues who have provided me with emotional support and kept me going particularly: Andrew Dunning, Jasmin Turner, Heather Taylor, Charlie Mikan, Charlotte McIvor, Alex Walker, Kate Nicholson, Blake Kesic and Matthew Reynolds.

The biggest thankyou goes to my Mam, Susan Donnelly and stepdad, Harry Donnelly who have always believed in me and have supported me every step of the way in any way they could. I would not be where I am today without you both.

## **Declaration**

I declare that the work contained in this thesis has not been submitted for any other award and that it is all my own work. I also confirm that this work fully acknowledges opinions, ideas and contributions from the work of others.

Any ethical clearance for the research presented in this thesis has been approved. Approval has been sought and granted by the Faculty Ethics Committee on 19 February 2016.

**I declare that the Word Count of this Thesis is 41972 words**

Name: Samantha Louise Bowerbank

Signature:

Date: 21<sup>st</sup> June 2021

# Chapter 1: Introduction

## **1. Introduction**

### **1.1. The changing face of analytical chemistry**

Advances in analytical capabilities over the past 50-60 years has opened up new possibilities in the way in which analysis takes place and the information which can be obtained. Since the 1960s the field of analytical chemistry has transformed from mainly destructive, simply spectroscopic tools which mainly utilised the visible regions of the electromagnetic spectrum, into a field with large complexity in both the nature and the methodological approaches. The introduction of instrumental techniques incorporating a wider range of the electromagnetic spectrum, alongside the introduction of mass spectrometry, allowed for more information to be obtained from increasingly smaller sample sizes. The rapid developments in analytical chemistry were driven by ideas from the top-down with developments in microelectronics, instrument manufacturer and nanotechnology and was also driven bottom up by the development of general scientific processes in chemistry, biology and physics.<sup>1</sup> These changes led to a shift in approach from a singular results focused approach to a combined data approach utilising a combination of tools. This increased the scope and footprint of analytical chemistry by the expansion into other areas, such as bioanalysis, which has occurred over the past decade bringing with it the possibility to use a systematic approach whereby a whole process can be evaluated.<sup>2</sup>

A wide range of techniques are available for analysis and are chosen based on a number of factors, including what information is required, whether the analysis is qualitative or quantitative, ease of use, availability and speed of analysis. In some instances, the techniques are often used as this is what has been used historically or from a form of governance; the use of a specific method in a pharmacopeia for example.<sup>3</sup> In recent years liquid chromatography coupled to a mass spectrometer has become applied across a wider range of applications than previously seen. This increase has been driven by a number of factors including the advancement in instrumentation and the advancement in column technologies, allowing for a wide range of analytes to be chromatographically separated in a shorter analysis time, all while systems being more robust and user friendly. The advances in ultra-high performance liquid chromatography allows for systems to be operated at greater pressure which, in turn, led to development of narrower bore, smaller

particle size columns that not only allows for a more efficient separation but allows reduction in consumable costs due to the low flow rates that are utilised by these instruments.<sup>1, 4</sup>

The advances in mass spectrometry have allowed for further developments, particularly in the field of biology, allowing for the identification and characterisation of large complex compounds with a high sample throughput and high degree of sensitivity for a miniscule amount of sample.<sup>3, 5, 6</sup> The ability to understand ion motion had benefitted mass spectrometry leading to the development of instrumentation optimised for a range of applications. This, in turn, has led to an increase in the complexity of samples which are being investigated.<sup>1, 7</sup> Complex samples from an analytical perspective can be described as samples in which, not only is the analytes of interest present, but a wide range of other components. This can incorporate a range of different materials including biological samples such as blood and urine, food samples, environmental samples such as river water or soils, plant materials and many others. Each sample type brings with it a unique set of analytical challenges which must be overcome in order to obtain a sensitive, robust and reliable method of analysis, many of these being dependant on the analysis technique being employed.<sup>8, 9</sup> A common problem encountered when analysing complex samples by liquid chromatography-mass spectrometry (LC-MS) using electrospray ionisation (ESI) is the signal suppression due to the sample matrix.<sup>5, 9</sup> The signal suppression is caused by the matrix components and the analyte competing within the droplet surface of the gas phase resulting in the analyte signal being suppressed.<sup>10</sup> This can cause issues particularly in quantification, as the standard solutions will not exhibit these matrix effects.<sup>11, 12</sup> In order to address the issues around matrix effect an effective clean up procedure must be developed. In this work, complex matrices of serum, tablet preparation, gastrointestinal fluid (thyroid hormones) and plant materials (plant toxins) were used.

Thyroid hormone diseases are commonplace in the United Kingdom with around 1 in 20 people having a thyroid problem however numbers are estimated to be higher due to individuals not being aware they have issues.<sup>13, 14</sup> The diagnosis and management of thyroid disorders relies on thyroid function testing which measure thyroid stimulating hormone as an initial screen, thyroxine as a confirmation and triiodothyronine alongside thyroxine in the management of treatment.<sup>15, 16</sup>

However, a separate assay must be performed for each test and due to the limitations of the clinical method accuracies of 30 % at the limit of quantification can be observed.<sup>17, 18</sup> Therefore LC-MS would be a suitable alternative allowing for the simultaneous detection of thyroxine and triiodothyronine with the potential benefits of increase sensitivity and accuracy. Plant toxin analysis was carried out in collaboration with Alnwick Garden, which is located in Northumberland and has the largest poison garden in the UK, housing plants ranging from stinging nettles to poisonous and UK Home Office licence controlled plants.<sup>19, 20</sup> The plants chosen for the study were based on the availability of standards within the UK and also the potential of exposure. For example, *Heracleum mantegazzianum* which is often found on water banks, *Salvia Divinorum* contains Salvinorin A which is used as a recreational drug and numerous plants which can be purchased from garden centres and nurseries.<sup>21-24</sup> Due to the number and varying complexity of the compounds, liquid chromatography-mass spectrometry would be the most suitable technique for simultaneous analysis as the larger molecular weight compounds would be better suited to liquid chromatography-mass spectrometry than gas chromatography-mass spectrometry as these would have limited volatility and would therefore require derivatisation in order to be analysed via gas chromatography.

The reduction in matrix effects for LC-MS can be achieved via a range of sample clean up procedures, which can either be performed on-line, whereby the procedure is performed via programming parameters in the instrument or off-line, whereby the procedure is performed manual by the analyst. There are a range of clean up procedure available and common LC-MS sample clean up techniques include, liquid-liquid extraction (LLE), solid-liquid extraction (SLE), solid phase extraction (SPE)<sup>9, 25, 26</sup> dilution and filtration, as shown in Figure 1.1.<sup>8, 27</sup> SLE utilised solvent and compound properties to remove the compounds of interest into the solvent phase and typically the solid material is then removed via techniques such as centrifugation or filtration. Depending on the solid material, the material can be used whole, crushed, sieved or freeze dried and made into a powder in order to maximise the surface area. The solid material is then extracted into the solvent phase utilising techniques such as sonication or Soxhlet extraction. Sonication uses ultra-sonic vibrations by converting an electrical signal into physical vibrations which agitate the material within the solvent. In Soxhlet extraction the solid material is place in a thimble and a solvent reflux is used to

continuously extract the material into pure solvent which maintains the extraction efficiency of the solvent, as shown in Figure 1.2. Commonly, due to the larger volumes of solvent present when using Soxhlet extraction, the extract is then concentrated using a rotary evaporator, which utilises a water bath and vacuum to rapidly remove solvents below the boiling point.<sup>28, 29</sup>

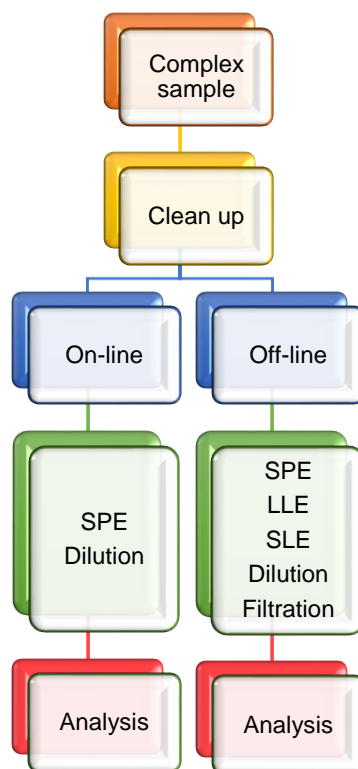


**Figure 1.1: Examples of complex sample treatment**

As with SLE, LLE exploits solvent and compound properties to remove the compounds of interest into the solvent phase but the compounds of interest are present as or within a liquid and the two liquids must be immiscible in order to form separate layer. LLE is generally performed in a separating funnel in which the two liquids are mixed by shaking before being allowed to settle as shown in Figure 1.3. Repeat extraction of performed and the extracts combined to maximise on the compound recovery. As with SLE, LLE extracts are commonly concentrated following the extraction.<sup>30</sup>

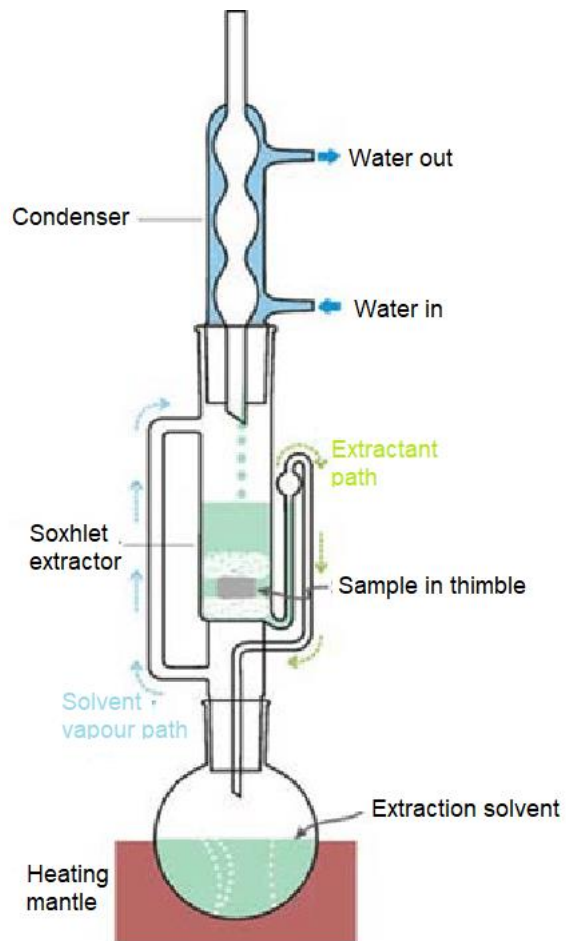


Figure 1.2: Soxhlet extraction set up<sup>29</sup>

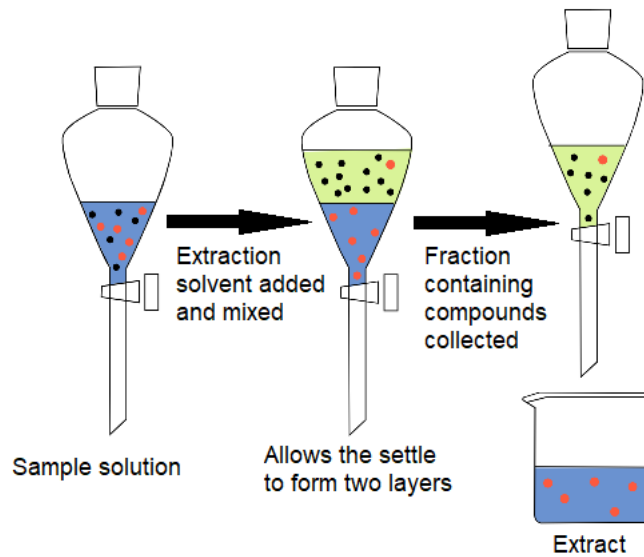
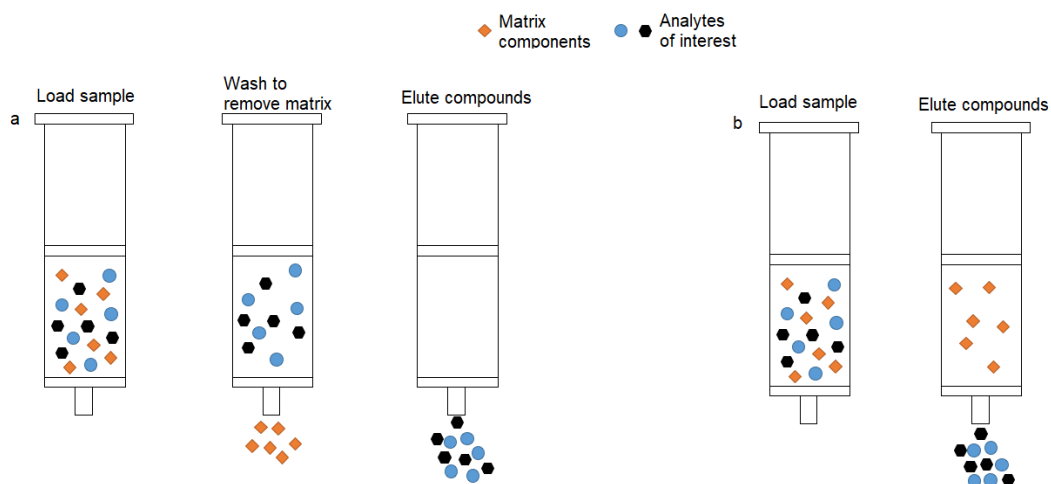


Figure 1.3: Schematic of LLE. Adapted from<sup>30</sup>

SPE involves the loading of the sample onto a sorbent which on washing either retains the compounds of interest as shown in Figure 1.4a, or the matrix components as shown in Figure 1.4b. Then via washing and elution stages, the compounds of interest are collected with minimal matrix compounds present. A typical SPE procedure would be to precondition the column with methanol then equilibration of the sorbent to match the matrix. The sample would then be loaded onto the sorbent and the sorbent wash with a water:organic mix followed by the elution of the compounds using organic solvent.<sup>31</sup> Various types of SPE sorbent are available include amide, ion exchange and alkyl chain of various length, e.g. C2, C8 and C18. SPE sorbents are also available in a number of formats including cartridges which connect to a vacuum manifold and pipette tip which can be used with a positive displacement pipette. The pipette tip format have the advantage of being able to be used for small volume sample of as low as 1  $\mu$ L however, each sample must be processed individually.<sup>32</sup> Where as a vacuum manifold allows for the simultaneous processing of up to 24 samples when using the cartridge format.



**Figure 1.4: Schematic of SPE modes. Adapted from<sup>33</sup>**

Dilution and filtration are simple clean up technique which involve the reduction in the concentration of matrix component in the case of dilution and the removal of particulate and some matrix component in the case of filtration. When performing filtration, care must be taken when selecting the filter material so that compounds of interest do not adhere to the filter. Filtration can be performed on small volume

samples via the use of syringe filters or large volume sample via the use of filter membranes and a vacuum filtration unit.

Sample preparation techniques are required for each sample type due to the difference in sample make up. For example serum contains albumin, globulin electrolytes and circulating hormones; gastro-intestinal fluid contains electrolytes, cholesterol, lipids, proteins and enzymes and plant materials contain proteins, organic molecules, electrolytes and chlorophylls, all of which can impact on the analysis.<sup>34-36</sup> In this study, SPE and dilution were used for the sample clean up for the analysis of thyroid hormones via low-resolution LC-MS and high-resolution LC-MS, respectively and SLE extraction is used for the plant toxins.

## **1.2. Liquid Chromatography-Mass Spectrometry**

### **1.2.1. Liquid chromatography**

Chromatography is an overarching term which covers a range of techniques including liquid chromatography (LC), gas chromatography (GC) and ion chromatography. The first work naming and using LC was just over 100 years ago by Tswett.<sup>37</sup> However, this original work was not accepted by his peers and it was not until the 1930s that the technique was reinvestigated. Work completed by Martin and Synge<sup>38</sup> on the separation of amino acid derivative saw the beginning of partition chromatography, for which they received a Nobel prize in 1952. Their work led to the development of paper chromatography in 1944, thin layer chromatography in 1956 and eventually high performance liquid chromatography (HPLC) in 1967-69.<sup>37, 39</sup>

The advancement over the years has led to HPLC now being common place within pharmaceutical testing laboratories.<sup>3, 40, 41</sup> Typical separation modes employed within pharmaceutical analyses have included reversed phase (RP), normal phase (NP), and size exclusion (SEC), with reversed phase being the most widely used mode of separation with pharmaceutical and clinical analyses.<sup>37</sup> However, as the complexity of the samples increases, more sophisticated separations are required in order to obtain analytically reliable results. This has resulted in techniques such as hydrophilic interaction liquid chromatography

(HILIC), supercritical fluid chromatography (SFC) and chiral chromatography starting to make an appearance in analytical laboratories. This study utilises both high performance liquid chromatography (HPLC), for initial investigation and development of sample clean up, and LC-MS for the analysis of thyroid hormones and plant toxins (Figure 1.5).

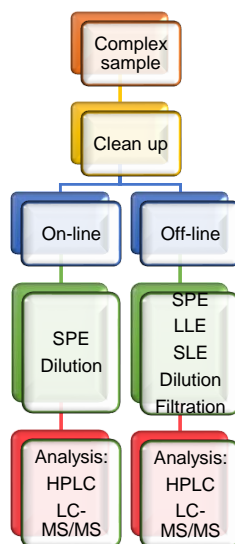


**Figure 1.5: Stages in the analytical process for complex samples**

Modern HPLC systems are based on a modular set up with the following elements; a solvent reservoir, a high pressure pump, injection device with optional autosampler, column, detector and chromatography data system (CDS) as shown in Figure 1.6.<sup>39, 42</sup>

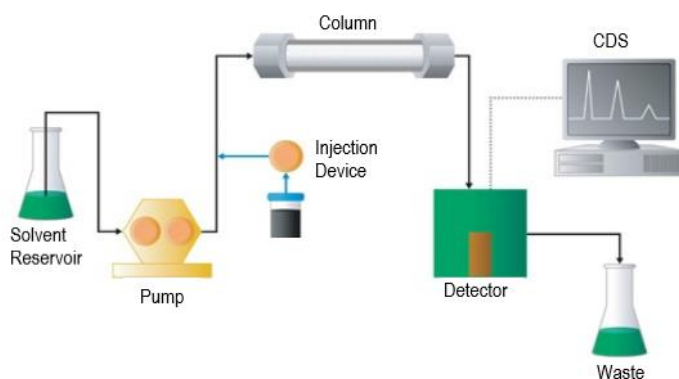
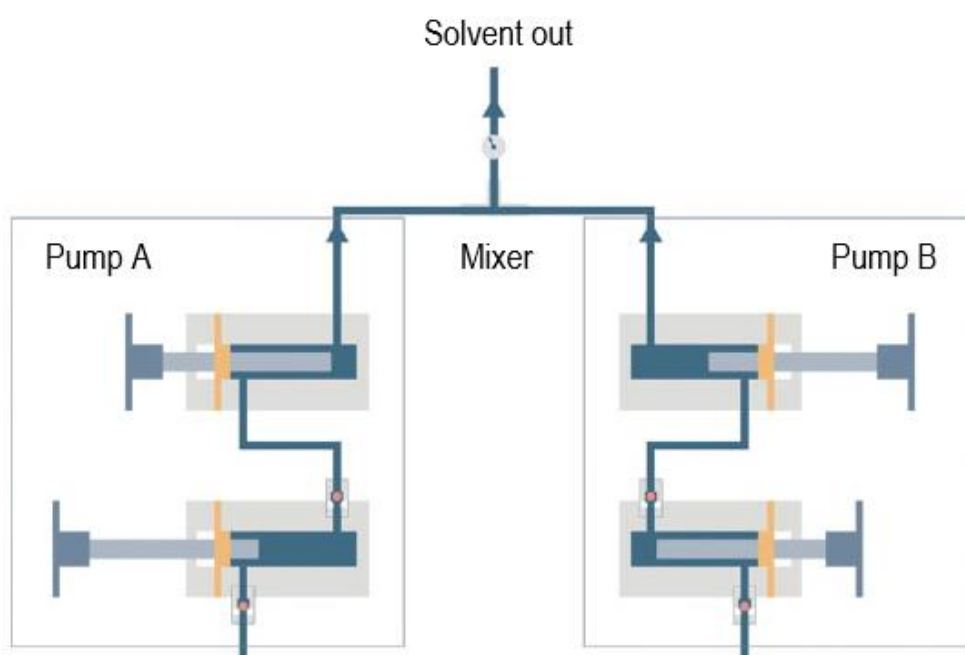


**Figure 1.6: Schematic of HPLC system. Adapted from<sup>42</sup>**

The HPLC pump can either be isocratic, delivering the same composition of mobile phase, or gradient, delivering a changing composition of mobile phase,

during the analysis, and must be able to operate with minimal pulsing of flow. Gradient HPLC pumps can either be binary which mix the mobile phase components in a high-pressure mixing design downstream from two pump heads or quaternary, which mix the various mobile phase components in a low-pressure mixing design where one pump draws each component via a four-port proportioning valve as shown in Figure 1.7.<sup>43</sup>

a)



b)

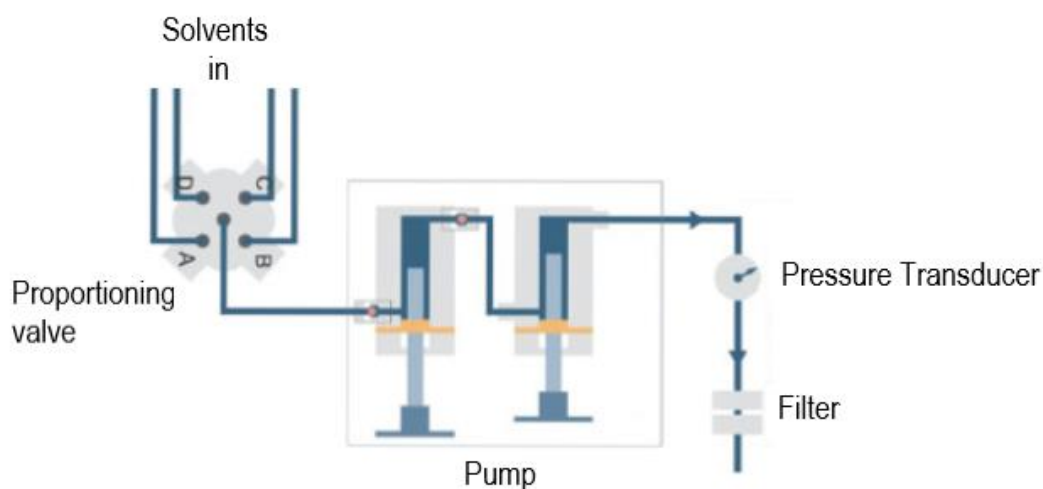


**Figure 1.7: Schematic of a) binary pump and b) quaternary pump. Adapted from<sup>43</sup>**

The separation of analytes within a chromatographic system can be described by the column efficiency. Column efficiency can be determined by the number of theoretical plates or the height equivalent to a theoretical plate. The theoretical plates model proposed that a column can be divided into plates with equilibrations of the analyte between the mobile and stationary phase occurring in each plate. Analytes move through the column by transfer from one plate to the next. The larger the number of theoretical plates the better the column efficiency. The number of theoretical plate (N) can be calculated by the following:

$$N = 16(t_r / W)^2 \quad (1.1)$$

$$N = 5.54(t_r / W_{0.5})^2 \quad (1.2)$$

$$N = 2\pi(t_r \cdot H / A)^2 \quad (1.3)$$

Where:  $t_r$  is retention time,  $W$  is peak width,  $W_{0.5}$  is peak width at half height,  $H$  is peak height,  $A$  is peak area

The theoretical plate number can be expressed as a function of the column length to give the height equivalent to the theoretical plate (HETP). The smaller the height equivalent to the theoretical plates the better the column efficiency. The height equivalent to theoretical plates is calculated by the following:

$$\text{HETP (mm)} = L / N \quad (1.4)$$

Where:  $L$  is the column length (mm) and  $N$  is the number of theoretical plates

The limitations of the plate model is the assumption that the equilibrium of the analyte between mobile and stationary phase is instantaneous and that there is a single pathway for the analyte to travel through the stationary phase particles. Both factors effecting the peak broadening of an analyte as it passed through the column. The mechanisms of peak broadening and its relationship to the height equivalent to the theoretical plates were discussed in work carried out by van Deemter *et al.* in 1956.<sup>44</sup> The relationship between the column efficiency and the

mechanisms resulting in band broadening can be described by the van Deemter equation.<sup>37, 39, 45</sup>

$$HETP = A + (B/u) + Cu \quad (1.5)$$

Where: A is Eddy diffusion, B is Longitudinal diffusion, C is resistant to mass transfer and  $u$  is mobile phase velocity

In order to determine the optimum mobile phase, flow a van Deemter curve can be constructed as a function of the van Deemter equation of the mobile phase velocity. (Figure 1.8)<sup>37, 39, 45</sup>

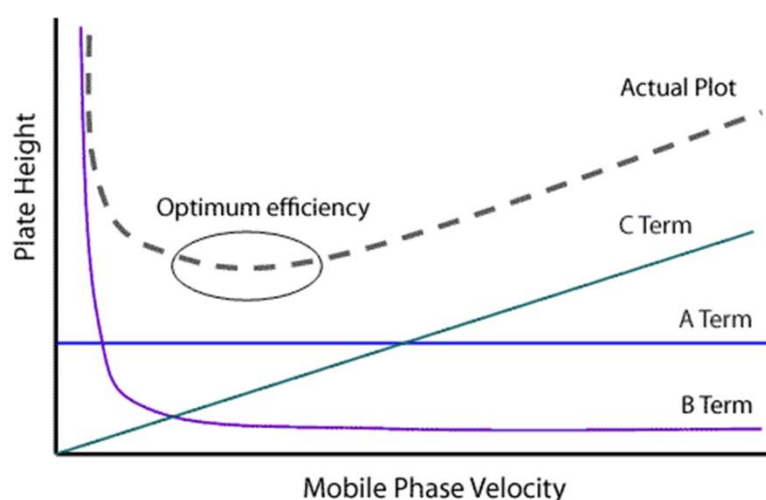


Figure 1.8: Example van Deemter curve.<sup>46</sup>

In order to access the separation, the resolution for each neighbouring peaks using the following calculation.

$$\text{Resolution} = (t_2 - t_1) / 0.5(w_1 + w_2) \quad (1.6)$$

Where:  $t_1$  is the retention time of the first peak  
 $t_2$  is the retention time of the second peak  
 $w_1$  is the retention time of the first peak  
 $w_2$  is the retention time of the second peak

Historically the most common form of detection used for liquid chromatography has been ultraviolet/visible. This technique has for many years been the common

work horse in a range of different industries. The technique is suitable for compounds with a chromophore, or those which can be reacted to give a chromophore. However, this technique will only yield the retention time and the peak area of a particular compound. Therefore, not allowing for the identification of an unknown compound without the use of a reference standard.

### 1.2.2. Column chemistry

HPLC column housings are commonly made from 316 grade stainless steel, are resistant to high pressure, are relatively chemically inert and are polished or electropolished to ensure a smooth surface. HPLC columns are packed with particle or monoliths, which are single piece synthesised stationary phases typically made from organic polymers or silica. In order to achieve a large number of theoretical plates, microparticles are used with a range of particle types available including porous, nonporous and core shell particles and porous and nonporous monoliths as shown in Figure 1.9.<sup>39, 47, 48</sup> The most common packing material are fully porous spherical particle however there has been an increase in popularity of monolithic and solid core packing materials.<sup>49</sup>

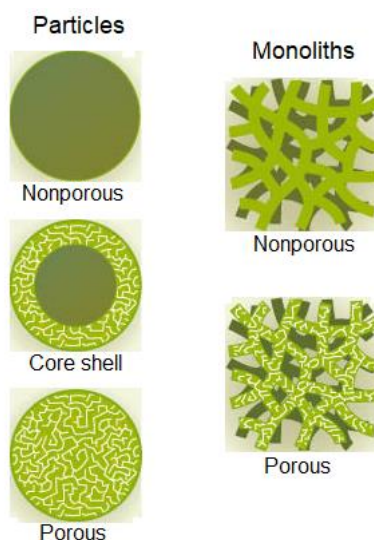


**Figure 1.9: Column packing materials. Adapted from<sup>48</sup>**

The most widely used material for the preparation of column packing material is silica, consisting of silicon atoms which are three-dimensionally bridged with -OH groups and dependent upon the reaction used the silica obtained will either be

irregular or spherical.<sup>39</sup> The physical and mechanical stability of silica allows for controllable pore structure and morphology which is characterised by the surface silanols and siloxanes and structural heterogeneity as shown in Figure 1.10. Silanol groups fall into one of three groups; free isolated silanols, vicinal silanol, formed by hydrogen bond with neighbouring silicon, or geminal silanols, formed by hydrogen bonds to the same silicon. Free isolated silanols and geminal silanols form polar active centres and have the greatest influence on retention. The condensation of vicinal and geminal silanol groups results in siloxane groups being formed. Structural heterogeneity is based on the properties of the silica, including pore shape (cylindrical, funnel shaped or inkbottle shaped), pore size and surface area. The pore shape and curvature impacts on the bonded phase coverage due to steric hindrance, particularly in the application of long hydrocarbon chains. One of the main features of the chromatographic column bed is the particle size with small particle sizes increasing in popularity due to the ability to use lower flow rate, less solvent and achieve separation in a shorter run time, however they require instrumentation capable of handling the higher pressures produced.<sup>49</sup>

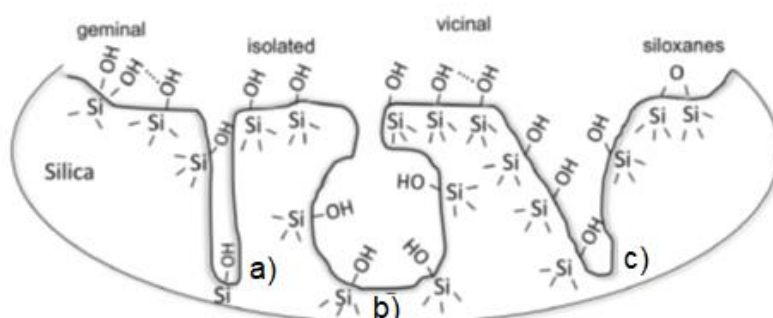


**Figure 1.10: Types of silanol groups and pore shapes where a) cylindrical, b) inkbottle shaped and c) funnel shaped.<sup>49</sup>**

The particles, and commonly monoliths, in the HPLC column can be either used as a silica column or can be chemically bonded to various stationary phases such as C8, CN, phenyl and OH in order to achieve specific separation properties.<sup>50</sup> Bonded siloxane based phases were developed by Aue and Hastings and commercialised by Kirkland in 1971.<sup>49</sup> Chemically bonded phases involve substitution reactions of the silanol moieties via esterification, silane coupling and organosilanisation to form stable covalent bonds. With the most common bonded stationary phase being a C18 bonded column.<sup>49</sup> In the work two separate columns

were used, a pentafluorophenyl (F5) column for the analysis of thyroid hormones and a C18 column for the analysis of plant toxins. Figure 1.11 shows the stationary phase of both columns.

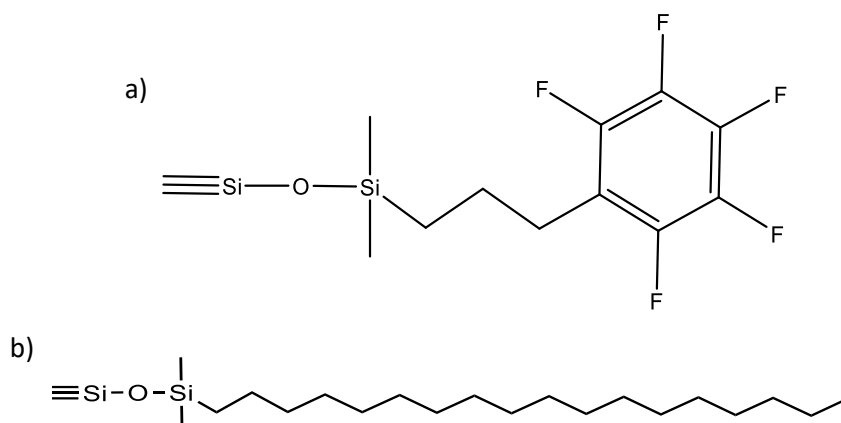


**Figure 1.11: Structure of stationary phase for a) F5 column and b) C18 column**

Both columns utilised reversed phase interactions but the F5 column is a blended column which also utilises HILIC interactions. Reversed phase interactions utilises the compound hydrophobic nature with the column material being spherical silica coated with hydrophobic alkyl group. Separation predominantly occurs due to Van de Waals interactions, which are weak electrostatic forces attracting neutral compounds to each other, between the functional groups on the stationary phase and the alkyl groups present on the compound.<sup>4, 51, 52</sup> HILIC interaction utilise partitioning, ionic and polar interactions with pentafluorophenyl phases being shown to enhance dipole,  $\pi$ - $\pi$ , charge transfer and ion exchange interactions.<sup>49, 50, 53</sup> It has been found that fluorophenyl phases have greater cation exchange properties than phenyl phases due to the partial negative charge present on the fluorine atoms on the phenyl ring structure resulting in a partial negative charge on the outer edge of the ring and a partial positive charge in the internal region.<sup>49</sup> In both systems the compound are adsorbed onto the stationary phase until such a time that the mobile phase has sufficient solvent strength to compete with the forces, at which point the compounds will be eluted from the column.<sup>54-57</sup> In the mode of chromatography used the mobile phase are a mixture of aqueous and organic solvent phases operated in either an isocratic, same composition during the run, or gradient, composition changes during the run, elution. The aqueous phase can also be buffered using a variety of salts such as ammonium formate,

sodium dihydrogen phosphate and ammonium acetate depending upon the required pH needed. The buffering of mobile phase ensures that any ionisable compounds are either fully ionised or fully unionised based upon the compound pKa. A general rule of thumb is that the solution should be pH buffered to  $\pm 2$  pH units from the pKa. The use of a buffer can improve retention time repeatability and peak shape.<sup>39, 58, 59</sup>

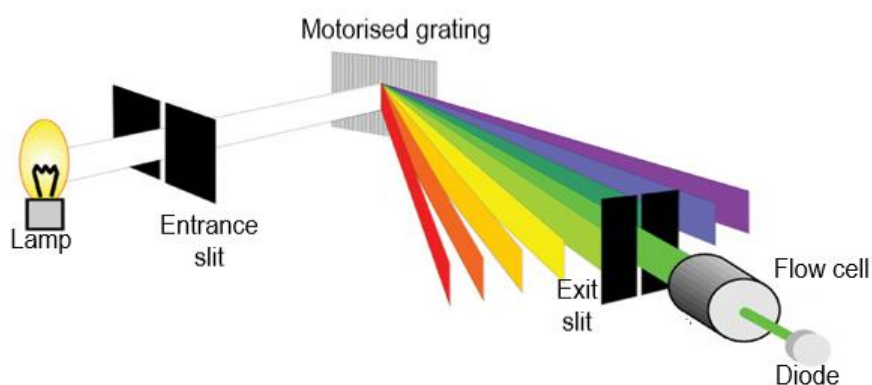
### **1.2.3. Detectors**

#### **1.2.3.1. Ultraviolet/visible detector**

The first ultraviolet/visible (UV/Vis) detectors used in HPLC were fixed wavelength detectors in the late 1960s, with variable wavelength detectors becoming popular during the 1980s which are now the most common detector found within routine analytical laboratories. UV/Vis detectors for HPLC are now commercially available as fixed wavelength, variable wavelength, multi wavelength and photo diode array formats. Fixed wavelength detectors are commonly found in low cost and portable system and are capable of operating at a single fixed wavelength. Variable and multi wavelength detectors are the most common work horses of the analytical laboratory. Allowing for the wavelength to be set as any point across the UV and visible regions of the spectrum, 100 – 700 nm, with multi wavelength detectors being able to simultaneously monitor more than one wavelength. Photo diode array detectors also allows for the scanning across the UV/Vis region. In all forms of UV/Vis detector the column eluent is passed through a flow cell which in analytical applications are commonly have a path length of 10 mm. UV/vis light is produced from a deuterium lamp, for UV and low vis region and if required a tungsten lamp, for the remaining visible region. In variable and multi detectors the light emitted from the lamp is passed through an entrance slit towards a motorised grating or prism which disperses the beam of light. The beam of light then passes through an exit slit to the flow cell and a reference diode via a beam splitter. The positioning of the grating controls the wavelength of light which passes through the exit slit. The specific wavelength of light is then absorbed by the compounds as they exit the column resulting in an excitation of electrons from a resting state to a higher energy state and the amount of light absorbed is detected via a diode as shown in Figure 1.12a. In photo diode array (PDA) detectors, the light emitted from

the lamp is passed through an entrance slit then through the flow cell before passing towards the grating or prism which disperses the beam of light. The dispersed light is then detected via a diode array across a specified nm range Figure 1.12b. The advantages of UV/Vis detectors are that they are non-destructive, relatively cheap and easy to use, have a large dynamic linear range and have high precision. However, a compound must have chromophore activity or be able to be reacted to give a chromophore and the mobile phase must be transparent to UV light, which is why wavelengths of less than around 210 nm are not routinely monitored in UV/Vis detection. UV/Vis detectors also cannot provide structural information but are highly effective in quantitative analysis based on the Beer-Lambert law which states that the absorbance is the product of the molar absorptivity ( $\epsilon$ ), path length ( $b$ ) and concentration ( $c$ ).

a)



b)

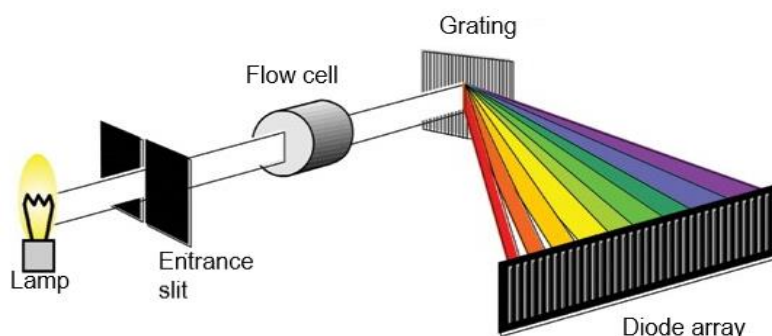


**Figure 1.12: Schematic of a) variable wavelength detector and b) photo diode array detector.<sup>60</sup>**

### 1.2.3.2. Fluorescence

Fluorescence detectors can be used with compounds that fluoresce or can be reacted to form a fluorescing derivative and can be up to 1000 times more sensitive than UV detection, however this type of detector requires a larger amount of capital to purchase and can have relatively low linear ranges depending on the solvents, sample components and analytes of interest.<sup>39</sup> Fluorescence detector use typically a Xenon lamp which produces wavelength of 200 – 900 nm which is passed through an excitation filter or monochromator before passing through the flow cell depending upon the type of instrumentation.<sup>61</sup> The use of a monochromator allows for the selection of the excitation and emission wavelength and are commonplace in more advanced modern instruments.<sup>39</sup> Typically the flow cell in fluorescent detectors is larger than that of UV detectors, typically 20  $\mu$ L in volume.<sup>61</sup> The light, of a specified wavelength, passes through the sample causing the analyte(s) to enter an excited state, when the analytes return to a normal state the energy is emitted and is detected by a photodiode via an emission filter which is at a right angle to the flow cell, as shown in Figure 1.13.

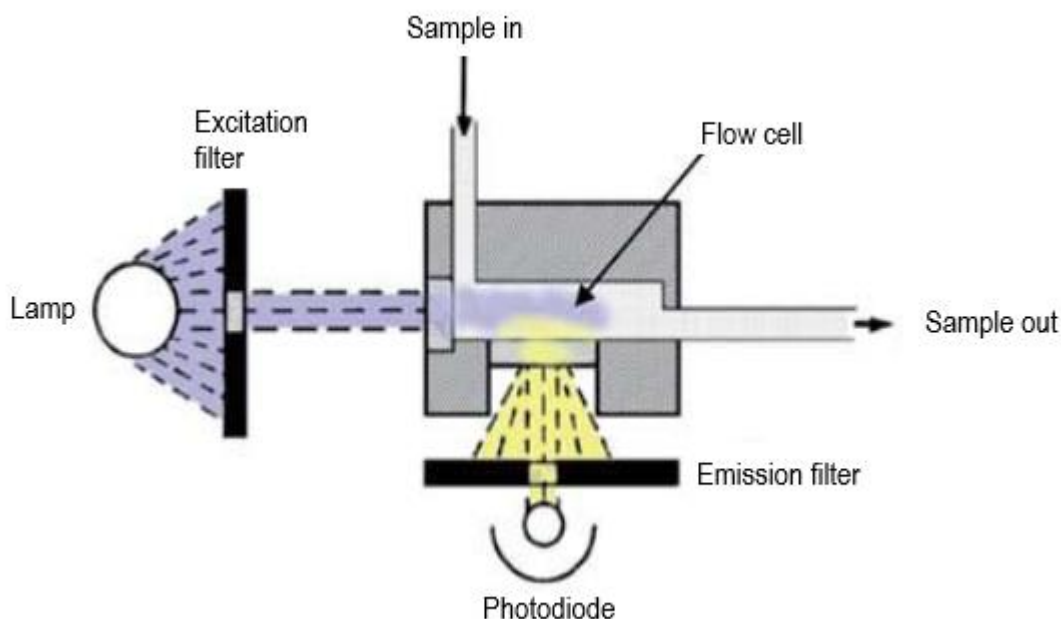


**Figure 1.13: Schematic of fluorescence detector.<sup>61</sup>**

### 1.2.3.3. Refractive index

Refractive index (RI) detection is a universal detector which can be utilised in HPLC and work on the principles of light refraction, the change in the angle of light

as it passes through a substance. Refractive index detection is commonly used for the detection of sugars and polymers and in SEC applications.<sup>62, 63</sup> Refractive index detectors use a tungsten lamp or light emitting diode (LED) with the light passing through the flow cell and the components present resulting in slight changes in the angle of light. Most manufacturer utilise a static reference flow cell filled with mobile phase which is then subtracted from the sample flow cell response. The light is then detected via two diodes with the shift in light resulting in the amount of light on each diode to increase and decrease as shown in Figure 1.14.<sup>39, 62, 64</sup>

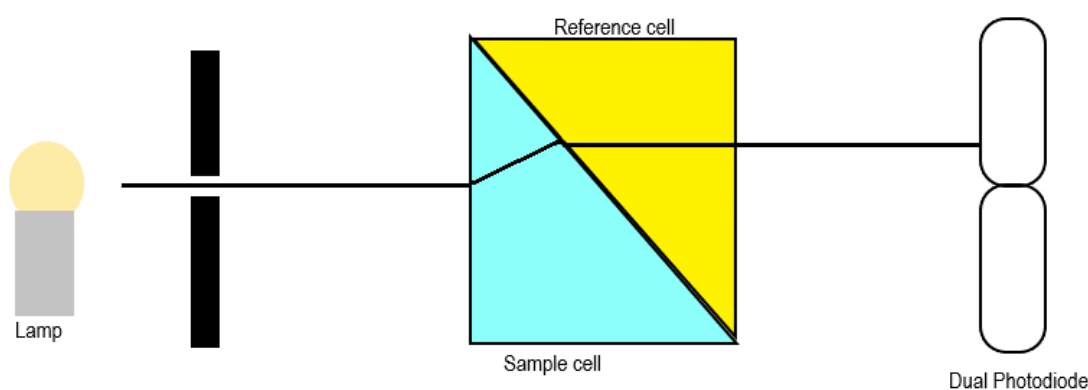


**Figure 1.14: Schematic of refractive index detector. Adapted from<sup>62, 64</sup>**

Due to the fact that the refractive index of a liquid is based upon the temperature of the light refractive index detectors are housed within insulated compartments which can be temperature control by the operator. The mobile phase eluting from the column must also be the same temperature as the flow cell for which a heat exchanger is used, with the large volume of heat exchangers resulting in broader peaks when utilising refractive index detection.<sup>64</sup>

#### **1.2.3.4. Mass Spectrometry**

Development into mass spectrometers capable of handling liquid samples has come a long way over recent years, and LC-MS is becoming more reliable and robust. This has led to the increase in LC-MS instruments in analytical laboratories.<sup>3, 12, 40, 65</sup> Sample introduction for single compounds can be achieved

by direct injection into the ionisation source. However, when more than one compound is present, separation is required prior to mass spectrometer analysis. This is achieved by coupling the mass spectrometer to another analytical technique such as liquid chromatography. In LC-MS the mobile phase must be removed before the sample can be introduced into the analyser. This led to the development of ionisation sources which allowed for the simultaneous removal of mobile phase and ionisation of the compounds of interest within a low vacuum system before the ions could then be passed into the high vacuum mass analyser.

#### **1.2.3.4.1. Ionisation mechanisms for Mass spectrometry**

A number of mechanisms exist to form ions in LC-MS; the most widely available and therefore most commonly used ionisation techniques are electrospray ionisation (ESI) and atmospheric pressure chemical ionisation (APCI). The technique of ionisation is often termed “soft ionisation” as there is limited fragmentation seen at this stage during LC-MS applications, unlike GC-MS. Physicochemical properties such as molecular weight and polarity are useful in the determination of ionisation mechanism with separation parameters used for HPLC also requiring consideration.<sup>65-67</sup> Figure 1.15 shows the use of ESI and APCI based upon molecular weight and polarity.

##### **1.2.3.4.1.1. Electrospray ionisation**

Electrospray ionisation (ESI) forms charged gas phase analyte ions from the liquid phase HPLC eluent and is capable of forming both positively and negatively charged quasi-molecular ions depending on the operation mode. The HPLC eluent is infused into the ionisation source, at a flow rate of typically around 100-400  $\mu\text{L}/\text{min}$ , via a metal capillary held at an electrical potential which causes dissociation of the analyte. In conventional ESI, which is typically used for flow rate of around 5-10  $\mu\text{L}/\text{min}$ <sup>68</sup>, the eluent is distorted to form a Taylor cone at the tip of the capillary which emits a fine mist of droplets. (Figure 1.16a) However due to the high flow rates now used (50-300  $\mu\text{L}/\text{min}$ ) pneumatically assisted ESI is now common place. Pneumatically assisted ESI uses an inert nebuliser gas, e.g. nitrogen, to create a mist of charged droplets which disrupts the formation of the

Taylor cone.<sup>68, 69</sup> (Figure 1.16b) (stage 1) The droplets undergo rapid desolvation assisted by heat and drying gas resulting in an increasing charge density within the droplet until the Rayleigh limit is reached (stage 2). Producing smaller highly charged droplets via jet fission; a process which is repeated until nanometre droplets are produced from which the charged species are obtained via one of two possible models, charge residue model (CRM) and ion evaporation model (IEM). (stage 3) In CRM the constant evaporation of solvent from the droplet leads to an isolated analyte ion. In IEM once the droplet reaches a small radius of ~ 10 nm the analyte ion is able to evaporate to the gas phase due to the electrostatic forces on the surface of the droplet being able to counteract the solvation forces. The charged species then pass through a skimmer cone and heated transfer capillary (stage 4) and are directed to the mass analyser via a series of lenses as shown in Figure 1.16.<sup>11, 65, 70-72</sup>

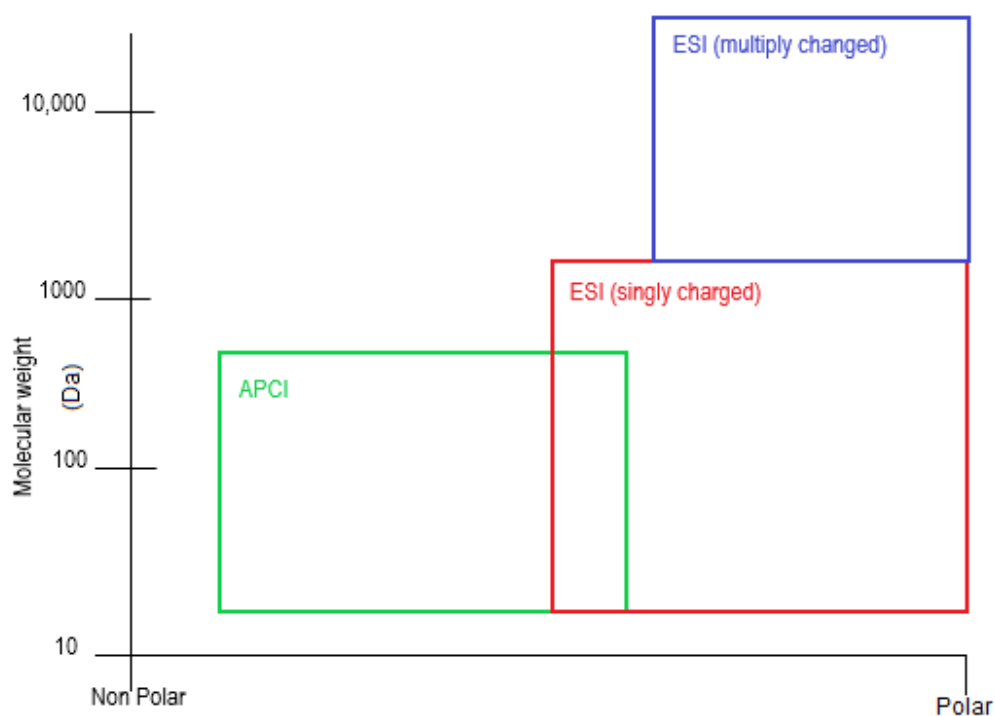


**Figure 1.15: Ionisation technique relative to analyte physiochemical properties. Adapted from<sup>73</sup>**

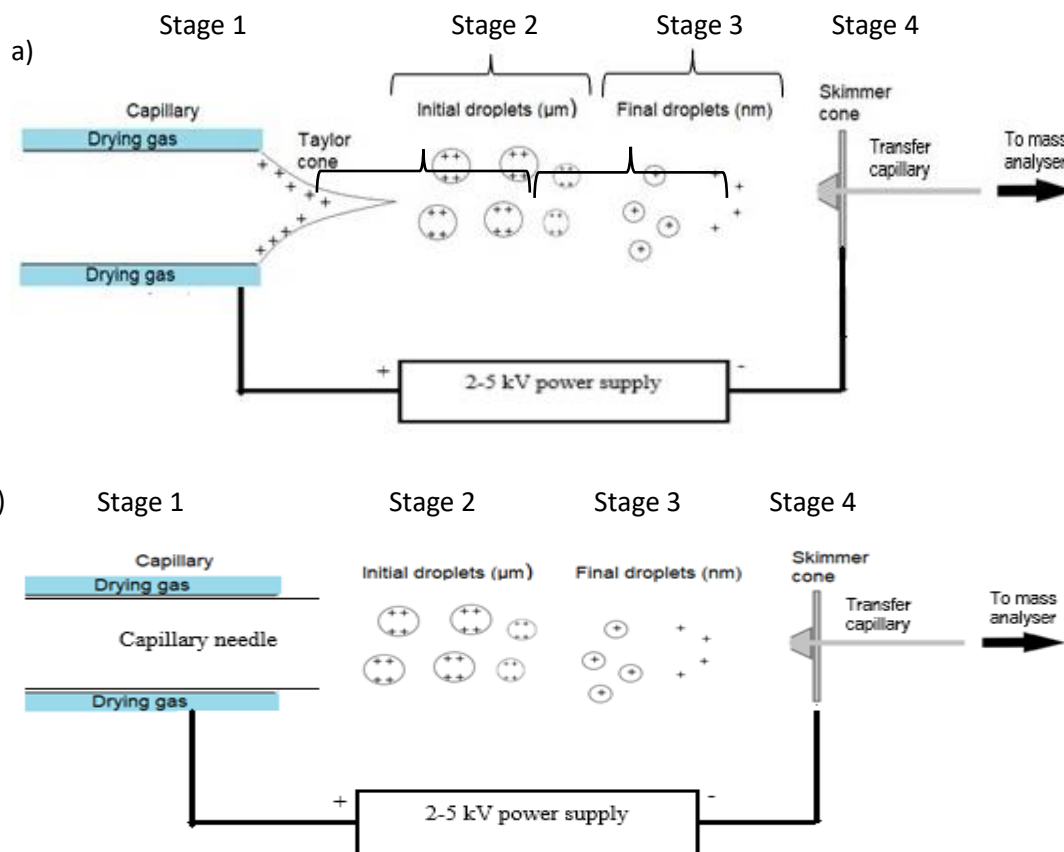


**Figure 1.16: Schematic of a) ESI operation and b) pneumatically assisted ESI operation in positive mode. Adapted from<sup>65</sup>**

#### 1.2.3.4.1.2. Atmospheric Pressure Chemical Ionisation

In atmospheric pressure chemical ionisation (APCI) ionisation occurs using similar mechanisms to that of ESI however the process of solvent evaporation and analyte ionisation is obtained via two separate processes. In APCI a corona needle is used to ionise the drying gas and the solvent molecules (stage 1). The interaction of these charged ions with the analyte results in ionisation through charge transfer once the charged analyte is formed it enters into the mass analyser in the same way described above (stage 2) as shown in Figure 1.17. Atmospheric pressure chemical ionisation is typically used for smaller, non-polar compounds which are not readily ionisation by ESI.<sup>65</sup>

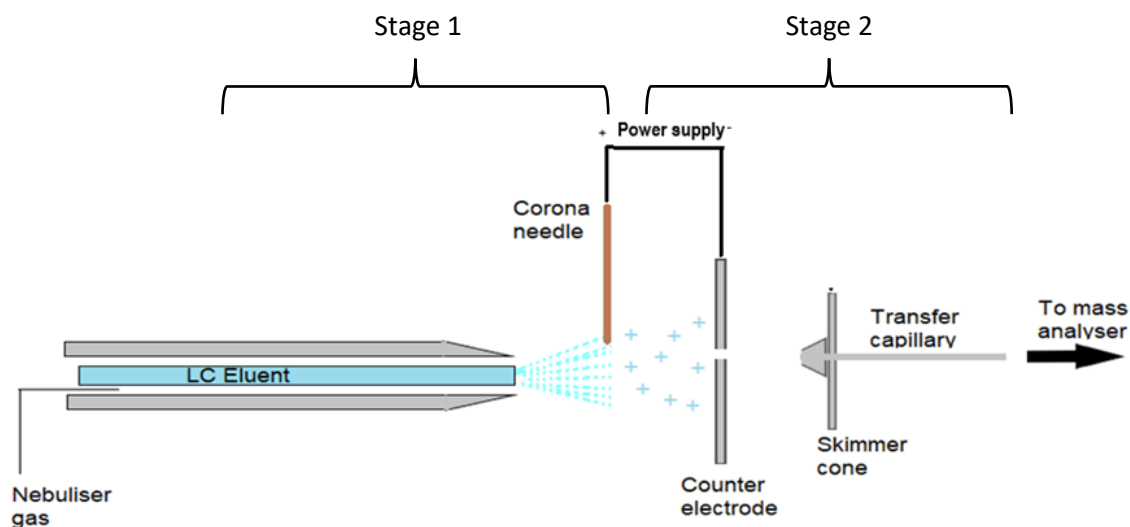


**Figure 1.17: Schematic of APCI source. Adapted from<sup>65</sup>**

#### 1.2.3.4.2. Mass spectrometer analysers

The mass analyser is used to filter ions based upon their mass to charge ratio ( $m/z$ ) prior to detection based upon the ion's behaviour within a specific electrical or magnetic field. Some mass analysers are also used to induce fragmentation via collision, usually with a gas. For the instruments used in this work fragmentation can be induced via collision induced dissociation (CID) or pulsed Q collision induced dissociation (PQD). In CID the precursor ion is accelerated toward collision gas, usually argon, nitrogen or helium, which has an electric potential applied. The repeated collision with the gas converts the kinetic energy into internal energy until a fragmentation threshold is reached which results in dissociation of the precursor ion and the formation of product ions.<sup>74-76</sup> Pulsed Q collision induced dissociation was developed and patented by Thermo Scientific and generated spectra allowing for the observations of low  $m/z$  fragments. In PQD the precursor ion is kinetically excited by short exposure, around 100  $\mu\text{s}$ , to a high amplitude resonance excitation pulse. The excited state precursor ion is held at a high state for around 100  $\mu\text{s}$  and exposed to collision gas which converts the kinetic energy into internal energy but the short duration limits dissociation. The RF amplitude is then rapidly dropped resulting in fragmentation (Figure 1.18).<sup>65, 77-79</sup> Tandem mass spectrometry fall into 2 categories MS/MS in time or MS/MS in space. For MS/MS in time ions are held in a region of the mass spectrometer where fragmentation and separation takes place over time an example of which

would be an ion trap mass spectrometer. For MS/MS in space, they utilise the coupling of more than one mass analyser, connected in series, with each analyser having a set function. The ions move through the analysers in space and are fragmented and separated, an example of which would be a triple quadrupole.<sup>80-82</sup> Types of mass analysers include quadrupole, time of flight, ion traps and orbitraps.

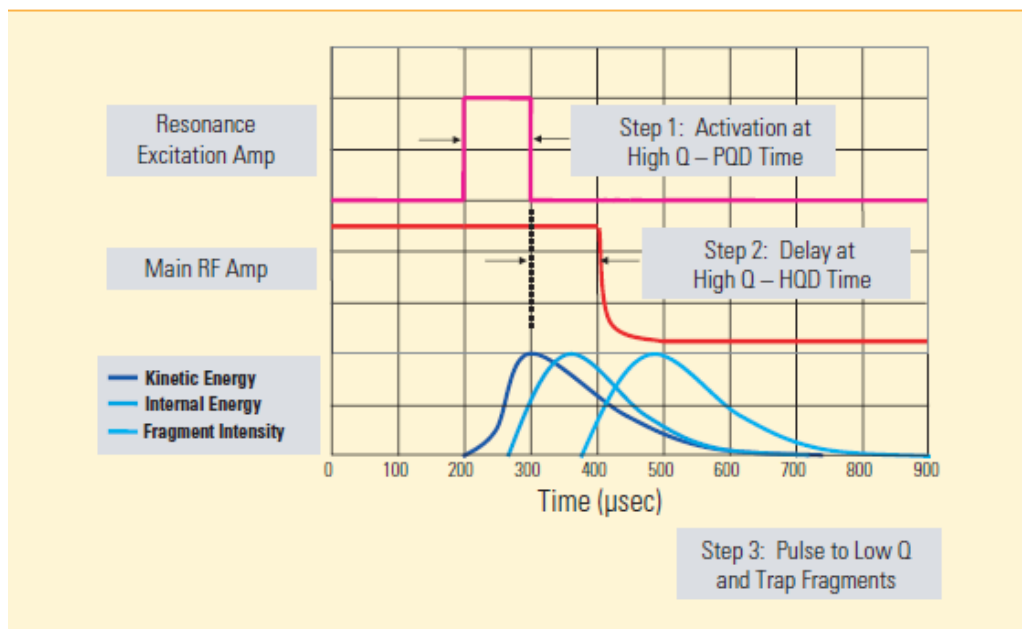


**Figure 1.18: Schematic of PQD process<sup>77</sup>**

#### 1.2.3.4.2.1. Single quadrupole

The quadrupole consists of four rods which are positioned symmetrically in a linear arrangement which have a RF and DC voltage applied. An RF potential is applied to each opposite sets of rods which results in a field which alternates between reinforcing and dominating the DC field. The alternating field causes ions to oscillate along the plane of the quadrupole based on their mass to charge ratio. If the oscillation of the ion is stable then the ion will continue moving through the rod assembly and reach the detector. However, if the oscillations are unstable the trajectory of the ion will be distorted resulting in either collision with one of the quadrupoles or dropping out of the quadrupole assemble. The RF and DC voltages can be rapidly adjusted to allow for scanning across multiple  $m/z$  or to scan across a range (Figure 1.19).<sup>65</sup> In order to obtain a stable trajectory for the ions the parameters for the movement of ions inside an electric field,  $a$  and  $q$ , must be known through Mathieu equations.<sup>83-86</sup>

$$1.1 \quad a_u = 8eU / m\omega^2 r_0^2$$

$$1.2 \quad q_u = 4eV / m\omega^2 r_0^2$$

Where U is the DC voltage, V is oscillating voltage, e is the ion charge, m is the mass of the ion,  $\omega$  is the radio frequency and  $r_0$  is the radius between electrodes.

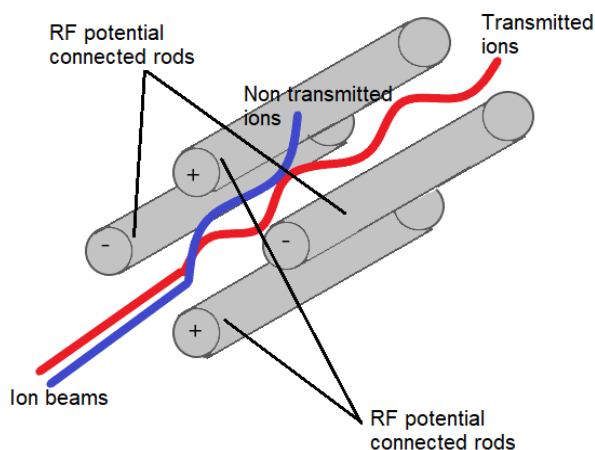


**Figure 1.19: Schematic of quadrupole mass analyser. Adapted from<sup>65</sup>**

In a quadrupole  $r_0$  and  $\omega$  are constant resulting in the mass being directly related to  $a_u$  and  $q_u$ . The stability areas obtained for  $a_u$  and  $q_u$  can be plotted to give a stability diagram as shown in Figure 1.19. For ions of difference masses the stability areas are calculated as a function of U and V as shown in Figure 1.20.<sup>83-86</sup>

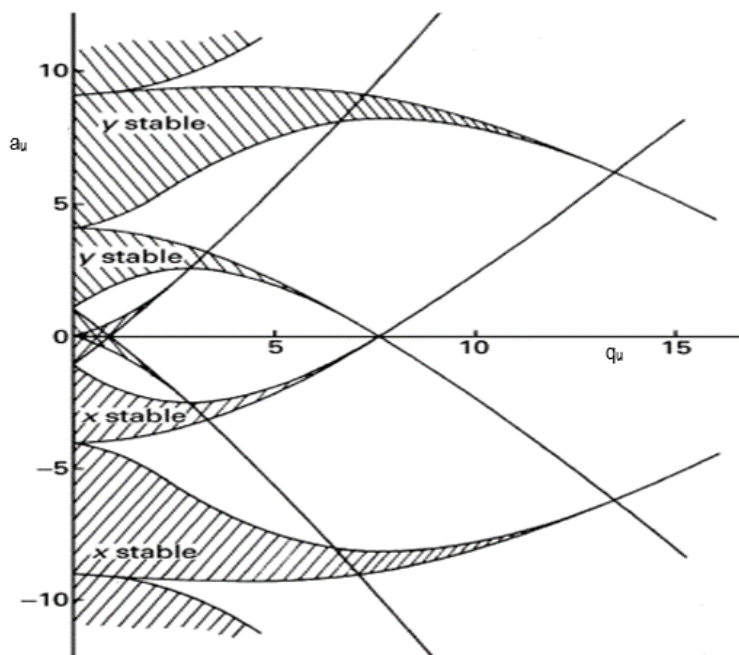


**Figure 1.19: Mathieu stability diagram for ion motion in an electrical field.<sup>85</sup>**

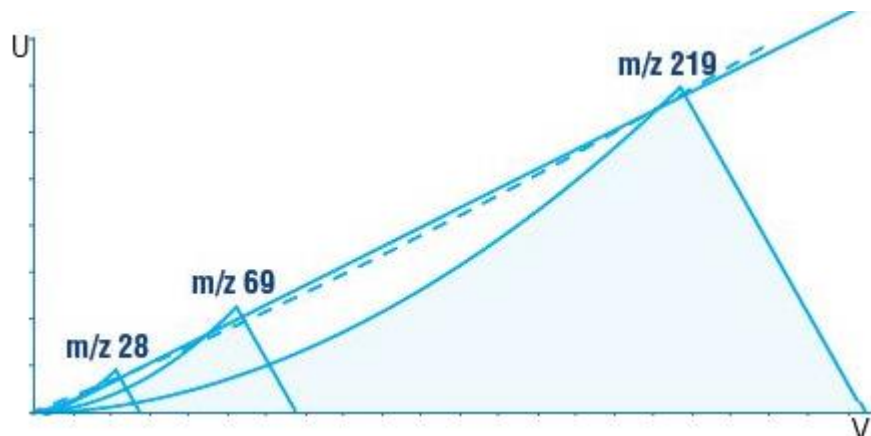


Figure 1.20: Ion stability as function of U and V.<sup>86</sup>

#### 1.2.3.4.2.2. Triple quadrupole

As suggested by the name a triple quadrupole consist of three quadrupoles, termed Q1, Q2 and Q3, to separate, filter and induce fragmentation of the ionised compounds. The compounds enter the mass analyser from the ionisation source and are filtered based on mass to charge ratio in Q1 using RF and DC voltage as described in section 2.1.3.5.1. The ions then enter Q2 where they are focused and fragmented due to a presence of a low-pressure collision gas such as helium which results in dissociation. The resulting fragment ions then pass through to and are then separated and filtered in Q3 via the same principles employed in Q1 as shown in Figure 1.21.<sup>65, 76</sup>

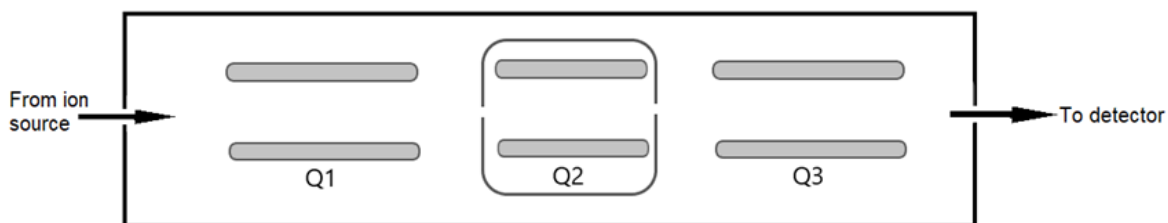
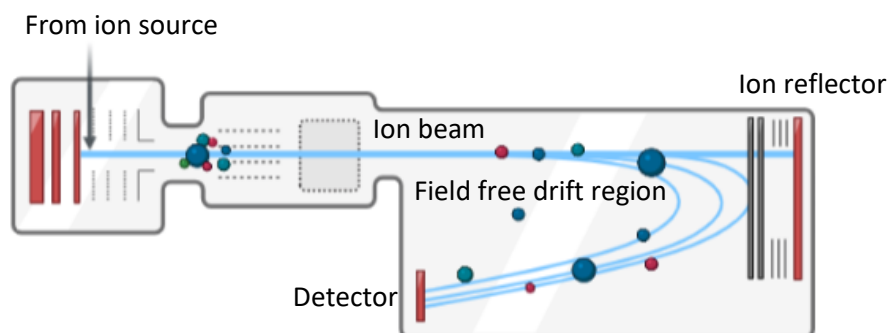


Figure 1.21: Schematic of triple quadrupole mass analyser. Adapted from chromacademy®

### 1.2.3.4.2.3. Time of flight

A time of flight (TOF) mass analyser filters charged ions based on the time taken to reach the detector. Ions are accelerated in a field free region by an electrical field of known strength. The velocity and therefore the time taken to reach the detector is dependent on the mass to charge ratio, with heavier ions having a lower velocity than lighter ions with the same charge and therefore taking longer to reach the detector. However multiple charged ions have an increased velocity. A reflectron can be used in TOF MS to correct for the initial kinetic energy distribution which reflects the ion beam towards the detector and is referred to as time-of-flight focusing (Figure 1.22).<sup>65, 87</sup>



**Figure 1.22: Schematic of time-of-flight mass analyser. Created with BioRender.com**

### 1.2.3.4.2.4. Ion Trap

Ion traps are three dimensional analogues of the quadrupole mass filter consisting of three electrodes, a ring electrode and two end cap electrodes, where ions are subjected to a RF field which produced forces across three dimensions. Ion trap mass analysers allow for higher sensitivity and resolution when compared to a quadrupole, can perform tandem mass spectrometry and can be used to study ion/molecule reactions with the ability to vary reaction time allowing for the study of kinetics and equilibrium. The ions travel through an octapole and one of the end cap electrodes to enter the trap which has an RF voltage applied which traps the ions by generating an electrical quadrupole field. The ion trap is also filled with helium dampening gas in order to remove kinetic energy of the ions. The

amplitude of the RF voltage is then increase causing movement of ions and instability of the ion field resulting in ions exiting the trap via the end cap electrode and entering the detector. As the RF voltage is raised ions of increasing mass-to-charge ratio ( $m/z$ ) are ejected and detected resulting in a mass spectrum. Due to the electrical field generated within the trap, ion trap can hold around  $10^5$ - $10^6$  ions before repulsions effect the resolution due to the effect on the ion trajectories. In order to obtain fragmentation, the octapole is used to accelerate the ions into the ion trap so that collision with the helium gas results in fragmentation (Figure 1.23).<sup>65, 88-91</sup> A limitation in ion trap mass spectrometers is that traditionally only the selected ion is fragmented and the ions formed do not undergo subsequent fragmentation. In order to overcome this WideBand Activation™ technology, developed by Thermo Scientific, can be used. In WideBand Activation the excitation energy is applied over a mass range to give fragmentation after the subsequent loss of water ion from the precursor ion. (Figure 1.24) In a traditional MS experiment the additional fragmentation would require the use of MS<sup>2</sup>, resulting in longer scan cycles and a reduced number of data points across the peak which would affect the precision of the data obtained.<sup>92</sup>

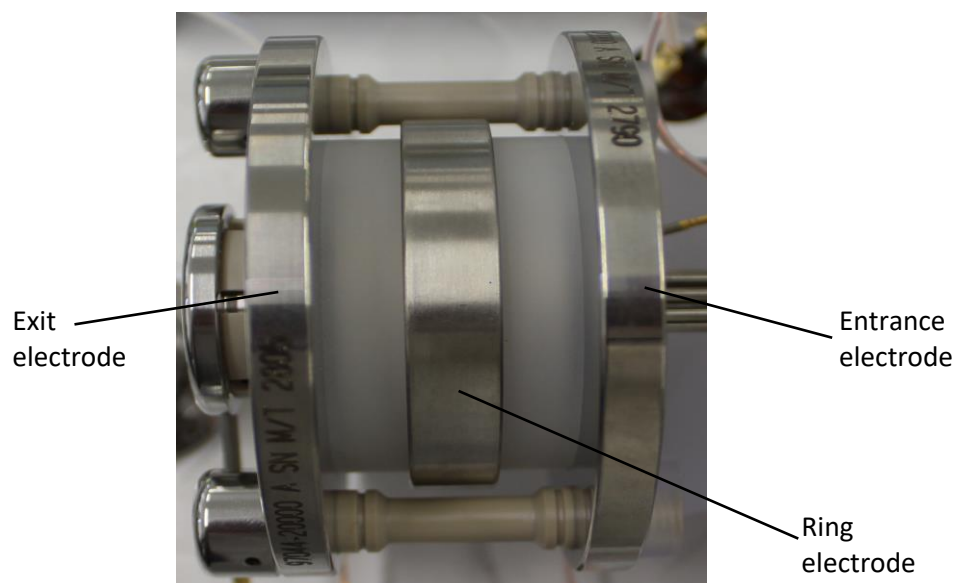


**Figure 1.23: Ion trap mass analyser**

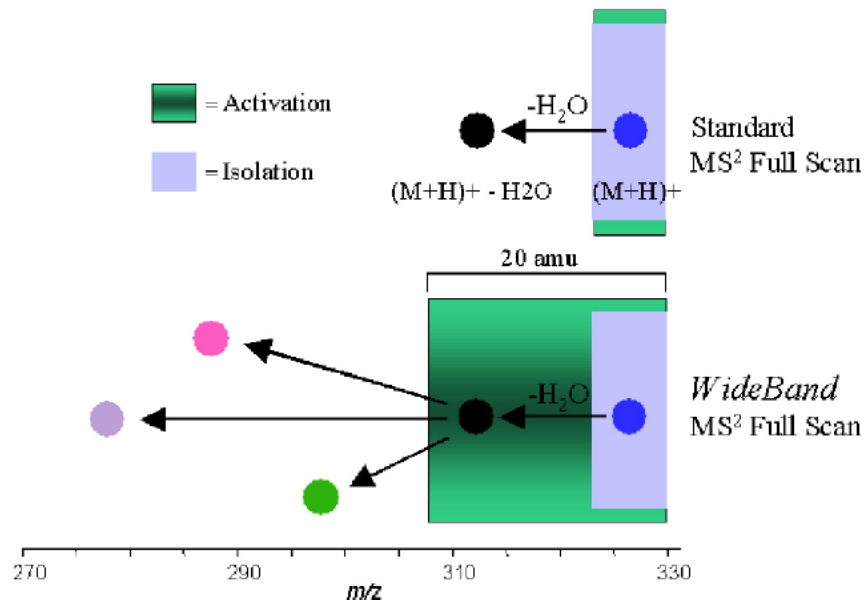


**Figure 1.24: WideBand Activation™.92**

#### 1.2.3.4.2.5. Orbitrap

Orbitrap mass spectrometers are hybrid and tribrid high resolution mass analysers which utilise one or more of the above analysers alongside an orbitrap analyser allowing for the simultaneous and independent acquisition of different scan types. For example, a LTQ orbitrap uses a linear ion trap, a Q Exactive uses a quadrupole and an ID-X uses both a linear ion trap and quadrupole (Figure 1.25).<sup>93-95</sup>

The orbitrap mass analyser is an adaptation of the Kingdom trap developed in the 1920's,<sup>96</sup> which consisted of a wire central electrode, an outer cylindrical electrode (electrically isolated) and two endcap electrode which utilised electrostatic fields.<sup>96</sup> In an orbitrap mass spectrometer, ions pass from the initial mass analyser via a transfer octapole to the C-trap, which is a curved RF quadrupole with a C shaped central axis. The C-trap is enclosed by two lenses with the lens between the octapole and C-trap being a gate electrode and the second lenses being a trap electrode. The C-trap is filled with nitrogen gas as a collision dampener causing ions to lose energy but with mild enough collisions to not cause fragmentation, resulting in the ions forming a thin thread along the curved axis. A voltage distribution forces the ions into the centre of the curvature where they pass through a slot in the pull-out electrode where they pass through curved ion optics and are accelerated to form an ion cloud which then passes through the entrance

aperture of the orbitrap where they are captured by a rapidly increasing electric field where they oscillate along the inner electrode (Figure 1.26).<sup>1, 65, 95, 97-101</sup>

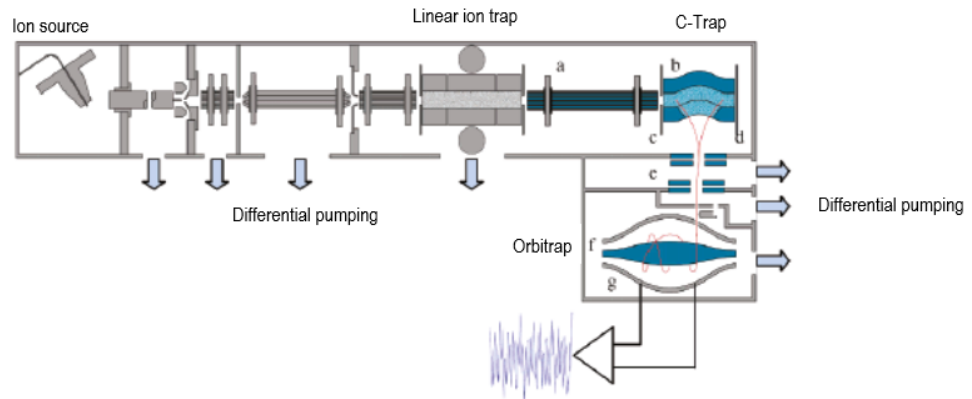
Fringing fields are compensated via a deflector electrode near the entrance slit of the orbitrap. Once the inner electrode has stabilized the signals are amplified using a differential amplifier and are converted into a frequency spectrum by Fourier transformation which is then converted into a mass spectrum via the chromatography data system (CDS) software. The axial frequency is used to determine mass to charge ratio as it is the only frequency completely independent of velocities and coordinates of the ions.<sup>1, 65, 95, 97-101</sup>

### **1.2.3.4.3. Mass spectrometry detectors**

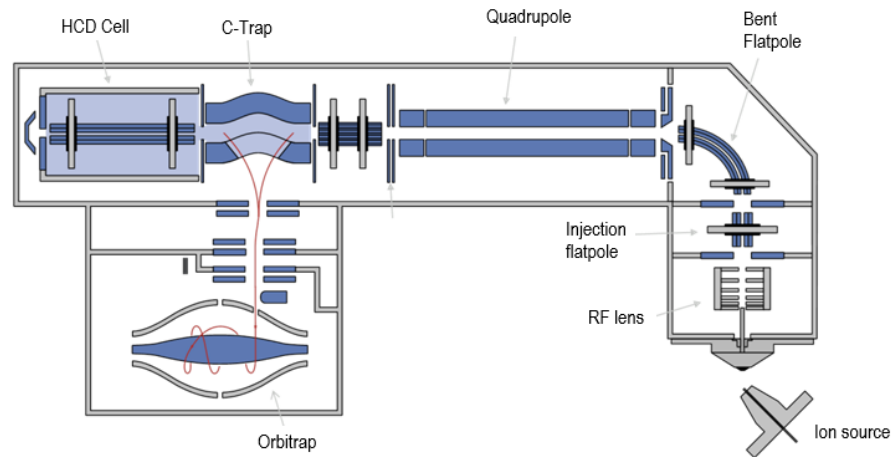
#### **1.2.3.4.3.1. Electron multiplier**

An electron multiplier is used to detect the ions exiting the mass analyser in a range of mass spectrometers including the linear ion trap used in this study. An electron multiplier operates on the principle of secondary electron emission whereby a charged particle strikes the surface of the electron multiplier and causes a secondary electron to be emitted from the surface atoms of the multiplier. The electron multiplier can be either discrete dynode or continuous dynode as shown in Figure 1.27. A discrete dynode electron multiplier typically has 12-24 dynodes present positioned in such a way that the electron bounce between each dynode. A continuous dynode electron multiplier uses a horn shaped glass funnel which is coated with a thin film of semi-conductive material and electrons are funnelled down the horn. The continuous dynode electron multiplier is utilised in the LTQ XL mass spectrometer.<sup>65</sup>

a)



b)



c)

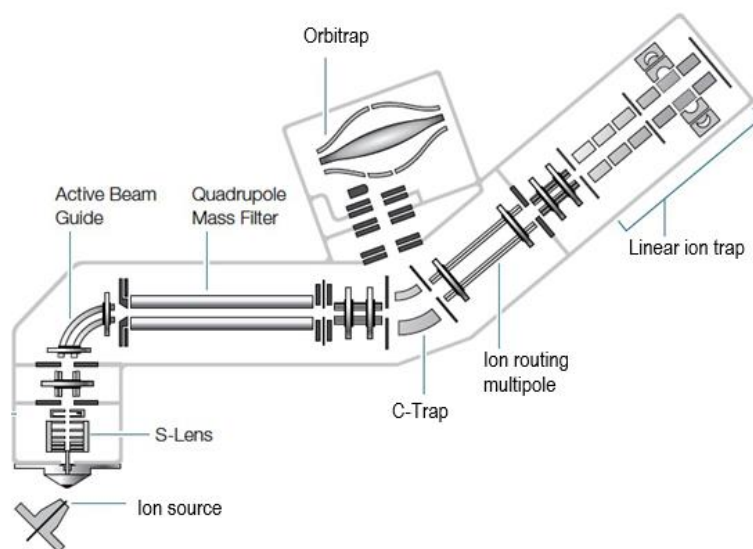


Figure 1.25: Schematic of a) LTQ orbitrap<sup>95</sup>, b) Q Exactive orbitrap<sup>93</sup> and c) ID-X orbitrap mass analysers<sup>94</sup>

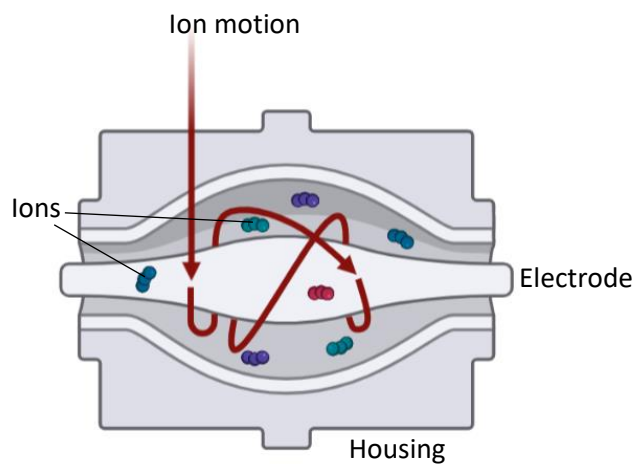


Figure 1.26: Orbitrap mass analyser. Created with BioRender.com

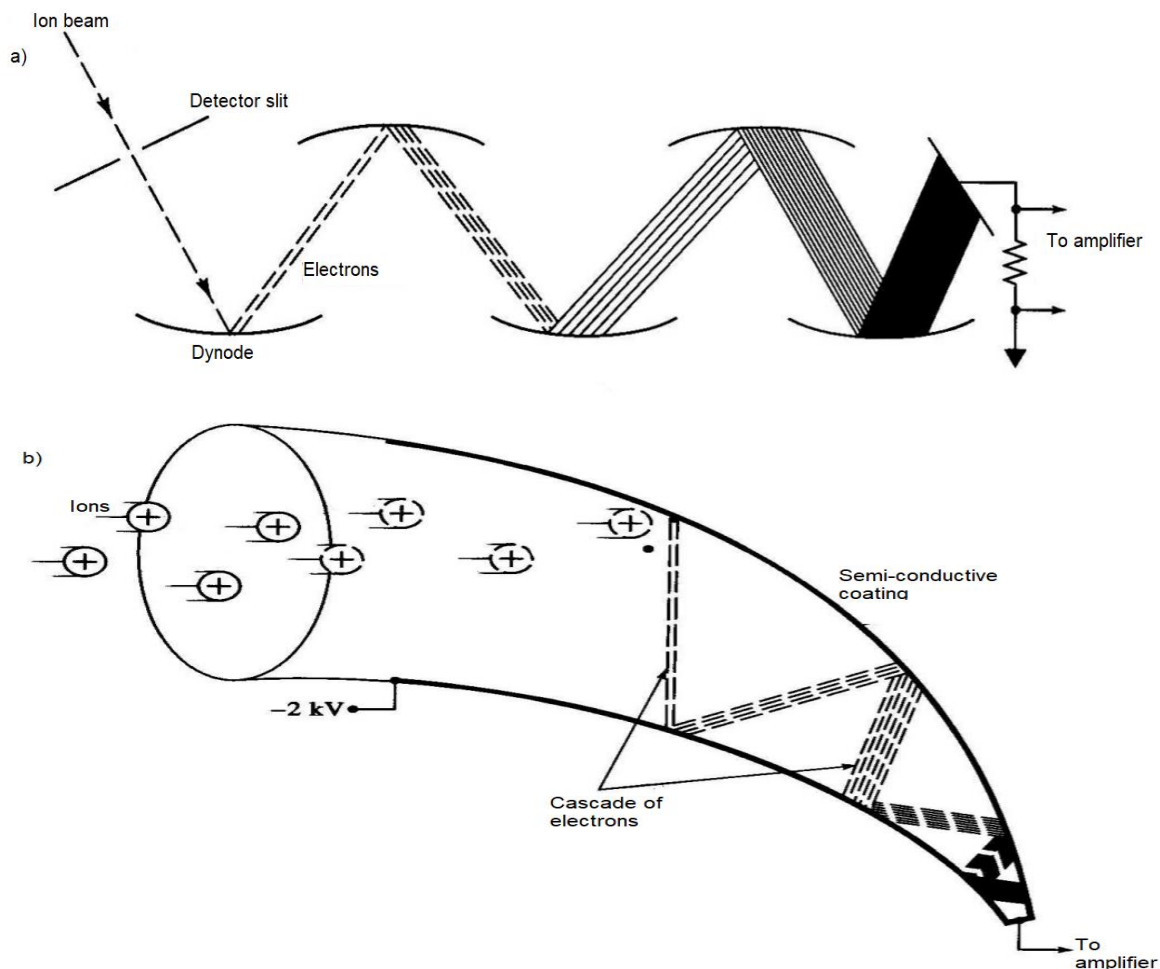


Figure 1.27: Schematic of a) discrete dynode and b) continuous dynode electron multiplier<sup>102</sup>

### 1.3. Method development and validation

One of the aims of this research is to establish analytical methods for the simultaneous detection and quantification of four thyroid hormones and plant toxins. It is therefore necessary to develop and validate a method for the detection and quantification of these analytes. The development of an analytical method for LC-MS involves covering all aspects of the analysis from sample preparation to instrument parameter in order to obtain a method which is robust and capable of producing reliable results. In order to assess the reliability of the results obtained from the method are validated to ensure it will perform in the manner it was intended for and this performance is consistent.<sup>8, 103, 104</sup>

The International Council for Harmonisation (ICH) guidelines propose the validation testing required for methods of analysis for drugs to be administered to humans. The typical validation parameters included in the guidelines are accuracy, precision, specificity, limit of detection (LOD), limit of quantification (LOQ), linearity, range and robustness. These guidelines are used within the pharmaceutical industry today. The ICH guidelines have also been adapted for use in bioanalytical method validation by the European Medicines Agency (EMA).<sup>103</sup> A brief description of each parameter is defined below:<sup>103, 105</sup>

- **Accuracy:** This is a measurement of the closeness of agreement between a reference value and the result obtained
- **Precision:** this is a measurement of the degree of scatter between a series of measurement from the same homogeneous sample under specific condition. Precision can be broken up into repeatability, intermediate precision and reproducibility. Where:
  - **Repeatability:** Precision over a short period of time
  - **Intermediate precision:** Expresses within lab variations such as different days or equipment
  - **Reproducibility:** Precision between laboratories
- **Specificity:** the ability to unequivocally detect the analyte of interest in the presence of other component such as matrix or impurities

- **Lower limit of detection (LLOD):** The lowest analyte concentration at which the analyte can be detected but not necessarily quantified to an exact value
- **Lower limit of quantification (LLOQ):** The lowest analyte concentration at which the analyte can be quantified accurately and precisely
- **Linearity:** The analyte concentration range which produced a signal response which is directly proportional to the concentration
- **Linear dynamic range (LDR):** The range between the upper and lower concentration of analyte which is able to demonstrate accuracy, precision and linearity. This can be inferred from the results obtained from the parameters above
- **Robustness:** The ability for the method to remain unaffected by small but deliberate variations in the method parameters.
- **Carry-Over:** The presence of the compounds of interest in blank injections following the injection of a high standard.
- **Matrix effects:** The effect of matrix components on the performance of the analytical method.
- **Stability:** The effect of storage conditions on the concentration of analytes present.

The agreement of these parameters within the limits of the guidelines infer that the method is reliable, accurate, precise and robust allowing for the application to the analysis of sample across the applications investigated.

## Chapter 2: Complex matrices

## **2. Complex matrices**

When developing an analytical method, it is necessary to consider the sample matrix when dealing with anything other than a pure compound. The sample matrix can be defined as any other components within a sample in addition to the compound or compounds of interest. The matrix composition will vary depending upon the types of samples being analysed and the matrix effects will vary depending upon the technique being used. Therefore, each potential sample type for which the method will be applied must be considered when developing the analytical method. For this study the matrices used were tablet formulations, gastrointestinal fluid and human serum for thyroid hormones and plant materials for plant toxins. Tablet formulations contain a number of excipients in addition to the active pharmaceutical ingredients which are present for functions such as bulking, binding, to aid dispersion, protective coating and to aid in the manufacturing process. Common excipients found in tablets include sugars such as sucralose, starch such as dextrin, calcium and magnesium salts and cellulose derivatives. Gastrointestinal fluid contains a number of components to add in the pH control, break down and absorption of ingested items including proteins such as albumin and mucin, enzymes such as amylase and lipase, sugar and sugar derivative such as glucose and glucuronic acid and salts such as sodium chloride, sodium sulphate and potassium chloride.<sup>106</sup> Serum is a straw coloured liquid which is formed when whole blood clots resulting in a liquid containing blood components minus any clotting agent including items such as proteins such as transferrin, red blood cell by-products such as bilirubin, lipids such as triglyceride and immunoglobulins such as IgG in addition to various hormones, antibodies and antigens.<sup>107</sup> The various parts of the plants, flower, stem, foliage and roots contain a variety of levels of components including polysaccharide such as cellulose and pectin, chlorophylls, glycoproteins such as extension and non-structural proteins such as glycosidase.<sup>108, 109</sup>

### **2.1. Thyroid hormones**

#### **2.1.1. Thyrotropin releasing hormone, Thyroid Stimulating Hormone and Thyroglobulin**

Thyrotropin releasing hormone (TRH) is a hypothalamic neurohormone which was initially termed a releasing factor as its hormonal action was unidentified and was

the first hypothalamic releasing factor identified. The structure of TRH, shown in Figure 2.1, was finally elucidated in 1969.

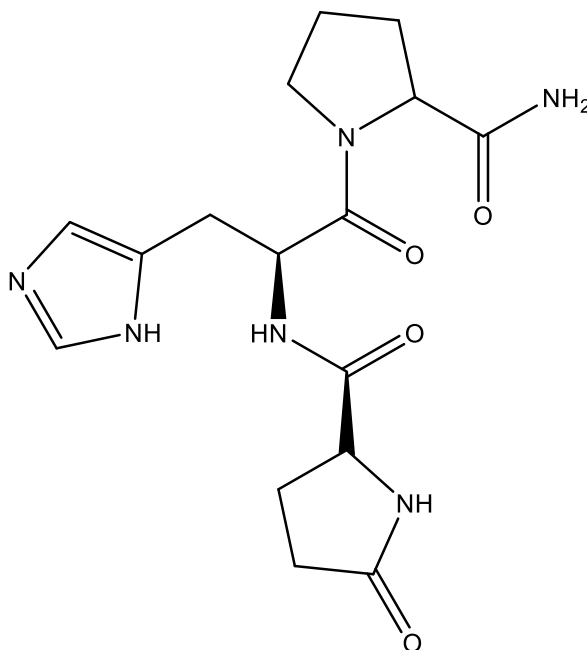


**Figure 2.1: Structure of TRH**

TRH is used by the body in the regulation of metabolism, energy levels and arousal and is primarily produced in the nuclei of the hypothalamus and is part of the endocrine system. The endocrine system involves the hypothalamus, pituitary glands, endocrine gland and target tissue and is regulated via feedback loops (Figure 2.2). The hypothalamus and pituitary gland are located in the base of the brain as shown in Figure 2.3 and are part of the limbic system. The main role of TRH is the regulation of the secretion of thyroid stimulating hormone which regulates the hormone secretion of the thyroid glands. Central nervous system expression of TRH starts around 2-3 months following birth with levels of TRH production decreasing at older age with the expression of TRH found in various locations throughout the body including the thyroid, brain, heart, hair follicles, testes and ovaries.

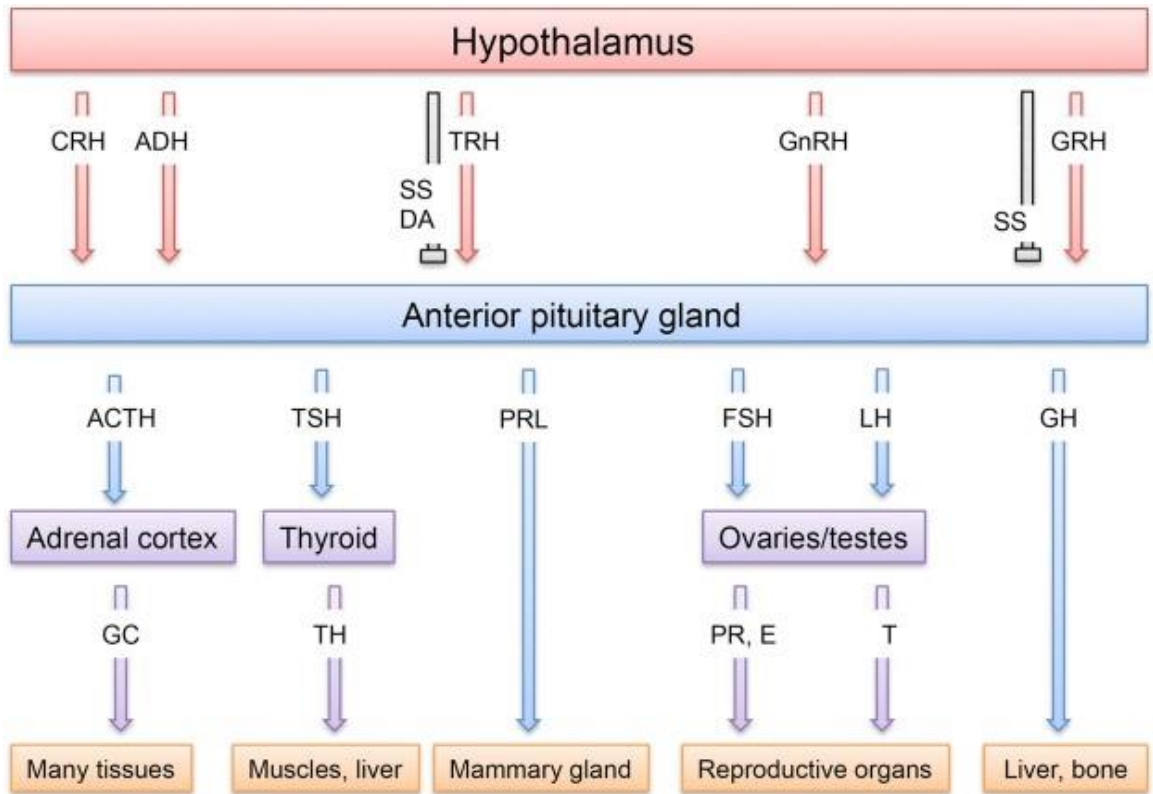


**Figure 2.2: Hierarchic regulation of endocrine system.<sup>110</sup>**

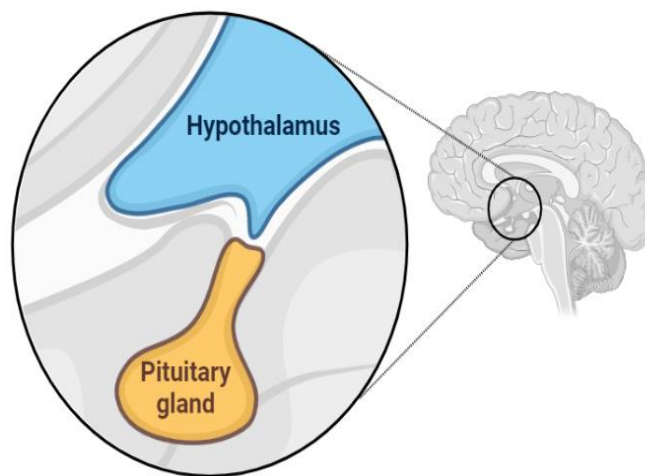


**Figure 2.3: Hypothalamus and pituitary gland location within the brain.**

**Created with BioRender.com**

In humans, TRH is produced via a prepro-hormone, located on chromosome 3, which encodes six copies of TRH. Gene translation produces the prepro-TRH precursor at the rough endoplasmic reticulum which is then transported to the endoplasmic reticulum and partially folded to form pro-TRH. The pro-TRH is then cleaved by prohormone convertases PC1/3 and carboxypeptidase E which is then

converted into the active hormone pyroGly-His-Pro-NH<sub>2</sub> via a two-step enzymatic process. TRH receptor (TRHR) ligation mediates the cellular action of TRH, humans have only one TRHR termed TRHR1, which consist of seven transmembrane domain G protein-coupled receptors (GPCR) which are activated by phosphorylation following the binding of TRH. Activation results in increase calcium levels and protein kinase C activated by the hydrolyses of phosphatidylinositol 4,5-biphosphate to 1,2-diacylglycerol and inositol 1,4,5-triphosphate. The production of TRH and TRHR is controlled via a negative feedback loop which decreases thyroid levels, stimulating the synthesis and expression.<sup>110-112</sup>

Thyroid stimulating hormone (TSH) is a glycoprotein anterior pituitary hormone responsible for the regulation of thyroid hormone production. TSH consist of two subunits, alpha and beta, which are tightly coupled but not covalently linked. Synthesis takes place on the ribosomes with the alpha unit being synthesised by chromosome 6 and the beta unit by chromosome 1. TSH is produced via co-translational glycosylation and the folding of the two subunits and are stored in pituitary basophils prior to release in response to TRH. Amongst the group of glycoprotein hormones produced in the anterior pituitary gland it is the beta unit which gives the hormones its physiological specificity, although the alpha and beta units both contribute to receptor binding. TSH is secreted in a basal and pulsed secretion from the pituitary gland in a circadian pattern with the basal secretion around for approximately a third of the circulating amount of TSH. Pulse secretion of TSH occurs roughly every 2-3 hours however, there is considerable variability. The secretion of TSH is inhibited by circulating thyroid hormone levels. Acute stimulation of the follicular cell by TSH causes the reuptake of thyroglobulin by a process called endocytosis. TSH binds to the thyroid follicular cell via a heptahelical G protein coupled receptor on the basolateral surface membrane, resulting in the activation of the adenylyl cyclase and phospholipase. This in turn leads to an increase in the cyclic adenosine monophosphate (cAMP) and diacylglycerol/IP3 messenger pathways. In addition to regulating biosynthesis and secretion, TSH also increases the blood flow to the thyroid gland, with prolonged stimulation also able to stimulate division of the follicular cell.<sup>112-115</sup>

Thyroglobulin (TG) is a large glycoprotein, around 660,000 Daltons, (Figure 2.4) which is synthesised by the thyroid follicular cell and is a matrix component for the

synthesis of thyroxine and triiodothyronine; it is also the form in which thyroid hormones are stored within the thyroid gland. Thyroglobulin is synthesised on the ribosomes, glycosylated and translocated to the Golgi apparatus where it is packaged in secretory vesicles and discharged from the surface of the lumen. After which iodination to form mature thyroglobulin takes place.<sup>112, 116</sup>

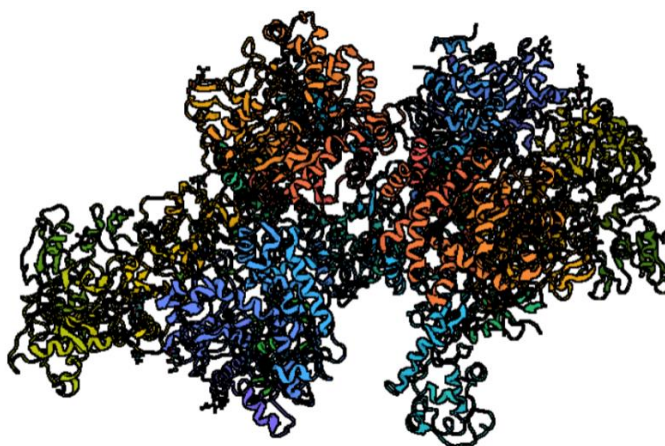


**Figure 2.4: Structure of Thyroglobulin. Protein data bank 6SCJ. Created with BioRender.com**

### 2.1.2. Thyroid hormones

Thyroid hormones are  $\alpha$ -amino acid derivatives consisting of two ether linked benzene rings with a hydroxyl group on the phenolic ring and an alanine chain on the inner ring. Both are found in the para position and are rich in iodine,<sup>112, 117, 118</sup> Chemical structures of the two main thyroid hormones are shown in Figure 2.5. Thyroxine, or tetraiodothyronine, (T<sub>4</sub>) was the first thyroid hormone to be isolated and characterised in 1914 by Kendall.<sup>119</sup>

Thyroxine is better characterised as a pre-hormone which is converted into the physiologically active form triiodothyronine (T<sub>3</sub>); This was not discovered until 1953 when it was identified by Gross and Pitt-Rivers.<sup>120</sup> Thyroid hormones are synthesised and stored within the thyroid gland, which is located in the bottom section of the front of the neck. As shown in Figure 2.6, the thyroid gland consists of two lobes which are connected around the trachea by an isthmus and in a normal human weighs around 20 g but is capable of reaching weights of several hundred grams when intensely stimulated for long periods of time. T<sub>4</sub> accounts for 85 % of the thyroid hormone content found within the thyroid gland and is also

more abundant in circulating levels with normal levels of T4 being 60-160 nmol/L and normal levels of T3 being 1.2-1.6 nmol/L.<sup>15, 120</sup>

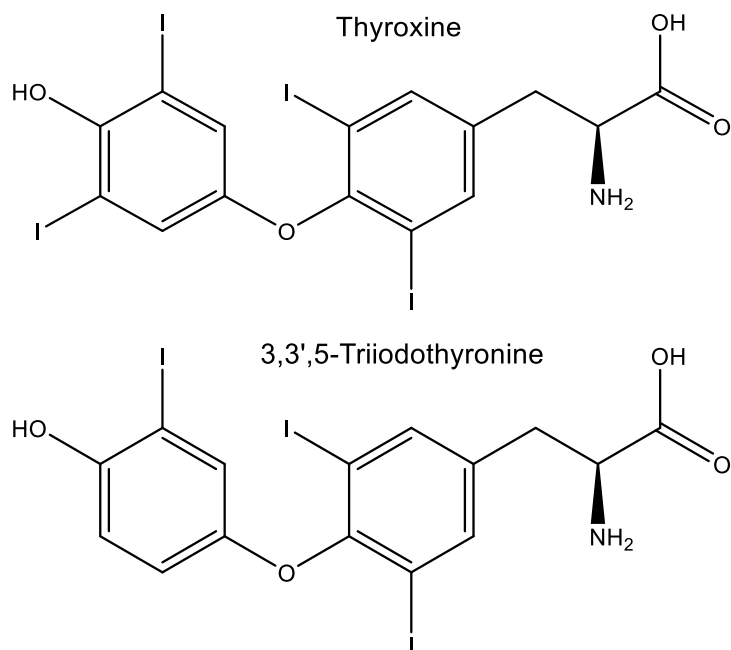


**Figure 2.5: Structures of thyroxine and 3,3',5-triiodothyronine**

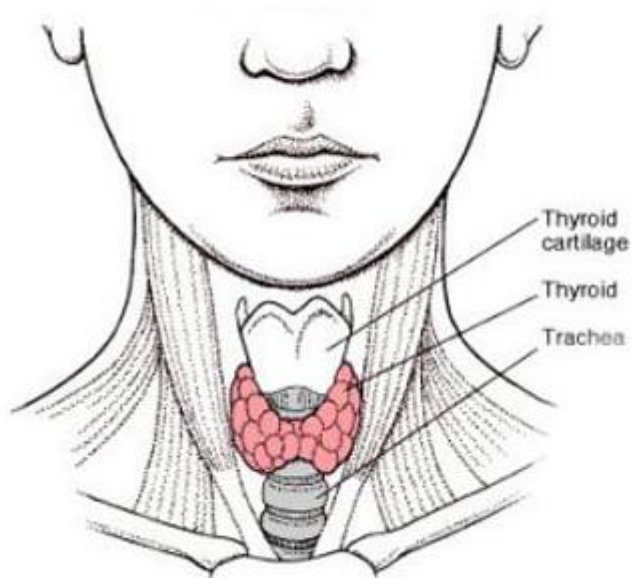


**Figure 2.6: Location and shape of thyroid gland<sup>121</sup>**

The biosynthesis of thyroid hormones involves a number of processes which occurs partially at the follicular lumen and required high concentration of iodide and are dependent upon three gene products: sodium iodide symporter (NIS),

thyroglobulin and thyroid peroxidase. The concentration of iodide within the thyroid follicular cells is 25-50 times more than in blood plasma, under normal circumstances, and can rise to as much as 250 times more concentrated during periods of active stimulation, which is obtained via the sodium iodide symporter. The sodium iodide symporter is an electrogenic pump located on the basolateral membrane of the follicle cell. The pump transfers one ion of iodide and two ions of sodium into the cell, against a steep concentration gradient. The transporting of iodine against the gradient is powered by the favourable electrochemical gradient of sodium. The sodium is then removed from the cell by the sodium potassium ATPase, adenosine triphosphate enzyme, to maintain the electrochemical membrane potential. The iodide diffuses into the lumen passively via the pendrin iodide transporter. The iodide is oxidized by the thyroid peroxidase in the presence of hydrogen peroxide and enters the follicular lumen via the sodium independent iodide transporter pendrin, allowing it to react with the thyroglobulin present in the follicular lumen to produce monoiodothyrosyl (MIT) and diiodothyrosyl (DIT). The final stage is the coupling of either two DIT molecules to form T4 or the coupling of one DIT and one MIT to form T3 which is also catalysed by the thyroid peroxidase (Figure 2.7).<sup>112, 116, 117</sup>

Although the exact mechanism is not known, it has been suggested that an ether linkage is formed by the production of free radicals by the action of the thyroid peroxidase. The suggested mechanism is shown in Figure 2.8. The thyroid hormones remain coupled to the thyroglobulin and are stored in the follicular lumen until required and in a normal individual around 2-3 months supply of hormones are stored in the thyroid gland.<sup>122-126</sup> In order for the hormones to be released the thyroglobulin must be brought back into the follicular cell by endocytosis. Upon stimulation of the follicular cell by thyroid stimulating hormones the thyroglobulin is surrounded by long strands of protoplasm forming an endocystic vessel. As the endosomes migrate towards the basal portion of the cell, they are fused with lysosomes which are simultaneously migrating towards the apical region.

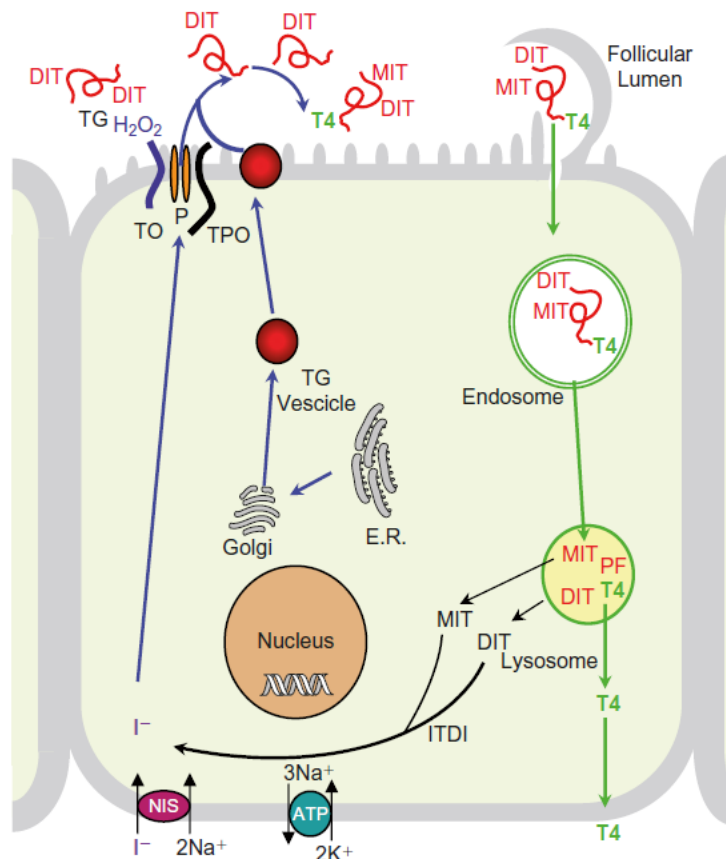


**Figure 2.7: Biosynthesis of thyroid hormones.**<sup>112</sup>

**P - Pendrin, TG – thyroglobulin, TO – thyroid oxidase, TPO – thyroid peroxidase, MIT – monoiodothyrosyl, DIT – diiodothyrosyl, ITDI – iodothyrosine deiodinase.**

Within the lysosome the thyroid hormones and remaining MIT and DIT are cleaved from the thyroglobulin which is then further broken down into peptide fragments via a number of hydrolytic reactions. Free T4 and free T3 are then released from the follicular cell via membrane transporters. The remaining MIT and DIT are deiodinated by iodothyrosine deiodinase in the presence of nicotinamide adenine dinucleotide phosphate (NADPH) (Figure 2.7).<sup>112, 126</sup>

The synthesis of thyroid hormones is autoregulated by thyroglobulin in the follicular lumen, which acts via a receptor on the apical surface of the follicular cells to decrease thyroid specific transcription factor expression. This results in the down regulation of the transcription of genes for thyroglobulin, thyroid peroxidase and TSH receptors. Thyroid hormone synthesis is also temporarily blocked by high plasma concentrations of iodide which has been exploited clinically to suppress thyroid hormone secretion in the short term.

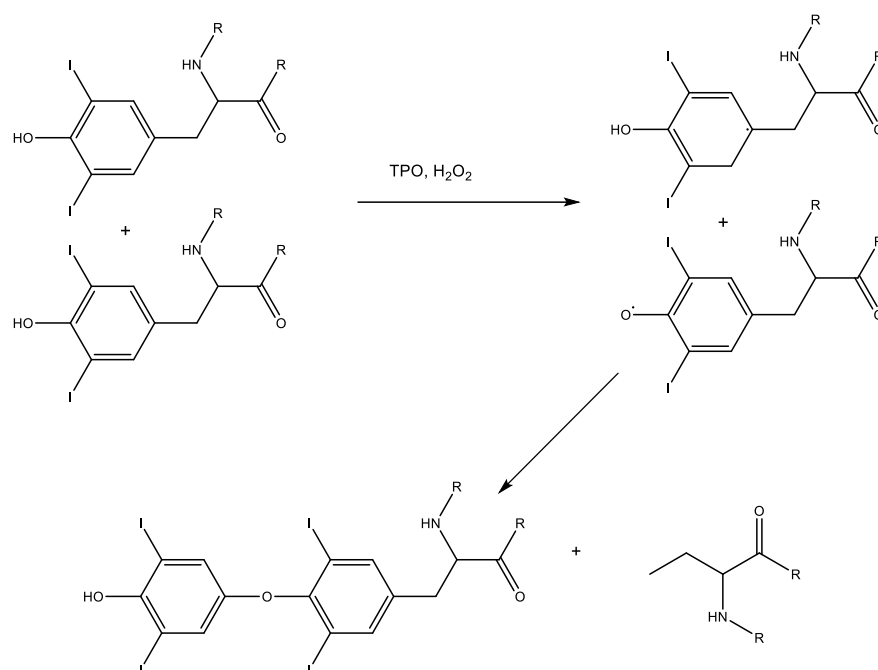


**Figure 2.8: Suggested mechanism for the coupling of thyroid hormones. R represents thyroglobulin protein linkage.<sup>112</sup>**

The blockage is short lived as the follicular cells downregulates the sodium iodide symporter to restore iodide concentrations. Thyroid hormone blood levels are maintained via a negative feedback loop whereby high levels of T<sub>4</sub> and T<sub>3</sub> inhibit the synthesis and secretion of TSH and TRH. T<sub>3</sub> binds to the receptors in the nucleus of the cell and downregulates the transcription of the genes responsible for the  $\alpha$  and  $\beta$  subunits of TSH as well as the genes for TRH receptors and inhibits hormone release. In addition to this T<sub>3</sub> accelerates the degradation of TRH receptors. The combined effects of T<sub>3</sub> result in the reduced sensitivity to TRH.<sup>112, 115, 127</sup>

Thyroid hormones are metabolized by the sequential removal of iodine by three enzymes called iodothyronine deiodinases: Type I, type II and type III. Type I deiodinase is found in the pituitary and thyroid glands, the central nervous system, the liver and the kidneys, and is capable of removing iodine from either the inner or outer ring. Type II deiodinase is found in the endoplasmic reticulum of extrahepatic tissues but is not present in the liver and is capable of removing iodine from the outer ring. Type II deiodinase is believed to be responsible for the local requirements for T<sub>3</sub> due to its rapid deactivation and activation. Type III deiodinase is found widely

amongst tissues in the body and is capable of removing iodine from the inner ring and is therefore solely present for the degradation of thyroid hormones. The combined actions of all three deiodinases results in the removal of all iodine from the thyroxine structure which is then up taken by the thyroid gland and recycled for thyroid hormone synthesis. The removal of iodine from the outer ring produces T3 which is the active form of the thyroid hormones, removal of the iodine from the inner ring produces reverse T3 (rT3) which is incapable of binding to thyroid hormone receptors. Figure 2.9 shows the breakdown of thyroxine to tyrosine via the three deiodinases.<sup>13, 112, 128, 129</sup>

### **2.1.3. Physiological effects**

Thyroid hormones are responsible for a number of physiological effects, most notably, the regulation of metabolism including oxidative, carbohydrate, lipid and nitrogen metabolism. Oxidative metabolism and basal metabolic rate (BMR) are highly sensitive to thyroid status with a thyroid hormone deficiency resulting in a decreased BMR and excess thyroid hormones causing an increased BMR across all tissues with the exception of the brain, testes and spleen. Thyroid hormones increase oxidative metabolism by increasing the rate of adenosine triphosphate (ATP) breakdown and decreasing the efficiency of ATP synthesis. The maintenance of cellular ionic gradients, an ATP consuming process, is accelerated by T3. The maintenance of the ionic integrity of cells, which is performed by the sodium/potassium ATPase, is estimated to account for around 20% of the BMR and even higher by the calcium ATPase, which is responsible for pumping calcium to the sarcoplasmic reticulum from the cytosol. Triiodothyronine is responsible for the upregulation of uncoupling proteins UCP-1, UCP-2 and UCP-3 which decreases the efficiency of ATP formation. The formation of ATP by the phosphorylation of ADP is driven by the proton gradient which is generated by the electron transport system in the inner mitochondrial membrane. The UCPs increase the leakage of protons in the inner mitochondrial membrane which partially dissipates the gradient, resulting in fewer high energy phosphate bonds being formed, and the energy being dissipated as heat.

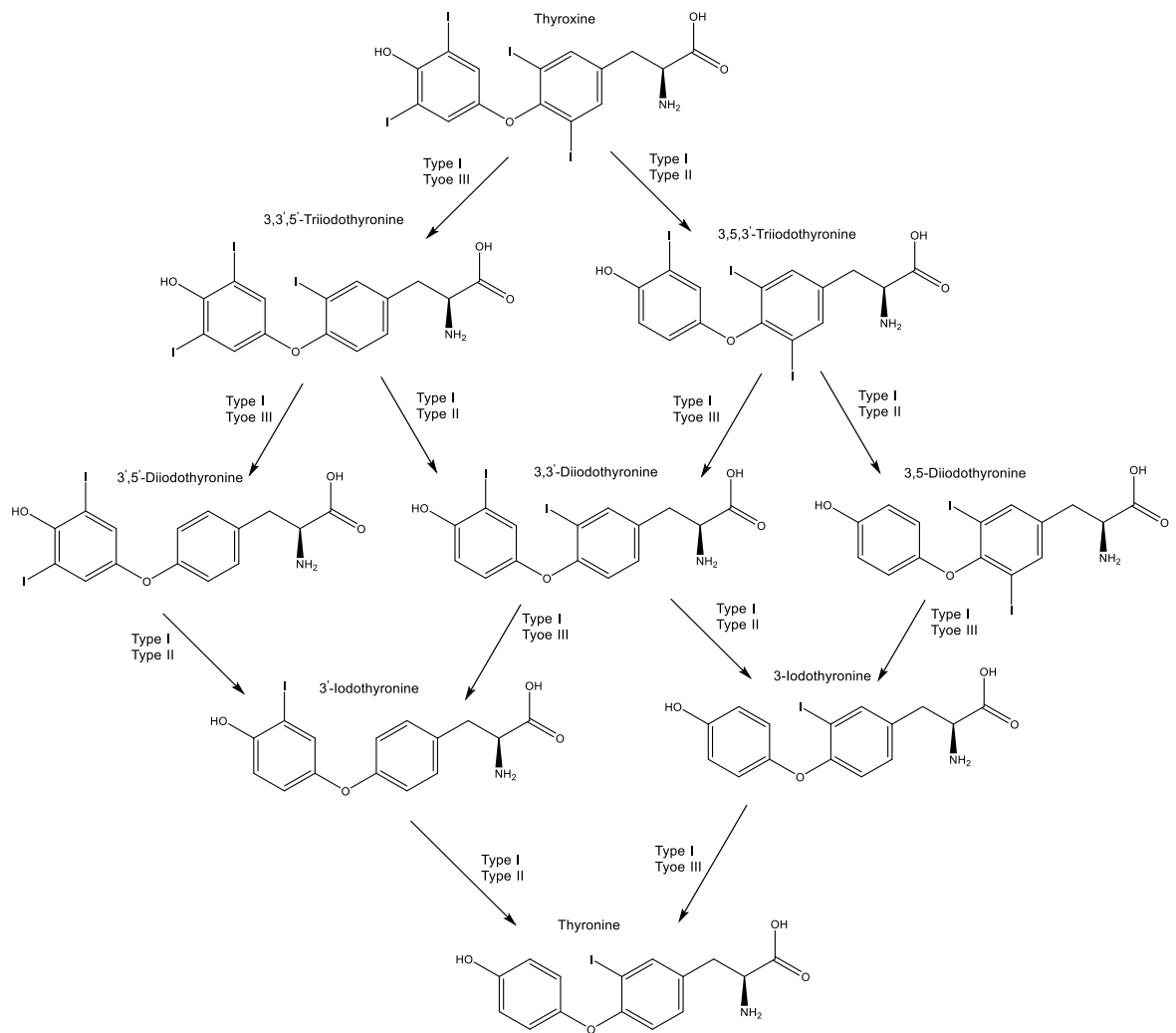


**Figure 2.9: Metabolism of thyroid hormones. Adapted from<sup>112</sup>**

The ATP-consuming cycles of carbohydrate, lipid and protein metabolism are also accelerated by thyroid hormones and therefore contribute to the increase in BMR. In carbohydrate metabolism T3 also increase the absorption of glucose from the digestive tract as well as increasing glycogenolysis, gluconeogenesis and glucose oxidation in hepatocytes, liver, fat and muscle cells. It is also believed that T3 induces the synthesis of malic enzyme, glucose 6-phosphate dehydrogenase and 6-phosphogluconate dehydrogenase. However, the main principle of T3 in carbohydrate metabolism is to behave as an amplifier to other signalling pathways. Similar to carbohydrate metabolism; T3 amplifies the signalling pathways in lipid metabolism.<sup>112, 116-118</sup>

Thyroid hormones also play an important role in the regulation of growth and maturation of the skeletal and central nervous system, although foetal bone

formation is independent of thyroid. Cartilage cells contain receptors for thyroid hormones and type 2 deiodinase with the development from undifferentiated precursors to hypertrophic stages being influenced by T3. Thyroid hormone is also required for the synthesis and secretion of growth hormone and they also act synergistically with growth hormones to promote bone formation. Thyroid hormones play a key role in the ossification and fusion of growth plates in skeletal maturation. In central nervous system development, thyroid hormones are present in the foetal brain prior to the thyroid gland becoming functional and are required during the perinatal period to allow for the proper cerebral and cerebella growth as well as the myelination of nerves. An absence or deficiency of thyroid hormones during this period can led to irreversible intellectual disability. In adulthood, thyroid hormones in the central nervous system produce physiological effects including hyper excitability, restlessness and exaggerated responses to environmental stimuli in hyperthyroidism and impaired memory, lack of energy and decreased sensory capacity in hypothyroidism.<sup>112, 116-118, 130</sup>

Thyroid hormones also show physiological effects on the autonomic nervous system and the cardiovascular system. In the autonomic nervous system, thyroid hormones exaggerate the responses which are mediated by norephedrine and ephedrine with many of the symptoms of hyperthyroidism resembling increased activity of the sympathetic nervous system. Thyroid hormones increase the abundance of  $\beta$ -adrenergic receptors in the myocardium and other tissues, they also increase the expression of stimulatory G-protein and down regulate the inhibitory G-protein, which results in greater production of cAMP. This in turn accelerated local conversion of T3 from T4 by activating the type II deiodinase. In addition to these sympathetic nervous system effects, T3 also accelerates the contraction and relaxation phases of the cardiac cycles due to the increased rate of calcium release from the sarcoplasm reticulum. In hyperthyroidism the peripheral resistance in the myocardium is lowered by a relaxation of the arteriolar smooth muscle and increased venous tone.<sup>112, 117, 118, 126</sup>

#### **2.1.4. Thyroid disorders**

An individual with a normal thyroid function is termed being in an euthyroid state with triiodothyronine levels between 3.1 – 6.8 pmol/L and thyroxine levels between

12-22 pmol/L. Thyroid disorders are diagnosed when patient levels fall outside of these ranges. (Table 2.1) <sup>17, 18</sup> Thyroid disorders fall into two general categories, hyperthyroidism and hypothyroidism, both of which can be caused by a number of factors, including iodine deficiency, inflammation caused by a viral or bacterial infection, thyroid cancer, thyroid nodules, certain treatments including radiation therapy and autoimmune diseases. Thyroid problems can also develop or worsen during pregnancy and if left untreated can lead to problems including miscarriage, premature birth and pre-eclampsia. <sup>131, 132</sup>

**Table 2.1: Thyroid hormone levels indicative of thyroid function.** <sup>133-136</sup>

	<b>Thyroid stimulating hormone concentration (mIU/L)#</b>	<b>Triiodothyronine concentration (pmol/L)</b>	<b>Thyroxine concentration (pmol/L)</b>
Hyperthyroidism	<0.5	>6.8	>22*
Euthyroid	0.5 – 5.0	3.1 – 6.8	12 - 22
Hypothyroidism	>5.0	Not routinely measured	<12

# indicative only T3 and T4 measurement required for diagnosis \* not always present. mIU/L: milli international units per litre.

Hyperthyroidism, or an overactive thyroid gland, is most commonly caused by the autoimmune condition Graves' disease and accounts for around 75 % of all cases of hyperthyroidism in the UK. <sup>136</sup> Although the exact cause of Graves' disease is unknown it is more commonly found in young and middle aged women, with women being 7 time more likely to be affected than men; it has also believed to be hereditary, although patterns are still being investigated. <sup>137</sup> Graves' disease causes the immune system to produce thyroid stimulating immunoglobulin (TSI). The TSI bind to the TSH receptors causing the thyroid to increase the release of thyroid hormone and causing the gland to enlarge. Hyperthyroidism is clinically indicated by low TSH level and high T3 level, sometimes coupled with high T4 levels. (Table 2.1) The symptoms of hyperthyroidism include increased appetite but with weight loss, irritability, restlessness, insomnia, tremors, muscle weakness,

excessive sweating, fatigue and reduced libido.<sup>138</sup> If left undiagnosed the growth of the thyroid gland can lead to a goitre, which is a visible enlargement of the thyroid gland on the neck as shown in Figure 2.10, which when caused by Graves' disease is termed a diffuse thyrotoxic goitre. Additionally, around half of patients which Graves' disease develop Graves' ophthalmopathy, which is an inflammatory disease effecting the eyes. The most common initial course of treatment is the use of anti-thyroid drugs, methimazole or propylthiouracil, which inhibit thyroid hormone synthesis to quickly bring the patient to an euthyroid, normal thyroid hormone level, state. Relapse after treatment with ATD is common, especially in individuals with extreme symptoms. Once the patient is in a euthyroid state further treatment performed with radioactive iodine treatment or via thyroidectomy, with radioactive iodine treatment being preferred. Radioactive iodine treatment, which was introduced in 1942, involves the patient being treated with iodine-131 which destroys the follicular cells via the emission of beta particles. Treatment can often require multiple doses with full effects taking an average of 3 months to reach a euthyroidism or hypothyroidism.<sup>139</sup>

However, there are instances where radioactive iodine treatment would not be suited, such as in women who are pregnant or breastfeeding, and thyroidectomy is preferred in these cases. Thyroidectomy was first used to treat Graves' disease in the 1800s and can be performed as either a total or subtotal thyroidectomy. A subtotal thyroidectomy can be performed bilaterally leaving around 2-4 g of thyroid remnant or unilaterally leaving around 7 g of remnant. Over the past few decades, total thyroidectomy has become the preferred surgical option. The main disadvantage of surgery for hypothyroidism is the requirement for lifelong thyroid hormone replacement.<sup>140-144</sup>

Hypothyroidism, or an underactive thyroid gland, is most commonly caused by the autoimmune disorder Hashimoto's disease or following treatment for hyperthyroidism.<sup>145</sup> Hypothyroidism can also be caused by medication prescribed for other conditions, e.g., lithium, interferons and amiodarone. Although the exact causes of Hashimoto's disease are unknown, it is more commonly found in individuals with other immune disorders, such as type 1 diabetes and vitiligo, it is hereditary and is more common in women than men.<sup>145-149</sup> Hashimoto's disease causes the immune system to produce antibodies which prevent thyroid hormone synthesis. In around 95 % of cases, thyroid peroxidase antibodies are present and

in around 60 % of cases anti-thyroglobulin antibodies are present.<sup>150</sup>  
Hypothyroidism can be either primary or secondary; with primary hypothyroidism clinically indicated by high TSH levels and low T4 levels and secondary hypothyroidism clinically indicated by non-elevated TSH levels and low T4 levels.  
(Table 2.1)<sup>148, 149, 151, 152</sup>

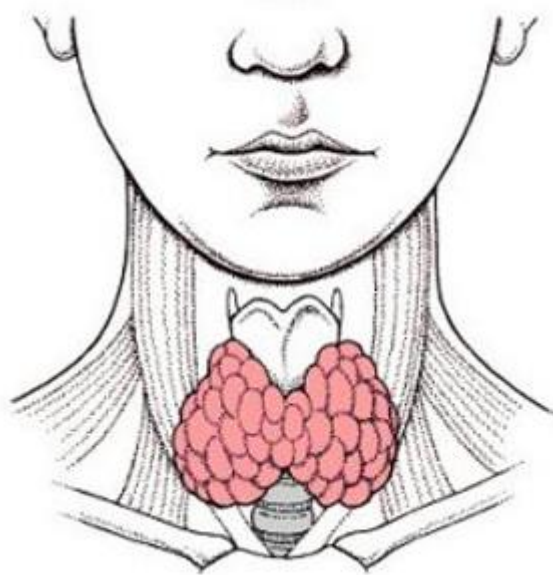


**Figure 2.10: Graphical representation<sup>121</sup> and Image of a goitre<sup>153</sup>**

The symptoms of hypothyroidism include unexplained weight gain, pale dry skin, brittle nails, memory lapses, depression, muscle weakness, sensitivity to cold, fatigue and sluggishness. Elderly individuals can suffer from a complication called hypothyroid crisis which is often caused by an infection where a reduced level of

consciousness is a common symptom. Other symptoms include hypothermia, heart failure, hypoxia and hypotension. Individuals are treated via multisystem support including ventilation, intravenous fluids and antibiotics and thyroid hormone replacement.<sup>149</sup> Synthetic levothyroxine is the most common treatment for hypothyroidism with the aim to bring patients into a euthyroid state. However, there are significant variation in the dosage required between individuals. Therefore, individuals are given dosage of levothyroxine and their serum levels monitored on a weekly basis for 6-8 weeks after which point, the dosage can be altered in order to obtain stable levels. Once a stable level is obtained the serum levels are tested monthly for 4-6 months and if they remain stable, the patient is then tested on an annual basis.<sup>154</sup> The use of combined levothyroxine and triiodothyronine therapies has been found to be preferred by some patients however, the clinical responses to a combined therapy are still an area of much debate.<sup>133, 147, 149, 150, 155, 156</sup>

## **2.1.5. Current methods of analysis**

### **2.1.5.1. Electrochemiluminescence immunoassay (ECLIA)**

Clinical analysis of patient samples for thyroid hormone testing is performed utilising electrochemiluminescent immunoassay (ECLIA), a quantitative method based on a change in electrochemiluminescence (ECL) caused by an immunoreaction for measurement of antigen or antibody.

Electrochemiluminescence is produced either directly or indirectly via an electrochemical reaction in which a potential is applied to an electrode resulting in the generation of an ECL-emitting species which emits light. Although the first ECL phenomenon was observed in the 1920s, detailed studies into ECL were not performed until the 1960s, but ECL is now a powerful analytical technique. ECL has a number of advantages over the conventional chemiluminescence (CL) method, including greater sensitivity due to the low background from not requiring an excitation light source, variation in electrochemical potential allows for greater control and compounds previously not suitable for CL reactions can be electrochemically modified on the surface electrode, giving a greater range of

applications. ECL has been used in areas such as medical diagnosis, food safety and environmental monitoring as a sensitive detection method.<sup>157</sup>

ECL can be produced by either an annihilation or a co-reactant pathway, although most modern applications are based upon the co-reactant pathway due to the need to use organic solvents in the annihilation pathway. In both pathways two species are electrochemically generated and then undergo redox reaction in order to produce an emissive species. In the co-reactant pathway, an emitter and co-reactant are exposed to a potential scan on the electrode causing oxidation. The co-reactant then forms a reducing intermediate via chemical decomposition which reacts with the emitter to generate an oxidised state.<sup>158-161</sup> The antigen is sandwiched between a primary antibody bound to a well plate and a secondary antibody which is labelled with a luminescent substrate. To prevent limiting of enzymatic activity the luminescent substrate is introduced using a nonenzymatic metal nanoparticle catalyst. ECLIA for the analysis of thyroid hormones uses a Tris(2,2'-bipyridyl) ruthenium(II)-complex with the amplification of the signal due to the repeated excitation with tripropylamine.<sup>14, 162</sup> As shown in Figure 2.11.

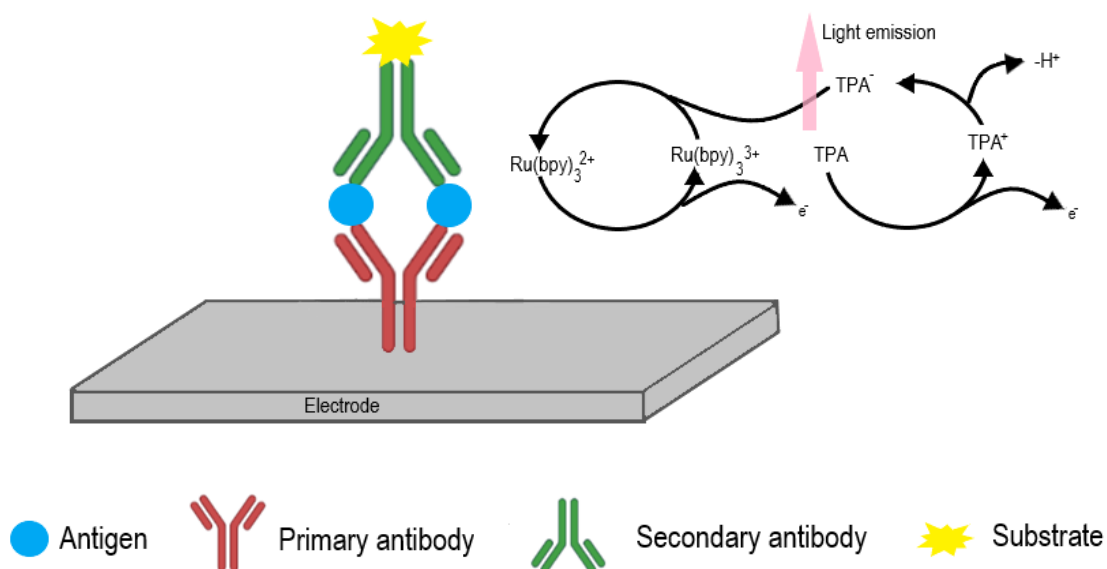


**Figure 2.11: Schematic of ECLIA reaction (adapted from <sup>163</sup>)**

The sensitivity of this techniques impacts on the diagnosis and management of hypothyroidism samples for hypothyroid patients were hormone levels are often below or close to the limits of quantification. Both of which can cause significant

problems when monitoring thyroid hormone levels, particularly in pregnant women.<sup>152, 164-167</sup> The method information sheets supplied by the manufacturer state a permissible error at the limit of quantification (LOQ) level of 30 % has the potential to cause inaccuracies in biological sample with lower thyroid level leading to misleading results.<sup>17, 18</sup>

### 2.1.5.2. Enzyme linked immunoassay (ELISA)

Alternatively, research samples are often analysed by enzyme linked immunosorbent assay (ELISA) as this is a relatively cheap alternative and requires less specialised instrumentation in comparison to ECLIA. The technique was first described by Engvall and Perlmann in the 1970s<sup>168</sup> and is a method of detection of antigens within a biological sample based upon antibody/antigen interactions. An ELISA assay can either be a direct, indirect (including competitive ELISA) and sandwich as indicated in Figure 2.12.

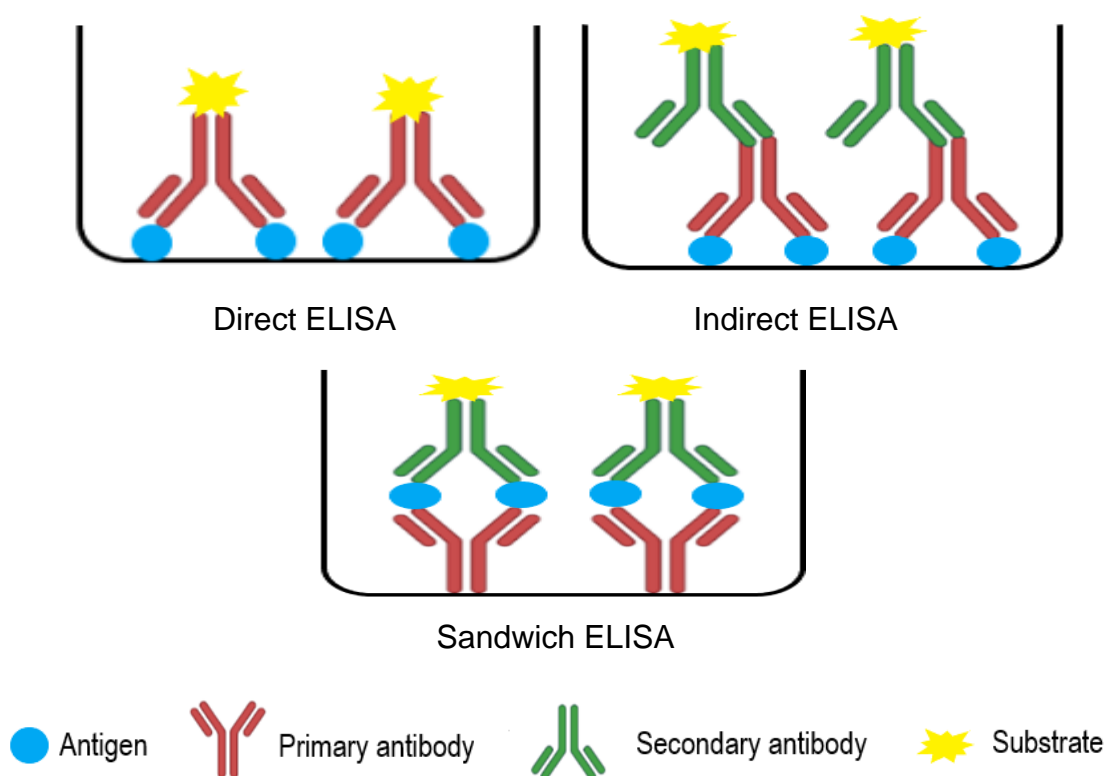


**Figure 2.12: Types of ELISA**

The basic principles of ELISA are a series of reactions which produce a chromogenic or fluorescence response which can be measured via a plate reader.

In direct ELISA the antigen is immobilised on the surface of a well plate which is then reacted with a specific antibody directly conjugated to the detection molecule. In indirect ELISA the antigen is also immobilised on the surface of a well plate. However, the primary antibody is not conjugated to the detection molecule and a secondary conjugated antibody carries the detection molecule. A competitive ELISA is a form of indirect ELISA however the antibody and antigen are incubated together and then added to an antigen coated well. The more antigen present within the sample results in less antibody binding to the well antigen, giving the type of ELISA the name competitive. The most common form of ELISA is the sandwich ELISA, as the name suggests the antigen is sandwiched between two antibodies which are specific for different epitopes of the antigen. The first antibody is immobilised onto the surface of a well plate and binds with the antigen the second antibody, which facilitates the detection, is then added to sandwich the antigen. The analysis of thyroid hormones utilises the competitive ELISA technique.<sup>14, 157, 168, 169</sup>

## **2.2. Plant toxins**

Plant toxins are usually secondary metabolites which are produced as protection against threats such as insects, bacteria and fungi. These compounds can have both useful and harmful effects in humans, and include classes of compounds such as alkaloids, glycosides, terpenes and steroids, causing a variety of actions within the body. Depending on the plant and the compounds, they can be present in specific parts of the plant or throughout the whole plant. Plant toxins have been used historically for a number of applications including assassinations, treatment of disease, pesticides and to add flavour to foods. Exposure to plant toxins can be oral, dermal or via inhalation and unintentional exposure is commonplace. The results of exposure vary greatly, depending on the plant and the route of exposure such as itching and rash from contact with plant sap to lethality.<sup>170-172</sup>

The median lethal dose ( $LD_{50}$ ) of a compound is a measure of lethality and is the concentration required to kill half of the test population. The partition co-efficient (P) of a compound is used to establish how well that compound will dissolve in

either an aqueous or organic phase. This provides an understanding of how a particular compound will react in different environments. The logarithm of P, commonly referred to as LogP, can be used to predict how compounds will react in plants and humans and is commonly used in drug discovery in order to understand drug distribution. A negative LogP indicates that the compound is at a higher concentration in the aqueous phase and a positive LogP indicates a higher concentration in the lipid phase. In the Lipinski's rule of 5, which was developed at Pfizer, a compound which is administered orally should have a LogP of <5 with the ideal LogP for central nervous system activity being around 2.<sup>173-175</sup> pKa is the measure of a strength of an acid and is the negative base 10 logarithm of the acid dissociation constant, with a lower value indicating a stronger acid. pKa values are useful in the controlling of protonation of the compound within a solution, for example, a solution with a pH value the same as the pKa value of the compound results in dissociation of half of the acid. As a rule of thumb, a pH of  $\pm 2$  pH units away from the pKa value will result in a fully ionised or fully unionised compound. The chemical properties of the compounds used within this study is shown in Table 2.2. Images of an example for each genus of plant analysed can be seen in Figure 2.13.

### 2.2.1. Aconitine

**Background:** Aconitine, as well as mesaconitine and hypoconitine, are diterpene alkaloids which are cardiotoxins and neurotoxins found within plants of the *Aconitum* L. genus from the *Ranunculaceae* family (Figure 2.13). They consist of over 300 species found all over the world. Aconitine is biosynthesised by a two step dual pathway process, firstly acetyl co enzyme A (CoA) or pruvate and D-glyceraldehyde-3-phosphate is converted to isoprenoid via the mevalonate and methylerythritol pathways, respectively. Secondly a diterpene alkaloid (DA) skeleton is formed via one of two pathways show in Figure 2.14 which is then converted to aconitine via mono-oxygenase and BAHD acyltransferase.<sup>176-178</sup> Around 76 species grown in China and surrounding countries are used for medical purposes, including *Aconitum Brachypodum*, known for its anti-rheumatic and analgesic effect. It grows at high altitude resulting in its Chinese name "snow grass", and is commonly applied as a treatment for abrasions and wounds.<sup>179-182</sup>

**Table 2.2: Compound properties**

Compound	LD <sub>50</sub> (mg/kg) (reference)	LogP <sup>183</sup>	pKa <sup>183</sup>	Molecular weight (g/mol)
Aconitine	1 <sup>(184)</sup>	-0.99	5.88	645.75
Atropine	75 <sup>(185)</sup>	1.83	9.43	289.38
Capsaicin	47.3 <sup>(186)</sup>	3.75	9.93	305.42
Cathinone	379.7 <sup>(187)</sup>	3.66	9.13	149.19
Colchicine	5.87 <sup>(188)</sup>	0.27	1.85	413.47
Coumarin	359.5 <sup>(189)</sup>	1.72	-6.90	146.04
Digitoxin	3527 <sup>(190)</sup>	2.30	7.18	764.95
Digoxin	28.27 <sup>(191)</sup>	2.37	7.15	780.95
Hellebrin	8.4 <sup>(192)</sup>	0.04*	Unknown	724.80
Psoralens	1700 <sup>(193)</sup>	1.44	-2.90	186.17
5- Methoxypsoralens	>3000 <sup>(194)</sup>	1.78	-2.90	216.19
8- Methoxypsoralens	791 <sup>(195)</sup>	1.78	-2.90	216.19
Salvinorin A	1400 <sup>(196)</sup>	2.39	16.45	432.50
Scopolamine	1300 <sup>(197)</sup>	0.98	7.75	303.36
α-Solanine	590 <sup>(198)</sup>	1.29 <sup>+</sup>	12.33 <sup>+</sup>	868.07
Strychnine	2.35 <sup>(199)</sup>	0.93	17.24	334.42
α-Thujone	500 <sup>(200)</sup>	1.74 <sup>x</sup>	-7.40 <sup>x</sup>	152.24
Veratridine	1.35 <sup>(201)</sup>	Unknown	9.54 <sup>-</sup>	673.80

References: \*202 +203 x204 -205

**Pharmacological effects:** aconitine, mesaconitine and hypoconitine are potent cardio and neurotoxins found in all parts of the aconitum plant but are especially found in high density in the roots. Aconitine activates the voltage dependent sodium channels within the cell membranes of tissues including myocardium, nerves and muscles, influencing the release of neurotransmitter from nerve terminals.<sup>206, 207</sup> Affected patients present with a number of symptoms including cardiovascular, neurological and gastrointestinal symptoms including numbness, coldness and body tingles. Poisoning by aconite still occurs around the world due to accidental ingestion of wild plants and due to the fact that the root of aconite plants is still used in herbal medicines.

<i>Aconitum napellus</i>	<i>Aquilegia atrata</i> <sup>#</sup>	<i>Artemisia absinthium</i> <sup>+</sup>
		
<i>Atropa belladonna</i>	<i>Catha edulis</i>	<i>Daphne laureola</i>
		
<i>Brugmansia suaveolens</i>	<i>Digitalis purpurea</i>	<i>Fritillaria imperialis</i>
		
<i>Helleborous orientalis</i>	<i>Heracleum mantegazzianum</i>	<i>Hyoscyamus niger</i>
		
<i>Ruta graveolens</i> <sup>*</sup>	<i>Salvia divinorum</i>	<i>Veratrum album</i>
		
<i>Capsicum chinense</i> <sup>x</sup>	<i>Solanum tuberosum</i>	<i>Colchicum autumnale</i>
		

Figure 2.13: Example of a plant from each family analysed. References <sup>\*208</sup>, <sup>+209</sup>, <sup>#210</sup>, <sup>x211</sup>

Symptoms of aconite poisoning display in a number of areas including cardiovascular, gastrointestinal and neurological but the main cause of death is refractory ventricular tachyarrhythmias and asystole.<sup>180, 206, 207, 212</sup>

Estimated lethal dose is 12 mg of aconitine or 1 g of raw plant material. In traditional medicine, the aconitum is processed to remove up to 90 % of the alkaloid content, with methods such as soaking and boiling, however due to inadequate processing fatal poisoning still occurs.<sup>180, 206, 212</sup> Tincture preparations, the dissolving of a compound in alcohol, of aconitum cause the highest percentage of poisoning cases at around 55 % of cases. Additionally, due to the long half-life of aconitum alkaloids, the repeated use of medicines causes an accumulation within the body.<sup>181</sup>

**Uses:** Aconitum root, harvested in late August and early September, continues to be used in traditional Chinese medicine for the treatment of joint pain, rheumatic fever, asthma and diarrhoea, amongst other conditions, due to their analgesic, anti-inflammatory and cardiotoxic effects.<sup>206, 207</sup> In regions of China aconite is also consumed as a herbal soup or a medicinal liquor and has been used to treat illness for around 2000 years.<sup>212</sup> For use in traditional medicine the aconite root is processed to reduce the amount of aconitum alkaloids present and can be found in formulations including proprietary medicines, tinctures, powders and lotions.<sup>212</sup> The state food and drug administration of China stipulates that only processed tubers and roots can be administered orally, for which there are over 70 traditional and modern processing techniques, and the Chinese pharmacopeia stipulating titrimetric and colorimetric tests for determining alkaloid content. However fatal aconite poisoning cases are still reported every year.<sup>179</sup> In a case example from 2010, Ms Singh was sentenced to life in prison for the murder of her ex-partner, Mr Cheema, and grievous bodily harm with intent of his fiancée, Ms Choongh, after entering his home and adding Indian aconite to a curry in the fridge. Mr Cheema died within hours of consuming two portions of the curry and Ms Choongh was left fighting for her life but later recovered. Due to the nature of the method of poisoning Singh was dubbed “the curry killer”.<sup>213-216</sup>

### 2.2.2. Atropine and scopolamine

**Background:** The tropane alkaloids atropine (hyoscyamine) and scopolamine are found within many plants of the *Solanaceae* family including *Atropa L. belladonna*, *Hyoscyamus L. niger*, *Datura L. spp.* and *hyoscyamine L. spp.* commonly known as deadly nightshade, henbane, jimsonweed and daturine, respectively (Figure 2.13). *Atropa belladonna* is a large perennial plant native to Europe, north Africa and western Asia and considered the most dangerous member of the *Solanaceae* family.

The plant produces cherry like berries which are dark purple/ black and are the most toxic part of the plant. The berries have a sweet and pleasant taste which often leads to accidental poisoning when mistaken for edible berries. Although the berries of the plant are the most toxic, the whole plant is considered to be toxic. The berries on average contain 65% alkaloid content and can cause lethality after the ingestion of 2-5 berries in children and 10-20 berries in adults, if left untreated.<sup>217</sup>

Atropine and scopolamine function as the plant's chemical defence when in a condition of stress. Atropine and scopolamine are synthesised within the plant from tropane and phenylalanine utilising polyketide synthase, cytochrome P450 enzyme, tropinone reductase I/II, littorine synthase, littorine mutase/monooxygenase, hyoscyamine dehydrogenase and hyoscyamine 6 $\beta$ -hydroxylase as shown in Figure 2.15.<sup>218, 219</sup> Synthesis occurs within the roots of the plants and the alkaloids are subsequently transported to the aerial plant parts where the compounds are stored.<sup>218</sup>

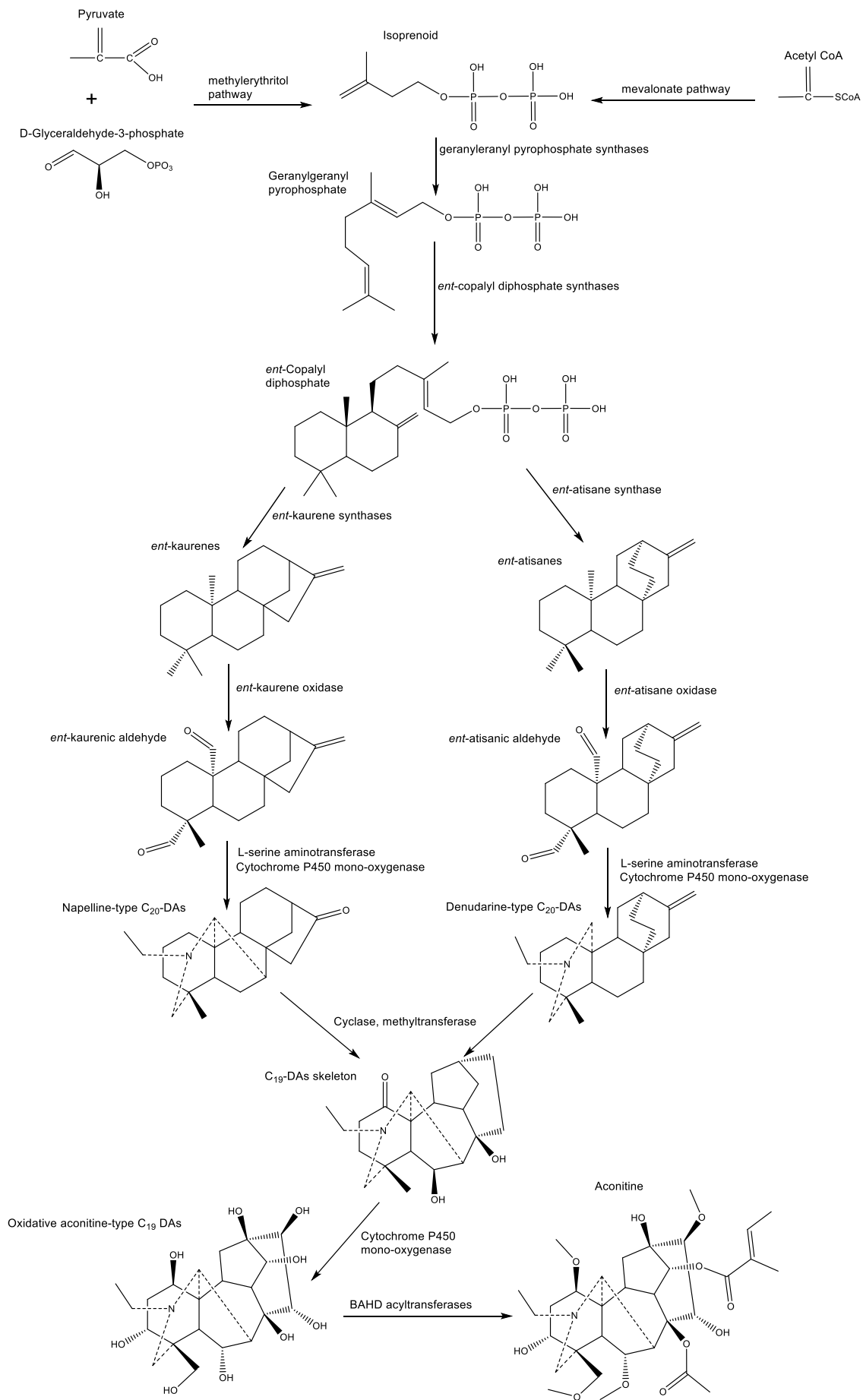


**Figure 2.14: Biosynthesis of aconitine.** 176-178

**Pharmacological effects:** Atropine and scopolamine exhibit dose dependant hallucinations and psychoactive effects due to their ability to cross the blood-brain barrier. The effect the peripheral and central nervous system as a competitive, non-selective muscarinic acetylcholine receptor antagonist, preventing the binding of acetylcholine, a physiological neurotransmitter.<sup>217, 220</sup> Muscarinic acetylcholine receptors are split into five subtypes, M1-M5; M1 is involved in the memory and learning process, M2 are found in the heart, M3 are involved in smooth muscle contraction, M4 is involved in the pain process and the physiological effects of M5 have not been determined. Both atropine and scopolamine cause pupil dilation (mydriatic), relieves muscle spasms (spasmolytic) and are used as a local anaesthetic. However, its side effects are hallucinogenic and potentially fatal.<sup>218</sup>

**Uses:** The use of atropine dates back to the late century BC where it was reported to have been used by Cleopatra to dilate her pupils to be more alluring, a practice which has twice seen a resurgence. Firstly, in renaissance Venice and then again in the late 19<sup>th</sup> and early 20<sup>th</sup> century in Paris and is believed to be where belladonna in the name of *Atropa belladonna* originates, meaning beautiful lady.<sup>221</sup> Atropine was widely used as a medicine to treat hepatitis, edema, scarlet fever and mental diseases during ancient times but the poisonous effects were also known. Attalos III used *Solanaceae* plants on animals and individuals condemned to death to establish the poisonous effects on the plant. *Atropa belladonna* is also believed to be used by King Duncan I. of Scotland in food to poison enemies before battle. During the middles ages Atropine was being widely used by witches and sorcerers but by the 16<sup>th</sup> and 17<sup>th</sup> century was being studied by herbalist and apothecaries for application to the treatment of bronchial spasm, cough and colds. In the 1800s the uses of jimson weed in India as a treatment for asthma by smoking and inhalation was observed by British colonists who introduced it into Western medicine. By the 19<sup>th</sup> century *Atropa belladonna* was being used as an anticholinergic, to treat jaundice and epilepsy, as a sedative for bronchial spasms, as an analgesic and to treat hyperkinesis associated psychiatric disorders.

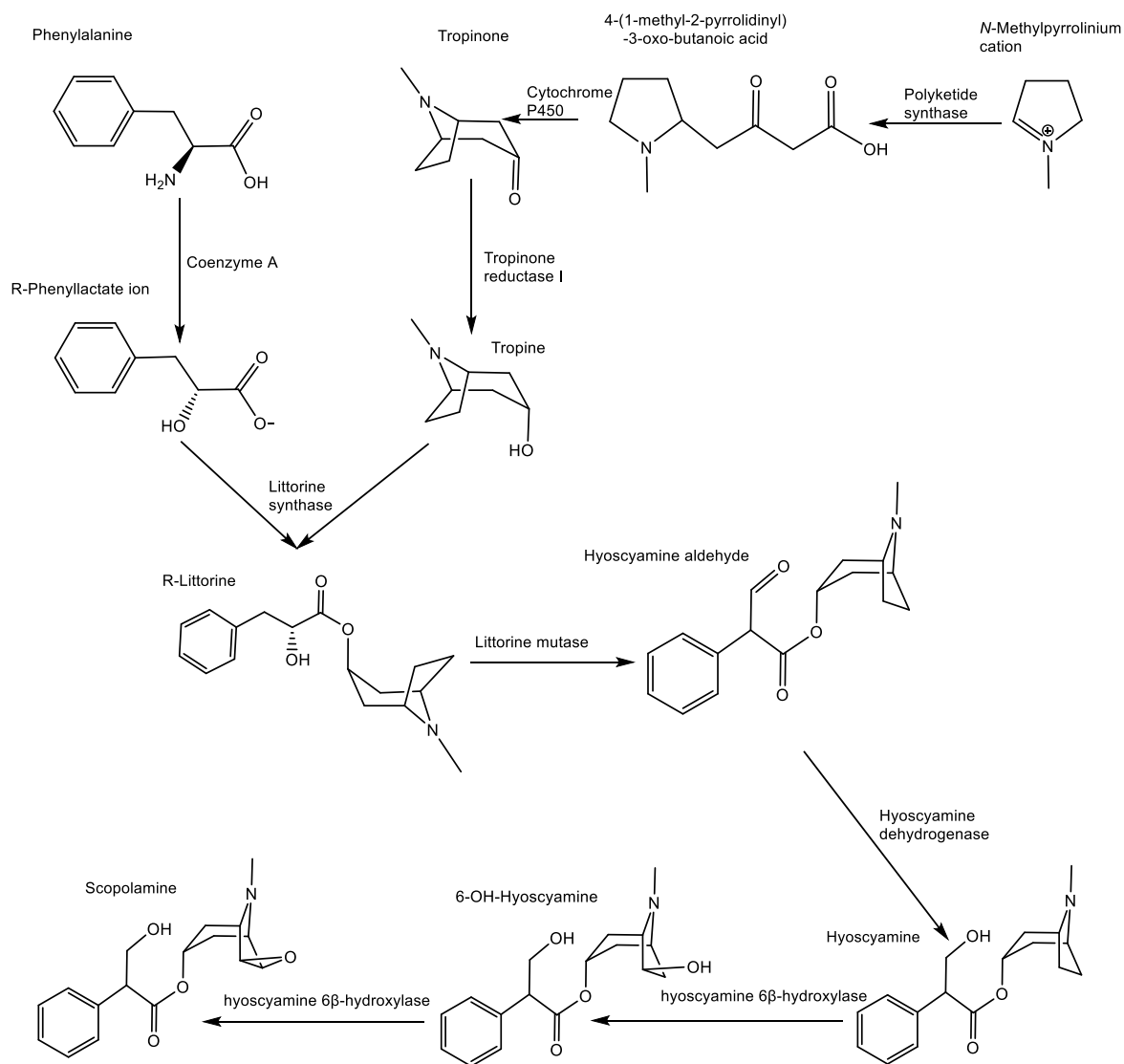


**Figure 2.15: Biosynthesis of hyoscyamine (atropine) and scopolamine.**<sup>218, 219</sup>

Currently, topical atropine preparations are used to temporarily dilate pupils in order to aid in ophthalmic examinations and, until its removal in 2010, injections of atropine were recommended for resuscitation following a cardiac arrest associated with asystole and pulseless electrical activity due to its action of blocking the vagus nerve.<sup>217, 221, 222</sup>

### 2.2.3. Capsaicin

**Background:** Capsaicin (trans-8-methyl-N-vanillyl-6-nonenamide) is a capsaicinoid which is found within many plants within the *Capsicum* L genus of the *Solanaceae* family and is responsible for the spicy taste (Figure 2.13). Capsaicin is

biosynthesis by the condensing of vanillylamine and 8-methyl-6-nonenic acid which are produced by the phenyl propanoid and valine pathways, respectively by capsaicin synthase, as shown in Figure 2.16.<sup>223-225</sup> Capsaicin is capable of creating heat, flavour and an endorphin rush and accounts for almost 70% of the total capsaicinoids in spices. Capsaicin content is classified on the Scoville scale which is the industrial standard for the degree of spiciness but it is subjective due to the fact it relies on tasters.<sup>226-229</sup> The chilli plant which has held the Guinness world record since 2017 as the hottest chilli is the Carolina reaper with an average of 1,641,183 Scoville heat unit.<sup>230</sup>

**Pharmacological effects:** Capsaicin has many benefits as a medicinal herb including enhancing metabolism, reducing cholesterol and the risk of stomach ulcers. Many people have allergic reactions to capsaicin causing lip swelling, nasal congestion, nausea and diarrhoea. The neurobiological effects of capsaicin are linked to the transient receptor potential vanilloid 1 (TRPV1) which is responsible for the coding of the capsaicin receptor. TRPV1 is a non-selective cationic ion channel and is a critical receptor in the sensing of stimuli, including noxious heat. The receptor desensitization of TRPV1 is believed to be the mechanism by which topical capsaicin preparations reduce pain. It has also been found to have antiepileptic activity by blocking sodium channel activation.<sup>226, 227, 231, 232</sup> The slimming effects of capsaicin are caused by two processes related to fat oxidation and energy consumption. Firstly, capsaicin reduces the accumulation of adipose tissue by inhibiting gene transcription for the proteins which stimulate adipogenesis and secondly it influences the genes responsible for fat reduction enzymes. Both of which lead to a reduction in adipose tissue and therefore a drop in body weight.<sup>231</sup>

**Uses:** Chillies are widely used around the world in cooking. There are also a number of topical preparations, such as creams and dermal patches, which are used for the temporary reduction in pain and it has been used as an analgesic since 7000 BCE. Capsaicin also has anti-microbial and anti-bacterial properties.<sup>226, 227, 231</sup>

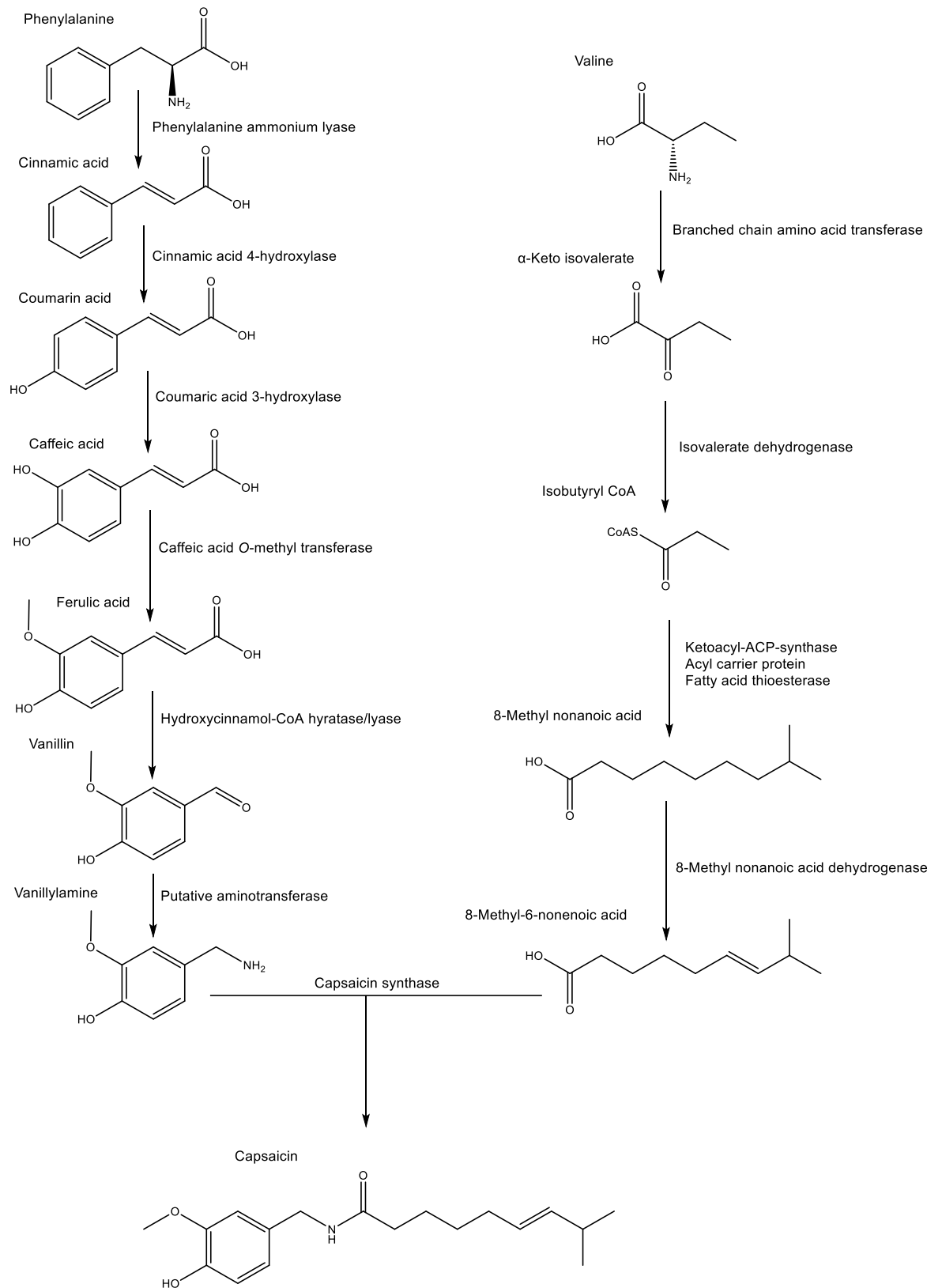


**Figure 2.16: Biosynthesis of capsaicin.**<sup>223-225</sup>

#### 2.2.4. Cathinone

**Background:** Cathinone is found in the young leaves and shoots of the shrub *Catha edulis* commonly known as khat (Figure 2.13). It is chewed for its psychoactive stimulating effects recreationally in the Middle East and Africa, with over 80% of adult males in some eastern African areas chewing khat on a daily basis.<sup>233</sup> The plant *Catha edulis* is a member of the *Celastraceae* family.

Cathinone is biosynthesised from phenylalanine via two separate pathways; a non- $\beta$ -oxidative CoA independent pathway, shown on the left of Figure 2.17, and a  $\beta$ -oxidative CoA dependent pathway, shown on the right of Figure 2.17.<sup>234-236</sup>

**Pharmacological effects:** Cathinone is a monoamine alkaloid similar in chemical structure to ephedrine, amphetamine and methamphetamine as seen in Figure 2.18 and as such, has the potential to produce similar effects, pharmacologically. Cathinone has been reported to increase the release of serotonin and dopamine while inhibiting the reuptake of both.<sup>233, 237</sup>

Of the two possible enantiomers of cathinone, only the S(-)-cathinone is naturally occurring. Cathinone is the main compound responsible for the psychostimulant nature of *Catha edulis*, however, as a keto-amine it is unstable and is found in higher concentrations in young leaves and shoots. Accounting for 70 % of the overall phenylalkylamine content of young foliage compared to not being present in older foliage. In older foliage cathinone is broken down into (+)-norpseudoephedrine and (-)-norephedrine, which are diastereoisomers due to the spatial arrangement of the -OH group. (Figure 2.19).<sup>238</sup> The release of active constituents is achieved by chewing the leaves and shoots of the plant which are dissolved in the saliva and then absorbed firstly in the buccal mucosa and then in the gastrointestinal tract. The increased lipophilicity of cathinone makes it a more potent psychoactive agent than norephedrine and norpseudoephedrine. Cathinone triggers presynaptic dopamine release and inhibits the reuptake of dopamine similar to amphetamine.<sup>237, 238</sup> Jones *et al.* found that cathinone also induces serotonin release and inhibits the uptake.<sup>233</sup> Peak plasma levels of active compounds following chewing of *Catha edulis* are observed after 1-3.5 hours with cathinone levels peaking at 2.3 hours. Cathinone is rapidly metabolised to

norpseudoephedrine and norephedrine by the reduction of the ketone to an alcohol which is catalysed by liver microsomal enzymes.<sup>237</sup>

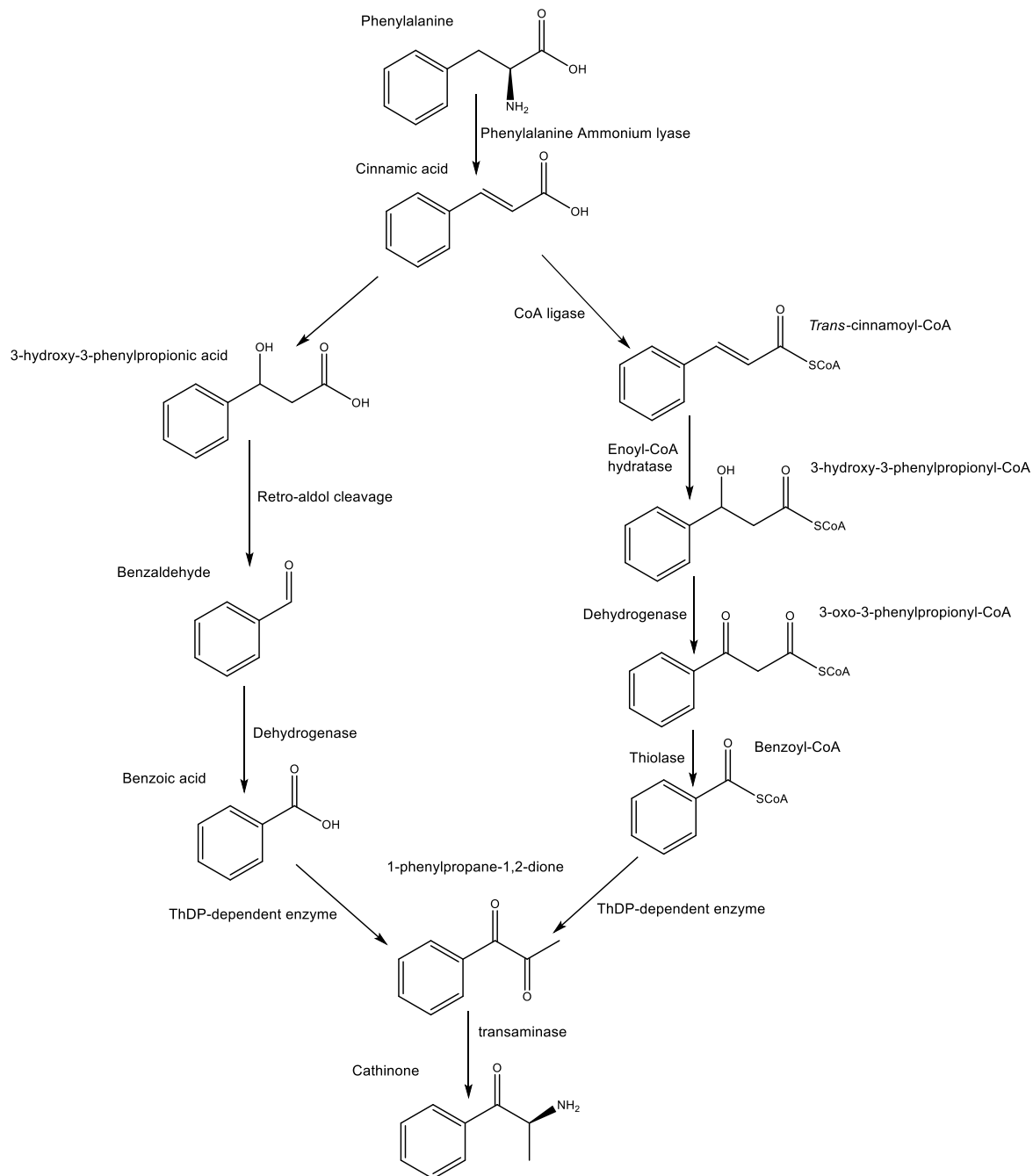


**Figure 2.17: Biosynthesis of cathinone.**<sup>234-236</sup>



**Figure 2.18: Comparison of cathinone with similar monoamine alkaloids.**<sup>233,</sup>

237

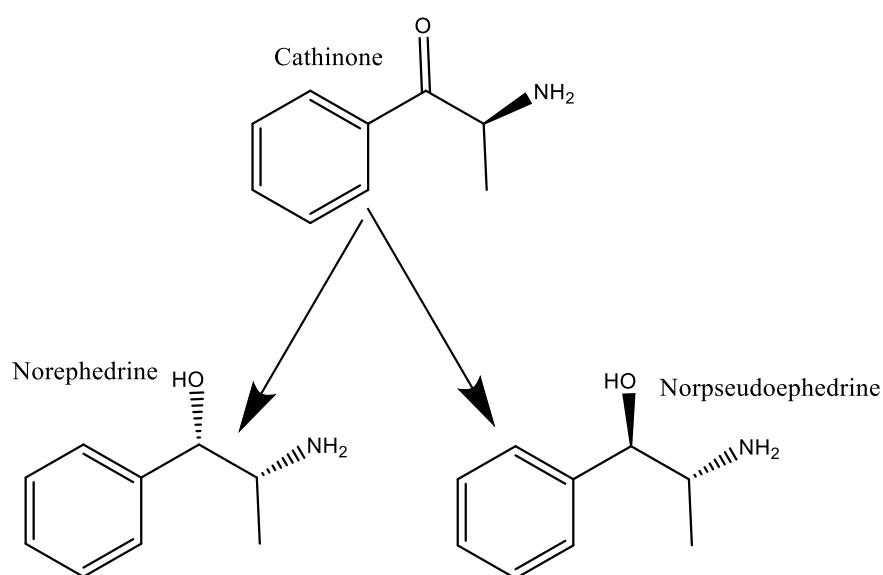


**Figure 2.19: Conversion of cathinone to norephedrine and norpseudoephedrine.**<sup>238</sup>

**Uses:** The chewing of khat has been reported dating back to the fourteenth century where leaves were chewed by medieval Islamic sultanates in what is now the southern region of Ethiopia where it was subsequently moved to the horn region via the historic trading routes. A 15<sup>th</sup> century historian and geographer, Al-Maqrizi, reported the chewing of plants leaves promoting appetite suppression while increasing levels of euphoria and intelligent performance. By the late 19<sup>th</sup> century, due to the widespread chewing of khat in Zeyla, the members of the Sufi order were condemned for promoting the plant as aid during Ramadan. Ultimately

consumption reaching a critical point causing a law to be passed in 1921, by the British authorities of the Somaliland protectorate, forbidding the cultivation, import and sale of khat. However, it was estimated that by 1945 around 3000 kg per day was being smuggled into the protectorate. By the early 20<sup>th</sup> century chewing of khat became a cultural practice and after the 1930s became a common place past time across all classes, cultures and religious affiliations.<sup>239</sup>

During the last three decades the use of khat, for recreational purposes, has increased in western countries; believed to be due to the immigration of individuals from the Horn of Africa and the Middle East. An increase in immigration has resulted in importing of khat to other countries including Europe and the United States of America.<sup>237</sup> As a result an advisory for the adding of cathinones to the UK Misuse of Drugs Act 1971 was presented in 2010.<sup>240</sup> Synthetic derivative of cathinone, mephedrone and methcathinone, are increasing in popularity in countries including the UK as a recreational drug, resulting in the synthetic derivative mephedrone being classified as a controlled substance in 2010. However, the use of khat remained legal until it was added to the misuse of drugs act as a class C substance in 2014.

### 2.2.5. Colchicine

**Background:** Colchicine is a phenethylisoquinoline alkaloid found in the plant *Colchicum L. autumnale* (Figure 2.13). Colchicine is biosynthesis from tyrosine and phenylalanine to form autumnaline which undergoes para-para phenol coupling followed by ring expansion and nitrogen modification with the use of methyltransferase and cytochrome P450 enzymes as shown in Figure 2.20.<sup>241-245</sup> *Colchicum L. autumnale* is a perennial herb which belongs to the family *Colchicaceae*, commonly known as wild saffron or meadow saffron, and is one of the more widespread species within the *Colchicum L.* genus and is the only species which is found in Northern Europe and Great Britain. *Colchicum autumnale* contains around 20 tropolone alkaloids including colchicine at varying levels found throughout the plant. Due to the resemblance of the bulb to onion and the leaves to wild garlic, accidental poisoning is not uncommon. Colchicine and derivatives are highly toxic leading to death after ingestion of as little as 7 mg has

been known to be fatal with a fatal blood concentration of between 0.09 – 0.16 mg/L.

**Pharmaceutical Effects:** The cytotoxic effects of colchicine are due to disturbing the cell replication in tissues. Colchicine inhibits mitosis by suppressing or blocking cell division and symptoms of poisoning normally follow three stages. The first stage includes symptoms such as vomiting including a burning sensation in the mouth and throat, diarrhoea and abdominal pain. The second stage includes symptoms such as arrhythmias (abnormal heart rhythm) liver failure, respiratory distress, pancreatitis and hypocalcaemia (low calcium level) which can lead to multiorgan failure. Recovering patients often experience hair loss, the third stage. This has led to *Colchicum autumnale* being regarded in central Europe as one of the most dangerous grassland weeds, especially in livestock areas.<sup>246, 247</sup>

A case reported by Klintschar *et al.* reports the miss identification of colchicum Autumnale leaves as wild garlic and subsequently being used in a meal with a larger consumption of the meal by the older individual.<sup>248</sup> The paper reported that around 3 hrs after consumption the individual suffered from vomiting, severe diarrhoea and abdominal cramps. After approximately 48 hours the individual collapsed and soon after died from multi-organ failure.

The second individual reported the same initial symptoms around 2 hours later than individual 1 and was admitted to intensive care at the same time as individual 1 with symptoms subsiding entirely after 3 days. The initial echocardiogram and laboratory tests were consistent of intoxication by digitalis, however the death of individual 1 was inconsistent with digitalis toxicity. Post mortem bile samples found a concentration of 7.5 µg/mL of colchicine present in individual 1 with no colchicine detected in either individuals blood samples.<sup>248</sup> There is no specific antidote for colchicine, therefore treatment must be administered symptomatically as soon as possible following ingestion.<sup>247, 249</sup>

**Uses:** Colchicine is used in pharmaceutical preparations, in the form of tablets, for its anti-inflammatory and analgesic properties and is commonly used for the treatment to prevent flare-ups of familial Mediterranean fever and to treat flare ups of gout.<sup>250</sup>

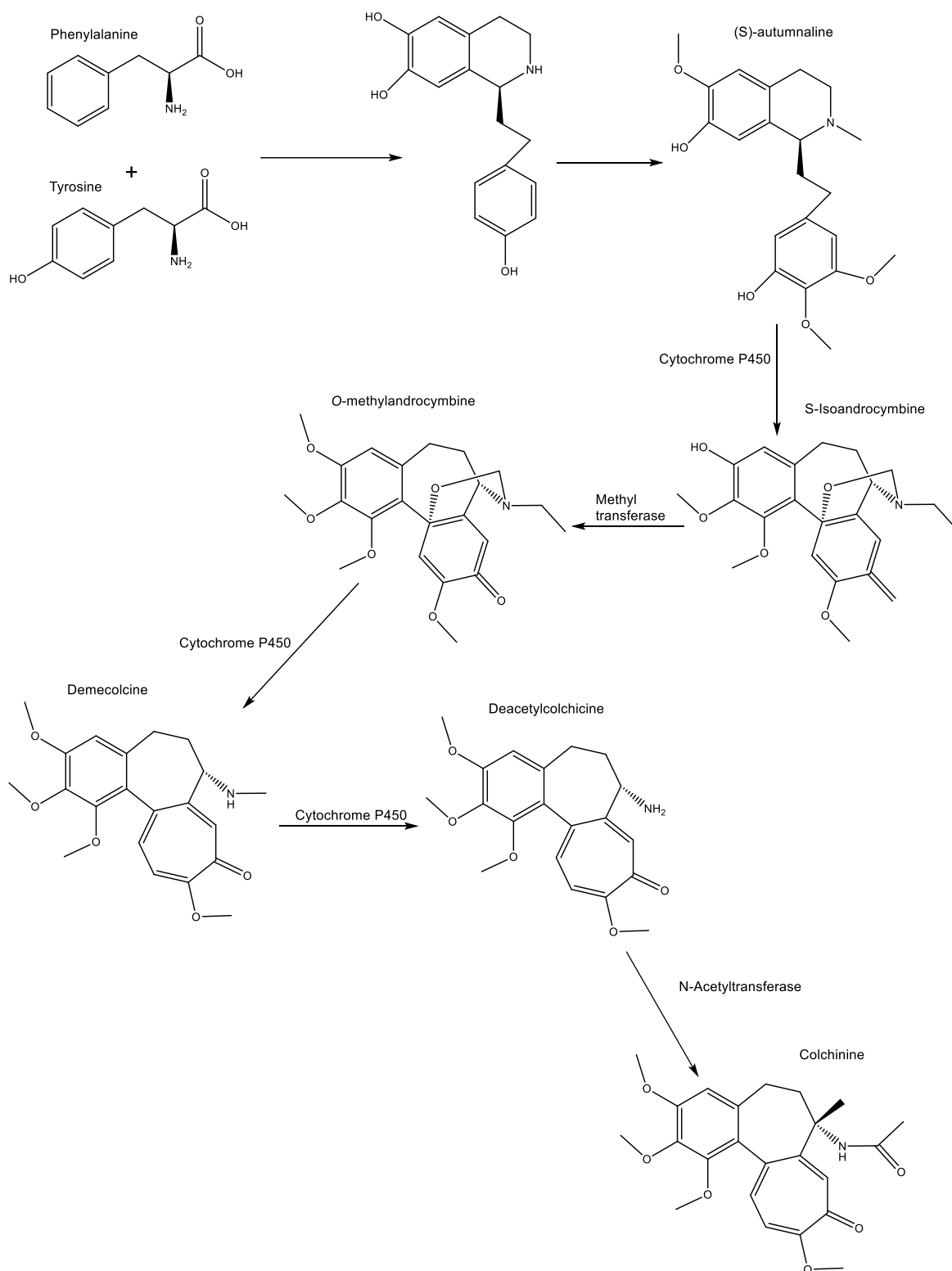


**Figure 2.20: Biosynthesis of colchicine.**<sup>241-245</sup>

## 2.2.6. Coumarins

**Background:** Coumarins are polyphenolic compounds belong to the family of benzopyrones consisting of a benzene ring joined to a pyrone ring. Coumarin related compounds are based on the coumarin structure with additional ring and side chains. These are split into four main classifications; simple coumarins, furocoumarins, pyrano coumarins and pyrone substituted coumarins.<sup>251-255</sup>

Coumarin is classified as a simple coumarin and is found within cassia cinnamon and *Symphoricarpus* L. *albus*, commonly known as snowberry. Psoralen is one of the two basic furocoumarin which is a precursor to other furocoumarin such as 5-methoxypsoralen and 8-methoxypsoralen. Furocoumarins are a class of compounds found natural in plant species with phototoxic properties, which are synthesis by binding of coumarin to a furan ring in either a linear (psoralen) or angular (angelicin) fashion in a response to stress (Figure 2.21).

Coumarin and furocoumarins are biosynthesis from phenylalanine via cinnamic acid and coumaric acid to form basic coumarins of which umbelliferone is converted into psoralens as shown in Figure 2.22 and are found within the plants families *Apiaceae*, *Caprifoliaceae*, *Thymelaeaceae* and *Rutaceae* (Figure 2.13).<sup>256-</sup>

259

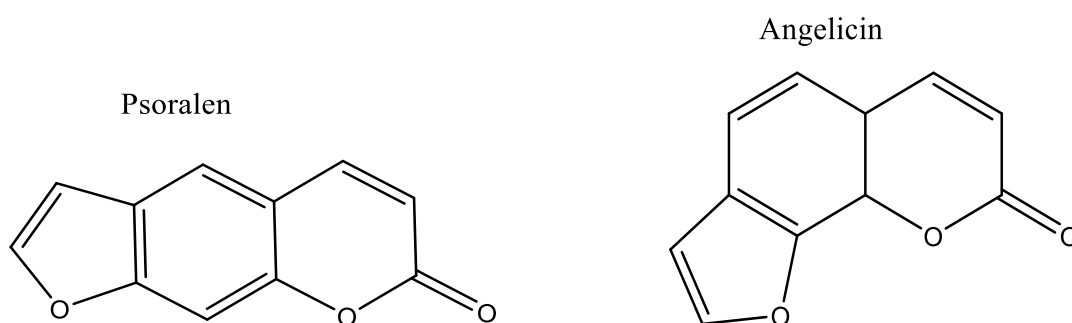


**Figure 2.21: Structure of linear and non-linear furocoumarins**

The *apiaceas* family contains a number of edible plants and herbs and spices such as carrot, dill, cumin, fennel and parsley. However, the family also includes a number of toxic plants including water hemlock and giant hogweed.<sup>260</sup> The

*Caprifoliaceae* family, commonly known as the honeysuckle family, generally form with flowers and berries in pair and are closely related to the *Adoxaceae* family. Many species produce edible berries but the vegetation have a diaphoretic and laxative effect.<sup>261</sup>

**Pharmacological effects:** Furocoumarins when exposed to ultra-violet (UV) light react with the deoxyribonucleic acid (DNA), disrupting the replication and in contact with skin caused burns and blisters known as phytophotodermatitis. Photosensitisation occurs when furocoumarins and the nucleic acids of the DNA form molecular complexes through Van der Waal's attraction and hydrogen bonding, which is then bonded to pyrimidine bases through cyclo-addition on exposure to UV radiation. Finally cross-linking is formed between this and another pyrimidine moiety on the opposite strand of DNA when. The cross linked furocoumarin, known as bifunctional psoralens are more toxic compared to monofunctional psoralens as they have the ability to create extensive damage to the DNA. Due to the type of reaction taken place it is uncommon to occur in angular furocoumarins.<sup>262, 263</sup> The furocoumarins form molecular complexes with the DNA nucleic acids via weak forces such as Van de Waal's attraction. UVA light (320-400 nm) is then absorbed by the compound resulting in excitation of electrons from the ground state to an unoccupied orbital. The compound is then converted to the triplet state by a change in the electron spin, resulting in a cyclo addition of the pyrimidine base and the furocoumarin (Figure 2.23). Finally is the furocoumarin absorbs additional UVA light then cross-linking between opposite DNA strands may occur.<sup>263</sup>

**Uses:** Furocoumarin are used in photo ultra-violet A (PUVA) therapy for treatment of conditions such as eczema, psoriasis, vitiligo and skin conditions linked to certain lymphomas. Psoralen based preparation are taken orally or topically through bathing and the patient is then exposed to ultraviolet A light.<sup>264-269</sup>

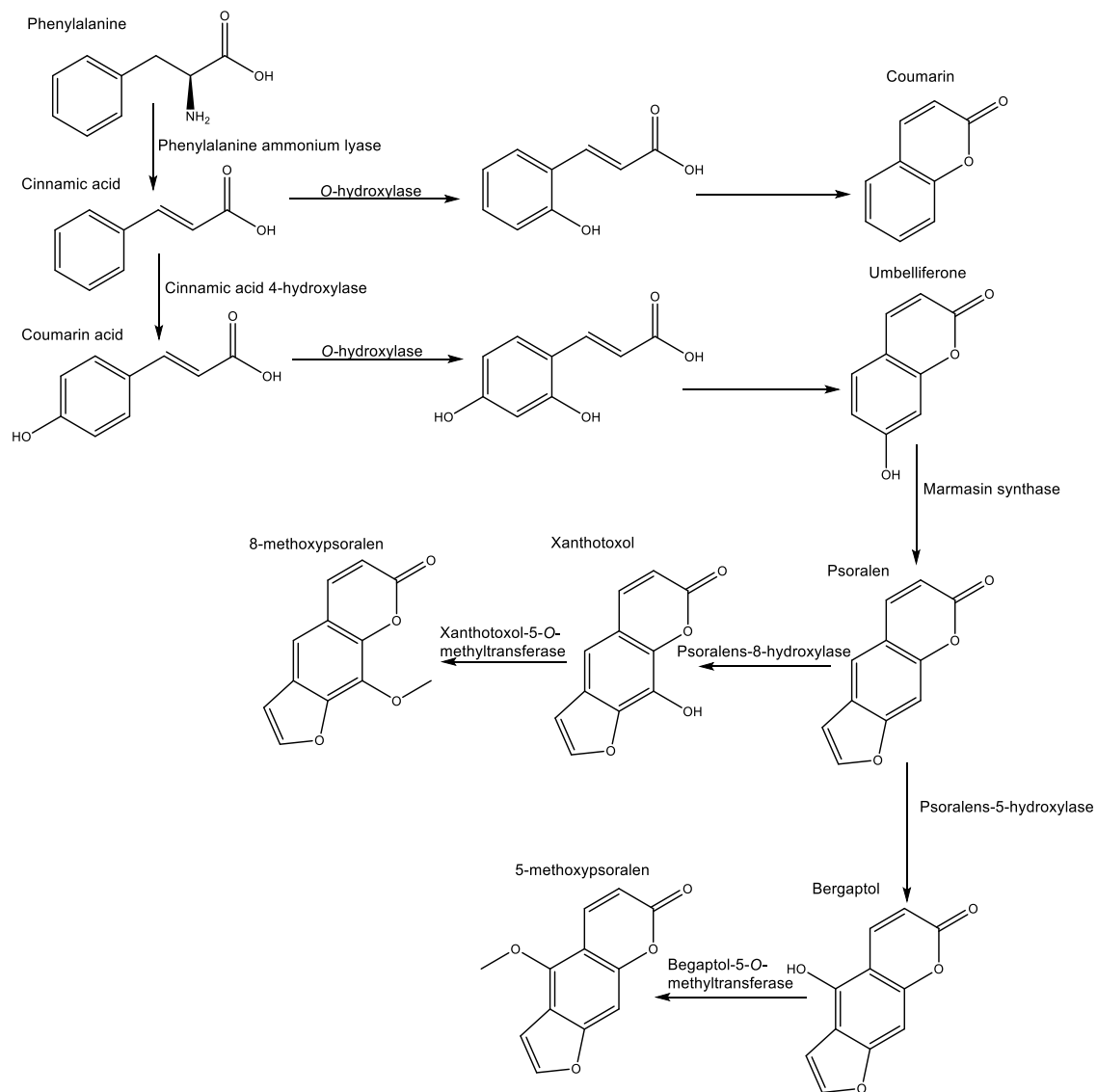


Figure 2.22: Biosynthesis of coumarin and coumarin related compounds.<sup>256-</sup>

259

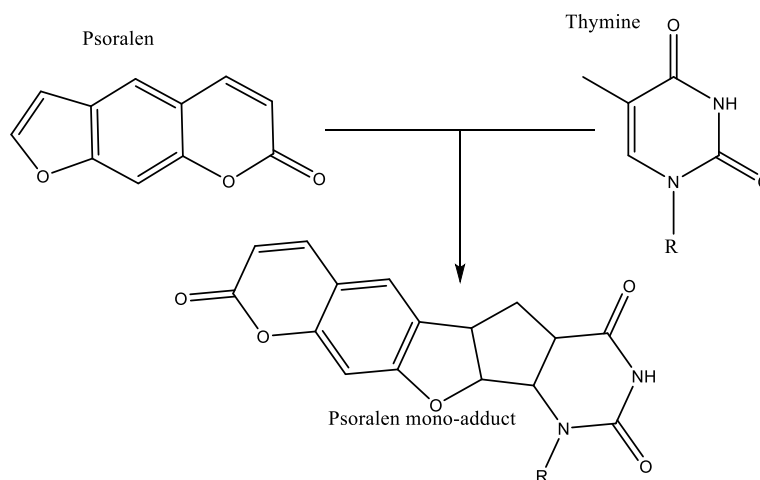


Figure 2.23: Formation of adduct between psoralen and a thymine base. R represents the DNA linkage.<sup>263</sup>

### 2.2.7. Digitoxin and Digoxin

**Background:** Digitoxin and digoxin are secondary cardiac glycosides which occur naturally in the *Digitalis* L. genus, commonly known as fox glove, such as *Digitalis purpurea* and *Digitalis ferruginea* which are member of the *Scrophulariaceae* family (Figure 2.13). The genus *Digitalis* contains over 20 species of herbaceous perennial plants, shrubs, and biennials which are native to Europe, western Asian and northwest Africa.<sup>270-272</sup> Digoxin is a hydrolysed form of digitoxin which is synthesised from cholesterol via a multi-step enzymatic process as shown in Figure 2.24.<sup>273</sup>

**Pharmacological effects:** Cardiac glycoside block the myocardium  $\text{Na}^+/\text{K}^-$  ATPase which produces a positive inotropic effect. The binding of digitoxin and digoxin to the  $\text{Na}^+/\text{K}^-$  ATPase activates tyrosine kinase Src P13K, phospholipase C and Ras/mitogen-activated protein kinase (MAPK) pathways leading to apoptosis.<sup>271, 274, 275</sup> The sodium potassium ATPase was first characterised around the turn of the 19<sup>th</sup> century and is one of the first membrane proteins to be characterised. In 1957 Post and Jolly showed that ATPase is responsible for the transfer of three sodium ions and two potassium ions across the plasma membrane.<sup>276-278</sup> ATPase also facilitate the secondary transport of molecules and other ions across the membrane.

*Digitalis* inhibits the  $\text{Na}^+/\text{K}^+$  ATPase in cardiomyocytes resulting in an increase in cytoplasmic sodium levels which causes the inhibition of the sodium calcium exchanger which has a direct effect on heart contractility. Cardiotonic steroids bind, from the extracellular side, to the  $\text{Na}^+/\text{K}^+$  ATPase. The cytoplasm gate opens allowing three sodium ions to bind to the sites in the middle of the membrane then the gate closes, and the P-domain is phosphorylated by ATP resulting in the opening of the outer gate and the release of the three sodium ions. This then allows potassium to bind to the binding site and the P-domain is dephosphorylated causing the cytoplasmic release of the potassium ions.<sup>279, 280</sup> *Digitalis* reduces the

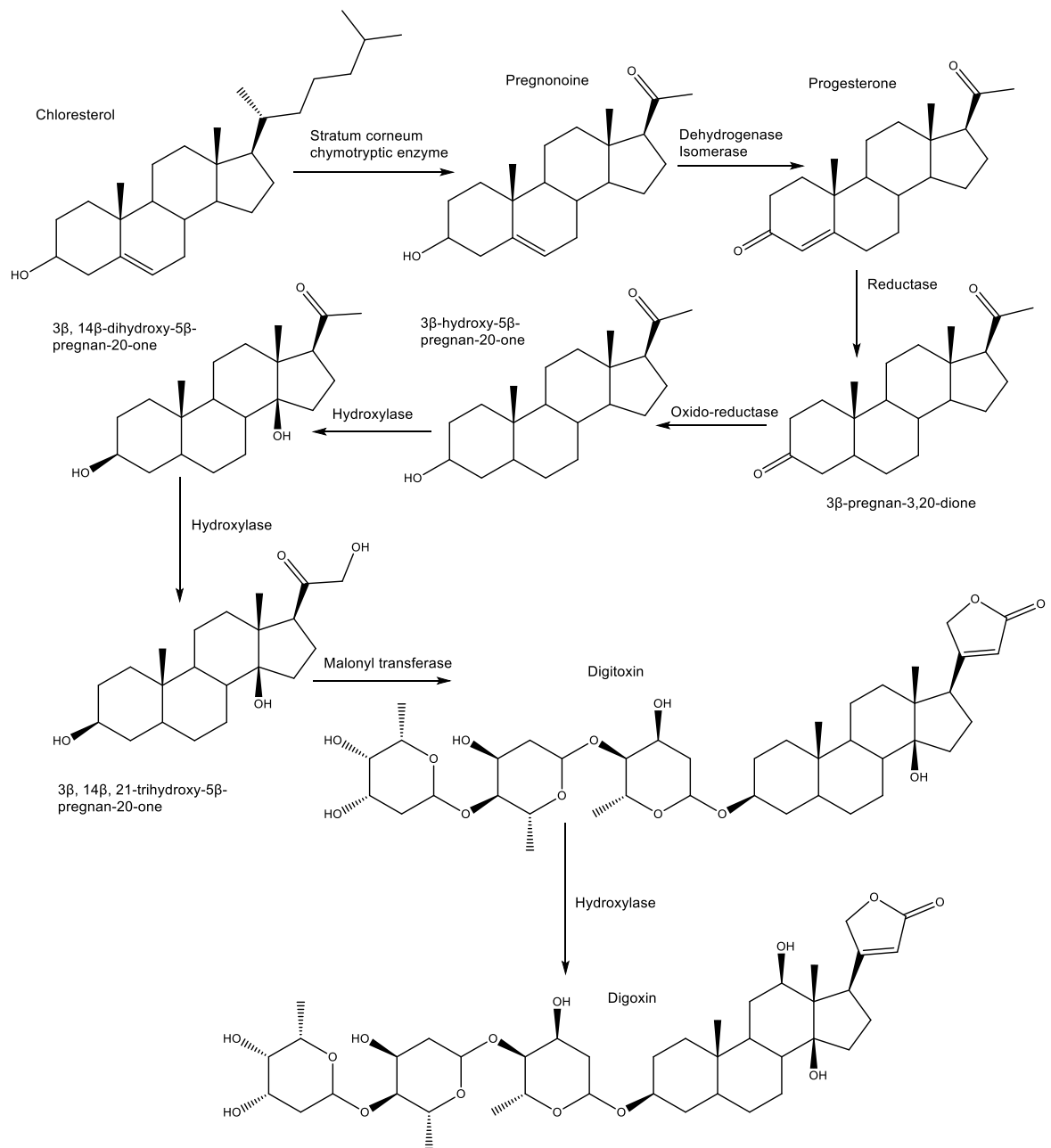


**Figure 2.24: Biosynthesis of digitoxin and digoxin.**<sup>273</sup>

active pumping of sodium ions out of the cell which decreases the sodium concentration gradient resulting in the sodium calcium exchanger moving calcium out of the cell. In addition when the ATPase is inhibited the resting membrane potential, normally between -30 and -70 mV, increases which causes an increased risk of arrhythmias due to membrane excitability.<sup>276, 281</sup> Ingestions of large amounts causes severe symptoms after 6 hours including nausea, vomiting arrhythmia and vision disturbances. More dangerous in elder individuals with previous kidney failure or heart attack. Treatment can include replenishing of potassium.<sup>270, 281</sup>

**Uses:** Digitoxin and digoxin are clinically approved for the treatment of heart failure and arrhythmia in both human and veterinary medicine and has been used as a treatment for congestive heart failure for more than a century. Preparations are available in oral and intravenous forms including elixirs, capsules, pills and ampoules. They have also been shown to have anti-cancer effects through cytotoxicity and anti-proliferation effects on tumour cells.<sup>271, 272, 274, 275, 277, 281-283</sup>

### 2.2.8. Hellebrin

**Background:** Hellebrin is a bufadienolides, which are a type of steroid with a 2-pyrone ring and show cardiotoxic, anaesthetic and cytotoxic activity, found within plants of the genus *Helleborus* L (Figure 2.13).<sup>284</sup> The genus *Helleborus* L. is a rhizomatous evergreen perennial belonging to the *Ranunculaceae* family native to Europe and western Asian which is mostly cultivated for ornamental purposes and is a popular garden flower due to the flowering during winter months.<sup>285-290</sup>

Hellebrin is synthesised from cholesterol following the same pathways as those used for the biosynthesis of digitoxin and digoxin as shown in Figure 2.25.<sup>291, 292</sup>

*Helleborus* L have also feature twice in Greek mythology, in the Greek myth of Melampus who used *Helleborus niger*, Black Hellebore, to cure the daughters of King Proteus from a madness which made them believe they were cows.

*Helleborus* L appears again in the myth of Heracles who was treated for madness which drove him to kill his wife and children with a hellebore from Antikyra.<sup>284</sup>

**Pharmacological effects:** Hellebrin causes cytotoxicity by the inhibition of Na<sup>+</sup>/K<sup>-</sup> ATPase as described in the section 1.3.7.<sup>289, 293-295</sup> Hellebrin promotes cell autophagy by activating the expression of caspase 3, 7 and cleaved caspase 7 proteins which causes the activation of the phosphoinositide 3-kinase (PI3K) protein resulting in an increase of the ratio of Bax to Bcl-2.<sup>294, 295</sup>

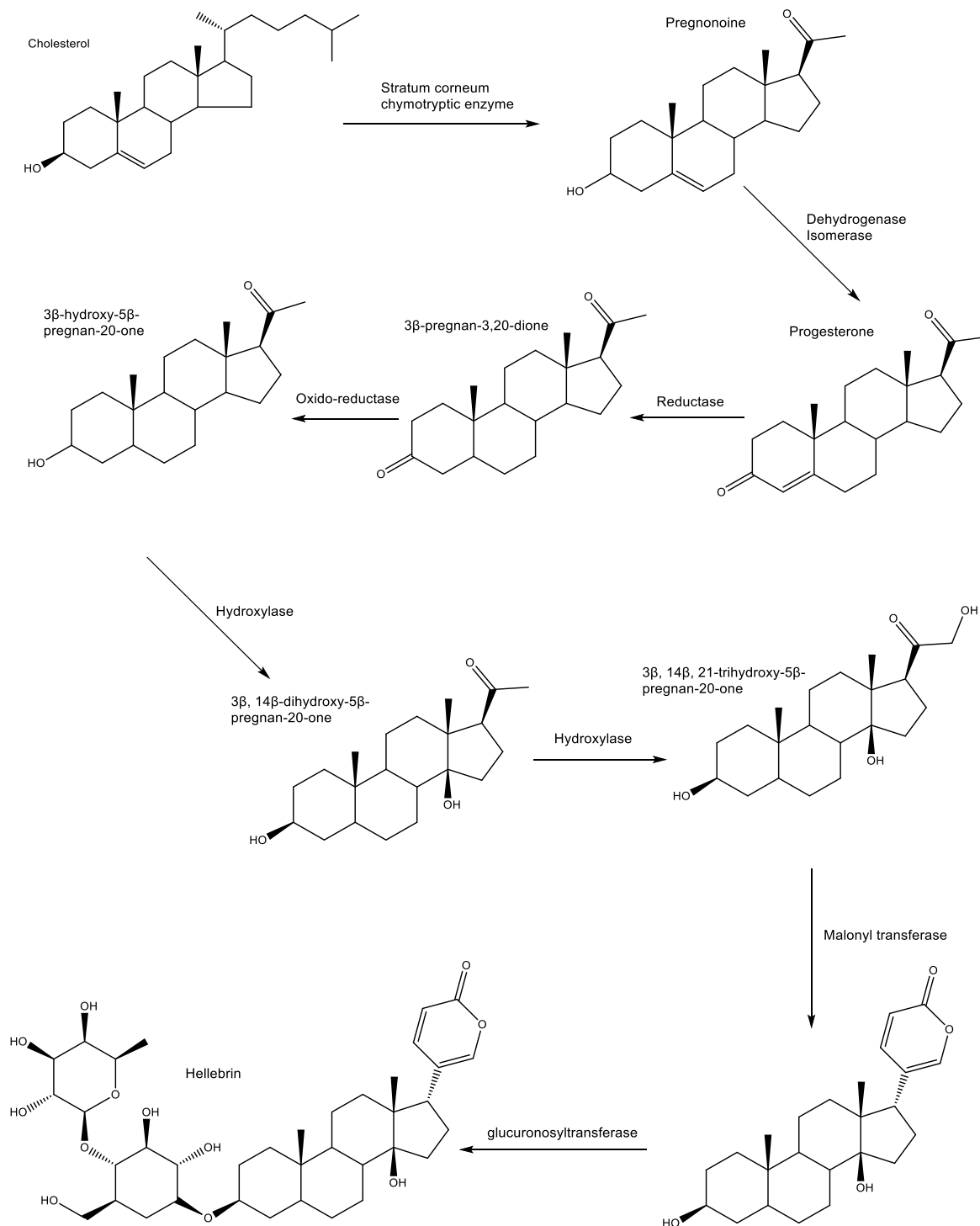


**Figure 2.25: Biosynthesis of hellebrin.**<sup>291, 292</sup>

**Uses:** Both Hippocrates and Theophrastus acknowledges the purgative and dangerous properties of the roots of black hellebore. Specific mentions of the use of black hellebore for the treatment of epilepsy date back to 40-90 AD where

Padanius Dioscorides described the use of black hellebore as a popular treatment for epilepsy and the insane. Around the same period Celsus also documented the effectiveness against “black bite disease” which resulted in madness. *Helleborus* species more recently have been reported to have anti-rheumatic, anti-inflammatory, anti-cancer, anti-diabetic, anti-bacterial and antioxidant properties and have been used for tooth ache, abortion, skin diseases and sore joints. However, the therapeutic effects have long been overshadowed by its high toxicity which have been known since the age of antiquity.<sup>284</sup> *Helleborus niger* is used in the treatment of tumour patients in Germany and *Helleborus purpurascens* was used in Romanian traditional medicine to aid in healing of chronic diseases.<sup>288, 296</sup>

### 2.2.9. Salvinorin A

**Background:** Salvinorin A, a diterpene, is believed to be the active component in *Salvia L. divinorum*. *Salvia L. divinorum* is a perennial herb, found originally in northern Mexico, commonly known as Diviner’s sage or Magic mint (Figure 2.13). Salvinorin A is biosynthesis via a two-step process, initially isoprenoid is form either from acetyl co-enzyme A via the mevalonate pathway or from pyruvate and D-glyceraldehyde-3-phosphate via the methylerythritol pathway. Isoprenoid is the converted into salvinorin A via a multi-step biosynthetic pathway utilising kolavenyl diphosphate synthase (KPS), diterpene synthase as well as general enzymatic reaction as show in Figure 2.26.<sup>297-299</sup>

**Pharmacological effects:** Salvinorin A effects the kappa opioid receptors which are found in the brain and spinal cord and has been found to have a variety of neurological effects including psychotomimesis, analgesia, sedation and diuresis. The effects of salvinorin A can be achieved via oral and sublingual exposure but is most commonly inhaled using dried leaves or plant extracts which effect lasting approximately 1 hours.<sup>298, 300, 301</sup> Studies in both animals and humans have shown that salvinorin A exhibits psychoactivity which profound hallucinations occurring after the inhalation of 200-500 ug of salvinorin A, with leaves found to contain 0.89 – 3.70 mg/g dried weight.

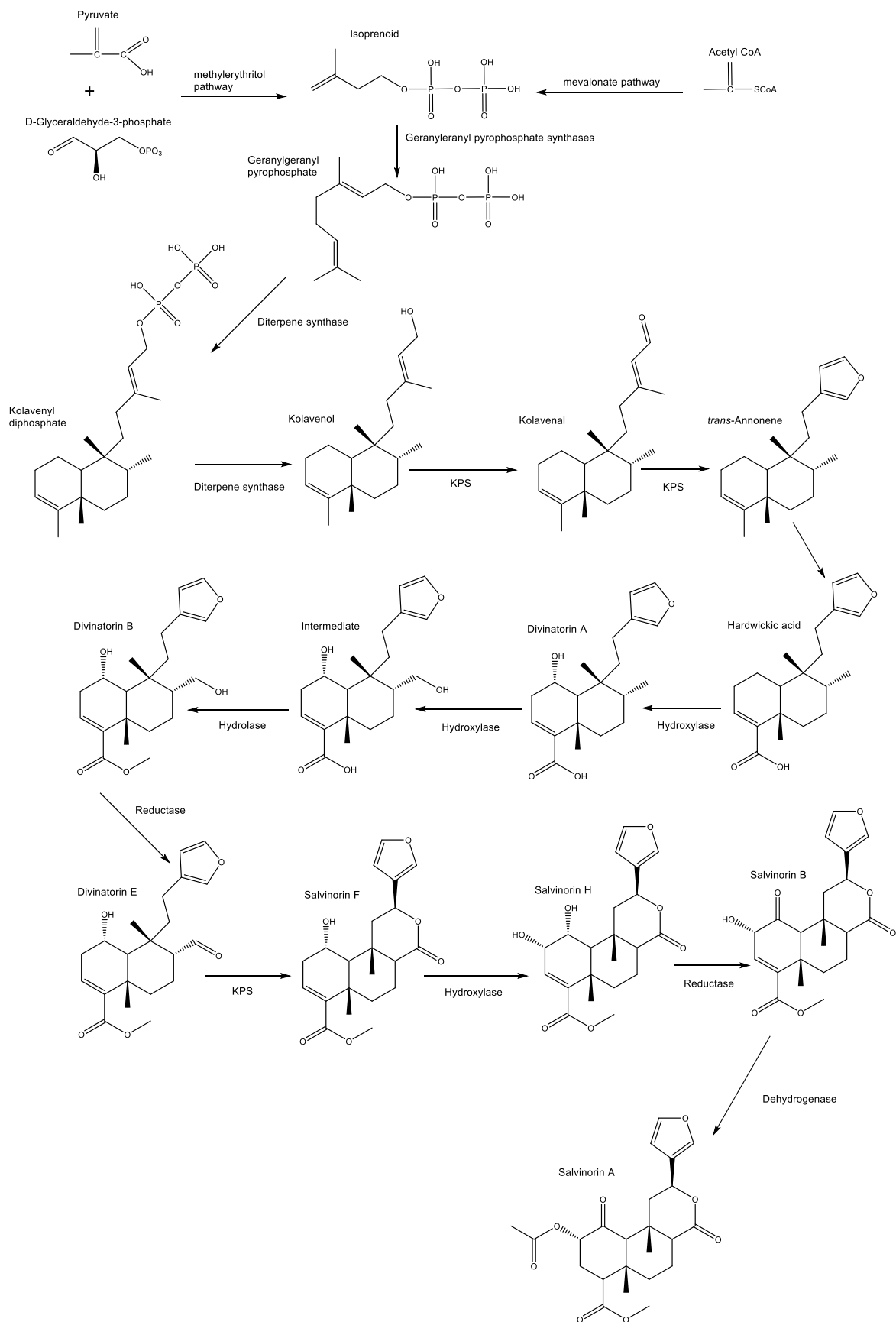


Figure 2.26: Biosynthesis of salvinorin A.<sup>297-299</sup>

With a study conducted by Johnson *et al.* which surveyed users suggesting that the effects of *Salvia divinorum* are brief and that users often feel an improved mood or insight, with reports of effects including neurological, cardiovascular and gastrointestinal effects particularly when mixed with other substances. With reports from a controlled study reporting “peoples experiences were classified as changes in spatial orientation, feelings of energy or pressure on different parts of the body and unusual and sometimes reoccurring themes across sessions such as revisiting childhood memories, cartoon-like imagery and contact with entities. Participants were largely behaviourally inactive”.<sup>302</sup>

**Uses:** Diviner’s sage was originally used for shamanistic purposes by the Mazatec population, it used in religious rites still continues in some indigenous Mexican cultures. The Mazatec believed that *Salvia divinorum* allowed the user to travel to heaven and speak to God and the saints, gaining its names from its use in divination. It is also used for the native treatment of diarrhoea, headaches, rheumatism and a semi-magical disease, panzon de barrego (swollen belly) caused by a curse from an evil sorcerer.<sup>303</sup> Traditionally the leaves would either chewed whole or crushed to extract the juice which was then drunk. Small doses, 4-5 leaves, were used as a healing tonic and large doses, 40-120 leaves, were used to induce hallucinations. Preparation of dried leaves, leaf extracts and tinctures are readily available online in “head” shops and are used as a recreational drug for its hallucinogenic properties.<sup>23, 24, 298, 300-304</sup>

### 2.2.10. Solanine

**Background:** Alpha-Solanine is a naturally occurring steroidal glycoalkaloids, synthesised from cholesterol via solanidine, found in plants of the *Solanum* family which is a member of the *Solanaceae* family including potato, *Solanum tuberosum* and the perennial climber *Solanum L. dulcamara* (Figure 2.13). Solanine is an effective defence against insects, worms and microbial pest but also affects the potato flavour at elevated level. The highest concentration of  $\alpha$ -solanine is found in areas undergoing high metabolic activity such as sprouts and peels with small

immature tubers also contain higher levels. Common ranges are 1-15 mg/100 g but are toxic to humans at around 20 mg/100 g. Elevated levels being triggered by stress caused by disease, light, mechanical damage and storage temperature meaning potatoes must be handled with care during and after harvest. Alpha-solanine is also poorly water soluble and not broken down during the cooking process.<sup>305-309</sup> The biosynthesis involves the conversion of cholesterol to solanidine, utilising dioxygenase for potato solanidine synthesis (DPS) which through the addition of three sugar moieties is converted into  $\alpha$ -solanine utilising solanidine galactosyltransferase (SGT1), solanidine glucosyltransferase (SGT2) and  $\beta$ -solanidine rhamnosyltransferase (SGT3) as shown in Figure 2.27.<sup>307, 310-312</sup>

**Pharmacological effects:** Daily consumption of potatoes leads to an accumulation of solanine. Poisoning causes gastrointestinal disorders and neurological issues. Symptoms include nausea, diarrhoea, vomiting, burning throat, heart arrhythmia, hallucinations, paralysis, fever, jaundice. Severe poisoning causes respiratory failure, heart failure and coma. Due to the bitter taste of the alkaloids, solanine poisoning is rare except in times of food shortages when stressed or green potatoes are consumed.<sup>309</sup>

**Uses:** Due to its potent pesticidal and fungicidal properties, solanine has been used in its hydrochloride salt form as an agricultural insecticide.<sup>313</sup>

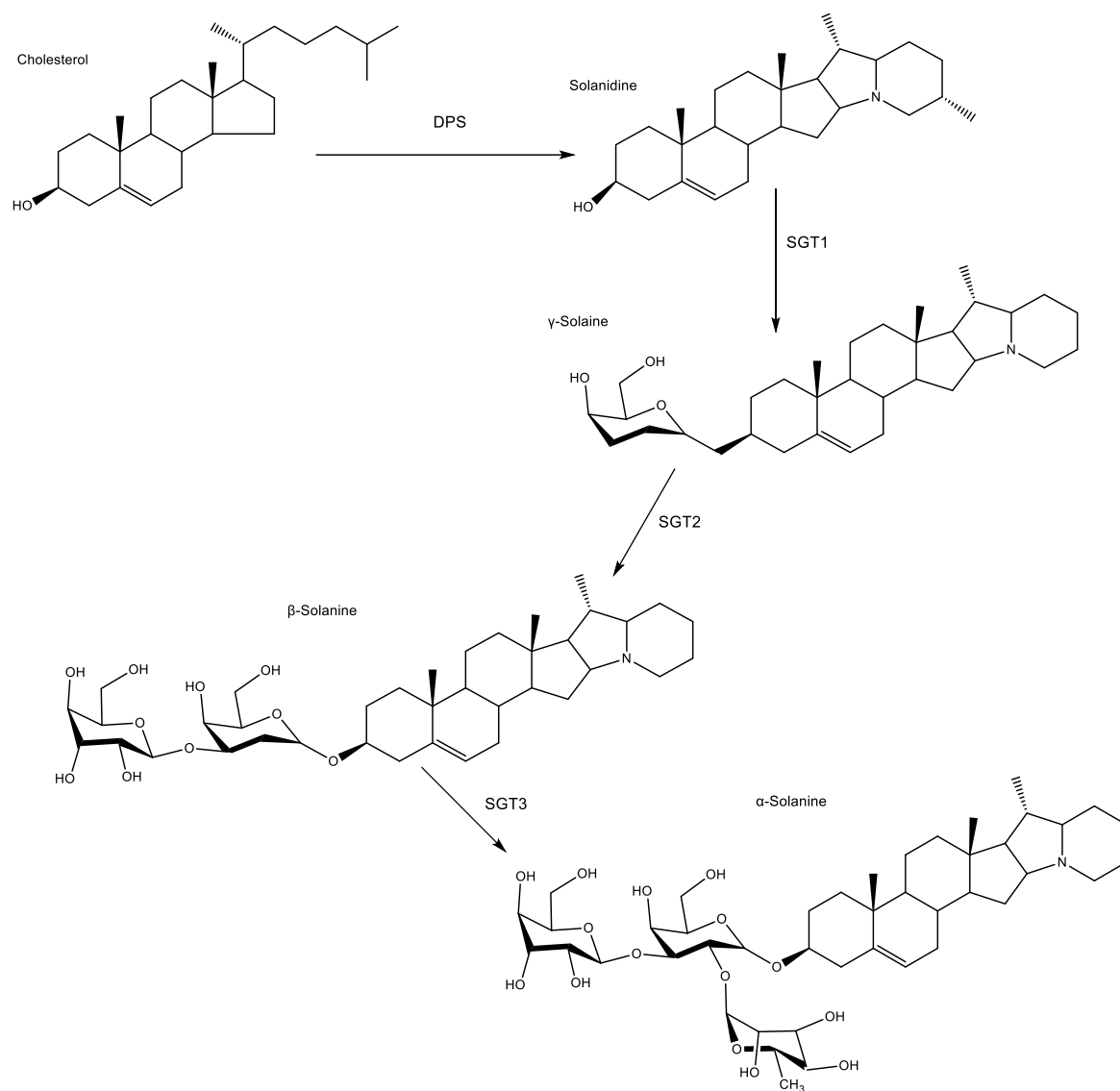


**Figure 2.27: Biosynthesis of  $\alpha$ -Solanine.**<sup>307, 310-312</sup>

### 2.2.11. Strychnine

**Background:** Strychnine is a monoterpene indole alkaloid found in the seeds of the *Strychnos* L. genus, a member of the *Loganiaceae* family. Strychnine and brucine are the main alkaloid found within the seed with strychnine being the most abundant and most toxic alkaloid present in the seeds with reported lethal doses of 50-100 mg in adults and 15 mg in children. Members of the strychnos genus are large trees native to Asia and Africa.<sup>314-324</sup> Strychnine is biosynthesised from the conversion of tryptophan to tryptamine utilising tryptophan decarboxylase which then reacts with secologanin in the presence of strictosidine synthase to form strictosidine. Strictosidine is converted into strychnine via a multistep enzymatic

pathway utilising Strictosidine- $\beta$ -D-glucosidase, glutamine synthetase and Geissoschizine oxidase as shown in Figure 2.28.<sup>325-327</sup>

**Pharmacological effects:** Strychnine is rapidly absorbed in the gastrointestinal tract and is a competitive inhibitor of the glycine receptor which is a neurotransmitter found in the family of ligand gated ion channels. The glycine receptor is an anionic Cl<sup>-</sup> channel, the receptor activation by glycine opens the anion selective channel causing an influx of Cl<sup>-</sup> which stabilizes the resting potential of the cell by hyperpolarisation resulting in the inhibition of neuron firing.<sup>314, 322, 324</sup> Strychnine blocks the postsynaptic receptor uptake of glycine in motor neurons of the spinal cord resulting in powerful long lasting contractions<sup>319</sup> Symptoms of strychnine include dizziness, nausea, restlessness and painful muscle spasms, with severe spasms leading to tachycardia, hyperthermia, respiratory failure and death by paralysis of the respiratory and spinal muscles or by cardiac arrest.<sup>314, 315, 319, 322</sup> There is no antidote for strychnine poisoning with treatment being with activated charcoal and the administration of benzodiazepines to control muscle spasms.<sup>314</sup>

**Use:** *Strychnos nux vomica* L. is used as a traditional Chinese medicine, included in the Chinese pharmacopeia, for the treatment of central nervous system diseases, pain, fever, vomiting, abdominal cramps and malaria and has been used for hundreds of years as a rodenticide.<sup>314-316, 318, 321-323</sup> Due to the level of toxicity of strychnine from *Strychnos* L. seed the use of unprocessed seeds is strictly prohibited.<sup>316, 321</sup>

### 2.2.12. Thujone

**Background:** Thujone is a monoterpene ketone which naturally occurs in two diastereomeric forms,  $\alpha$ -thujone and  $\beta$ -thujone within *Artemisia absinthium* L., a member of the *Asteraceae* family. The *Asteraceae* family is the largest flowering family in the northern hemisphere consisting of 19000 species worldwide.

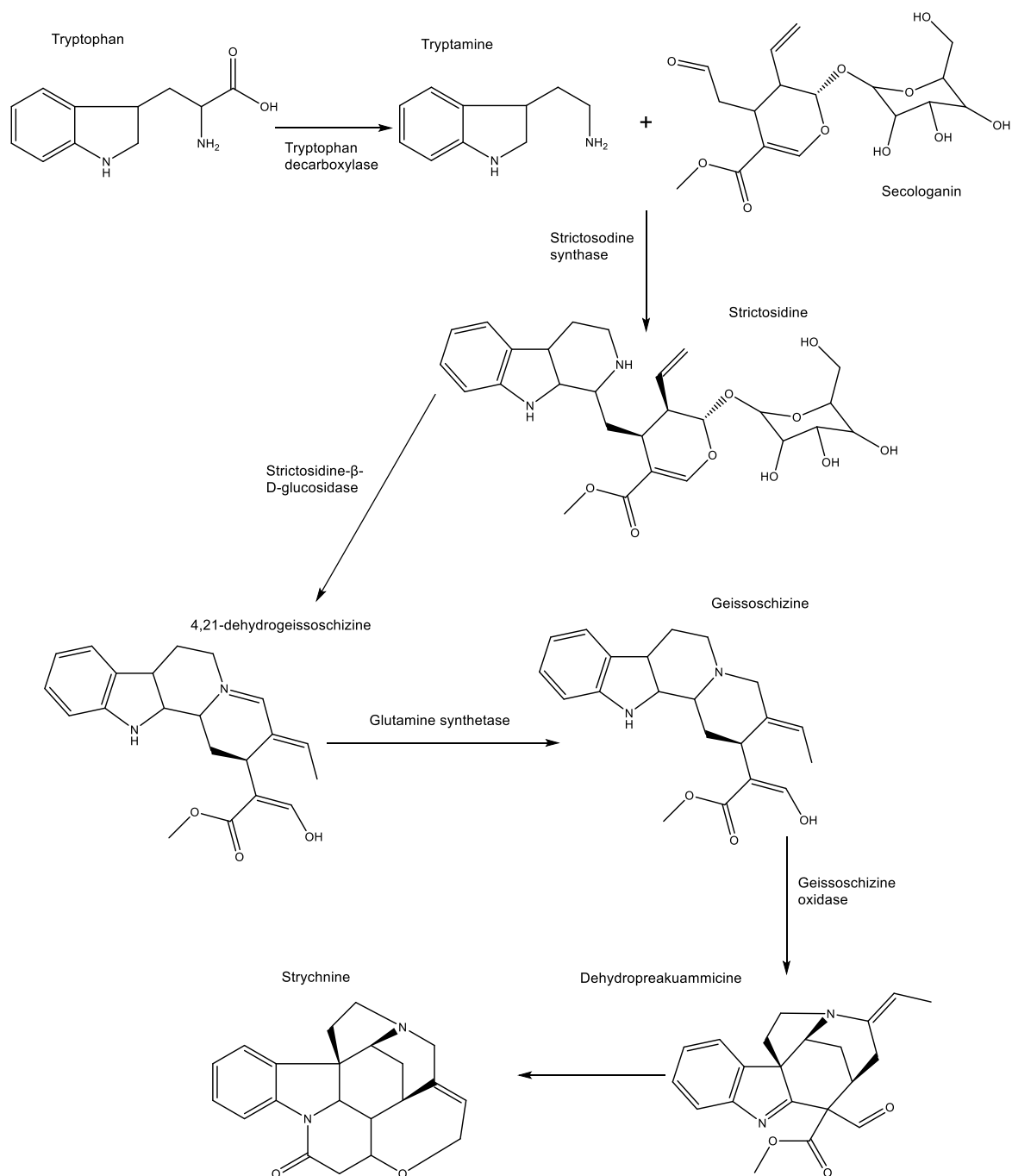


**Figure 2.28: Biosynthesis of strychnine.**<sup>325-327</sup>

Members of the *Asteraceae* family have flowers which comprise of multiple smaller flowers each as a disk flower or ray flower, a feature which is unique to the family . The family contains both ornamental and edible plants such as marigold, chrysanthemum, lettuce and artichoke. However, the family also contains a plant responsible for the well know hallucinogenic properties of the drink absinthe, *Artemisia absinthium* L (Figure 2.13).<sup>328</sup> *Artemisia absinthium* L. is a perennial herb native to Europe which is known for its aromatic leaves and bitterness, and

commonly called wormwood and absinthe. *Artemisia absinthium* essential oil contain the monoterpene thujone, occurring naturally as  $\alpha$  and  $\beta$  isomer at 33 % and 67 % respectively, which is responsible for the toxic effects on the central nervous system however,  $\beta$ -thujone is generally lower in toxicity.<sup>329</sup> Therefore,  $\alpha$ -thujone is generally considered to be the principle active ingredient in *Artemisia absinthium* and responsible for the hallucinogenic properties of absinthe. The biosynthesis of thujone involves the conversion of geranylgeranyl pyrophosphate to sabinene utilising sabinene synthase which is then converted into sabinone utilising two (+)-sabinene hydroxylases P450 enzymes (CYP750B1 and CYP76AA25). Sabinone is then converted into  $\alpha$  and  $\beta$ -thujone via an undetermined enzyme reaction as shown in Figure 2.29.<sup>325, 330, 331</sup>

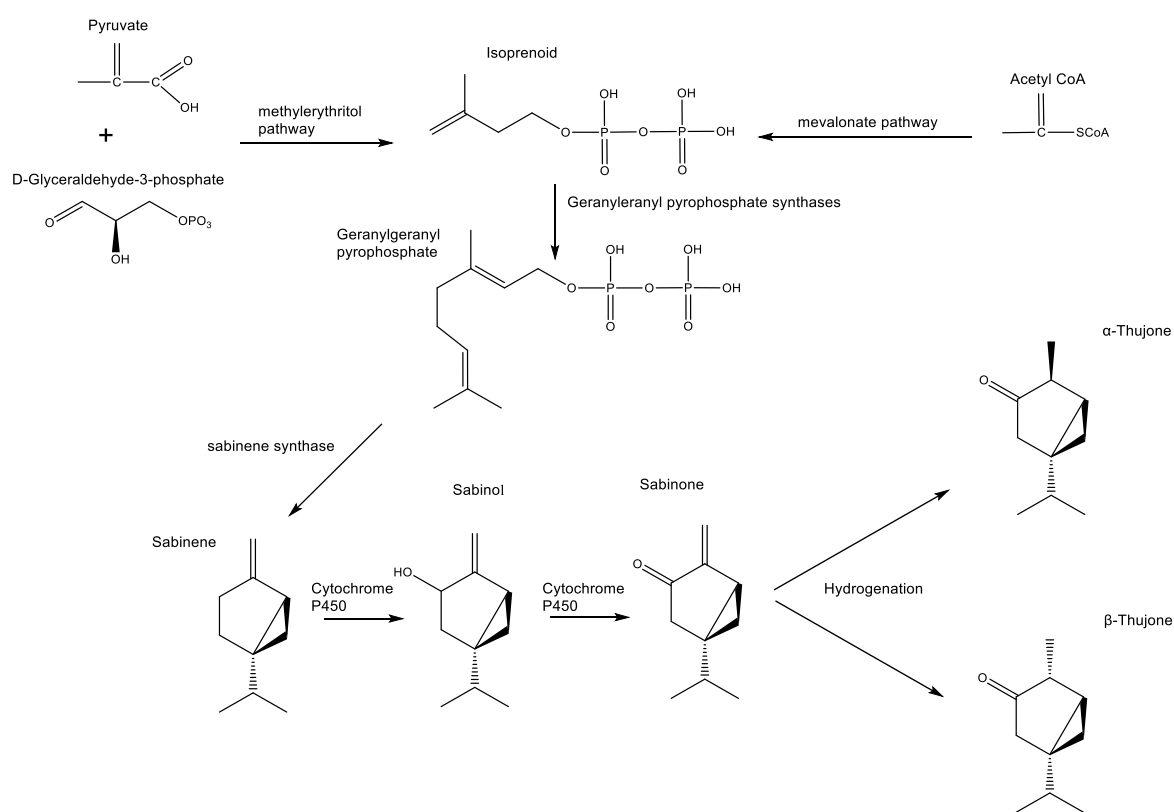


**Figure 2.29: Biosynthesis of  $\alpha$  and  $\beta$  –thujone.**<sup>325, 330, 331</sup>

**Pharmacological effects:** The major effects reported in humans is thought to be due to  $\gamma$ -aminobutyric acid type A receptor modulation of thujone causing epileptiform convulsions. However, there are only a few reports of wormwood intoxication generally caused by accidental or intentional ingestion of very large amounts of wormwood oil.<sup>332</sup> A study by K. Hold *et al.* established that  $\alpha$ -Thujone is a non-competitive blocker site of  $\gamma$ -aminobutyric acid A (GABA<sub>A</sub>) receptor which

is readily detoxified by metabolism to 7-hydroxy- $\alpha$ -thujone and other minor metabolites.<sup>333</sup>

**Uses:** *Artemisia absinthium* L. is known for its ethnopharmacological properties and documented medical uses can be dated back to an ancient Egyptian medical document dating to around 1552 B.C. It was recognised for its anthelmintic properties for which its name “wormwood” was derived. Wine-soaked wormwood leaves were recommended by Pythagoras to alleviate labour pains and by Hippocrates for the treatment of menstrual pain and rheumatism. Wormwood was considered a general remedy and was used as a purge and vermifuge during the middle ages. Due to the bitter taste of wormwood, it is believed that the name absinthe, used by the French for both the plant and the beverage, originated from the Greek word *apsinthion* meaning “undrinkable”. Large scale production of absinthe alcoholic extracts and distillates did not begin until the early 19<sup>th</sup> century when it began being considered not only as a cure-all but as an aperitif. During the French occupation of Algeria, absinthe was given to troops as a preventive measure for helminthiasis or fevers and mixed with water to kill germs and fend off dysentery. When troops returned, absinthe became a hit in bars and bistros all over France and at its peak, between 1880 and 1910, absinthe was conceived and marketed purely as an alcoholic beverage.<sup>332</sup>

The mass consumption of absinthe was claimed to produce a syndrome termed absinthism. A study by Valentin Magnan<sup>334</sup> defined absinthism as a separate syndrome to alcoholism causing auditory and visual hallucinations with alterations in consciousness after the consumption of absinthe. However, the study neglected the dose-response relationship as pure wormwood extract was injected into animals. A later study (Lachenmeier *et al.*, 2008) showed that the wormwood content was negligible, with additional studies hypothesising that absinthism was actually misdiagnosed alcoholism.<sup>332, 335</sup> Consumption of absinthe alcoholic beverage results in two effects, one from the ethanol and one from the thujone. Ethanol produces a sedative effect whereas thujone produces a state of excitation and is also a powerful convulsant.<sup>329</sup>

### 2.2.13. Veratridine

**Background:** Veratridine is a steroidal alkaloid found in members of the *Liliaceae* family including *Veratrum nigrum* L., *Veratrum album* L (Figure 2.13). and *Veratrum officinale* L.<sup>336, 337</sup> *Veratrum nigrum* L., commonly known as black false hellebore, and *Veratrum album* L, commonly known as white false hellebore, are native to Europe and parts of Asia are tall perennial herbs with pleated leaves which is commonly grown as an ornamental plant. Veratridine is biosynthesised from cholesterol to form verazine utilising cytochrome P450 enzymes specifically, cholesterol 22-hydroxylase (CYP90B27), 22-hydroxycholesterol 26-hydroxylase/oxidase (CYP94N1), 22-hydroxycholesterol-26-as transaminase (GABAT1) and 22-hydroxy-26-aminocholesterol 22-oxidase (CYP90G1). Verazine is then converted into veratridine via oxidation and esterification as shown in Figure 2.30.<sup>338, 339</sup>

**Pharmacological effects:** Veratridine acts on sodium channels causing the sodium channels to remain activated resulting in persistent depolarisation of excitable membranes increasing the permeability of sodium.<sup>336, 337, 340, 341</sup> The activated sodium channel causes an influx of Na<sup>+</sup> resulting in an increase in intracellular Na<sup>+</sup> concentration which stimulated ATPase activity in order to restore the ionic gradient. The depolarisation exacerbates neural cell damage and in addition trigger glutamate release which has a pivotal role in cell damage.<sup>342, 343</sup>

**Uses:** During the 19<sup>th</sup> century it was used a treatment for hypertension however side effects limited its clinical use. Poisoning from leaves of *Veratrum* plants have been reported in humans and cattle with symptoms similar to those of bioenergetic poisoning.<sup>337</sup>

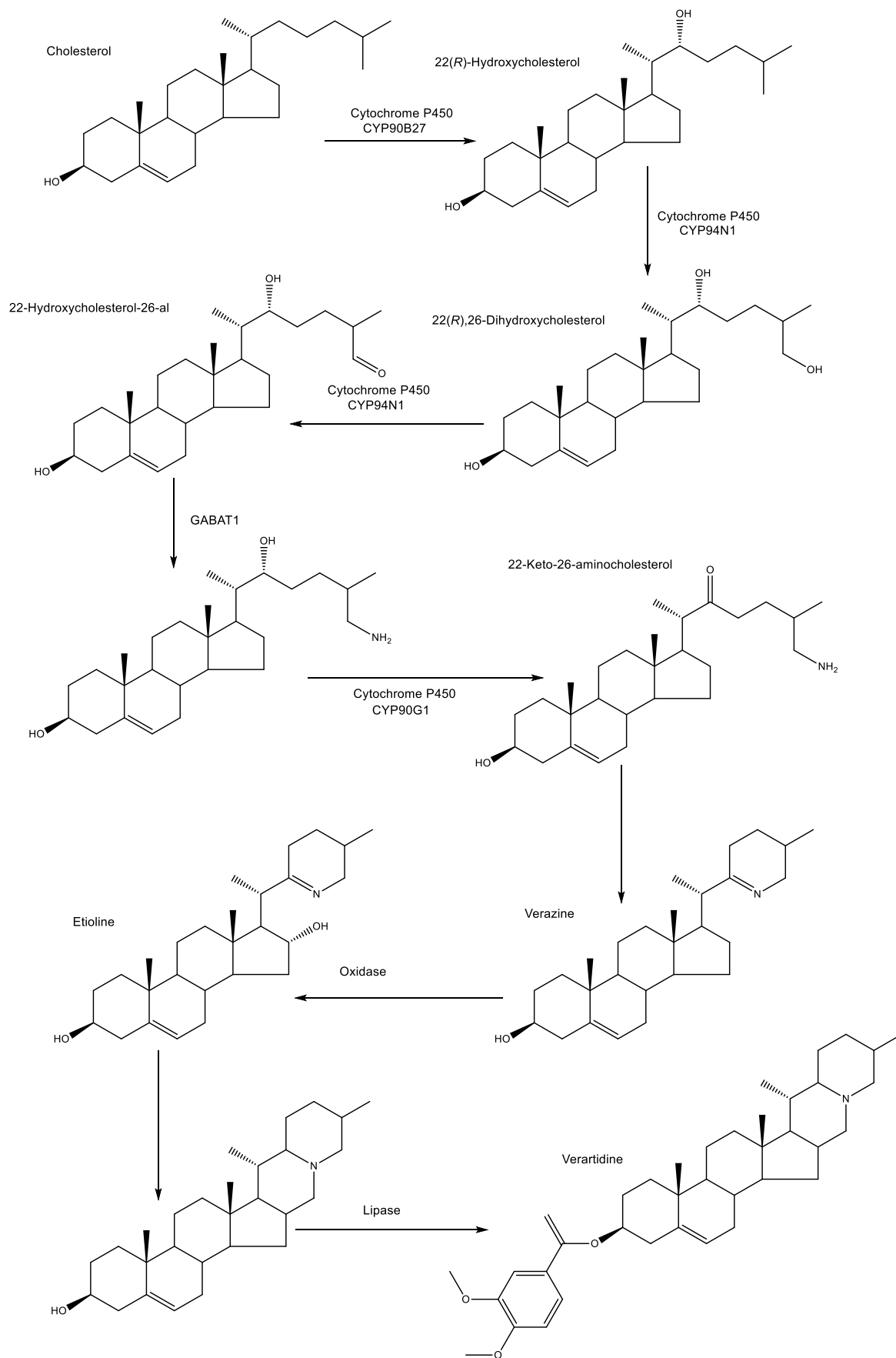


**Figure 2.30: Biosynthesis of veratridine.**<sup>338, 339</sup>

## Chapter 3: Aims

### 3. Aims

The main aim of this research is to develop applications for the analysis of complex samples via LC-MS. In order to achieve this aim, two methods will be developed and validated prior to the analysis of samples. The applications chosen were the analysis of thyroid hormones and the analysis of plant toxins.

Thyroid disorders are estimated to effect 1 in 20 people within the UK, however, many people remain undiagnosed. The current clinical method used within the NHS has limited sensitivity with a LOQ of 3 pmol/L and 1.5 pmol/L for T4 and T3 respectively with inaccuracies of 30 % at the LOQ which can often lead to a prolonged diagnosis period, particularly for hypothyroidism. In addition, each thyroid hormone must be tested for via a separate assay. The aim of developing a LC-MS method for the analysis of thyroid hormone is to reduce the analysis time as thyroid hormones would be analysed together whilst improving the levels of sensitivity and accuracy, which would in turn allow for better diagnosis. The method would also allow for the analysis of thyroid hormone supplements for content and dissolution testing. With the aim of having a method which can be applied to a variety of sample types. In addition this method will be used to support research within the Department of Sport, Exercise and Rehabilitation into the thyroid function in adolescent male academy footballers.

Alnwick Garden in Northumberland houses the largest poison garden in the UK, a brain child of the Dutchess of Northumberland which was opened in 2005.<sup>20</sup> The garden runs an extensive education program for school within the local areas leading to a collaboration to gain further scientific information regarding the plants within the garden. The aim of this study is to develop an LC-MS method for the analysis of 18 plant toxins found within a large variety of plants within the garden. In addition many of the plants analysed are available to purchase within garden centre however, there is little to no warning or safety information included. The developed method will allow for the simultaneous detection and quantification of all 18 compounds and will be applied to the analysis of plants materials obtained from Alnwick gardens. The results obtained will allow for the determination of risk based upon the dermal and ingestion risk models used by the environment protection

agency with the overall aim of providing comprehensive information which can be used to better inform the safe selling, purchasing and handling of these types of plants.

## Chapter 4: Experimental

## **4. Experimental**

### **4.1. Sample preparation**

Accelerated solvent extraction was performed using a Dionex ASE 200 consisting of control unit, solvent delivery system, extraction cell carousel and collection cell carousel from Dionex (Cheshire, UK). Sample concentration was performed using a Techne Sample Concentrator with dry heating block from Cole-Parmer (Staffordshire, UK). Sonication was performed using a Fisherbrand® ultrasonic bath operating at 50/60 Hz from Fisher Scientific (Loughborough, UK). Hellebrin extraction was performed using a Soxhlet extraction apparatus consisting of a heating mantle, round bottom flask, Soxhlet and condenser.

### **4.2. LC-UV**

For HPLC analysis the Thermo Surveyor HPLC (Thermo Finnigan, Hemel Hempsted, UK) used consisted of a quaternary pump, vacuum degasser, an autosampler, a thermostated column oven (set to 25°C) and photodiode array detector. Chromatographic separation was achieved using a reversed phase pentafluorophenyl column (Supelco 2.1 µm F5, 100 x 2.1 mm) from Sigma Aldrich (Dorset, UK). Sample aliquots of 10 µL were introduced onto the column at a flow rate of 200 µL/min. The analytes were separated using water + 0.2% formic acid (A) and methanol + 0.2% formic acid (B) as the mobile phase. UV detection was monitored at 240 nm with a bandwidth of 2.5 Hz, slit of 16 nm and attenuation of 1000 mAU

### **4.3. LC-MS**

For low resolution LC-MS analysis of thyroid hormones and plant toxins the Thermo Surveyor LC (Thermo Scientific, Hemel Hempsted, UK) consisted of a quaternary MS pump, vacuum degasser, a thermostated autosampler (set to 5°C) and a thermostated column oven (set to 25°C) coupled to a Thermo Scientific (Thermo Scientific, Hemel Hempsted, UK) LTQ XL ion trap mass spectrometer fitted with a heated electrospray ionisation (HESI) source. For high resolution LC-

MS of thyroid hormones analysis the Thermo Scientific ultimate 3000 LC (Thermo Scientific, Hemel Hempsted, UK) used consisted of a quaternary MS pump, a thermostated autosampler (set to 5°C) and a thermostated column oven (set to 25°C) coupled to a Thermo Scientific (Thermo Scientific, Hemel Hempsted, UK) Q-Exactive orbitrap mass spectrometer fitted with a heated electrospray ionisation (HESI) source.

For thyroid hormone analysis chromatography was achieved using a reversed phase pentafluorophenyl column (Supelco 2.1 µm F5, 100 x 2.1 mm) from Sigma Aldrich (Dorset, UK). Sample aliquots of 10 µL were introduced onto the column at a flow rate of 200 µL/min. The analytes were separated using water + 0.2% formic acid (A) and methanol + 0.2% formic acid (B) as the mobile phase. For plant poison analysis chromatographic separation was achieved using a reversed phase Eclipse™ Plus C18 column (3.5 µm, 100 x 4.6 mm) from Agilent (Stockport, UK). Sample aliquots of 10 µL were introduced onto the column at a flow rate of 300 µL/min. The analytes were separated using 0.1 % formic acid in water (A) and 0.1 % formic acid in methanol (B) as the mobile phase. The specific LC and MS parameters are show in Table 4.1 and the collision energies and monitored ions in Table 4.2.

#### **4.4. Prep-LC**

For preparative LC fractionation an Agilent Infinity semi-prep HPLC system was used (Agilent Technologies, Cheadle, UK) consisted of a binary pump, an autosampler, a UV/Vis detector and a fraction collector. Chromatography was achieved using a reversed phase SunFire® C18 ODS Prep column (10 mm x 150 mm, 5 µm) from Waters (Elstree, UK). Sample aliquots of 500 µL were introduced onto the column at a flow rate of 1.00 mL/min. The analytes were separated using water (A) and acetonitrile (B) as the mobile phase with the gradient profile shown in Table 4.3. UV detection was monitor at 250 nm with the fraction set to collect fractions greater than 100 mAU with a start and end peak detected at a 5 mAU/s slope.

**Table 4.1: Instrument parameters**

Parameter	Thyroid hormone analysis	Plant poison analysis		
Mobile Phase	A: water + 0.2% formic acid B: methanol + 0.2% formic acid	A: 0.1 % Formic acid in water B: 0.1 % Formic acid in methanol		
Pump program	Isocratic 70% B	Time (min)	% A	% B
		0.00	60	40
		10.00	10	90
		20.00	10	90
		20.10	60	40
		25.00	60	40
HESI temperature	200 °C	Ambient		
Ion source voltage	4.00 kV	4.50 kV		
Capillary voltage (V)	42	25, 45, 15, 14		
Transfer capillary temperature	350 °C	350 °C		
Auxiliary Gas	15	10		
Sweep Gas	1	5		
Sheath gas	60	10		
Ion Mode	Negative	Positive		
Scan mode	SRM	SRM		

#### 4.5. NMR

All nuclear magnetic resonance (NMR) spectroscopy analyses were performed using a JOEL ECS 400 NMR spectrometer operating at 400 MHz from Joel (Nieuw-Vennep, The Netherlands). Samples were submitted for proton, carbon and heteronuclear single quantum coherence (HSQC) NMR analysis.

**Table 4.2: Collision energies for LC-MS/MS**

<b>Compound</b>	<b>Collision energy (eV)</b>	<b>Fragmentation ion observed (<i>m/z</i>)</b>
T4 (low resolution)	28	776, 759, 605*
T4 (high resolution)	25	776, 759, 605*
T3 (low resolution)	27	650, 633*, 523
T3 (high resolution)	23	650, 633*, 523
rT3 (low resolution)	27	650, 633, 479*
rT3 (high resolution)	23	650, 633, 479*
T2 (low resolution)	29	524, 507*, 398
T2 (high resolution)	28	524, 507*, 398
5-methoxypsoralen	30.0	217, 202*, 185
8-methoxypsoralen	30.0	217, 202*, 185
Aconitine	24.0	646, 596, 586*
Atropine	24.0	290, 260, 124*
Capsaicin	35.0	328, 314*, 186
Cathinone	30.0	150, 132*, 105
Colchicine	23.0	400, 382*, 358
Coumarin	30.0	147, 119, 103*
Digitoxin	28.0	788, 743, 387*
Digoxin	29.0	804, 785, 387*
Hellebrin	32.0	747, 701, 585*
Psoralen	30.0	187, 159, 143*
Salvinorin A	30	455, 411*, 317
Scopolamine	23.5	304, 156, 138*
Solanine	40.0	869, 722, 706*
Strychnine	28.0	335, 307, 262*
Thujone	28.0	175, 133, 119*
Veratridine	25.0	674, 656, 492*

\* Quantification ion

**Table 4.3: Preparative LC gradient profile**

<b>Time (mins)</b>	<b>% A</b>	<b>% B</b>
0.00	90	10
100	90	10
200	70	30
240	70	30
240.1	90	10
245.0	90	10

## **4.6. Materials**

### **4.6.1. Thyroid hormone analysis**

Standards of T4, T3, rT3 and T2 were purchased from Sigma Aldrich (Dorset, UK) with a purity of  $\geq 98\%$ . Organic LC-MS grade solvents; methanol, acetic acid and formic acid were purchased from Fisher Scientific (Loughborough, UK). For dissolution media FaSSIF/FeSSIF/FaSSGF powder was purchased from Biorelevant (London, UK) and the additive; sodium hydroxide pellet and monobasic sodium phosphate monohydrate were purchased from Sigma Aldrich (Dorset, UK) and sodium chloride, hydrochloric acid and sodium hydroxide were purchased from Fisher Scientific (Loughborough, UK). Hypersep™ C18 100 mg solid phase extraction (SPE) cartridges were purchased from Thermo Fisher Scientific (Hemel Hempstead, UK). Nylon 0.2  $\mu\text{m}$  syringe filters were purchased from Thames Restek (High Wycombe, UK). Horse serum was purchased from TCS Biosciences (Buckingham, UK). Previously tested human blood serum samples were obtained from the Royal Victoria Infirmary, North Tyneside NHS trust. All biological samples were stored at  $-80^{\circ}\text{C}$  prior to analysis. Commercially available thyroid hormone tablets Cytomel®, Tiromel® were obtained from [www.uk-RXcart.com](http://www.uk-RXcart.com) and [www.buy-t3.co.uk](http://www.buy-t3.co.uk) respectively, and Dithyron® were obtained from [www.buy-t3.co.uk](http://www.buy-t3.co.uk).

#### **4.6.2. Plant toxin analysis**

Standards of aconitine, atropine, strychnine, (-)-scopolamine, veratridine, capsaicin, colchicine, coumarin, psoralen, 8-methoxypsoralen, 5-methoxypsoralen,  $\alpha$ -solanine, digitoxin, digoxin, (-)- $\alpha$ -thujone, S(-)-cathinone and salvinorin A were purchased from Sigma Aldrich (Dorset, UK) with a purity of  $\geq 95$  %. A Hellebrin standard was purchased from Enzo Life sciences (Exeter, UK) with a purity of  $< 99$  %. Organic LC-MS grade solvents; methanol, acetic acid and formic acid were purchased from Fisher Scientific (Loughborough, UK). The buffer additive: Ammonium formate was purchased from Fisher Scientific (Loughborough, UK). Nylon 0.2  $\mu\text{m}$  syringe filters were purchased from Thames Restek (High Wycombe, UK). Plant materials were obtained from Alnwick Gardens (Northumberland, UK) and online from [www.waitroseflorist.com](http://www.waitroseflorist.com), [www.crocus.co.uk](http://www.crocus.co.uk), [www.twelvenunns.co.uk](http://www.twelvenunns.co.uk) and [www.burncoose.co.uk](http://www.burncoose.co.uk).

#### **4.7. Preparation of standard solutions, samples and reagents.**

##### **4.7.1. Thyroid hormone analysis**

Stock solutions of each hormone were prepared at a concentration of 0.5 mg/mL in methanol and aliquoted into 100  $\mu\text{L}$  aliquots and stored at  $-20$  °C. Calibration standards were prepared daily for each analysis from the stock solution by diluting in mobile phase. Calibration standards were prepared over a concentration range of 0 – 200 ng/mL for low resolution LC-MS/MS and 0-150 ng/mL for high resolution LC-MS/MS for T4, T3/rT3 and T2, respectively. A full set of calibration standards were acquired at both the start and end of each chromatographic run cycle. In addition, a quality control standard was prepared at 50 ng/mL, by diluting stock standard solutions in mobile phase, and analysed at points throughout the run to ensure there was no deviation throughout the run. The concentration of the quality control was selected as it is mid-reference range for T4 [19]. Matrix matched calibration standards for LOQ and LOD determination were prepared in triplicate from the stock solution by diluting in horse serum and extracted by SPE. Calibration standards were prepared over a concentration range of 0.5 - 200 ng/mL for low resolution LC-MS/MS and 0.001 – 100 ng/mL for high resolution LC-MS/MS.

To make the fasted state small intestinal fluid (FaSSIF) buffer 0.84 g of sodium hydroxide pellet, 7.90 g of monobasic sodium phosphate monohydrate and 12.38 g of sodium chloride was added to approximately 1.8 L of type 1 water. The solution was pH adjusted to 6.5 with 1 M sodium hydroxide and make up to 2 L with type 1 water. To make the final FaSSIF media 4.48 g of FaSSIF/FeSSIF/FaSSGF powder was added to approximately 1 L of FaSSIF buffer. The solution was stirred until completely dissolved and make up to 2 L with FaSSIF buffer. The solution was allowed to stand for 2 hours prior to use. To make the fasted state gastric fluid (FaSSGF) buffer 3.2 g of sodium chloride was added to approximately 1.8 L of type 1 water. The solution was pH adjusted to 1.6 with 1 M hydrochloric acid and make up to 2 L with type 1 water. To make the final FaSSGF media 0.12 g of FaSSIF/FeSSIF/FaSSGF powder was added to approximately 1 L of FaSSGF buffer. The solution was stirred until completely dissolved and make up to 2 L with FaSSGF buffer.<sup>344</sup>

For tablet analysis the tablets were accurately weighed and then transferred to a 10 mL volumetric flask and made up to volume with methanol. The solution was sonicated for 10 mins and then further diluted to within the calibration range, based on the stated dosage, in methanol. Solutions were filter through a 0.22 µm and transferred to an autosampler vial.

For low resolution LC-MS serum samples were thawed and vortexed prior to extraction. The final developed method was applied to samples, prepared in triplicate, by transferring 500 µL to microcentrifuge tubes along with 500 µL of 0.1 % formic acid in water. Samples were vortexed and centrifuges at 5300 g for 5 minutes. The supernatants were loaded onto a HyperSep™ C18 solid phase extraction (SPE) cartridge, which were preconditioned sequentially with 2 mL of 0.1 % formic acid in methanol and 2 mL 0.1 % formic acid in water. The cartridge was washed with 1 mL of 30 % methanol in water and then the target compounds were eluted with 1 mL of 80 % methanol in water. The eluent was dried down under a stream of nitrogen and reconstituted in 50 µL of mobile phase. For high resolution LC-MS serum samples were thawed and vortexed prior to dilution. Samples were prepared by transferring 10 µL of sample to an autosampler vial and diluted with 990 µL of water and vortex mixed.

#### 4.7.2. Plant toxin analysis

Stock solutions of each compound were prepared at a concentration of 1.0 mg/mL in methanol, with the exception of hellebrin which was prepared at 0.5 mg/mL and Salvinorin A and cathinone which were provided as a 1 mg/mL solution and stored at -20 °C. Calibration standards were prepared daily for each analysis from the stock solution by diluting in mobile phase. Calibration standards were prepared over a concentration range of 0-100 ng/mL for 5-methoxypsoralen, 8-methoxypsoralen, aconitine, cathinone, capsaicin, colchicine digitoxin, psoralen, scopolamine, strychnine thujone and veratridine; a concentration range of 0-400 ng/mL for hellebrin; a concentration range of 0-300 ng/mL for digoxin and salvinorin A and a concentration range of 0-5000 ng/mL for coumarin. A full set of calibration standards were ran at both the start and end of each chromatographic run cycle. In addition, a quality control standard was prepared at a mid-calibration point by diluting stock standard solutions in mobile phase and analysed at points throughout the run to ensure there was no deviation throughout the run. For plant toxin analysis approximately 0.1 g of plant material was removed using a scalpel, which was cleaned with water and methanol between each collection, from various parts of the plant, root, stem, flower and foliage, was macerated and sonicated for 15 minutes in 10 mL of methanol. The solution was filtered through a 0.22 µm nylon syringe filter and diluted to within the calibration range with mobile phase before transferring to an autosampler vial.

For prep-LC and NMR of *Helleborus* root; approximately 20 g of *Helleborus purpurascens* was placed in a Soxhlet thimble and subjected to Soxhlet extraction with 250 mL methanol for 5 days. The resulting extract was then evaporated to approximately 20 mL using a rotary evaporator. An aliquot of 1 mL was placed into an autosampler vials and process by prep LC. From the fractions obtained 50 µL was removed and analysis by direct infusion mass spectrometry to obtain molecular weight information and the remaining solution was evaporated to dryness using a sample concentrator, with a nitrogen flow pressure of 1 bar, and then reconstituted in dimethyl sulfoxide (DMSO).

#### **4.8. Data Analysis**

LC-MS data analysis was performed using XCalibur™ 4.0 and 3.0 software packages for low resolution and high resolution respectively, supplied from Thermo Scientific (Hemel Hempsted, UK). For the Agilent prep-LC system and the Agilent LC-UV system data analysis was performed using OpenLab™ version C.01.07 supplied by Agilent Technologies (Cheshire, UK). All NMR spectra were analysed using the Delta™ 5.03 software package supplied by Joel (Nieuw-Vennep, The Netherlands). Statistical analysis was performed using SPSS™ version 25 from IBM (Portsmouth, UK).

## **Chapter 5: Thyroid hormone results and discussion**

## 5. Thyroid hormone results and discussion

### 5.1. Method development

#### 5.1.1. Evaluation of columns and mobile phase

A number of studies have been published looking at the analysis of a selection of thyroid hormones (Table 5.1) with varying degrees of successful chromatographic resolution obtained.<sup>345-353</sup> From the studies shown in Table 5.1 previous work for the analysis of thyroid hormones by LC-MS has been undertaken on a range of thyroid hormones and their chromatographic conditions. Of the studies shown, 6 previously published methods included the analysis of rT3.<sup>346, 348, 350-353</sup> The inclusion of rT3 in the study is of importance as any co-elution of T3 and rT3 could impact on the results obtained in the sample. The inclusion of rT3 within this study will allow for the assessment of an effective separation via chromatographic or mass spectrometry method parameters.<sup>354, 355</sup> The inclusion of T2 within the study is a of significance as previous studies have indicated that the levels of T2 could be indicative of underlying conditions including thyroid cancer.<sup>355-357</sup> Of the studies shown in Table 5.1 only three have included both rT3 and T2 within their studies however, only 1 study observed “visible” chromatographic resolution with a long run time (18 minutes). Therefore, significant improvement can be made in the separation of thyroid hormones, as well as the development of robust sample treatment methods, to allow for the adoption of the method for a number of applications such as the analysis of pharmaceutical preparation and clinical thyroid hormone level monitoring. Previous studies indicate that it is difficult to separate T3 and rT3 using basic carbon chain HPLC columns such as C8 or C18. Suggesting that more complex stationary phase interaction mechanism, such as, the  $\pi$ - $\pi$  interaction found in phenyl-hexyl or pentafluorophenylpropyl (F5) stationary phases are required. Therefore, initial investigations into columns using HPLC using F5, C18 and phenyl hexyl packing material were performed. The columns evaluated included Supelco Ascentis<sup>®</sup> Express F5 (15 cm x 2.1 mm, 2.7  $\mu$ m particle size), Thermo Scientific Accucore<sup>®</sup> phenyl-hexyl (15 cm x 2.1 mm, 2.6  $\mu$ m particle size) and Agilent ZORBAX<sup>®</sup> Eclipse Plus C18 (100 mm x 2.1 mm, 3.5  $\mu$ m particle size). Initial runs using a C18 column showed significant peak tailing and an inability to separate T3 and rT3. Phenyl based columns offer an additional retention mechanism by introducing the possibility of  $\pi$ - $\pi$  interactions. The initial mobile phase organic modifier used was acetonitrile; however, this still gave broad

peaks and some peak tailing which negatively impacted on the ability of the method to satisfactorily separate T3 and rT3. (Figure 5.1)

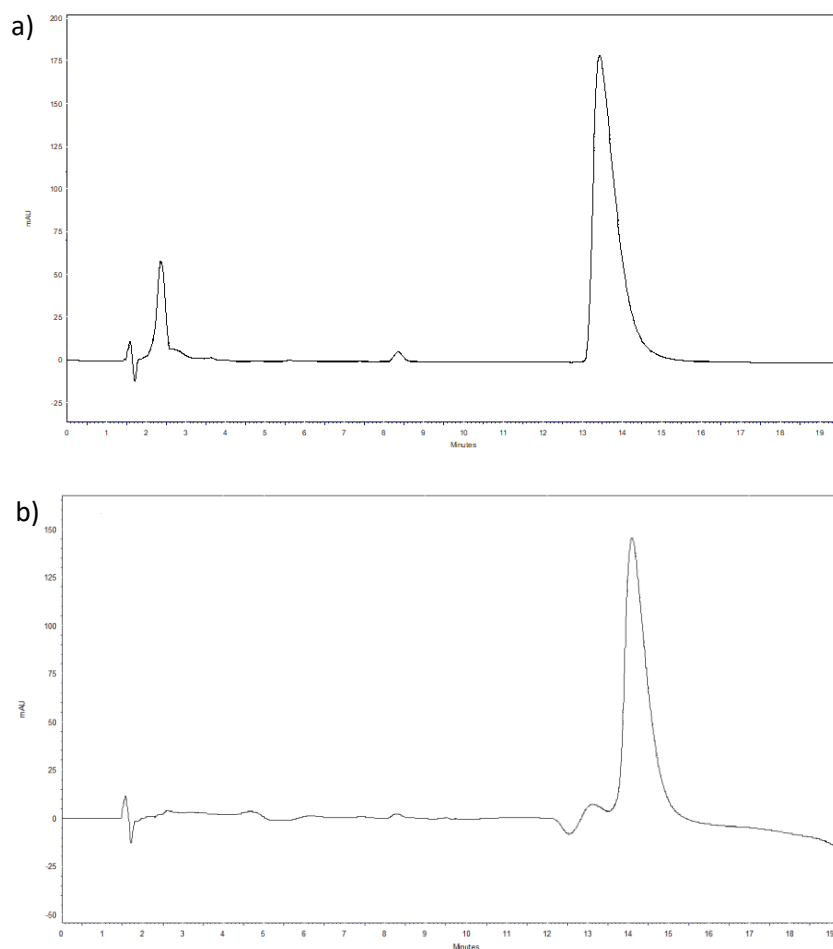


**Figure 5.1: HPLC-UV chromatogram of a) T3 and b) rT3 with acetonitrile as organic modifier**

Acetonitrile has previously been found to impede  $\pi$ - $\pi$  interactions between the analytes and the phenyl groups found on the stationary phase. Methanol however, has been shown to improve this selectivity as interaction are not impeded.<sup>53</sup> The use of methanol as the organic modifier was able to produce good separation, with a resolution value of  $\geq 1.0$  for all the compounds with a satisfactory peak shape with a tailing factor of  $\leq 1.8$  (Figure 5.2).

### 5.1.2. Optimisation of MS parameters

Tandem mass spectrometry parameters were optimised to allow for quantification of the four compounds. For the purposes of quantification, the precursor and two

product ions were monitored, with the most stable product ion used as the quantification ion (Table 5.2). Both collision induced dissociation (CID) and pulsed Q collision induced dissociation (PQD) were assessed for suitability.

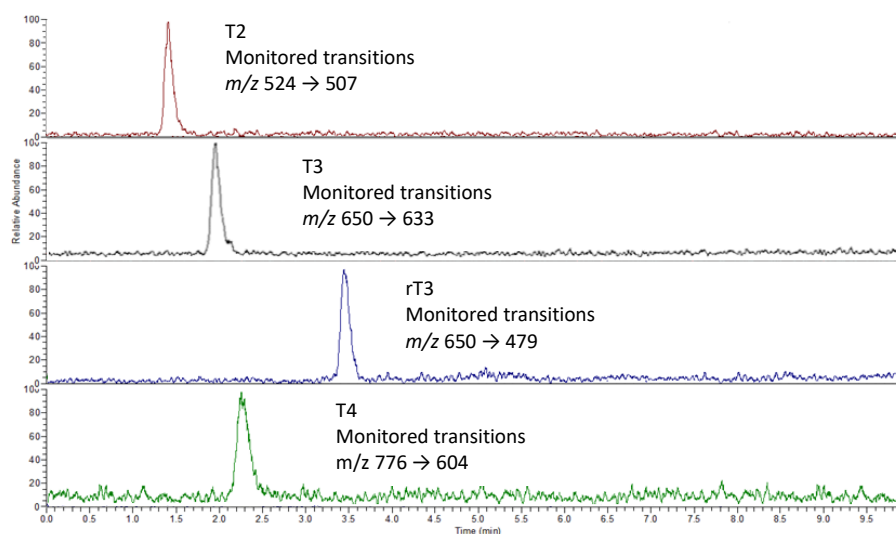


**Figure 5.2: Extracted ion chromatogram of T4, T3, rT3 and T2 by low resolution LC-MS/MS**

The only differences observed between the two fragmentation techniques was the ability for PQD to produce fragmentation ions in the lower range  $m/z$  region. However, as this is a fragmentation technique specific to Thermo Scientific instrumentation the decision was made to use CID to allow for a greater transferability of the method between instrumentation. With the collision energies for both low resolution and high-resolution liquid chromatography-mass spectrometry show in Table 5.2 with the mass spectrum for each compound shown in Figure 5.3. Figure 5.4 shows the fragments observed in both high-resolution LC-MS/MS and low-resolution LC-MS/MS.<sup>358</sup>

### 5.1.3. Use of internal standard

The use of an internal standard is common place in the development of analytical methods in order to assess and correct for inaccuracies. Inaccuracies within an analytical method can be due to a number of aspects, such as compound losses, sample pre-treatment, ion suppression and ion enhancement. Ion suppression and

enhancement, within the ionisation process (MS) are of particular concern when working with biological matrices due to their impact of the resultant data. In order to mimic the interaction effecting the analytes of interest the physiochemical properties of the internal standard need to be similar to those compounds. However due to the similar physiochemical properties of the analyte and internal standard this can lead to co-elution. It is for these reasons that the most common internal standards used in LC-MS are isotope labelled compounds such as deuterium, carbon-13, nitrogen-15 and oxygen-18. Due to the small variation in molecular weight of the isotope labelled compounds, co-elution can be overcome by MS separation based on their precursor and product ions.<sup>359, 360</sup> The use of C13 thyroxine was investigated as part of this study however the compound was found to be expensive and unstable (6 months). It was therefore concluded not to use the C13 thyroxine in the development of a new robust method.

#### **5.1.4. Tablet sample method development**

As the method is to be used for the analysis of tablets for total content which will also be required for dissolution profiling it is necessary to develop a method for the extraction of thyroid hormones from tablet preparation and to ensure no matrix effects are observed from excipients. For this study, brands of thyroid hormone supplements were used containing only T3, Tiromel<sup>®</sup> and Cytomel<sup>®</sup>, and containing both T3 and T4, Dithyron<sup>®</sup>. Initially the extraction solvent was investigated and due to the polarity of the compounds, methanol, acetonitrile, water and isopropanol were accessed. For each solvent, three tablets each batch were taken and the weight of the tablet was recorded.

**Table 5.1: Comparison of existing methods for the analysis of thyroid hormones**

Column	Compounds tested	Mobile phase	Flow rate (ul/min)	Run Time (min)	Visible chromatographic resolution observed	Sample preparation	Reference number
Supelco® LC-18 DB	T4 and T3	A: Methanol: water (98:2) + B: methanol	600	7	Yes	Liquid-Liquid	345
ACE phenyl	T4, T3, rT3, T2	A: 0.2% formic in water B: 0.2 % formic in 50:50 ACN:MeOH	350	18	Yes	SPE – Oasis HLB	335
Unison UK-C18	T4	Methanol: water 70:30 +0.1 % formic	300	5	N/A	HF-LPME	347
Ascentis Express® F5	T4, T3, rT3, T2, T1	A: 0.1 % Acetic acid in water, B: 0.1 % acetic acid in methanol	250	14	No	SPE – Oasis HLB	348
Hypersil® gold	T4	A: water + 0.1% formic, B: ACN + 0.1% formic	1000	3	N/A	N/A	349
Zorbax® extend-C18	T4, T3, rT3, T2, T1	A: 0.01% ammonium hydroxide in MeOH. B: Water	500	17	No	Solid-Liquid extraction	361
Ascentis Express® phenyl-hexyl	T4, T3, rT3	A: 0.1% acetic in water B: 0.1 % acetic in MeOH	Not stated	8	Yes	N/A	351
Ascentis Express® F5	T4, T3, rT3	30 % A: 0.1% acetic in water 70% B: 0.1 % acetic in MeOH	500	4.1	Yes	SPE – C18 and RP-Amine	352
Raptor® Biphenyl	T4, rT3, T3	A: 0.1% formic in water B: 0.1% formic in methanol	400	2.0	Yes	N/A	353

**Table 5.2: Fragmentation parameters and ions observed**

Compound	Collision energy (eV) (Low resolution, High resolution)	Fragmentation ion observed ( <i>m/z</i> )	Fragmentation
T4	28, 25	776	[M-H] <sup>-</sup>
		759	[M-H-NH <sub>3</sub> ] <sup>-</sup>
		605*	[M-H-ICO <sub>2</sub> ] <sup>-</sup>
T3	27, 23	650	[M-H] <sup>-</sup>
		633*	[M-H-NH <sub>3</sub> ] <sup>-</sup>
		523	[M-H-I] <sup>-</sup>
rT3	27, 23	650	[M-H] <sup>-</sup>
		633	[M-H-NH <sub>3</sub> ] <sup>-</sup>
		479*	[M-H-ICO <sub>2</sub> ] <sup>-</sup>
T2	29, 28	524	[M-H] <sup>-</sup>
		507*	[M-H-NH <sub>3</sub> ] <sup>-</sup>
		398	[M-H-I] <sup>-</sup>

\* Quantification ions

The tablet was then crushed with a pestle and mortar before being transferred to a 10 mL volumetric flask and made to volume with the appropriate solvent. The tablet solution was then sonicated for 30 minutes in an ultra-sonic bath. The solution was then diluted in the same solvent as the extraction to ensure the predicted concentration was within the calibration range. The diluted solution was then filtered through a 0.22 µm nylon syringe filter prior to analysis by low-resolution LC-MS/MS alongside calibration standards. From the % recovery results seen in Table 5.3 methanol gave the best recovery of at least 94 % with a % RSD of between 0.8 and 2.4 for the three replicates analysed. Therefore, methanol will be used as the extraction solvent for the remainder of the study.

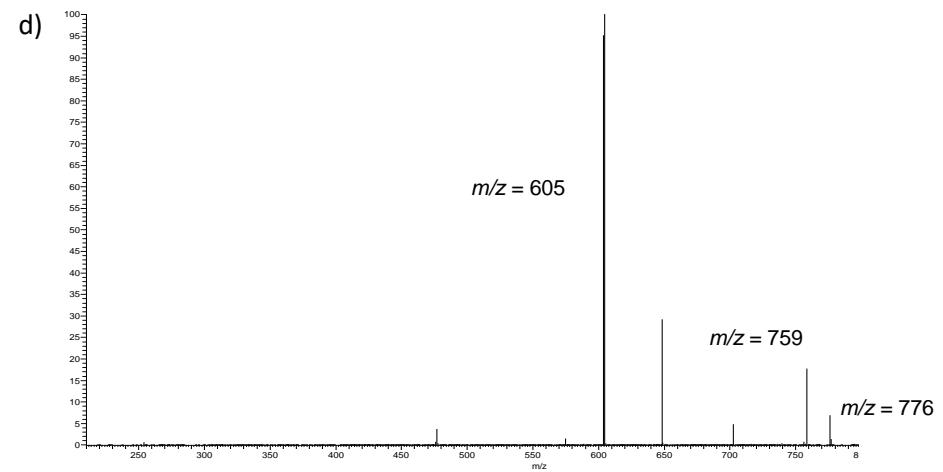
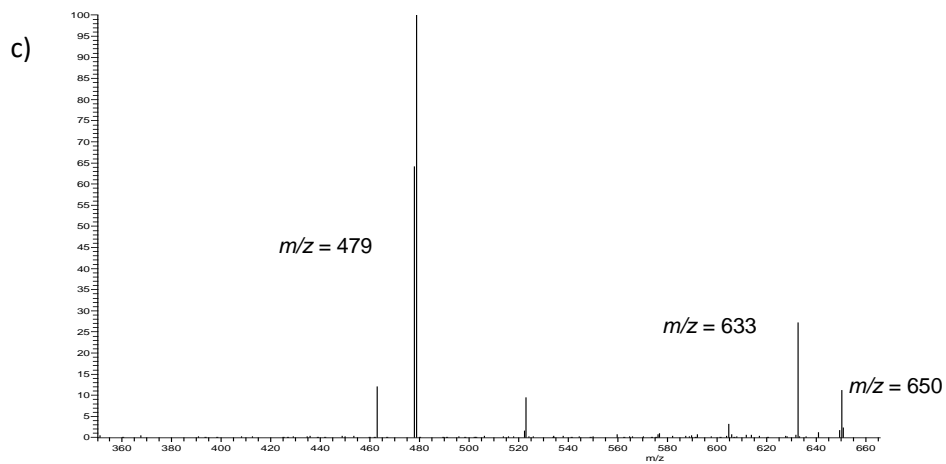
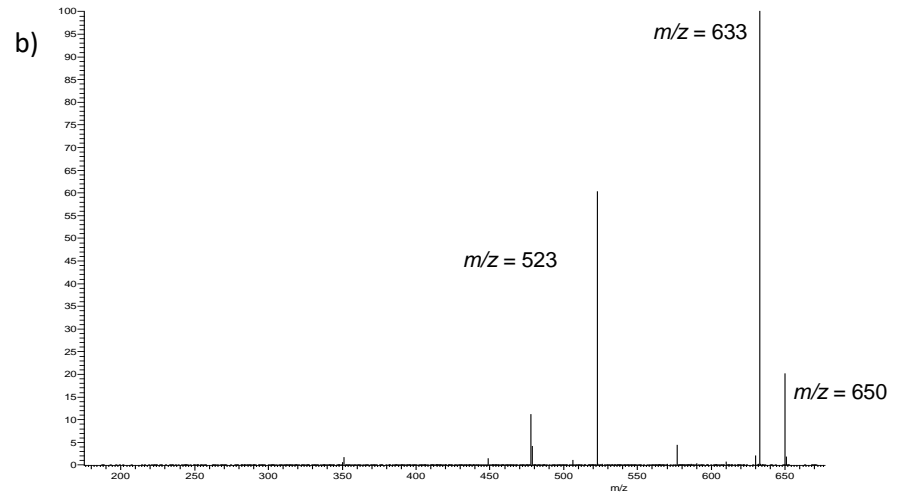
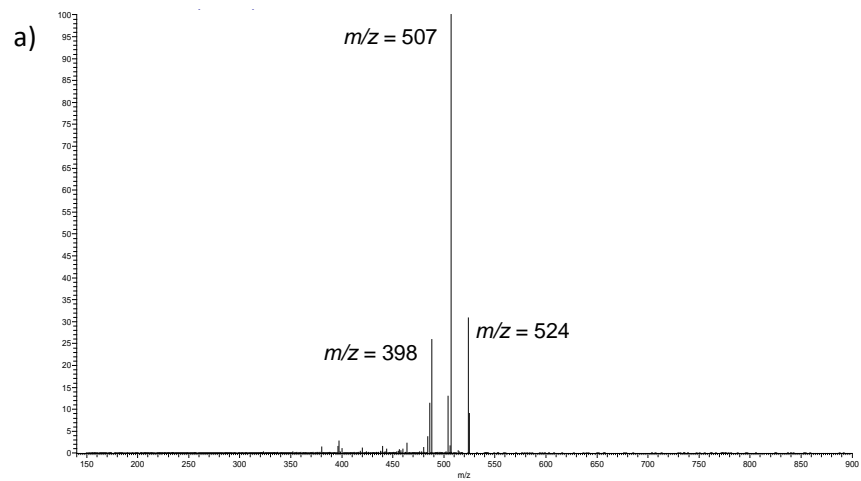


Figure 5.3: Low resolution ESI negative ion mass spectrum for a) T2, b) T3, c) rT3 and d) T4

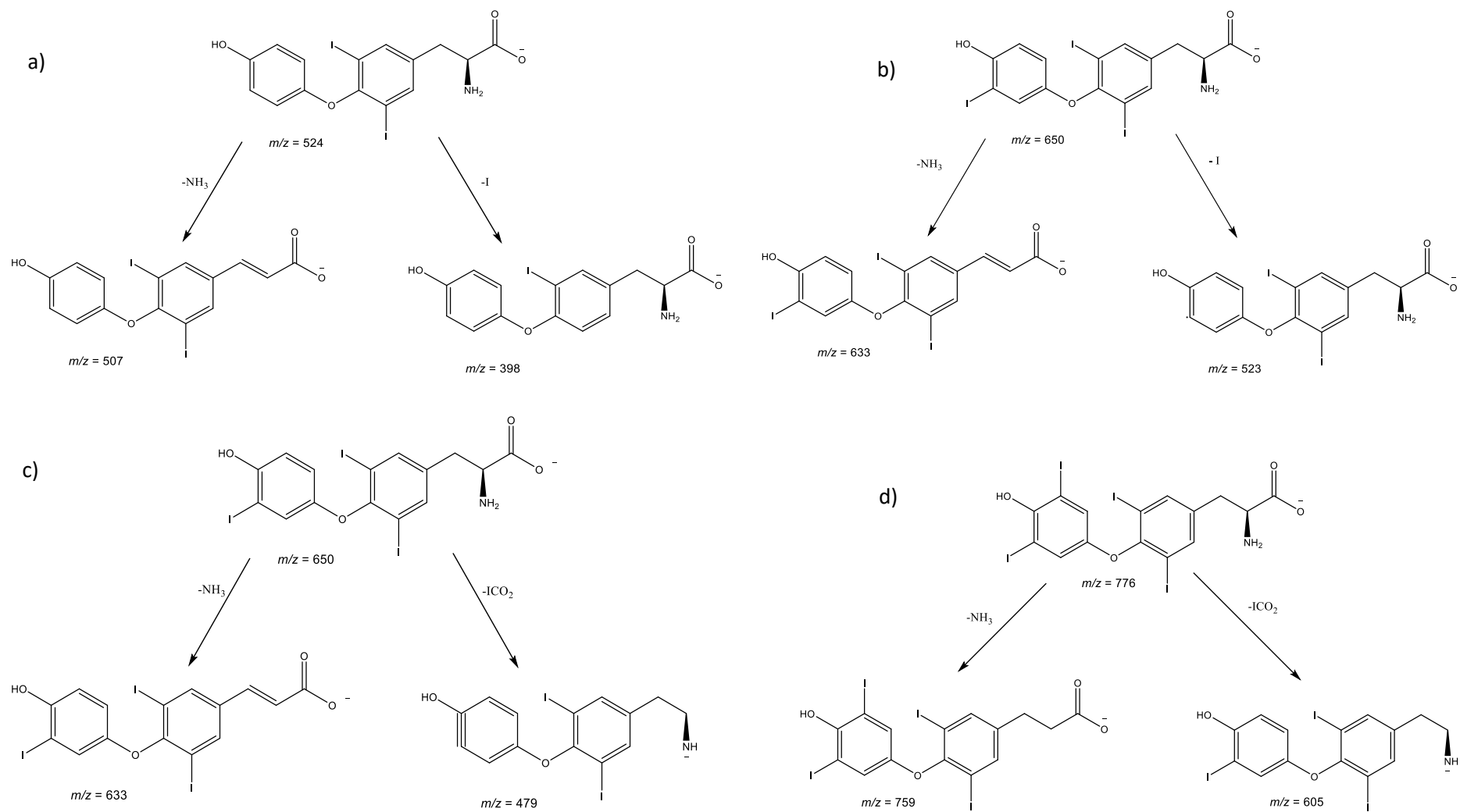
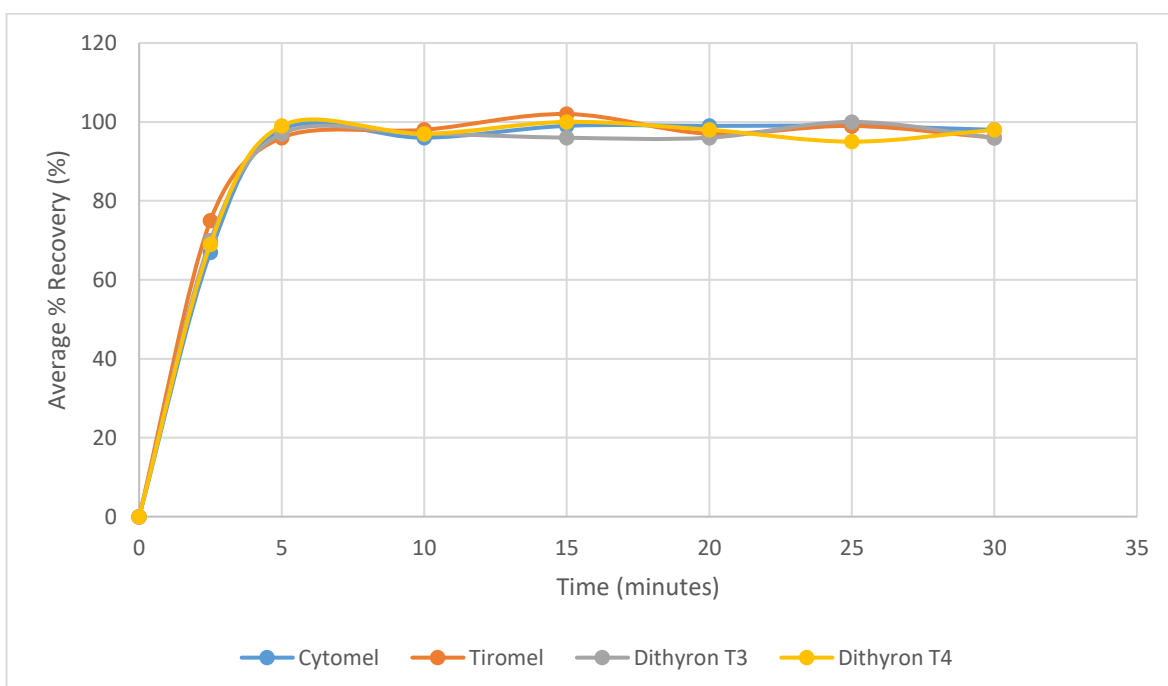


Figure 5.4: Mass spectrum fragments for a) T2, b) T3, c) rT3 and d) T4.<sup>358</sup>

**Table 5.3: Solvent recoveries for tablet extraction development**

Brand	Compound	% Recovery (% RSD)			
		Methanol	Acetonitrile	Water	Isopropanol
Cytomel®	T3	97 (1.2)	54 (2.4)	67 (0.8)	86 (2.4)
Tiromel®	T3	96 (0.8)	48 (2.8)	55 (0.9)	75 (1.4)
Dithyron®	T3	94 (2.4)	52 (1.6)	64 (1.5)	91 (2.2)
	T4	98 (1.7)	51 (2.1)	58 (1.2)	84 (1.0)

The next stage in the development was to investigate the sonication time to ensure an efficient extraction while maintaining the compound recovery. For this study the sonication times of 0, 2.5, 5, 10, 15, 20, 25 and 30 minutes were chosen. For each sonication time, three tablets each batch were taken and the weight of the tablet was recorded. The tablet was then crushed with a pestle and mortar before being transferred to a 10 mL volumetric flask and made to volume with methanol. The tablet solution was then sonicated for the above times in an ultrasonic bath. The solution was then diluted in methanol and then filtered through a 0.22 µm nylon syringe filter prior to analysis by low-resolution LC-MS/MS alongside calibration standards. The percentage recoveries were then plotted against extraction time. From Figure 5.5 it can be seen that the recoveries reach a plateau after 5 minutes for all of the tablets. Therefore, tablet content will be analysed by extraction in 10 mL of methanol with a sonication time of 5 minutes.



**Figure 5.5: Comparison of sonication times on % recoveries**

### 5.1.5. Serum sample method development

As the method is to be used for the analysis of biological material, it is necessary to develop a clean-up method to remove any matrix from the sample prior to analysis. Due to the volume available for each sample, between 0.1 – 1 mL, the most appropriate method for low resolution LC-MS would be solid phase extraction. Separate standard solutions in water were prepared at a concentration of 1500 ng/mL for each compound in order to investigate different cartridge interactions and wash and elution solvents. All initial clean up investigations were performed using HPLC-UV to prevent contamination of the LC-MS. Based on the previous studies shown above, reversed phase is the preferred mode of solid phase extraction. In order to determine the best extraction mode a range of cartridges were accessed for recovery. Two reversed phase and a mixed mode, reversed phase and ion exchange, were selected: C8, C18, Strata-X™ and Strata-SDB-L™ from Phenomenex (Macclesfield, UK). As per the manufacturer instructions, the cartridges were conditioned with 1 mL of methanol and then equilibrated with 1 mL of water prior to loading of 1 mL of standard solution. The cartridges were then washed with 1 mL of 10:90 methanol:water (%v:%v), dried down under vacuum for 5 minutes then the compounds eluted with 1 mL methanol as the standards were dissolved in methanol and methanol should therefore elute the compound from the cartridge. Both the wash and the eluent flow through were collected to assess cartridge performance. A second study was carried out simultaneously to access the best wash and elution percentages for each of the three cartridges. For this study, the cartridges were conditioned with 1 mL of methanol and then equilibrated with 1 mL of water prior to loading of 1 mL of standard solution. The cartridges were then washed with 1 mL of solutions increasing from 0 % methanol in water to 100 % methanol. Each wash step was collected and analysed via HPLC-UV in order to determine the % of methanol at which the compounds start eluting from the cartridge and the % of methanol at which the compounds are fully eluted from the cartridge.

The initial investigation found C18 cartridge gave recoveries of >95 % for the standard solution with no compound loss during the wash step. However, the

cartridge retention of both the Strata-X™ and Strata-SDB-L™ were too strong and the compounds were not fully eluted with 1 mL of methanol (Figure 5.6). As a preconcentration step will be required for LC-MS analysis the requirement to use more than 1 mL of elution solvent would not be favourable. This also confirmed that the retention on the Strata-X and Strata-SDB-L cartridges was too strong and that multiple washes would be required in order to obtain maximum recoveries (Figure 5.6). As seen from the data in Figure 5.5 the C18 cartridge was able to retain all four compounds strongly enough for a slightly organic wash solution to be utilised but not too strongly that the compounds were not fully recovered. Therefore, the C18 cartridge was used for the remainder of the studies.

The next stage was to determine which solvent would provide the best elution power. For this study commonly used reversed phase solvents were chosen, methanol, acetonitrile, ethanol, and isopropanol. Twelve C18 SPE cartridges, each solvent in triplicate, were conditioned, washed and loaded as per the wash procedure determined by the elution study then the compounds eluted with 1 mL of one of the four solvents. Then 10 µL of each solution was injected into the HPLC alongside calibration standards to determine the percentage recoveries. Methanol was found to give the best recoveries and will therefore be used as the elution solvent (Table 5.4). However, 100 % methanol is likely to also remove the unwanted components from the cartridge so a methanol:water, 80:20 (%v:%v) solution will be used as indicated in the wash profile from Figure 5.5.

An initial developed methodology for the extraction of thyroid hormones from biological samples was determined as, condition with 1 mL of methanol and then equilibrate with 1 mL of water prior to loading of 1 mL of sample. The cartridges were then washed with 1 mL methanol:water, 30:70 (%v:%v), dried down under vacuum for 5 minutes then the compounds eluted with 1 mL of methanol: water, 80:20 (%v:%v). However, this gave lower recoveries than expected and for some replicates the cartridges became blocked. Therefore, the use of an acid solution followed by centrifugation was investigated. The samples were diluted 1:1 with 0.1% formic acid in water, vortexed and centrifuged at 5300 g for 5 minutes following discussions with colleagues. The samples were checked to ensure the formation of two layers, one containing the particulate material and the liquid layer. This method gave good recoveries for all four compounds; however, there was still

a significant amount of matrix present in the samples. This could potentially cause problems with the analysis especially when using the LC-MS.

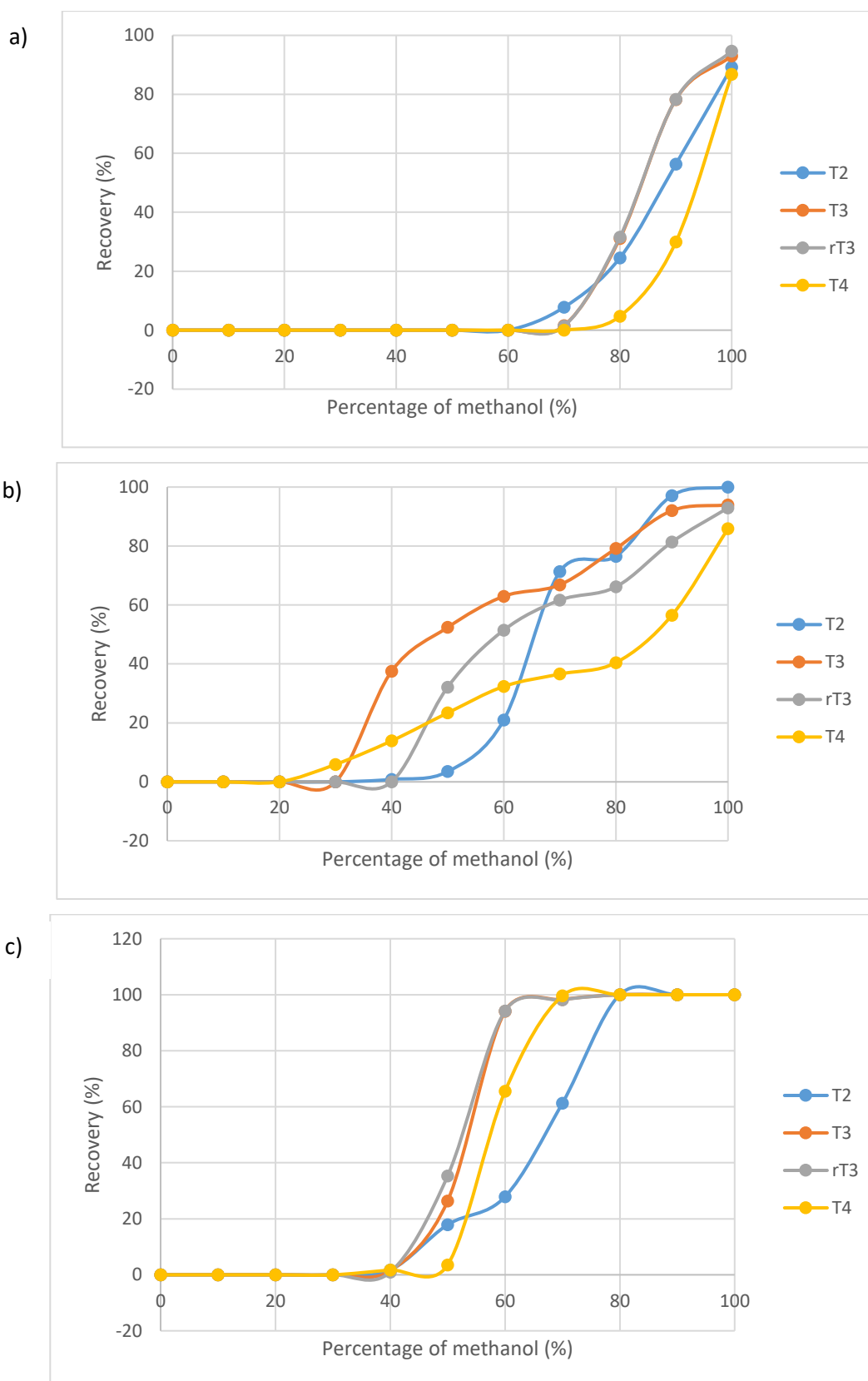


**Figure 5.6: Method development of SPE using HPLC-PDA. a) Strata-SDB-L™, b) Strata-X™ and c) C18**

Based on the data from the earlier wash and elution studies, it was not possible to increase the percentage of methanol without getting some of the compounds eluting from the cartridge. Therefore, the pH of the wash solution and pH of the sample was investigated. The next stage was to investigate the preconcentration step to allow for the analysis of biological materials by low resolution LC-MS. Based on the LOQ data and the normal range a minimum precentration of a factor of 5 would be required in order to be able to quantify T3 in the samples. This can be achieved in a number of ways including elution with a lower volume than the sample load volume or drying down of the sample after extraction. As the lowest sample volume likely to be loaded onto the SPE cartridge is 100  $\mu$ L it would not be possible to elute with a lower volume while maintain recoveries. Therefore, the extraction eluent will be dried down under nitrogen and then reconstituted in a smaller volume.

To assess the effective removal of matrix and the impact on the extraction procedure calibration standards and a matrix blank were extracted by SPE and analysed against standards prepared in mobile phase. Calibration standards for all four compounds were prepared over a range of 0-200 ng/mL, one set in mobile phase and one set in horse serum and analysed by low resolution LC-MS in triplicate. For the serum standards the developed SPE procedure was used using 1 mL of each standard. The peak areas obtained for both sets of standards were plotted on a calibration graph (Figure 5.7). There were no differences observed between the standards prepared in mobile phase and serum. The extracted serum blank also showed no interference peaks from the matrix.

Due to the increased levels of sensitivity obtained via high-resolution LC-MS it is possible to use a simple dilution for the sample preparation to limit the matrix effects. A study was performed at dilutions ranging from 1 in 10 to 1 in 200 dilutions with horse serum spiked at a concentration of 40 ng/mL and analysed alongside calibration standard to determine the % recovery and therefore the minimum dilution required. From the recoveries show in Table 5.5 it can be seen that a minimum of 1 in 100 dilution was required to remove the matrix effects.

**Table 5.4: C18 SPE solvent recovery comparison**

Elution solvent	Mean Concentration (ng/mL) (n = 3) (± SD)				Mean Recovery (%) (n = 3) (range)			
	T2	T3	rT3	T4	T2	T3	rT3	T4
Methanol	1429 (13.7)	1598 (17.8)	1494 (4.4)	1559 (2.1)	95.3	106.5	99.6	103.9
Acetonitrile	722 (7.0)	871 (9.1)	867 (8.3)	957 (4.5)	48.1	58.1	57.8	63.8
Ethanol	467 (7.5)	132 (3.2)	121 (9.1)	60 (6.0)	31.1	8.8	8.1	4.0
Isopropanol	0	54 (7.0)	60 (6.1)	0	0	3.6	4.0	0

Matrix matched standards were ran using the dilution obtained from the study above and compared to standards prepared in mobile phase. The dilution of 1 in 100 had no impact on the response of the calibration standard across the full calibration range, as can be seen in Figure 5.8.

## 5.2. Method Validation

### 5.2.1. Selectivity

Blank samples of mobile phase, blank serum, FaSSIF and FaSSGF were ran alongside the appropriate analysis at the beginning and end of each run. As no peaks were observed at the same retention time of the four thyroid hormones and no matrix effects were seen, selectivity for the method was established.

### 5.2.2. Linearity

Linearity was established for both high resolution and low-resolution LC-MS/MS by preparing mixed calibration standards of all four thyroid hormones.

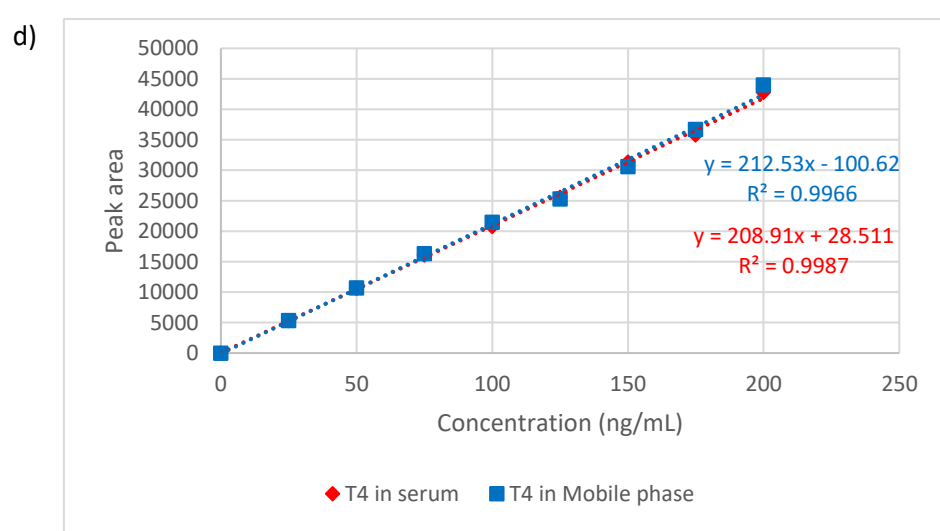
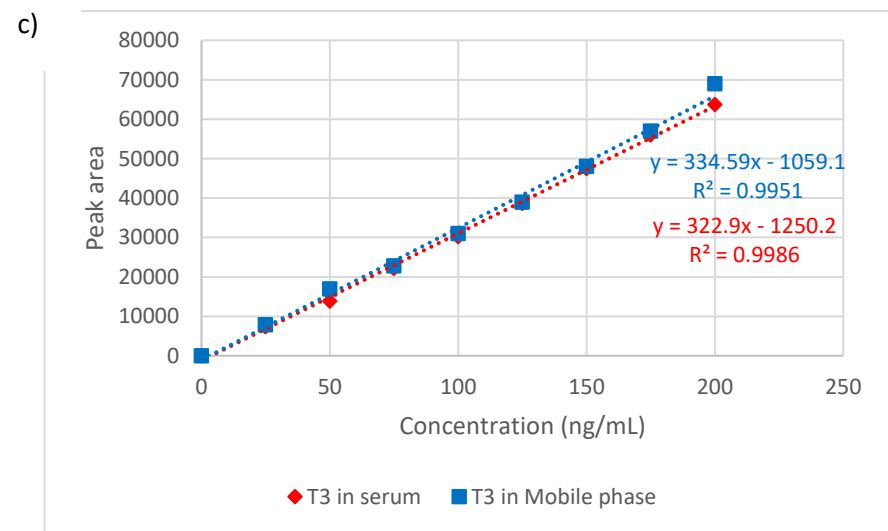
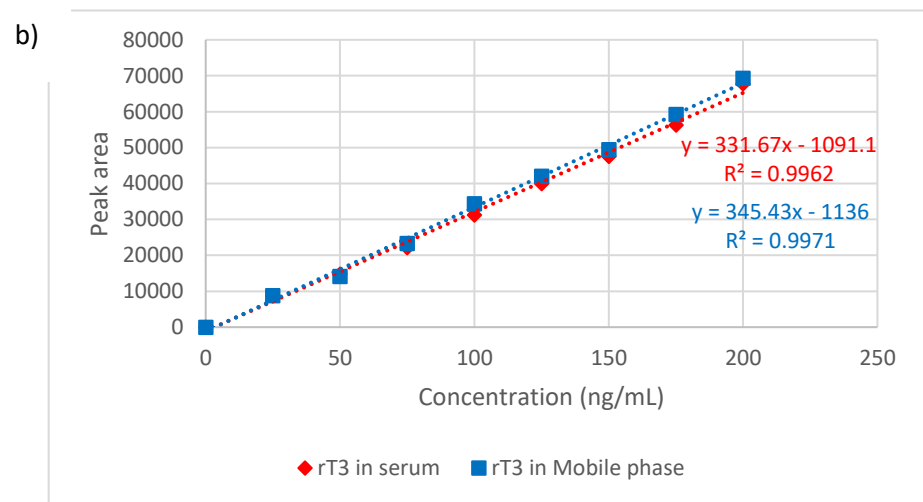
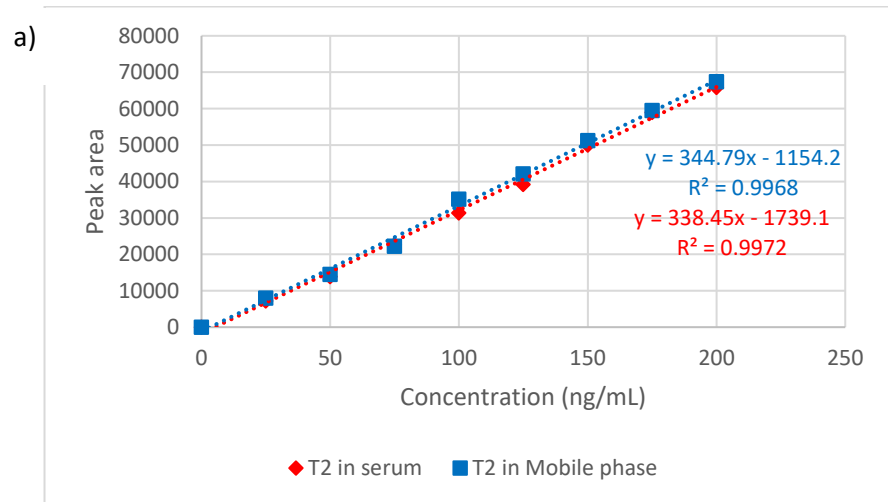


**Figure 5.7: Comparison of standards in mobile phase and serum by LR-LC-MS/MS. a) T2, b) rT3, c) T3 and d) T4**

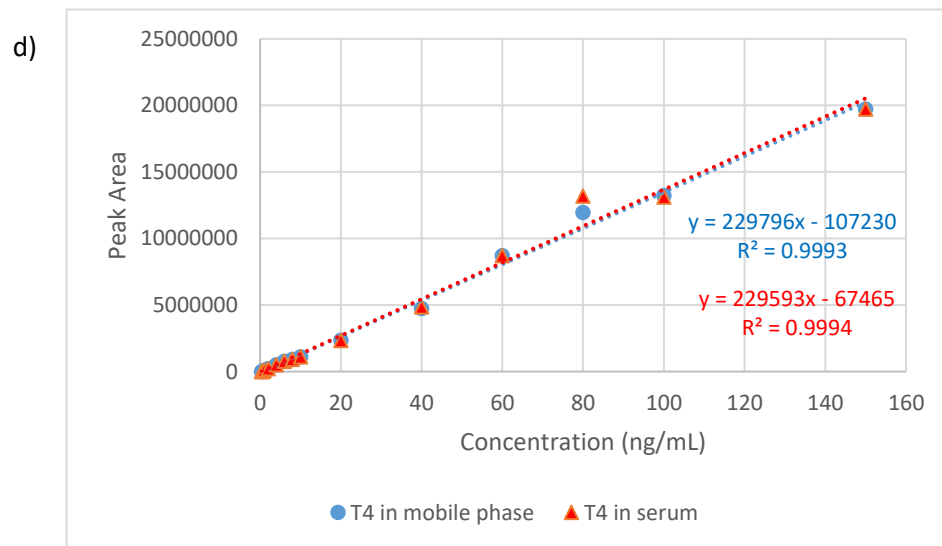
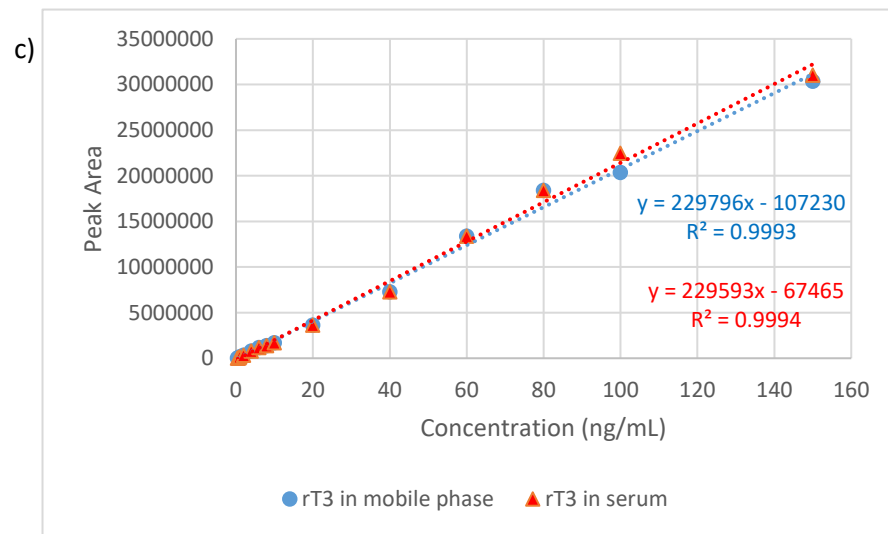
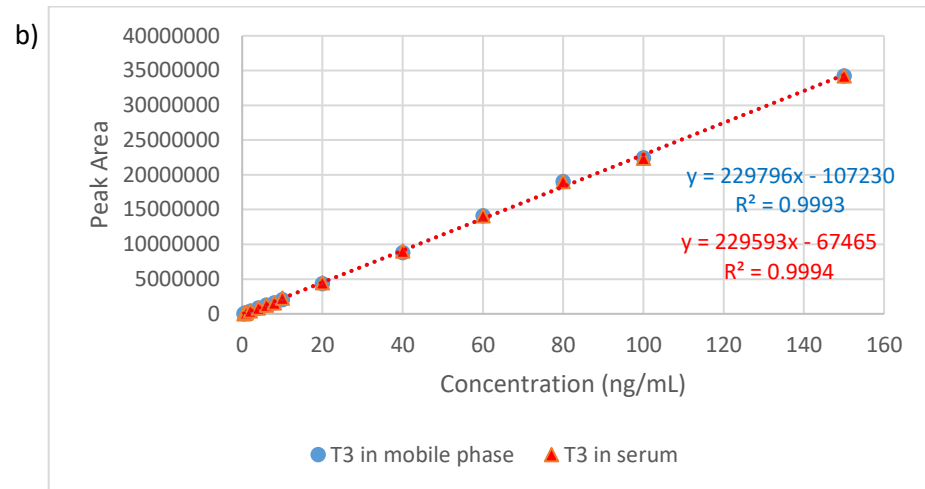
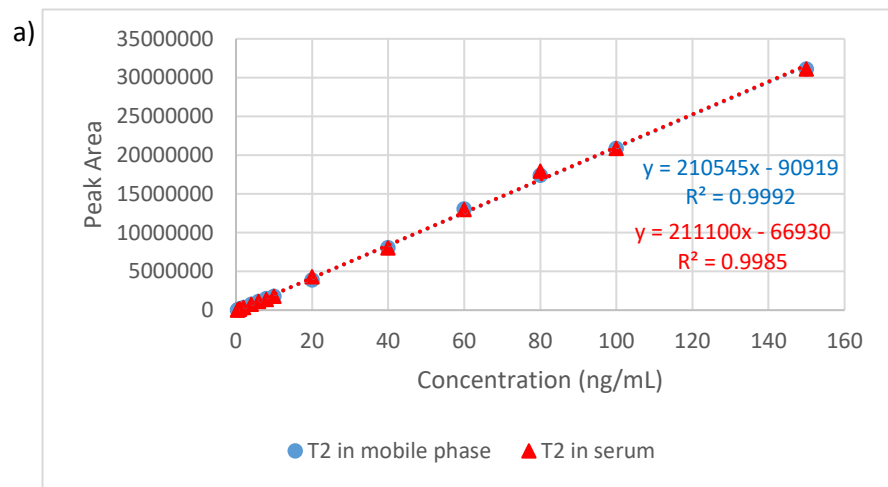


**Figure 5.8: Comparison of standards in mobile phase and serum by HR-LC-MS/MS. a) T2, b) T3, c) rT3 and d) T4**

**Table 5.5: % recovery for spiked serum dilutions**

Dilution	% Recovery (%) (n=3)			
	T2	T3	rT3	T4
1 in 10	57.9	38.4	78.7	69.3
1 in 20	64.2	59.8	79.1	72.5
1 in 40	68.3	73.1	82.8	88.9
1 in 60	71.8	75.7	92.5	90.2
1 in 80	75.0	94.2	96.3	94.8
1 in 100	98.1	104.7	103.4	99.2
1 in 120	98.5	99.4	101.8	100.4
1 in 140	100.2	100.5	101.3	100.3
1 in 160	99.3	102.3	98.9	98.7
1 in 180	98.9	99.7	100.5	99.5
1 in 200	100.5	98.6	99.4	99.7

For low resolution LC-MS/MS the calibration range was 0-200 ng/mL and for high resolution LC-MS/MS the calibration range was 0-150 ng/mL. Calibration standards were prepared and analysed in triplicate. Using the ions identified in Table 5.2 for quantification, the average peak areas were used to construct calibration graphs for the four thyroid hormones. The coefficient of determination ( $R^2$ ) was greater than 0.99 so the method can be described as linear for T4, T3, rT3 and T2 (Table 5.6).

### 5.2.3. Precision

Precision was established for both the standard and the extracted serum sample. For the standard precision low, medium and high calibration standards were injected in triplicate and the % coefficient of variance (%CV) calculated. The average %CVs obtained were 3.3 for T4, 2.1 for T3, 2.2 for rT3 and 3.2 for T2 and 3.9 for T4, 1.8 for T3, 3.2 for rT3 and 1.8 for T2 for low resolution LC-MS/MS and high-resolution LC-MS/MS, respectively. (Table 5.6) The individual results for the standard points can be seen in Table 5.7. For the sample precision, nine replicate sample extractions were performed from a single sample for each technique and

the %CV was calculated. The %CV obtained were between 2.2 – 3.3 and 1.8 -3.8 for low resolution LC-MS/MS and high-resolution LC-MS/MS, respectively (Table 5.6).

#### **5.2.4. Limits of detection and quantification**

Due to the analysis being performed in selection reaction monitoring the limits of detection and quantification were based on the replicate calibration curve preparations. The limit of detection (LOD) was calculated by multiplying the standards deviation for the y-intercept by 3.3 then dividing by the average slope of the calibration curve and the limit of quantification (LOQ) was calculated by multiplying the standards deviation for the y intercept by 10 then dividing by the average slope of the calibration.<sup>105</sup> Due to thyroid hormone ranges being reported in pmol/L the LOQ and LOD were converted from ng/mL to pmol/L

The calculated limit of detection was between 0.05 - 1.76 pmol/L and 0.4 – 1.8 fmol/L for low resolution LC-MS/MS and high-resolution LC-MS/MS, respectively.

The calculated limit of detection was between 0.168 – 5.9 pmol/L and 1.5 – 6 fmol/L for low resolution LC-MS/MS and high-resolution LC-MS/MS, respectively.

The limit of quantification for low resolution LC-MS/MS means that a preconcentration step will be required prior to analysis to ensure that T3 is within the limits of sensitivity of the instrumentation.

#### **5.2.5. Standard stability**

It was identified in the product information sheet provided from Sigma Aldrich for T3 that dilute solutions tend to adhere to glass when stored therefore the stock solutions of all four thyroid hormones were prepared and then aliquoted into small portions and stored at -20 °C. To assess the suitability of glass storage vials the portions were aliquoted into standard glass storage vials and assessed over the course of the study for stability. Aliquots were defrosted and used to prepare calibration and quality control samples and the remaining stock solution disposed of. The stability of the stock solutions was assessed based on the data obtained for each set of analysis over the course of 3 months. From Figure 5.9 it can be seen that the compounds are stable when stored at 2-8 °C for 10 days and for a period of up to 52 days when stored at -20 °C.

**Table 5.6: Linearity and LOQ/LOD results for the analytical techniques**

Compound	Technique	Calibration range (ng/mL)	No. of data points	Linearity $y = mx + c$	R <sup>2</sup> Value	Precision (%CV)	LOD (pmol/L)	LOQ (pmol/L)
						Sample	Standard	Standard
T4	LR-LC-MS	0-200	11	$33.834x + 1.2857$	0.9996	3.3	1.76	5.9
	HR-LC-MS	0-150	11	$128022x + 376.6945$	0.9965	3.8	0.0014	0.0045
T3	LR-LC-MS	0-200	11	$59.937x - 13.196$	0.9998	2.2	0.052	0.172
	HR-LC-MS	0-150	11	$264700x - 65.667$	0.9922	1.8	0.0017	0.0058
rT3	LR-LC-MS	0-200	11	$53.737x + 46.81$	0.9918	2.3	0.16	0.582
	HR-LC-MS	0-150	11	$127180x - 104.6175$	0.9944	3.0	0.0018	0.006
T2	LR-LC-MS	0-200	11	$38.461x + 42.429$	0.9912	3.2	0.05	0.168
	HR-LC-MS	0-150	11	$128270x - 202.8385$	0.9901	1.9	0.0004	0.0015

**Table 5.7: Individual %CV results**

<b>Compound</b>	<b>Technique</b>	<b>%CV Low standard</b>	<b>%CV Medium standard</b>	<b>%CV High standard</b>
T4	LR-LC-MS/MS	3.8	3.4	2.6
	HR-LC-MS/MS	4.2	3.8	3.6
T3	LR-LC-MS/MS	2.8	2.1	1.4
	HR-LC-MS/MS	2.5	1.7	1.2
rT3	LR-LC-MS/MS	3.0	2.1	1.4
	HR-LC-MS/MS	3.9	2.7	3.0
T2	LR-LC-MS/MS	4.0	2.2	3.3
	HR-LC-MS/MS	2.4	1.6	1.4

Additionally, a freeze thaw study was carried out by using the same aliquot of standards and spiked horse serum samples which were repeatedly thawed and refrozen. With each thawing a set of calibration and quality control solution were prepared and the sample extracted as per the procedure for low-resolution LC-MS/MS and compared to the previous thaw cycles. From Tables 5.8 and 5.9 it can be seen that there was minimal impact on the results obtained during the study which is in agreement with results previously reported in literature.<sup>362, 363</sup>

Therefore, the limiting factor for the analysis is the storage of standard solutions in glass vials and therefore the suppliers recommended storage must be followed. Additionally, where possible a thermostated autosampler should be used to maintain stability of the solution during analysis.

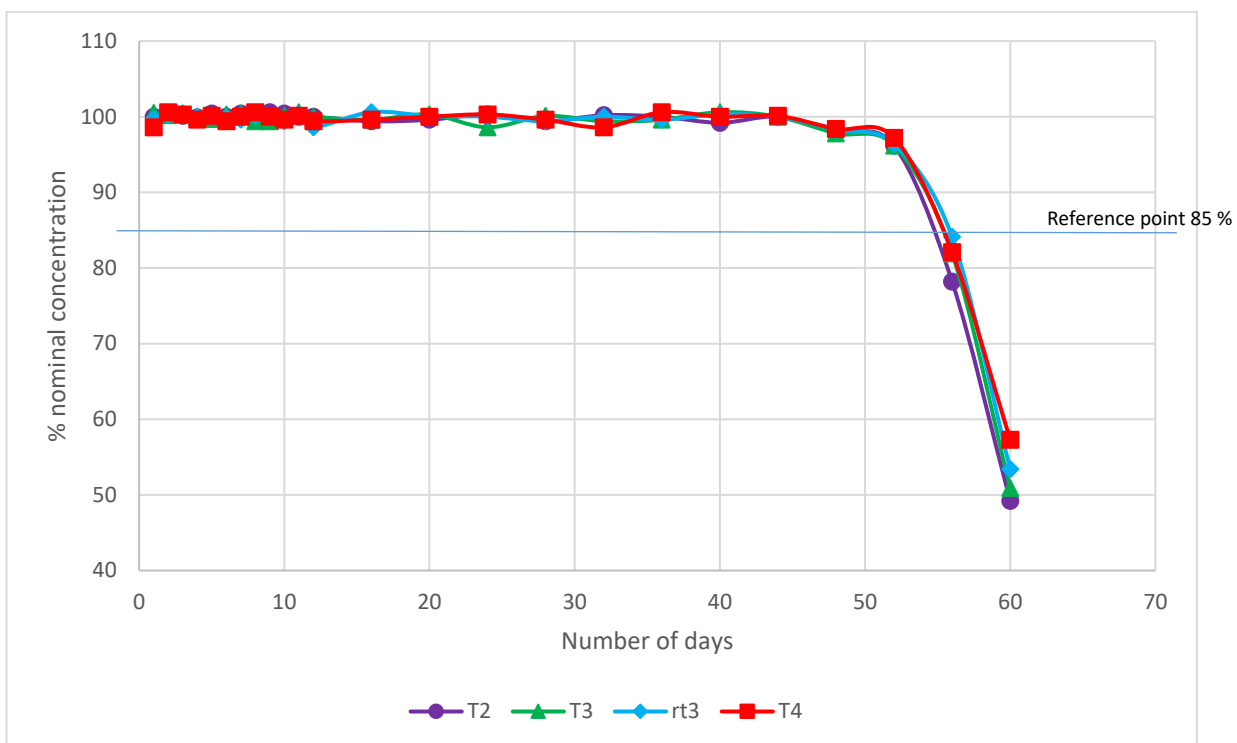
**Table 5.8: Impact of freeze-thaw cycles on standard solutions**

Cycle Number	Calculated concentration % Different (%)			
	T4	T3	rT3	T2
1	-0.47	-3.27	-1.21	1.74
2	-0.20	-1.14	-2.05	-1.46
3	1.40	2.49	3.43	-1.83
4	-1.96	-2.76	1.08	0.88
5	1.31	-3.64	0.76	-3.68
6	2.55	-1.65	0.34	-2.93
7	-3.82	3.54	1.27	0.30
8	-1.01	0.06	-0.45	1.42
9	-1.14	3.60	-2.55	-0.27
10	1.75	-3.23	1.35	-1.30

**Table 5.9: Impact of freeze-thaw cycles on spiked serum samples**

Cycle Number	Calculated concentration % Different (%)			
	T4	T3	rT3	T2
1	-2.85	-3.10	-0.24	1.59
2	-0.88	1.41	-3.58	-0.02
3	1.85	-1.71	-1.27	2.91
4	-1.43	1.29	1.70	0.32
5	0.69	1.12	2.70	1.88
6	0.58	-2.50	-1.54	-0.84
7	-2.45	-2.22	3.44	-0.20
8	-1.38	-2.26	-3.38	1.23
9	-2.94	2.26	0.41	3.91
10	-2.19	-1.20	-1.84	-0.92

a)



b)

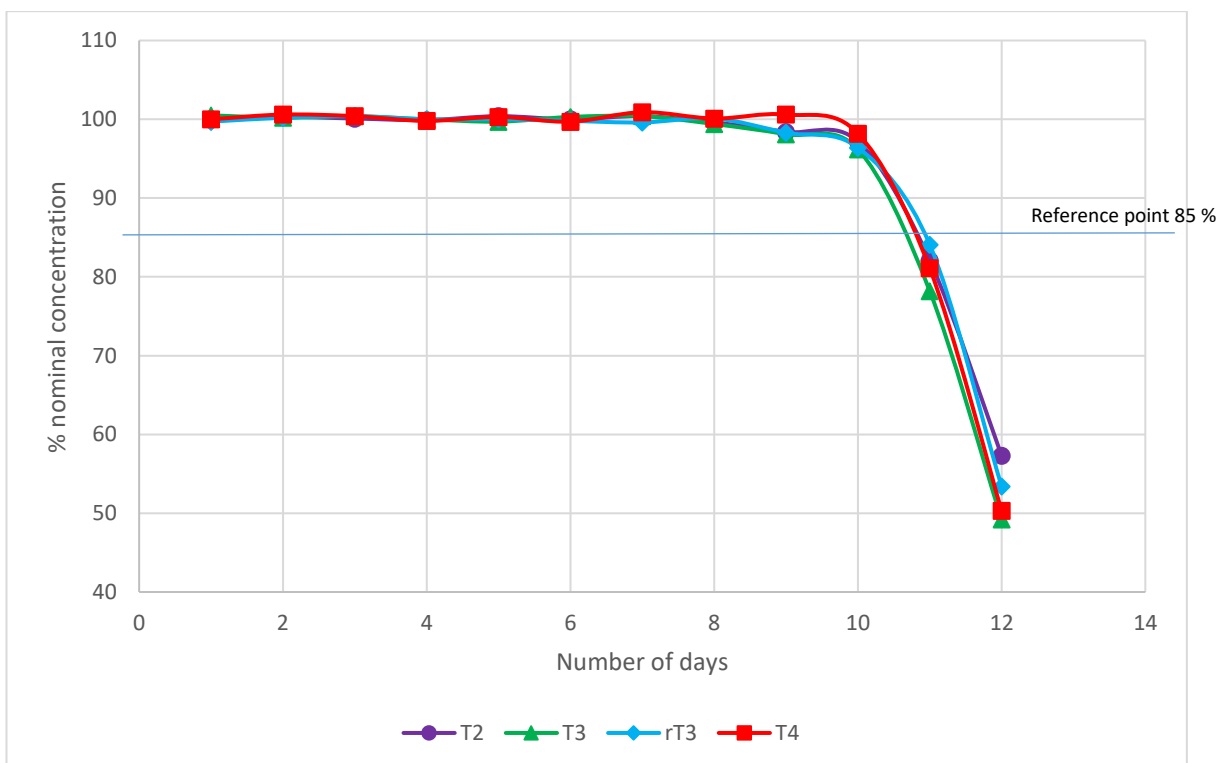


Figure 5.9: Stock solution stability for solutions stored at a) -20 °C and b) 2-8 °C

### **5.3. Tablet Analysis**

#### **5.3.1. Method**

In order to access the low-resolution LC-MS method for the analysis of commercially available tablets were obtained. Tiromel® and two batches of Cytomel® tablets containing 25 µg of T3 and Dithyron® containing 12.5 µg of T3 and 50 µg of T4 were obtained. The whole tablet was crushed using a pestle and mortar and transferred to a 10 mL volumetric flask, dissolved in methanol and sonicated for 5 minutes. Cytomel and Tiromel were diluted by taking 400 µL and made up to 10 mL with methanol. For Dithyron, to ensure that both T3 and T4 were within the calibration range, 200 µL was taken and diluted to 10 mL with methanol. The solution was filtered through a 0.22 µm syringe filter and analysis by LC-MS. Each batch of tablets was analysed in triplicate.

#### **5.3.2. Results and discussion**

Three batches of T3 and one batch of a combined T3 and T4 supplements were analysed for total content. The weight of the tablets were all consistent with an average weight of 0.06 g for all four. Visual differences were noted between the two manufacturers with Cytomel™ having a pink and nonglossy coating whereas Tiromel™ had a white glossy coating. The total content analysis showed that all four tablets contained T3 with Dithyron™ also containing T4, as identified by the retention time and tandem mass spectrometry (Figure 5.10). The tablet analysis was consistent with the dosages stated on the packaging for all four batches of thyroid supplement with a % content of >93.3 % for all batches and replicate preparations (Table 5.10). Good inter-batch and inter-tablet precision was also observed with a % RSD of <1.8 % and <3.4 %, respectively.

**Table 5.10: Tablet results**

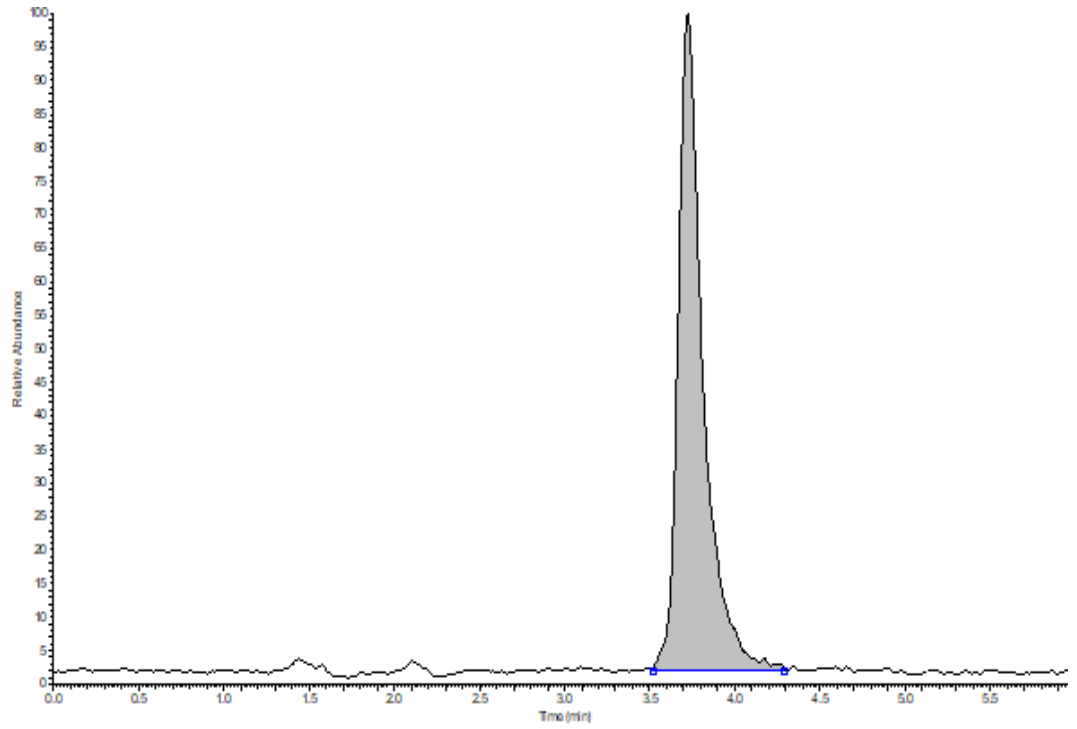
Sample	Replicate	$\mu\text{g per tablet}$ (n=3) $\pm$ SD	% Content (n = 3) (%RSD)	% Content Per batch (n = 9) (%RSD)
Cytomel batch 1	1	24.4 $\pm$ 0.83	97.6 (3.4)	95.6 (1.8)
	2	23.7 $\pm$ 0.27	95.0 (1.2)	
	3	23.6 $\pm$ 0.58	94.3 (2.4)	
Cytomel Batch 2	1	23.4 $\pm$ 0.46	93.6 (2.0)	94.0 (0.8)
	2	23.7 $\pm$ 0.38	94.8 (1.6)	
	3	23.4 $\pm$ 0.51	93.5 (2.2)	
Tiromel	1	23.3 $\pm$ 0.12	93.3 (0.5)	94.4 (1.3)
	2	23.9 $\pm$ 0.06	95.7 129(0.3)	
	3	23.5 $\pm$ 0.19	94.1 (0.8)	
Dithyron – T3	1	12.4 $\pm$ 0.08	99.2 (0.6)	96.3 (2.7)
	2	11.8 $\pm$ 0.13	94.4 (1.1)	
	3	11.9 $\pm$ 0.07	95.2 (0.6)	
Dithyron – T4	1	49.3 $\pm$ 0.21	98.6 (0.4)	98.4 (0.9)
	2	48.7 $\pm$ 0.09	97.4 (0.2)	
	3	49.6 $\pm$ 0.16	99.2 (0.3)	

## 5.4. Dissolution

### 5.4.1. Method

Dissolution was carried out using a SOTAX Smart AT7™ dissolution bath from Sotax (Finchley, London). The dissolution bath was set to 37 °C and 250 mL of FASSGF was added to each vessel, the rotor speed set to 75 RPM and allowed to equilibrate for at least 1 hour as specified in the United States and European pharmacopeia.<sup>364, 365</sup> The initial and final temperatures were recorded to ensure consistent temperature control. Tablet weights were recorded prior to being released into the relevant vessels simultaneously. Samples were taken at the following time point through probe filters and syringe filters; 5, 10, 20 and 30 minutes.

a)



b)

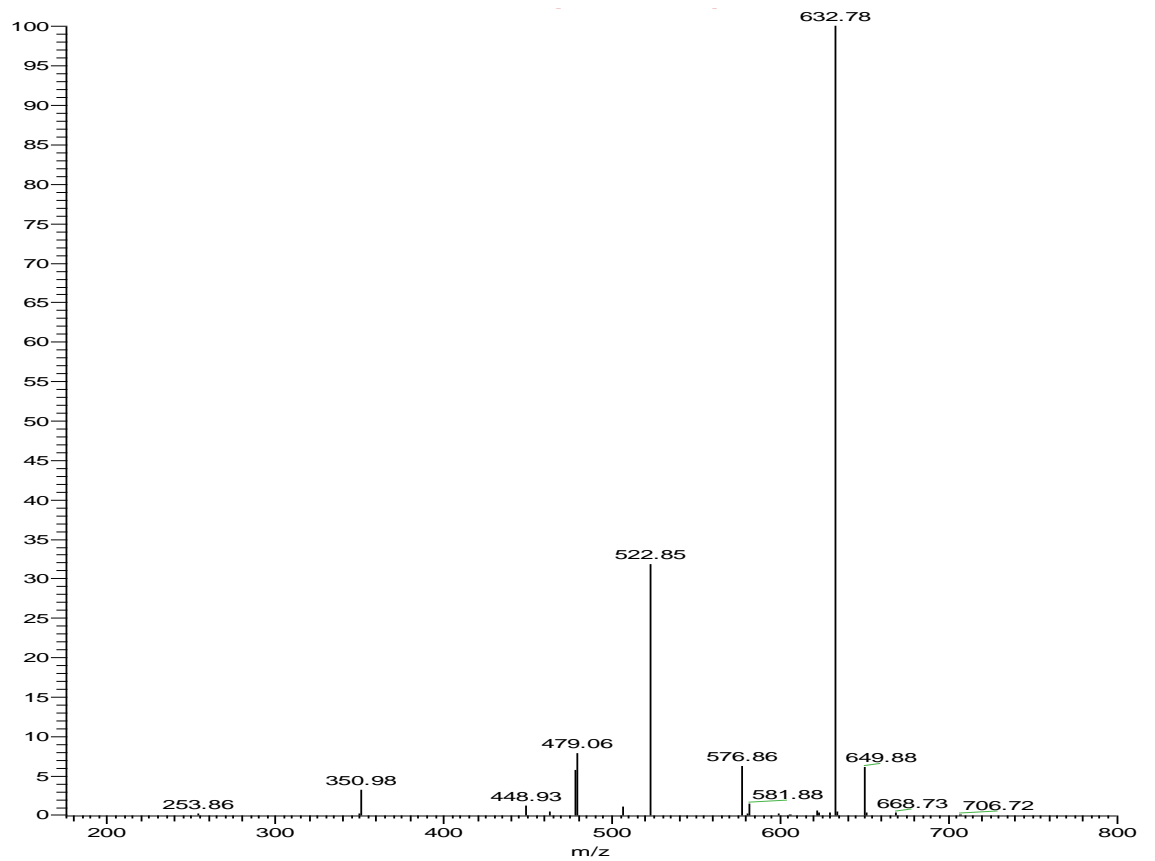


**Figure 5.10: Analysis of Cytomel™ tablet showing a) extracted ion chromatogram and b) product ion MS of  $m/z$  650 for triiodothyronine**

The paddles were stopped and 250 mL of FaSSIF added to each vessel and the paddles resumed. Samples were then taken at the following time point through probe filters and syringe filters; 35, 40, 50, 60, 90, 120, 150, 180, 210 and 240 minutes. Approximately 1 mL was transferred to an autosampler vial for analysis by LC-MS/MS. Calibration standards were prepared contained T3 and T4 over the range of 0-200 ng/mL by diluting the stock solutions in methanol which were ran at the beginning and end of each dissolution run. Quality control standards at 50 ng/mL were also prepared and injected throughout the run to ensure there was no inter-run variation.

#### **5.4.2. Results and discussion**

Throughout all runs there was minimal variation observed as can be seen from the combined calibration graph for the standards ran at the beginning and end of every acquisition (Figure 5.11). The inter run quality control standards showed good inter analysis precision with a calculated concentration of between 49.8 and 51.3 ng/mL for all injections.

From the dissolution profile it can be noted that there is minimal release during the first 30 minutes indicating that both T4 and T3 are poorly soluble in gastric fluid with a pH of 1.6. After the introduction of intestinal fluid there is a rapid release of the active pharmaceutical ingredient which is consistent across all batches (Figure 5.12). Dissolution testing is a procedure used within quality control testing and method development to assess the bioaccessibility of tablet formulations. The United States Pharmacopeia (USP) has a specification of at least 70 % of release after 45 minutes, which is displayed on the dissolution profile.<sup>366</sup> From the profile obtained, all four batches are consistent with the USP with 75 % release in approximately 45 minutes and total release is observed within 120 minutes. The USP used a quality control method for the dissolution testing of supplement containing either T3 or T4, however does not state a method for a combined supplement. The method in the USP uses an alkaline borate buffer at pH 10. A quality control method is used for the purpose of identifying variation in the manufacturing and formulation of tablets and does not account for the variations in the gastrointestinal tract. This could account for the small variations between the release when using the biorelevant media.

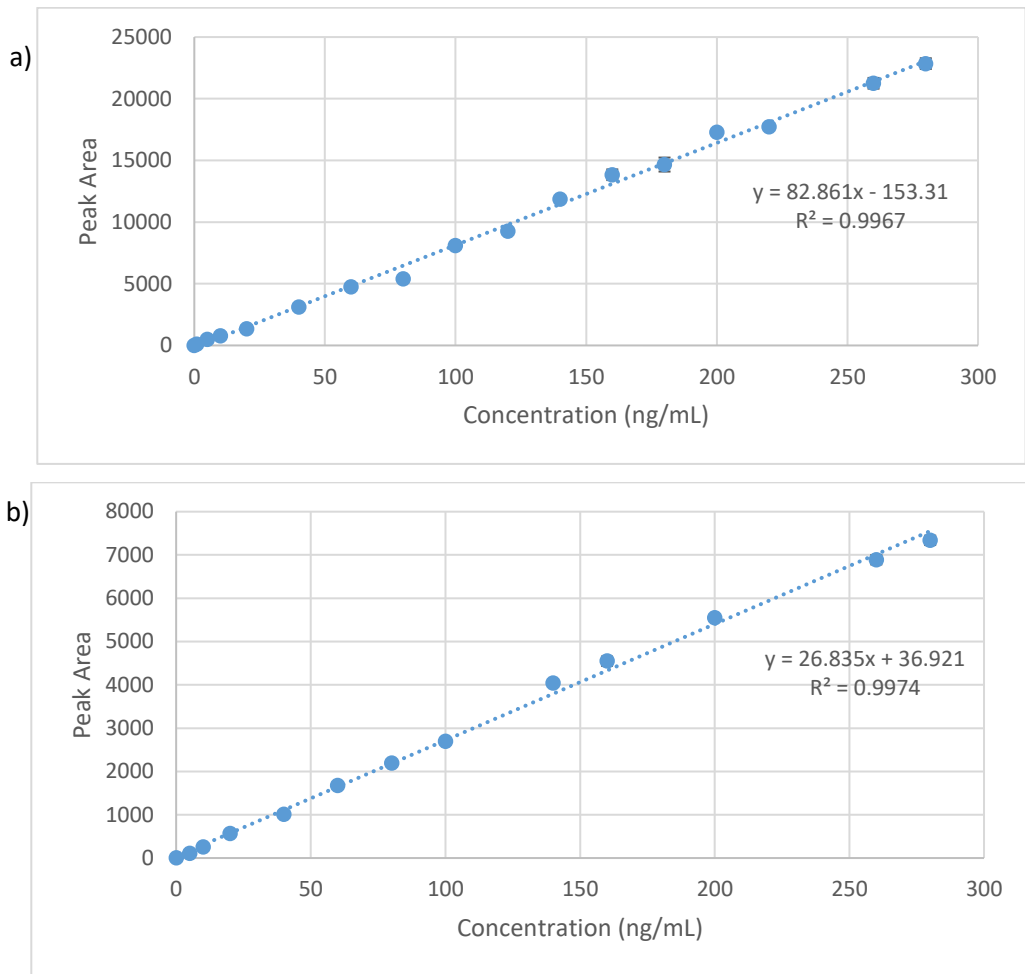


**Figure 5.11: Combined calibration graph from all dissolutions. a) T3 (n=8) and b) T4 (n=2)**

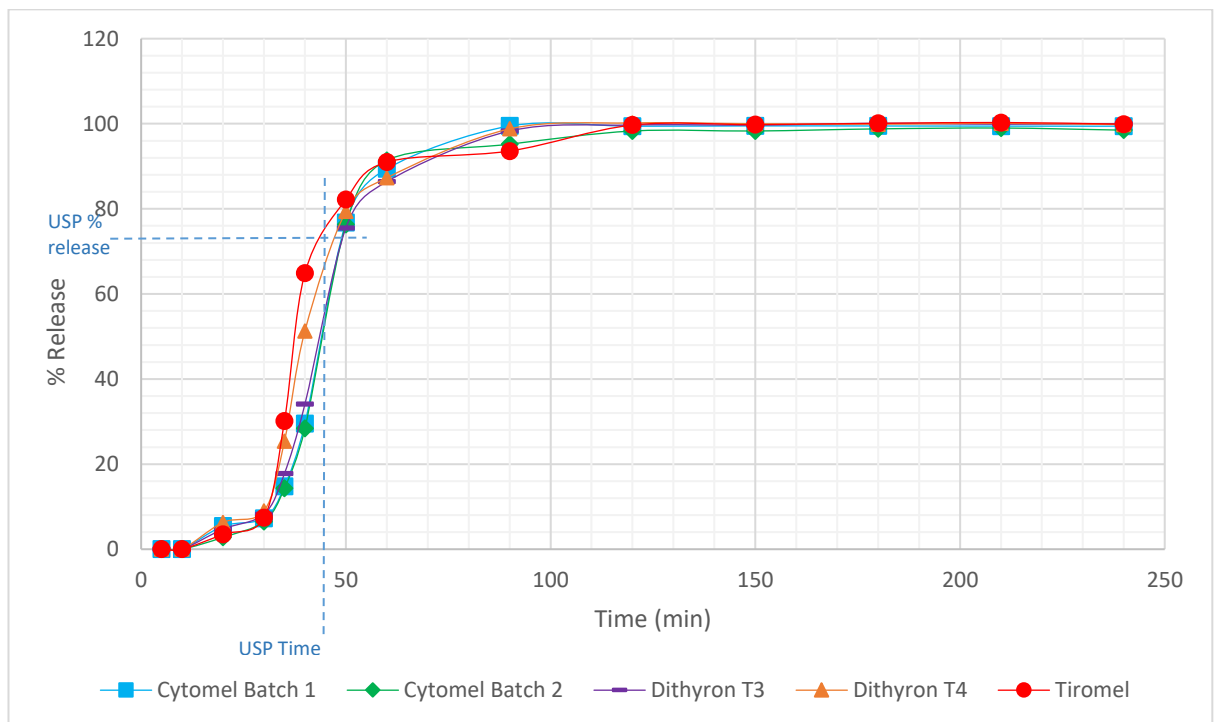


**Figure 5.12: Dissolution profile of 4 batches of thyroid supplements**

From the kinetic profile, Figure 5.13, it can be observed that a two-stage dissolution process occurs for both T3 and T4 based upon the 2 linear slopes of the log of the % drug remaining. The linear relationship within the two stages shows that both stage 1 and 2 are first order kinetics but identify as a 2-step process. In stage 1 the table coating is dissolved with minimal active pharmaceutical ingredient release. In stage 2 the active pharmaceutical ingredient is rapidly released from the tablet into the gastrointestinal fluid. Rate constants ( $k$ ) of between  $5.3 - 6.1 \text{ h}^{-1}$  and  $0.4 - 0.8 \text{ h}^{-1}$  with the first-order rate constant being consistent with the coating dissolution and then the tablet break down. The rate constant was calculated by a change in the % cumulative drug remain over time  $((y_2 - y_1)/(x_2 - x_1))$  with  $y$  calculated from the equation of the line.

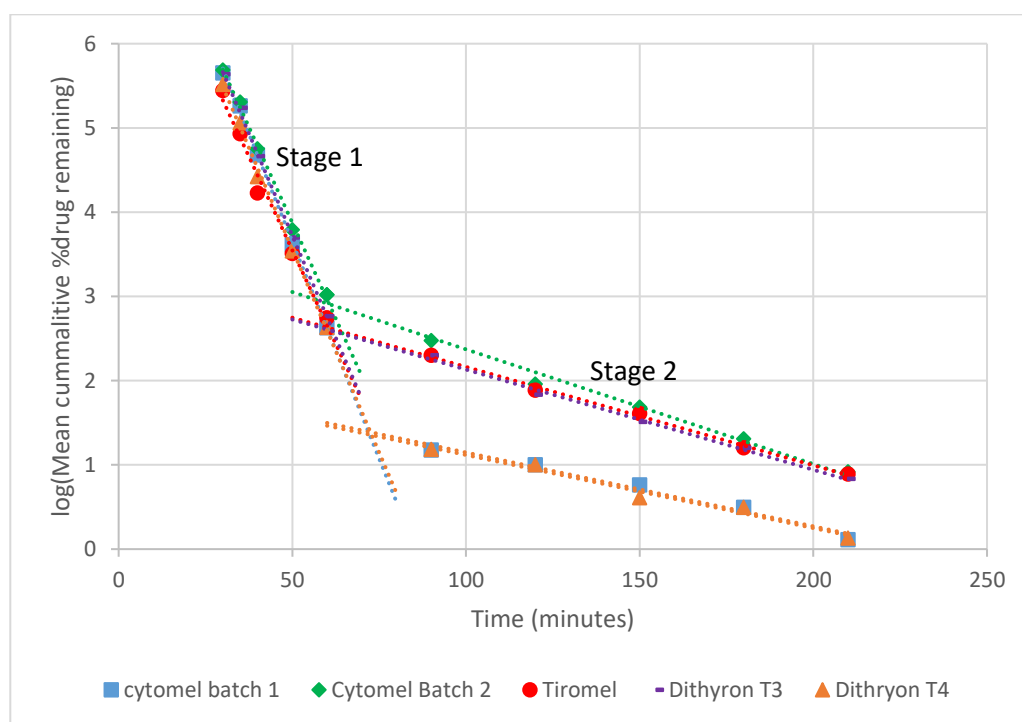


**Figure 5.13: Kinetic profile of the dissolution of T3 and T4**

## 5.5. Serum Analysis

### 5.5.1. Method

For low resolution LC-MS serum samples were thawed and vortexed prior to extraction. The final developed method was applied to samples, prepared in triplicate, by transferring 500  $\mu\text{L}$  to microcentrifuge tubes along with 500  $\mu\text{L}$  of 0.1% formic acid in water. Samples were vortexed and centrifuged at 5300 g for 5

minutes. The supernatants were loaded onto a HyperSep™ C18 solid phase extraction (SPE) cartridge, which were preconditioned sequentially with 2 mL of 0.1 % formic acid in methanol and 2 mL 0.1 % formic acid in water. The cartridge was washed with 1 mL of methanol:water, 30:70 (%v: %v) and then the target compounds were eluted with 1 mL of methanol:water, 80:20 (%v:%v). The eluent was dried down under a stream of nitrogen and reconstituted in 50 µL of mobile phase. For high resolution LC-MS serum samples were thawed and vortexed prior to dilution. Samples were prepared by transferring 10 µL of sample to an autosampler vial and diluted with 990 µL of water and vortex mixed.

### **5.5.2. Results and discussion**

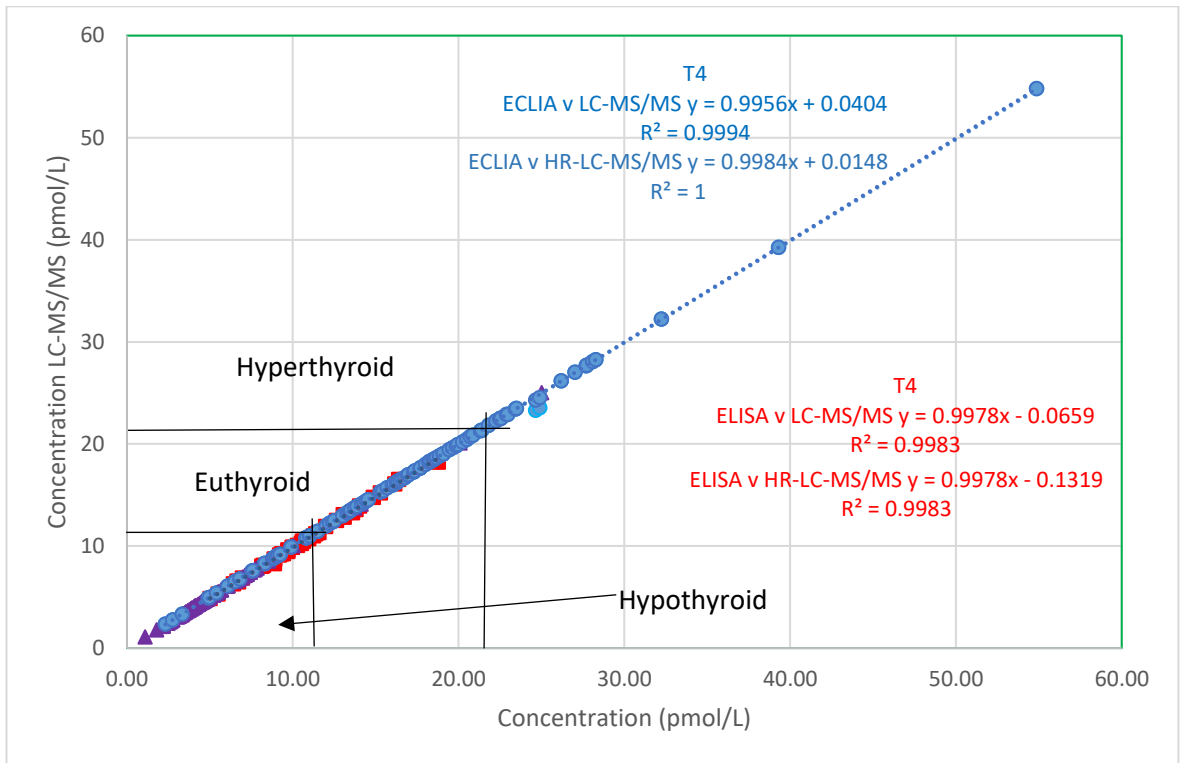
Human serum samples previously testing for T4 and T3 by ECLIA were provided by the Cellular pathology (CEPA) Biobank at the Royal Victoria Infirmary. As the samples are anonymised and not controlled under the human tissue act full NHS ethical approval was not required due to the biobank having ethical approval for the use of samples for external research work (Research Ethics Committee reference number 17/NE/0070).<sup>367</sup> Samples previously tested by ELISA were provided by the Department of Sports Exercise and Rehabilitation at Northumbria University and were analysed, in a blind study, using the validated LC-MS methods for both low resolution and high-resolution LC-MS. The analysis showed that the method for both low resolution and high resolution were comparable to the clinical routine testing methods of ECLIA and the more readily available ELISA. The null hypothesis for the comparison of the method was that there would be statistically no difference between the values obtained. In order to accept the null hypothesis at the 95% confidence interval a p-value of >0.05 should be obtained. Statistical paired sample t-test using SPSS found that there was no statistical difference between each set of data at the 95% confidence interval. Figure 5.14 shows the comparison of samples previously analysed via ECLIA and ELISA across hypothyroid, normal and hyperthyroid states in comparison to the data obtained using the developed LC-MS/MS method. The comparison shows that the analysis via LC-MS/MS is comparable across all the thyroid function states. However, it was not possible to obtain mean data for the ECLIA data as only a single clinical measurement was made for each sample.

A comparison of all four methods shows a significant reduction in analysis time for high resolution LC-MS and also batch analysis by low resolution LC-MS from 20 minutes to 7 and 8.75 minutes, respectively. Both LC-MS methods are also able to analyse all four hormones simultaneously meaning that repeat tests do not need to be performed for each hormone. However, due to the SPE extraction used for low resolution LC-MS a higher level of operator skill is required when compared with the other three methods, which mainly require the operator to be skilled in basic laboratory techniques and the use of specialist software. The increase in skill level and training requirements may still be a more favourable option over the high-resolution LC-MS for some laboratories due to the increase in capital cost associated with the high-resolution instrumentation.

## 5.6. Conclusion

A method has been developed and validated for the analysis of four thyroid hormones, T4 and T3, rT3 and T2 by low resolution and high-resolution LC-MS/MS. The inclusion of and the ability to separate rT3 ensures that quantification of T3 is not affected by co-elution. The inclusion of T2 within the method has the potential to aid in the diagnosis of additional underlying medical conditions. Separation of the four thyroid hormones was achieved using a Supelco 2.1  $\mu\text{m}$  F5, 100 x 2.1 mm column. The developed method used an isocratic method of 30 % water + 0.2 % formic acid (A) and 70 % methanol + 0.2 % formic acid (B) at a flow rate of 0.2 mL/min. Both mass spectrometers were operated in selected reaction monitoring mode with ions transitions of 524  $\rightarrow$  507  $m/z$ , 650  $\rightarrow$  633  $m/z$ , 650  $\rightarrow$  479  $m/z$  and 776  $\rightarrow$  604  $m/z$  being monitored for T2, T3, rT3 and T4, respectively. The developed method significantly improves on the currently used clinical method, ECLIA, both in terms of accuracy and limits of detection, with an increase in accuracy from 30 % to <3.8 % at the LOQ. In addition, the method also significantly improves on previously published thyroid hormone LC-MS/MS methods with a reduced run time allowing for greater sample throughput. The established method has then been applied to the analysis of thyroid hormones from tablet formulations, for total content and dissolution profiling, and human serum samples. The analysis of tablet formulations shows results consistent with the stated dosages and the USP dissolution specification.

a)



b)

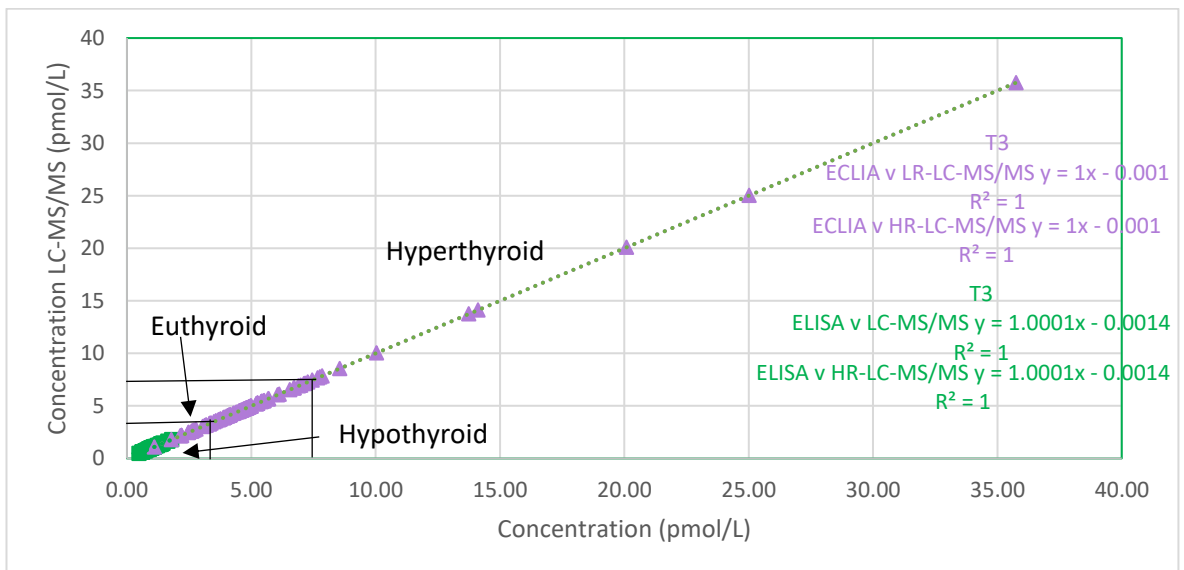


**Figure 5.14: Measurement Agreement plots for a) T4 by ELISA or ECLIA versus LC-MS and b) T3 by ELISA or ECLIA versus LC-MS.**

ECLIA, N = 118; ELISA, N = 40; LR-LC-MS, N = 158; HR-LC-MS, N = 158

For the analysis of serum samples, a clean-up method was developed utilising SPE for low-resolution liquid chromatography-mass spectrometry and dilution for high-resolution liquid chromatography-mass spectrometry to minimise any matrix effects. The developed SPE method utilised C18 cartridges which were preconditioned with acidified methanol and water prior to the loading of the acidified sample. Matrix removal was achieved by washing the cartridge with a 30 % methanol solution and compound elution was achieved with an 80 % methanol solution. Due to the higher levels of sensitivity of the high-resolution mass spectrometer a simple dilution procedure was required for the minimising of matrix effects. The dilution study found that a 1 in 100 dilution was required to remove any matrix effects observed. The developed sample preparation method show excellent recoveries (>95 %). The thyroid hormone results obtained from both the LR-LC-MS and HR-LC-MS were compared across all thyroid function states with previous results obtained for the samples via ECLIA and ELISA and were found to be comparable at a 95 % confidence interval using a paired sample T-test. The stability of thyroid hormones when stored in solution must be considered when performing the analysis and therefore stock solutions should be aliquoted into small portions and storage at -20°C for a maximum of 50 days. Due to the limited stability of the compounds at 2-8 °C a thermostated autosampler should also be used for all analysis, which in this study was set to 5 °C.

The developed method and assessed application highlight the advantages in the use of LC-MS within a variety of industries including clinical biochemistry and pharmaceutical analysis. With the ability to provide data with excellent precision while also providing high levels of sensitivity. The inclusion of both low resolution and high resolution mass spectrometry demonstrates the ability to obtain a very high level of sensitivity with minimal sample preparation requirements. The advantages for the development method in terms of sensitivity and precision would allow for more accurate and reliable diagnosis of thyroid hormone disorders which has previously discussed can go miss diagnosed, particular for hypothyroidism. In addition the method has been used to support the department of Sport, exercise and rehabilitation at Northumbria University to assess the affects of sports training on thyroid function with the hopes of the department to develop dietary interventions for adolescence involved in intense physical training.

## **Chapter 6: Plant toxins results and discussion**

## 6. Plant toxins results and discussion

### 6.1. Method development

#### 6.1.1. Evaluation of mobile phase

A number of studies have been performed analysing compounds within a specific plant genus however there has been limited studies performed focusing on compounds found across a range of plant genus. Table 14 shows a summary of some of the analysis previously performed and the compounds of the focus of these studies. While there are a number of published studies which identify the compounds which normally focus on specific chemical compound classifications or plant species. Of particular importance in this study is the range of compounds found in plants which are grown locally and therefore pose a risk to human health. Based on the information available, the use of prior analytical methods for the basis of method development was not able to give a comprehensive understanding of the influence of mobile phase composition and gradient profile. However, based on the previous literature the stationary phase most often used is reversed phase C8 and C18 columns. Therefore, due to the number of compounds and the greater separation capacity of a C18 column over a C8 column, a C18 column was used for the initial investigation. From the previous studies shown in Table 6.1 a variety of mobile phases have been used including acetonitrile:water, methanol:water, methanol:buffered aqueous and acetonitrile:buffered aqueous therefore, the mobile phase selection will be based on these four systems. Based on the pKa of the compounds of interest, shown in Table 2.1, an acidic environment would be best suited to the compounds therefore, the unbuffered solutions will be acidified with formic acid and a buffered mobile phase system based on the suitability of buffering compounds with LC-MS applications and buffering range as per Table 6.2 was investigated. Due to the pKa of the compounds an ammonium formate buffer solution adjusted to pH 3.5 was chosen.

From the extracted ion LC-MS/MS chromatograms shown in Figure 6.1 it can be seen that there was a loss of compounds observed when using acetonitrile as the organic modifier and also when using a buffered aqueous solution. The loss of compound when using acetonitrile could be caused by the variation in organic strength and therefore affecting the retention mechanisms observed. To access

this a longer chromatographic method was used and the compounds were observed eluting from the column at a greater retention time.

The use of the buffered aqueous solution also observed a decrease in the peak areas observed for some of the compounds and as such it was concluded that the presence of the buffer ions was resulting in either a reduction in ionisation in the source or ion suppression within the ion trap. Therefore, the remaining mobile phase optimisation was performed using water and methanol as the mobile phase as this showed peaks for all the compound within an adequate run time. Initially co-elution of atropine, scopolamine and cathinone and of solanine, coumarin and veratridine was observed therefore, the gradient system was adjusted. A lower starting percentage of methanol was used in order to improve the chromatographic separation of the co-eluting compounds however, full resolution could not be observed within a suitable run time resulting in separation based on MS ions. (Figure 6.1) In order to assess the separation, the resolution was calculated for each neighbouring set of peaks using the resolution calculation in section 1.2.1.

The final developed method showed good retention stability with % RSDs of <4.3 % for all compounds. The chromatograms for the final separation method can be seen in Figures 6.2-6.4.

### **1.1.1. Optimisation of MS parameters**

Tandem mass spectrometry parameters were optimised by direct infusion of individual standard preparation at 600 ng/mL into the mass spectrometer. For each compound collision energies (ce) were determined to give a precursor ion and a minimum of two product ions. For quantification purposes the two most stable product ions were chosen along with the precursor ion to be monitored in selected reaction monitoring (SRM) mode.

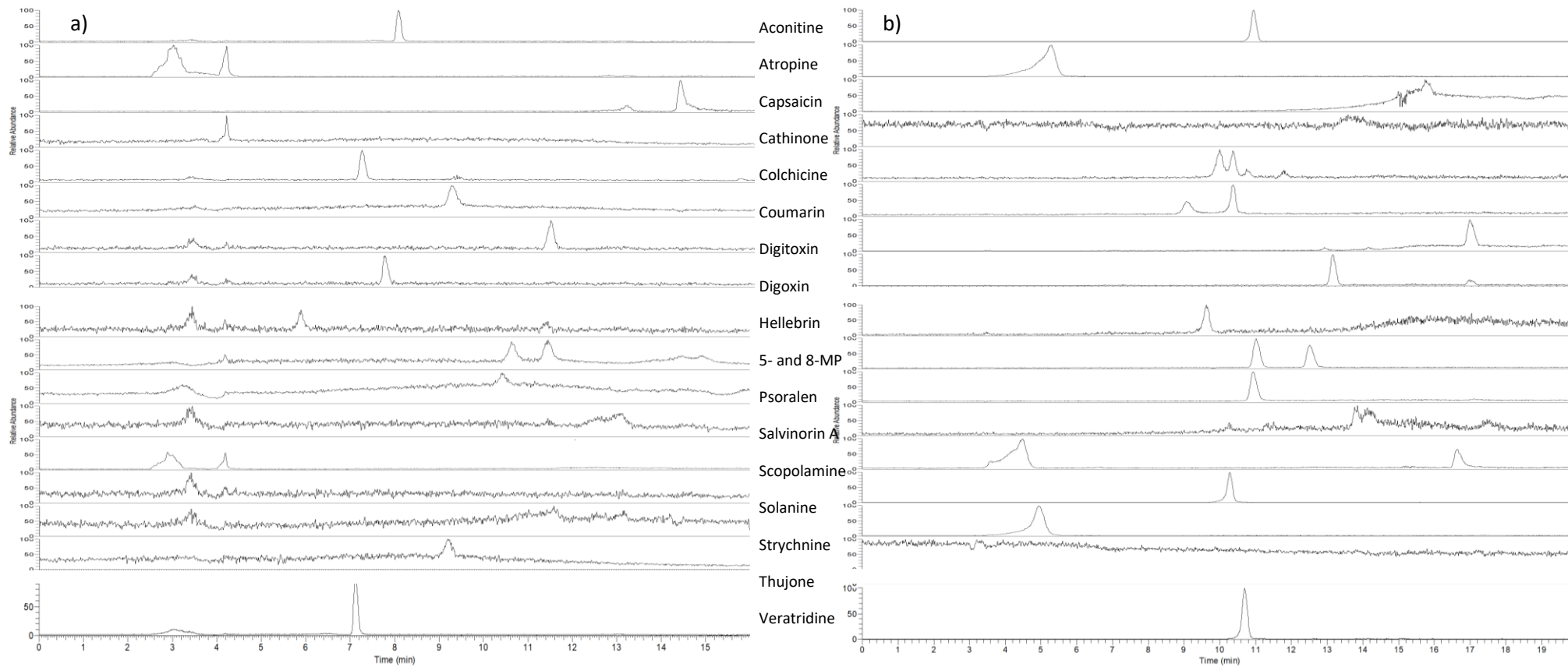


**Figure 6.1: Standard solution extracted ion chromatograms for a) water:acetonitrile and b) buffer:methanol using the gradient in Table 4.1**

**MP: Methoxypsoralen**

**Table 6.1: Comparison of existing methods for the analysis of plant toxins**

Column (i.d, length, particle size)	Compounds tested	Mobile phase	Flow rate (ul/min)	Run Time (min)	Visible chromatographic resolution observed	Reference number
XTerra RP 8 (2.1 x 150 mm, 3.5 µm)	Aconitine	A: 0.1 % ammonium acetate pH6, B: methanol	200	10	N/A	368
XTerra RP 18 (2.1 x 150 mm, 3.5 µm)	Aconitine, mesaconitine, hyaconitine and jesaconitine	A: 0.1% (v/v) formic acid in acetonitrile. B: 0.1% (v/v) formic acid in water	200	25	Yes	369
Inertsil ODS-2 (4.6 x 150 mm, particle size not reported)	Aconitine, mesaconitine, hypoconitine and jesaconitine	A: Tetrahydrofuran, 0.3 % tetrafluoroacetic acid and glycerine (19:81:0.3, v:v:v)	1000	30	Yes	370
Shiseido UG80 C 18 (not reported)	Aconitine, mesaconitine, hypoconitine and jesaconitine	A: 20 mM Ammonium acetate B: Acetonitrile	200	35	Yes	371
Superspher160 RP Select B (2 x 125 mm, particle size not reported)	Aconitine, atropine, colchicine, scopolamine, coniine, cotinine, cytosine, nicotine and physostigmine	A: 50 mM Ammonium formate (pH 3.5) B: Acetonitrile	400 – 600 gradient	10	No	372
XTerra MS C18 (2.1 x 100 mm, 3.5 µm)	Atropine, scopolamine	A: Formate buffer B: Acetonitrile	200	10	Yes	373
BDS C18 (3 x 50 mm, 3 µm)	Atropine	A: Acetonitrile: methanol: 10 mM Ammonium acetate (625:375:150, v:v:v)	500	2	N/A	374
Eclipse XDB C8 (2.1 x 30 mm, 3 µm)	Colchicine	A: 50 mM Ammonium acetate (pH 4) + 5 % Acetonitrile, B: Acetonitrile	500	6	N/A	375
XTerra C18 (2 x 150 mm, 3.5 µm)	Colchicine	A: acetonitrile. B: 2mM formate buffer (pH 3)	200	10	N/A	376
Alltech C18 (1 x 250 mm, 5 µm)	Colchicine	A: acetonitrile: 2 mM ammonium formate (pH 3.0) (75:25, v:v)	50	10	N/A	377

**Table 6.1 (continued): Comparison of existing methods for the analysis of plant toxins**

Column (i.d x length, particle size)	Compounds tested	Mobile phase	Flow rate (ul/min)	Run Time (min)	Visible chromatographic resolution observed	Reference number
Zorbax SCX (2.1 x 150 mm, 5 µm)	Cathinone, norephedrine, norpseudoephedrine, ephedrine, pseudoephedrine, methylephedrine, methylpseudoephedrine, methcathinone, mescaline and synephrine	A: 5 mM ammonium formate (pH 3) B: Acetonitrile	1500	10	No	378
Hypersil Gold (2.1 x 50 mm, 1.9 µm)	Capsaicin and dihydrocapsaicin	A: 2 mM ammonium formate. B: methanol	500	2	Yes	379
MetaSil Basic (3 x 100 mm, 3 µm)	Capsaicin, nonivamide and dihydrocapsaicin	A: water + 0.1% (v/v) formic acid B: methanol + + 0.1% (v/v) formic acid	250	16	No	380
LUNA 3U C18 column (2.1 x 100 mm, 3 µm)	Coumarin, psoralen, 5-methoxypsoralen, 8-methoxypsoralen, isoscopoletin, daphnetin-7-methylester, umbelliferone, 6- methylcoumarin, isopimpinellin, isobergapten, imperatorin, 4- methyl-daphnetin, esculetin, 6-hydroxycoumarin, 6,7-dihydroxy- 4-methylcoumarin, 5,7-dihydroxy-4-methylcoumarin, 8-acetyl- 6-hydroxy-7-methoxycoumarin, herniarin, 6-methoxy-4- methylcoumarin, 8-acetyl-6,7-dimethoxycoumarin, 3- acetylcoumarin, 7-methylcoumarin, nordalbergin, 6-methoxy-4- methylcoumarin, 7-methoxy-4-methylcoumarin, 6- methylcoumarin, dalbergin, citrophen, 7-ethoxycoumarin, 4- hydroxycoumarin, 4-ethoxycoumarin, 4-methylumbelliferone, 4- methyl-7-ethoxycoumarin, bergapten and osthol	A: water B: ACN	500	37	No	381

**Table 6.1 (continued): Comparison of existing methods for the analysis of plant toxins**

Column (i.d, length, particle size)	Compounds tested	Mobile phase	Flow rate (ul/min)	Run Time (min)	Visible chromatographic resolution observed	Reference number
Luna 5 µm Phenyl-Hexyl (2 x 50 mm, 5 µm)	Digitoxin	A: Ammonium acetate in water + 0.1 % acetic acid. B: Ammonium acetate in methanol + 0.1 % acetic acid	600	4.5	N/A	283
octadecylsilane analytical column (2 x 50 mm, particle size not reported)	Digitoxin, digoxin, digitoxigenin bisdigitoxoside, digitoxigenin monodigitoxoside, digitoxigenin, digoxigenin bisdigitoxoside, digoxigenin monodigitoxoside and digoxigenin	A: water B: Acetonitrile	1000	15	Yes	272
ACQUITY UPLC® HSS C18 (2.1 x 150 mm, 1.8 µm)	Solanine, Aconitine, Atropine, colchicine Digitoxin, Digoxin, Scopolamine, α-lobeline, ajmaline, brucine, cephalomannine, convallatoxin, cymarine, cytisine, emetine, gelsemine, ibogaine, jervine, kavain, lanatoside C, lupanine, mitragynine, neriifolin, oleandrin, ouabain, paclitaxel, physostigmine, pilocarpine, podophyllotoxin, proscillaridin A, reserpine, retrorsine, ricinine, senecionine, sparteine, strophanthidin, strychnine, veratridine and yohimbine	A: Acetonitrile (0.1% formic acid) B: Ammonium formate buffer pH 3.0	400	15	Yes	382
Zorbax C18 (1 x 50 mm, 3.5 µm)	Salvinorin A	A: 99.0 % H <sub>2</sub> O + 1.0 % acetonitrile. B: 99.92 % acetonitrile + 0.08 % formic acid	135	11	N/A	383
ACQUITY UPLC® HSS T3 (2.1 x 30 mm, 1.8 µm)	Salvinorin A	A: Water + 0.1 % formic B: Acetonitrile + 0.1 % formic	600	2	N/A	384
Kinetex C18 (4.6 x 250 mm, 5 µm)	α-solanine, α-chaconine and solanidine	A: 0.1 % Formic acid, B: 100 % acetonitrile and 0.1 % formic acid	500	20	Yes	385

**Table 6.1 (continued): Comparison of existing methods for the analysis of plant toxins**

Column (i.d, length, particle size)	Compounds tested	Mobile phase	Flow rate (ul/min)	Run Time (min)	Visible chromatographic resolution observed	Reference number
Waters C18 Acquity bridged ethylene hybrid (2.1 x 100 mm, 1.7 µm)	α-solanine, α-tomatine, solanidine and tomatidine	A: Water + 0.1% formic acid B: Acetonitrile + 0.1% formic acid	400	Not reported	Not reported	<sup>386</sup>
ZORBAX Eclipse XDB-C18 column (2.1 x 150 mm, 3.5 µm)	strychnine, brucine, strychnine-N-oxide and brucine-N-oxide	A: Ammonium acetate pH 4, B: methanol	200	10	No	<sup>321</sup>
ZORBAX Eclipse XDB C8 column (4.6 x 150 mm, 5 µm)	aconitine, atropine, scopolamine, strychnine, colchicine, hyaconitine, mesaconitine, yunaconitine, crassicauline A, benzoylaconine, benzoylmesaconine, benzoylhyaconine, deacetylyunaconitine, deacetylcrassicauline A, anisodamine, anisodine, matrine, sophoridine, oxymatrine, cytisine, N-methylcytisine and brucine	A: ammonium formate + 0.1 % formic acid in water B: ammonium formate + 0.1 % formic acid in acetonitrile	NR	24	No	<sup>387</sup>
Acquity BEH C18 (2.1 x 50 mm, 1.7 µm)	Thujone	A: 0.05 % formic acid in water B: acetonitrile	400	9.9	Not reported	<sup>388</sup>
Supelco® Rx-C18 (4.6 x 250 mm, particle size not reported)	Veratridine and cevadine	A: methanol: acetonitrile: 10 mM ammonium acetate (20:20:60, v:v:v)	900	40	Yes	<sup>389</sup>
Waters Symmetry C8 (4.6 x 250 mm, 5 µm)	Veratridine and cevadine	A: ammonium formate pH 3.0 B: methanol	200	35	Yes	<sup>390</sup>

**Table 6.2: LC-MS buffer suitability<sup>391</sup>**

Buffer	Buffering range	LC-MS compatible
Phosphate	1.1-3.1	No
	6.2-8.2	
	11.3-13.3	
Acetate	3.8-5.8	Yes – as ammonium
Citrate	2.1-4.1	No
	3.7-5.7	
	4.4-6.4	
Ammonium formate	2.7-4.7	Yes
Ammonium bicarbonate	6.6-8.6	Yes
Borate	8.3-10.3	Yes

**Table 6.3: Resolution of neighbouring peaks**

Compound 1	Compound 2	Resolution
Cathinone	Strychnine	2.0
Strychnine	Atropine	0.5
Atropine	Scopolamine	0.4
Scopolamine	Colchicine	2.3
Colchicine	Hellebrin	2.7
Hellebrin	Solanine	1.3
Solanine	Coumarin	0.2
Coumarin	Veratridine	0.2
Veratridine	Aconitine	1.1
Aconitine	Digoxin	2.4
Digoxin	Psoralen	0.9
Psoralen	8-Methoxypsoralen	0.9
8-Methoxypsoralen	5-Methoxypsoralen	2.9
5-Methoxypsoralen	Thujone	1.1
Thujone	Salvinorin A	1.9
Salvinorin A	Capsaicin	7.2
Capsaicin	Digitoxin	6.4

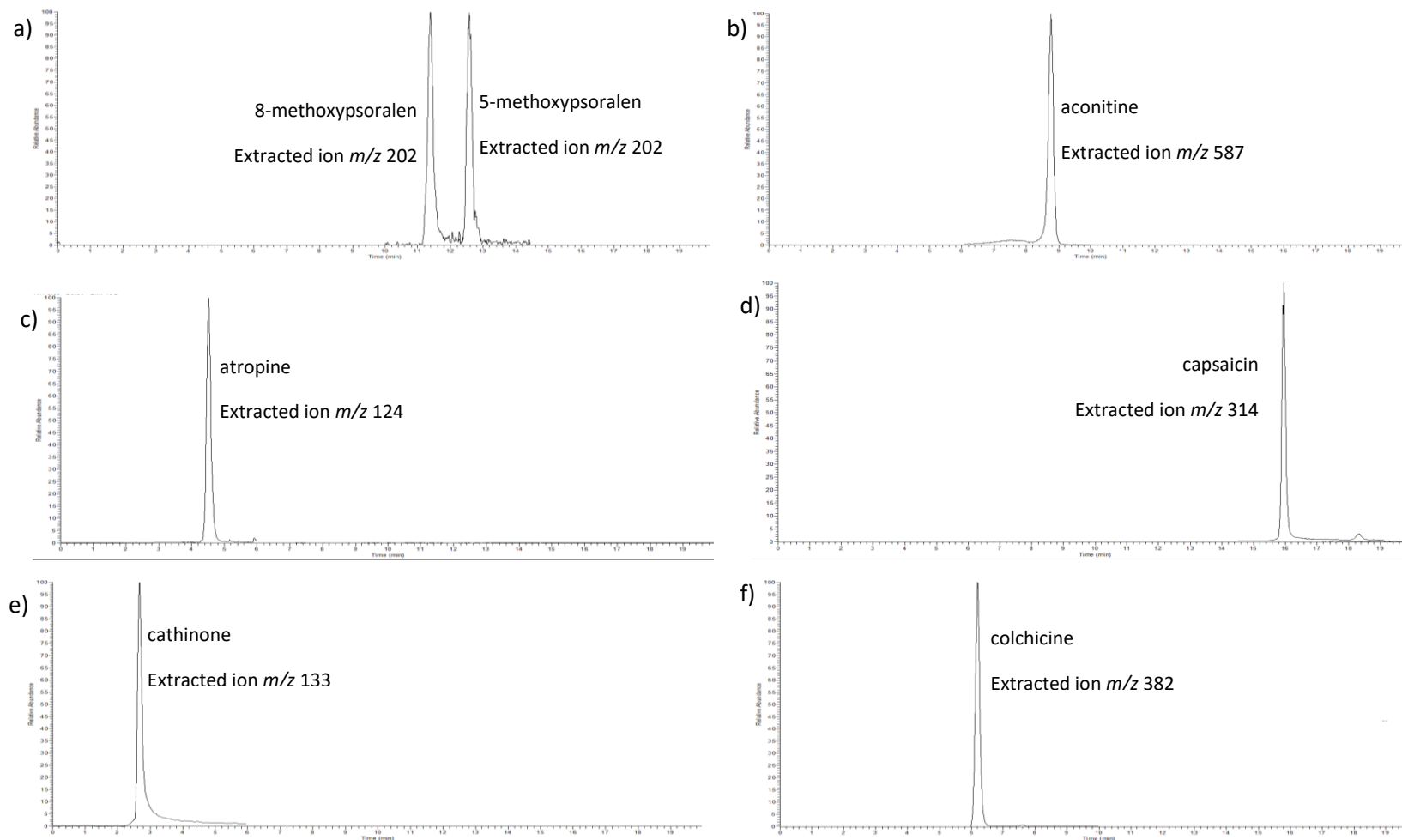


**Figure 6.2: Standard solution extracted negative ion ESI SRM chromatograms for a) 5- and 8- methoxypsoralen, b) aconitine, c) atropine, d) capsaicin, e) cathinone and f) colchicine**

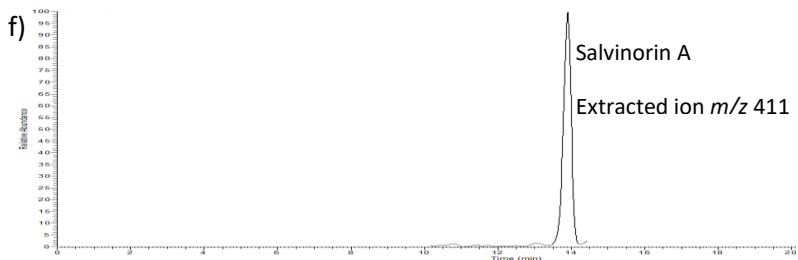
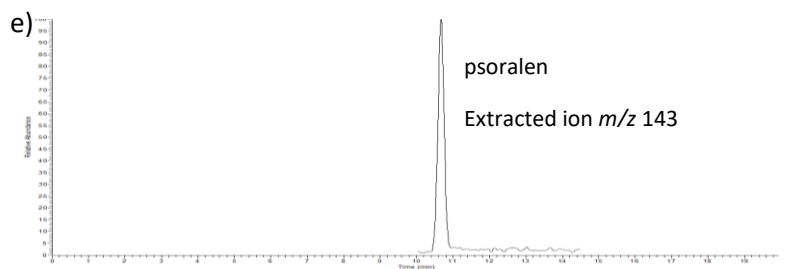
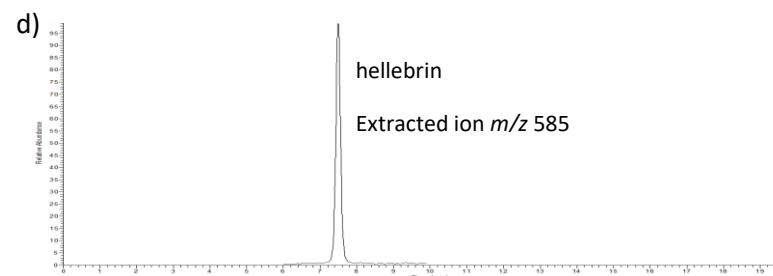
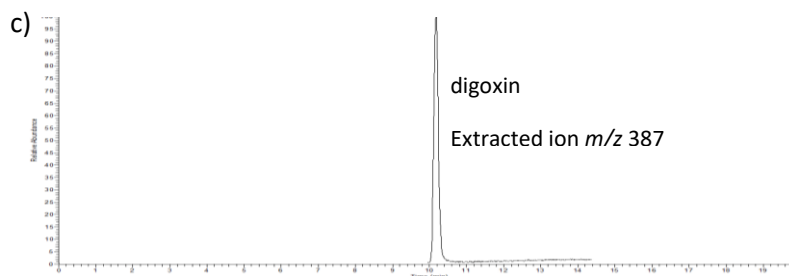
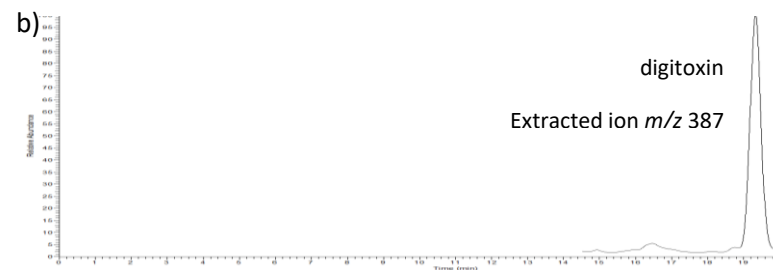
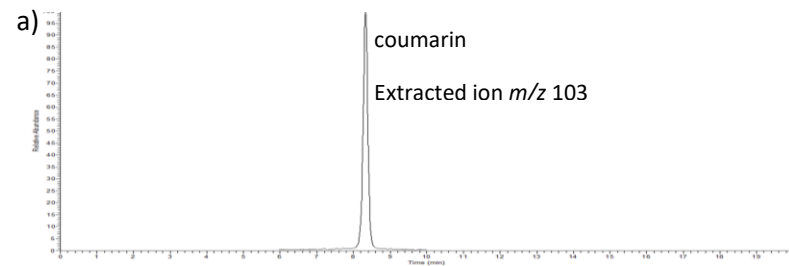


**Figure 6.3: Standard solution extracted negative ion ESI SRM chromatograms for a) coumarin, b) digitoxin, c) digoxin, d) hellebrin, e) psoralen and f) salvinorin A**

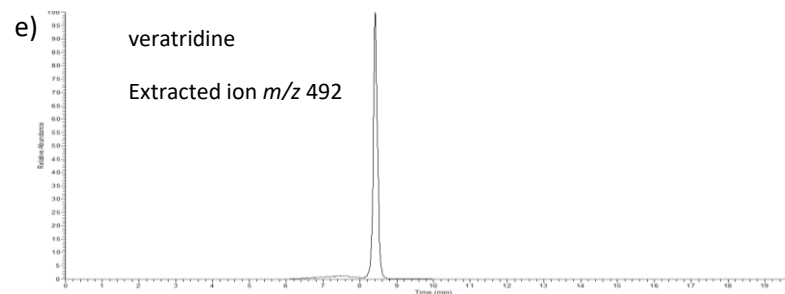
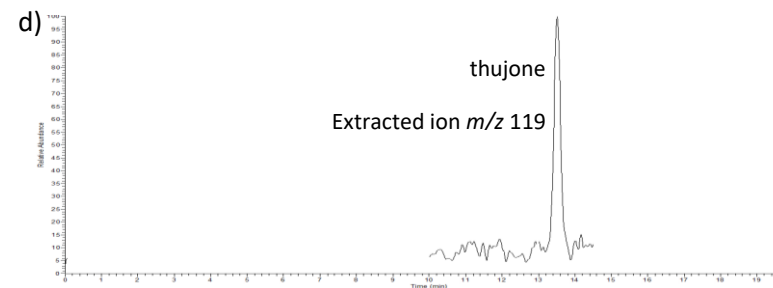
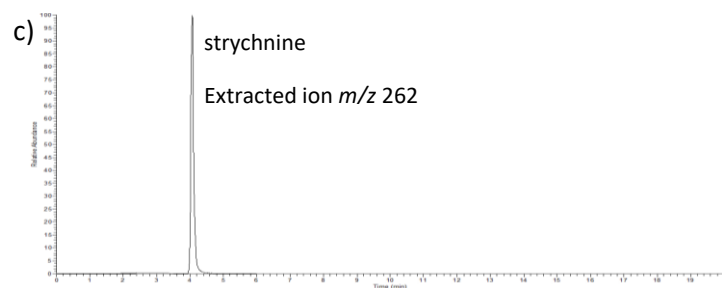
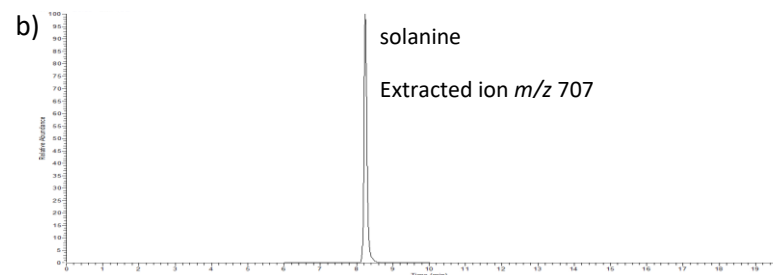
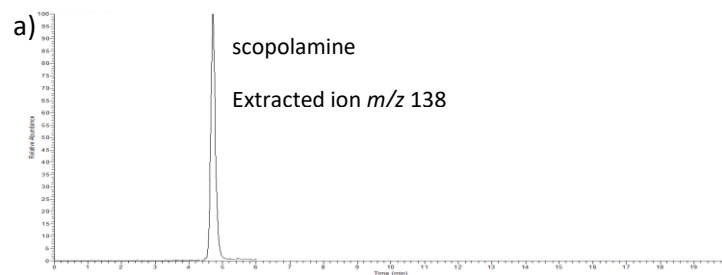


Figure 6.4: Standard solution extracted negative ion ESI SRM chromatograms for a) scopolamine, b) solanine, c) strychnine, d) thujone and e) veratridine

The collision energies, precursor and product ions can be seen in Table 6.4. The fragmentation losses for each compound can also be seen in Table 6.4 and in Figures 6.5-6.21. A combined method of breaking the method into segments and scan events was used in order to achieve the best level of sensitivity for the method as using scan events alone reduced the overall sensitivity of the method due to the number of compounds being analysed. In addition, the use of segments allowed for the tune file to be selected for each segment resulting in parameters which are better optimised across the whole method. To achieve this each segment was assessed with each of the tune files for the compounds present within that segment and the responses of each of the compounds was noted. The tune file which gave the best overall response for all of the compounds within the segment was then used in the final method. A breakdown of the individual segments can be seen in Table 6.5.

**Table 6.5: MS/MS method per segment**

<b>Segment number</b>	<b>Time window (min)</b>	<b>Compounds</b>	<b>Tune File used</b>
1	0-6	atropine, strychnine, cathinone, scopolamine	Atropine
2	6-10	aconitine, coumarin, hellebrin, solanine, veratridine, colchicine	Hellebrin
3	10-14.5	digoxin, 5- and 8- methoxypsoralen, psoralen, thujone, salvinorin A	Psoralen
4	14.5-20	capsaicin, digitoxin	Digitoxin

**Table 6.4: Fragmentation ions observed**

Compound	Collison energy (eV)	Fragmentation ion observed ( <i>m/z</i> )	Fragmentation
5-methoxypsoralen	30.0	217, 202*, 173	[M+H] <sup>+</sup> , [M+H-CH <sub>3</sub> ] <sup>+</sup> , [M+H-CO <sub>2</sub> ] <sup>+</sup>
8-methoxypsoralen	30.0	217, 202*, 173	[M+H] <sup>+</sup> , [M+H-CH <sub>3</sub> ] <sup>+</sup> , [M+H-CO <sub>2</sub> ] <sup>+</sup>
Aconitine	24.0	647, 597, 587*	[M+H] <sup>+</sup> , [M+H-HO <sub>3</sub> ] <sup>+</sup> , [M+H-C <sub>2</sub> H <sub>4</sub> O <sub>2</sub> ] <sup>+</sup>
Atropine	24.0	290, 260, 124*	[M+H] <sup>+</sup> , [M+H-OH] <sup>+</sup> , [M+H-C <sub>8</sub> H <sub>7</sub> O <sub>2</sub> ] <sup>+</sup>
Capsaicin	35.0	328, 314*, 186	[M+Na] <sup>+</sup> , [M+Na-CH <sub>3</sub> ] <sup>+</sup> , [M+Na-C <sub>10</sub> H <sub>15</sub> O <sub>2</sub> ] <sup>+</sup>
Cathinone	30.0	150, 133*, 105	[M+H] <sup>+</sup> , [M+H-NH <sub>3</sub> ] <sup>+</sup> , [M+H-C <sub>2</sub> H <sub>7</sub> N] <sup>+</sup>
Colchicine	23.0	400, 382*, 358	[M+H] <sup>+</sup> , [M+H-H <sub>2</sub> O] <sup>+</sup> , [M+H-C <sub>2</sub> H <sub>2</sub> O] <sup>+</sup>
Coumarin	30.0	147, 119, 103*	[M+H] <sup>+</sup> , [M+H-CO] <sup>+</sup> , [M+H-CO <sub>2</sub> ] <sup>+</sup>
Digitoxin	28.0	788, 743, 387*	[M+Na] <sup>+</sup> , [M+Na-CO <sub>2</sub> ] <sup>+</sup> , [M+Na-C <sub>17</sub> H <sub>36</sub> O <sub>10</sub> ] <sup>+</sup>
Digoxin	29.0	804, 786, 387*	[M+Na] <sup>+</sup> , [M+Na-H <sub>2</sub> O] <sup>+</sup> , [M+Na-C <sub>17</sub> H <sub>36</sub> O <sub>11</sub> ] <sup>+</sup>
Hellebrin	32.0	747, 701, 585*	[M+Na] <sup>+</sup> , [M+Na-CH <sub>2</sub> O <sub>2</sub> ] <sup>+</sup> , [M+Na-C <sub>6</sub> H <sub>10</sub> O <sub>5</sub> ] <sup>+</sup>
Psoralen	30.0	187, 159, 143*	[M+H] <sup>+</sup> , [M+H-CO] <sup>+</sup> , [M+H-CO <sub>2</sub> ] <sup>+</sup>
Salvinorin A	30.0	455, 411*, 317	[M+Na] <sup>+</sup> , [M+Na-CO <sub>2</sub> ] <sup>+</sup> , [M+Na-C <sub>5</sub> O <sub>5</sub> +H <sub>2</sub> ] <sup>+</sup>
Scopolamine	23.5	304, 156, 138*	[M+H] <sup>+</sup> , [M+H-C <sub>9</sub> H <sub>8</sub> O <sub>2</sub> ] <sup>+</sup> , [M+H-C <sub>9</sub> H <sub>10</sub> O <sub>3</sub> ] <sup>+</sup>
Solanine	40.0	869, 723, 707*	[M+H] <sup>+</sup> , [M+H-C <sub>6</sub> H <sub>10</sub> O <sub>4</sub> ] <sup>+</sup> , [M+H-C <sub>6</sub> H <sub>10</sub> O <sub>5</sub> ] <sup>+</sup>
Strychnine	28.0	335, 307, 262*	[M+H] <sup>+</sup> , [M+H-C <sub>2</sub> H <sub>4</sub> ] <sup>+</sup> , [M+H-C <sub>4</sub> H <sub>11</sub> N] <sup>+</sup>
Thujone	28.0	175, 133, 119*	[M+Na] <sup>+</sup> , [M+Na-C <sub>3</sub> H <sub>6</sub> ] <sup>+</sup> , [M+Na-C <sub>4</sub> H <sub>8</sub> ] <sup>+</sup>
Veratridine	25.0	674, 656, 492*	[M+H] <sup>+</sup> , [M+H-H <sub>2</sub> O] <sup>+</sup> , [M+H-C <sub>9</sub> H <sub>10</sub> O <sub>4</sub> ] <sup>+</sup>

\* Quantification ions

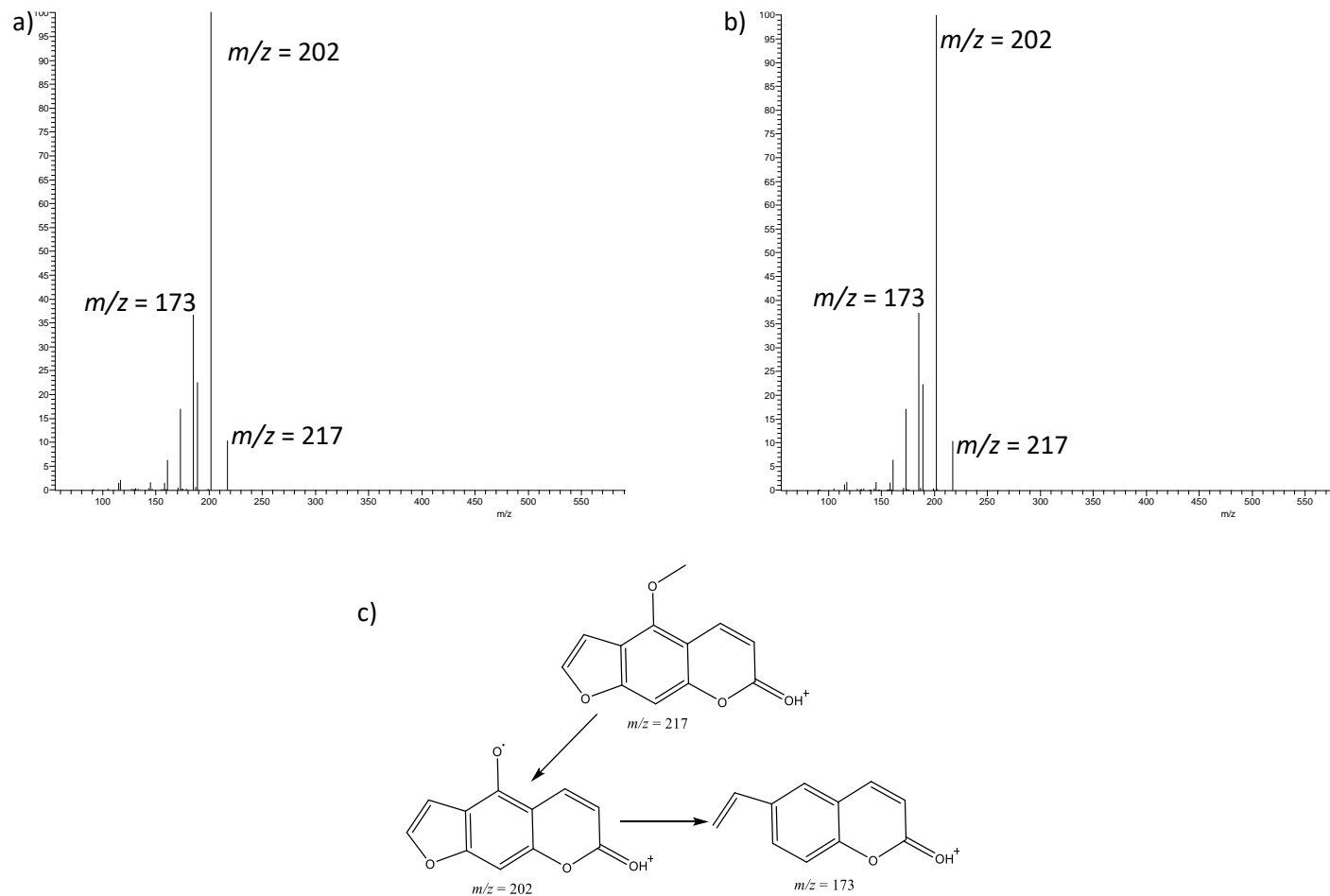


Figure 6.5: Full scan MS/MS spectrum for a) 5-methoxypsoralen, b) 8-methoxypsoralen and c) compound fragmentation.<sup>392</sup>

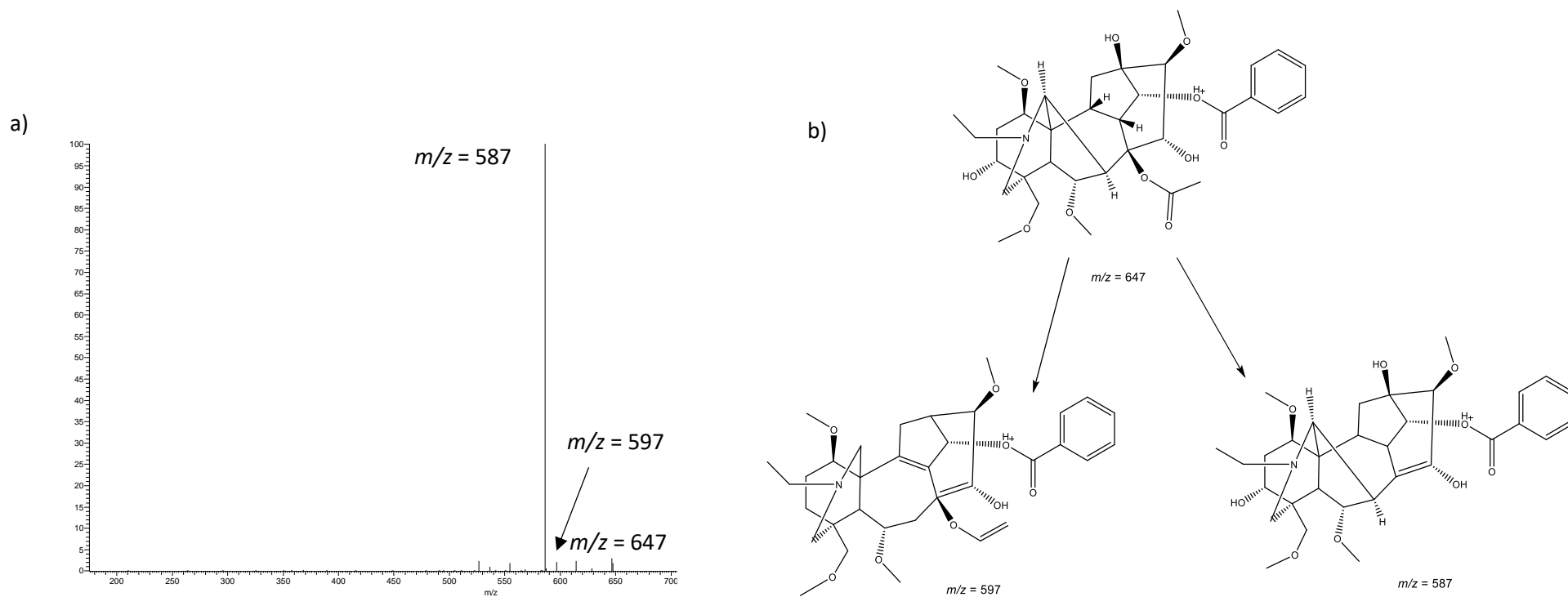


Figure 6.6: Full scan MS/MS for a) aconitine and b) compound fragmentation.<sup>393</sup>

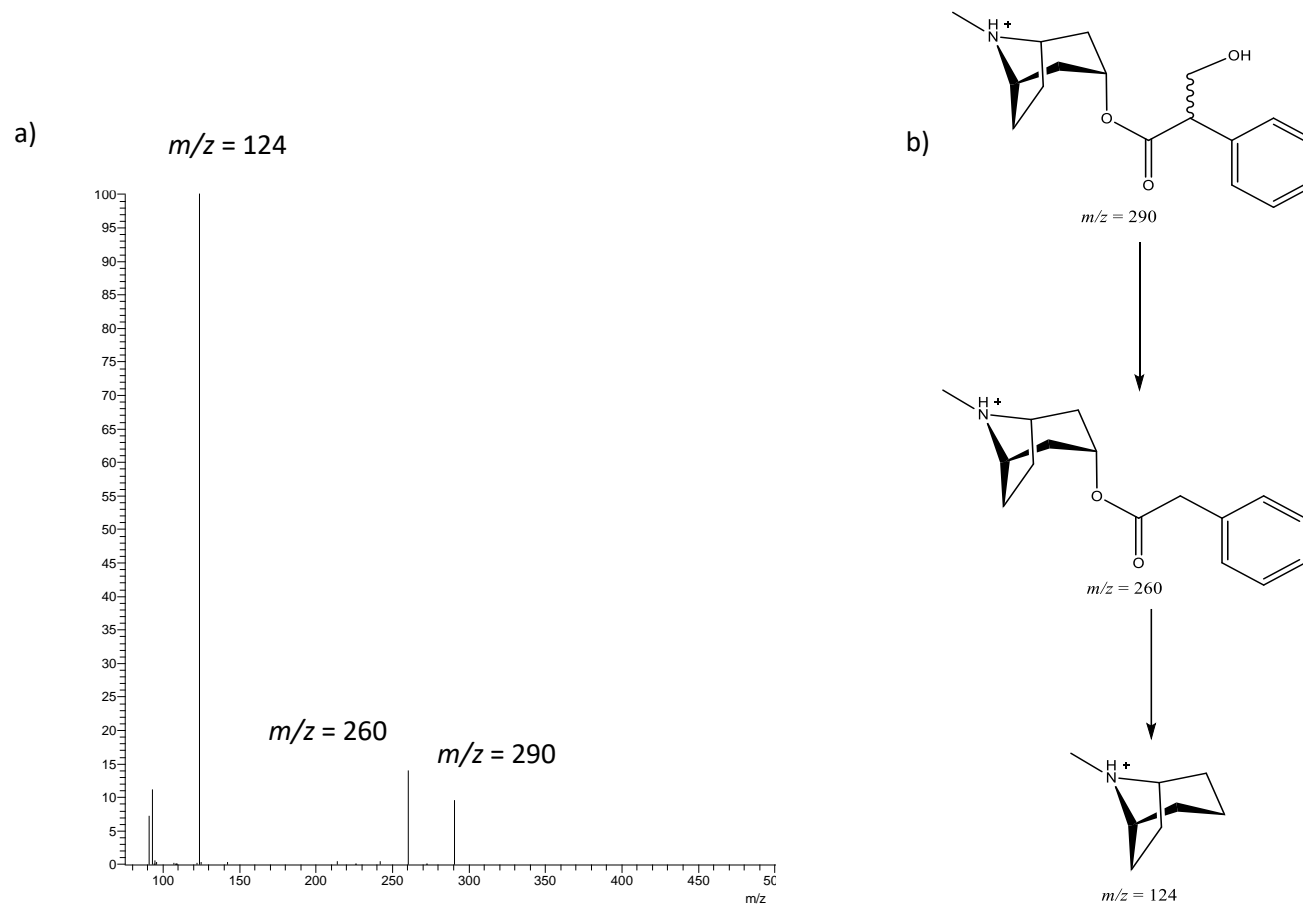


Figure 6.7: Full scan MS/MS for a) atropine and b) compound fragmentation.<sup>394</sup>

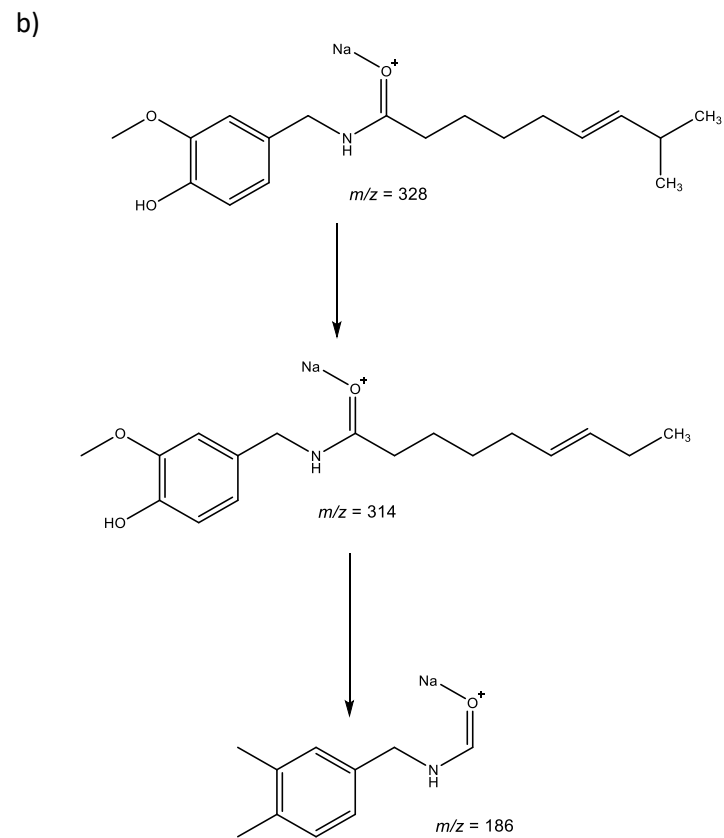
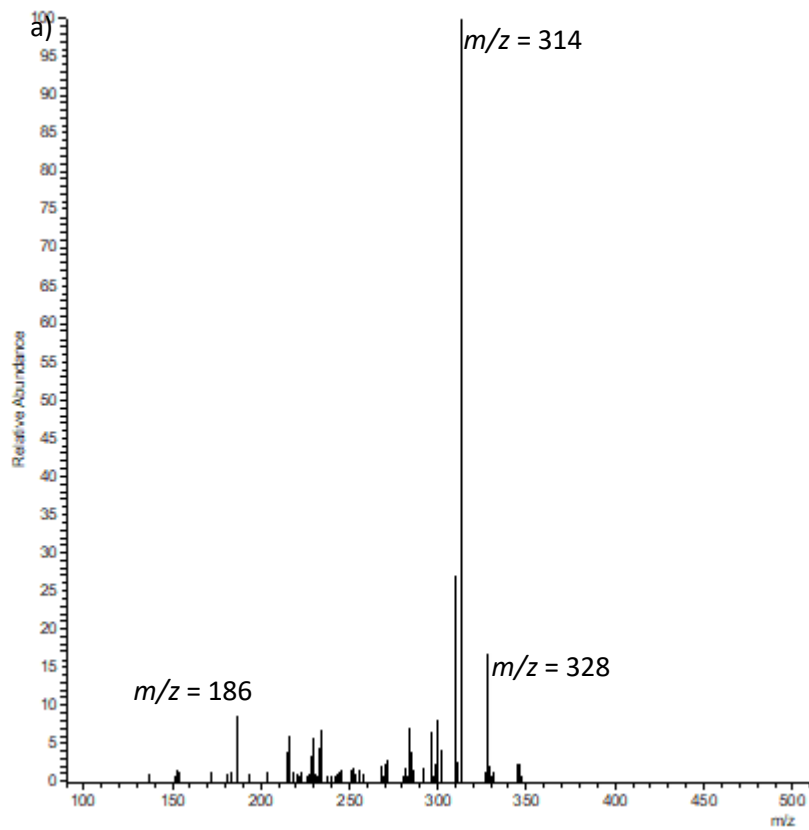


Figure 6.8: Full scan MS/MS for a) capsaicin and b) compound fragmentation.

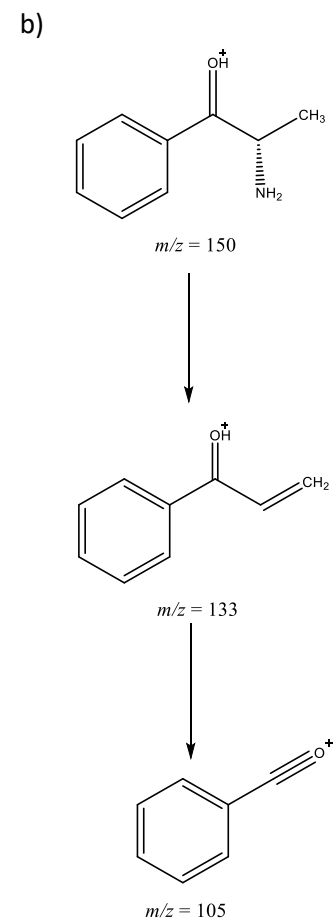
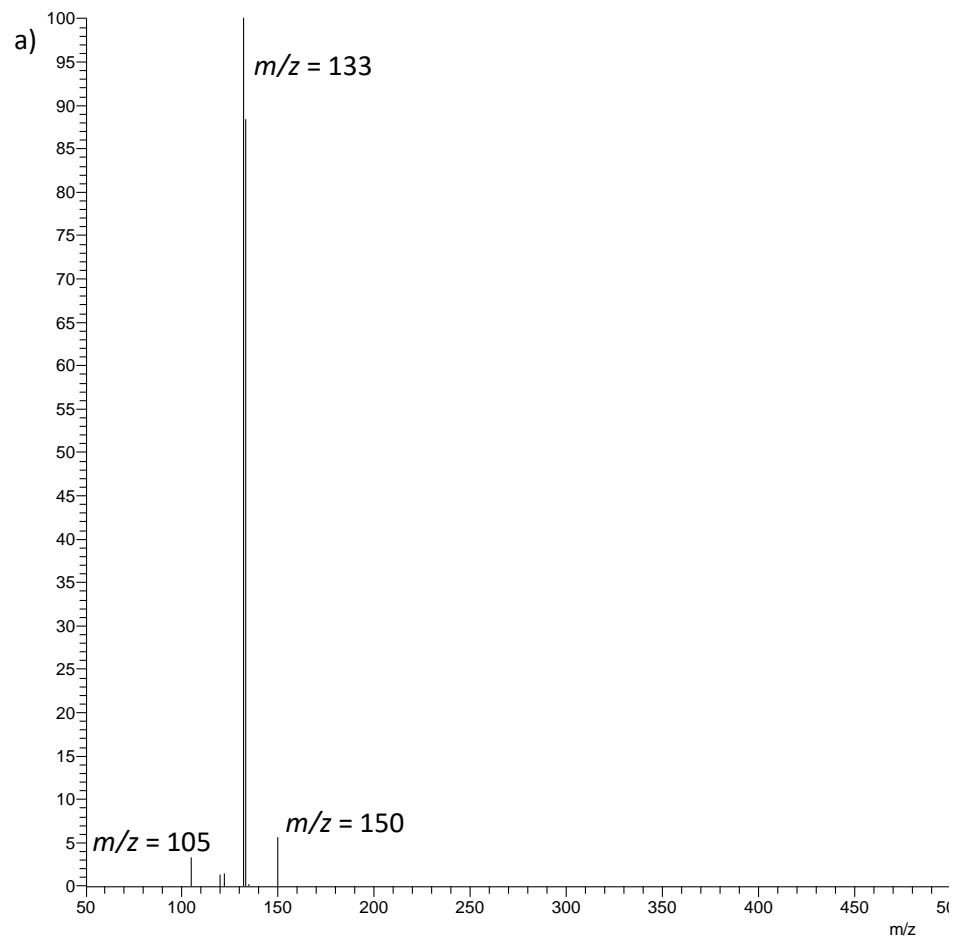


Figure 6.9: Full scan MS/MS for a) cathinone and b) compound fragmentation.

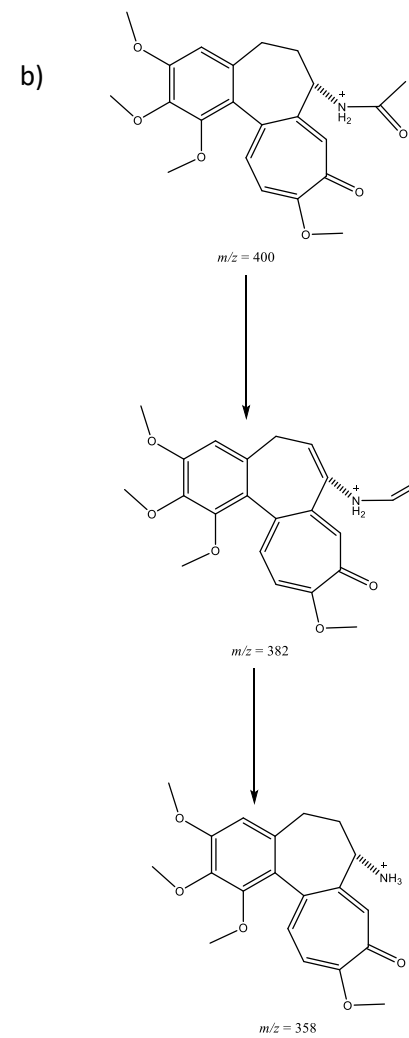
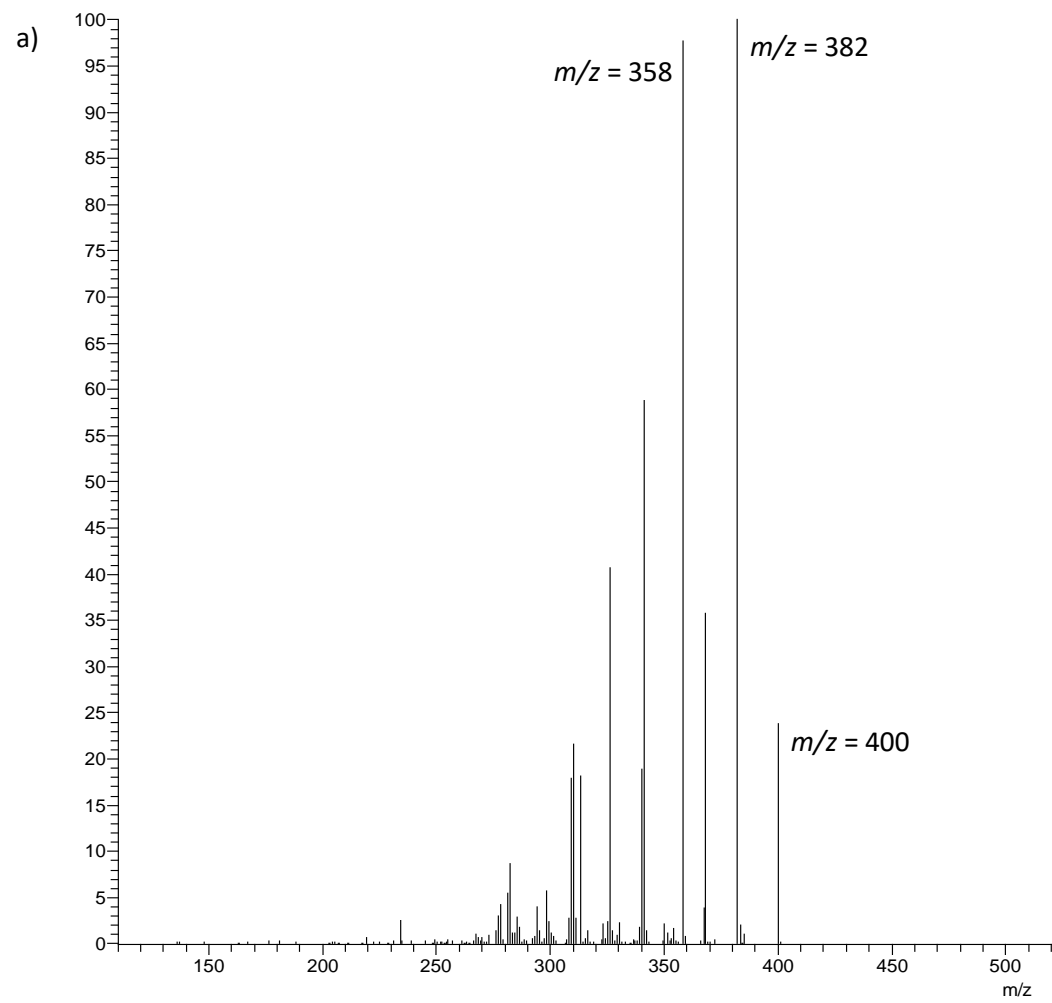


Figure 6.10: Full scan MS/MS for a) colchicine and b) compound fragmentation.<sup>395</sup>

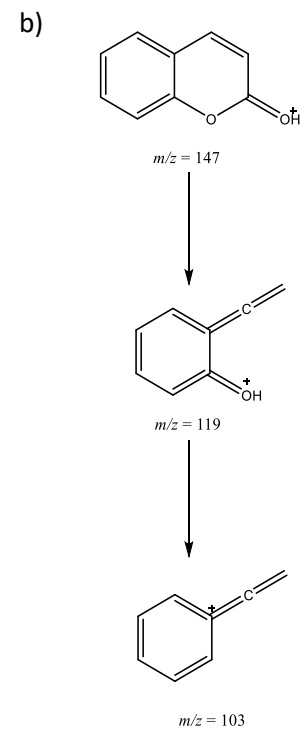
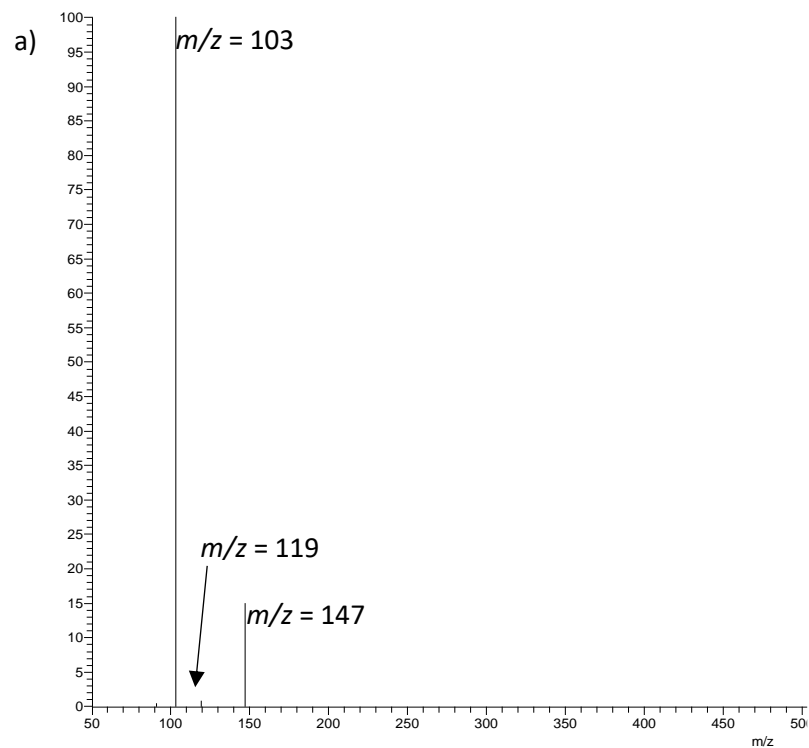


Figure 6.11: Full scan MS/MS for a) coumarin and b) compound fragmentation.<sup>396</sup>

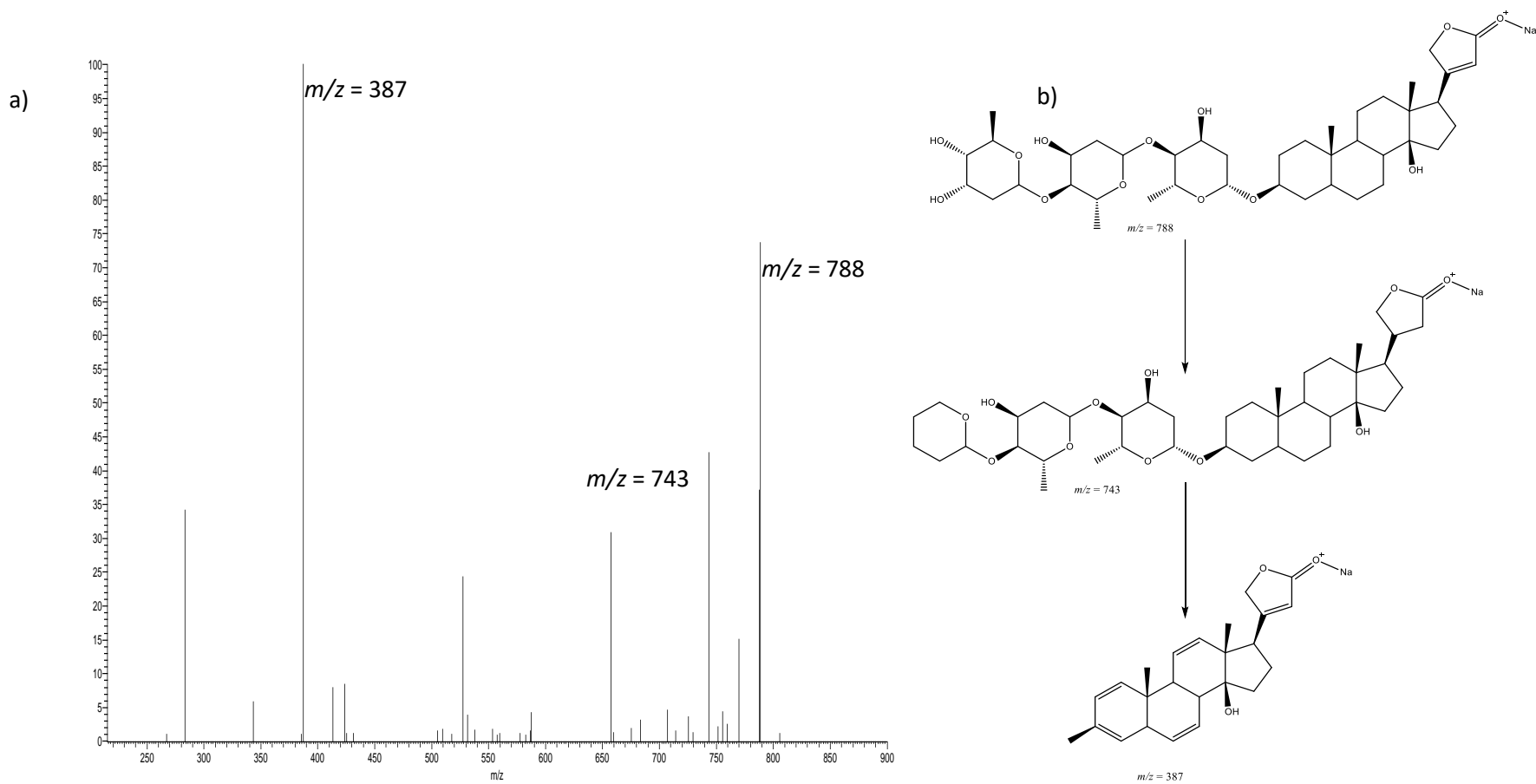


Figure 6.12: Full scan MS/MS spectrum for a) digitoxin and b) compound fragmentation.

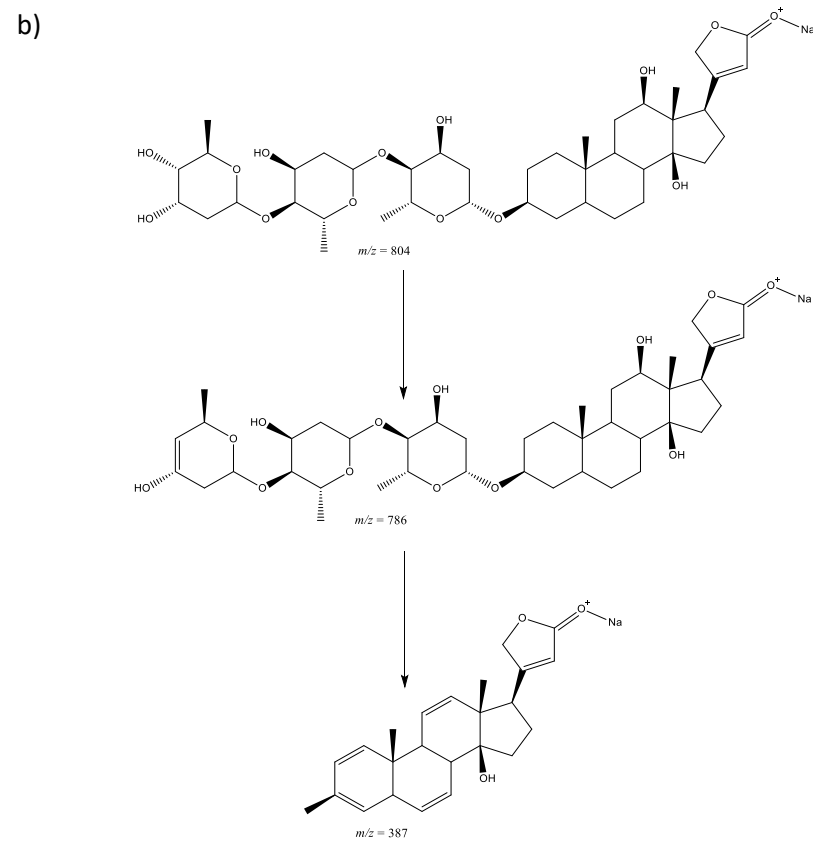
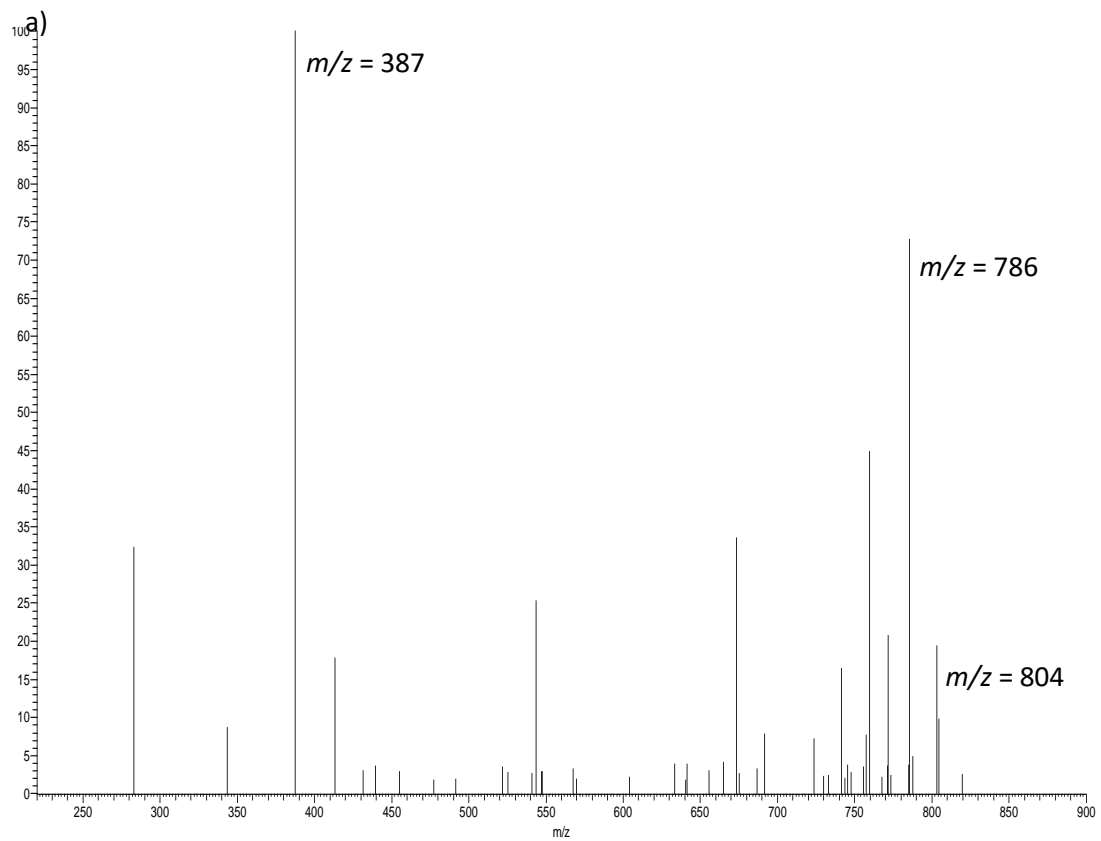


Figure 6.13: Full scan MS/MS spectrum for a) digoxin and b) compound fragmentation.

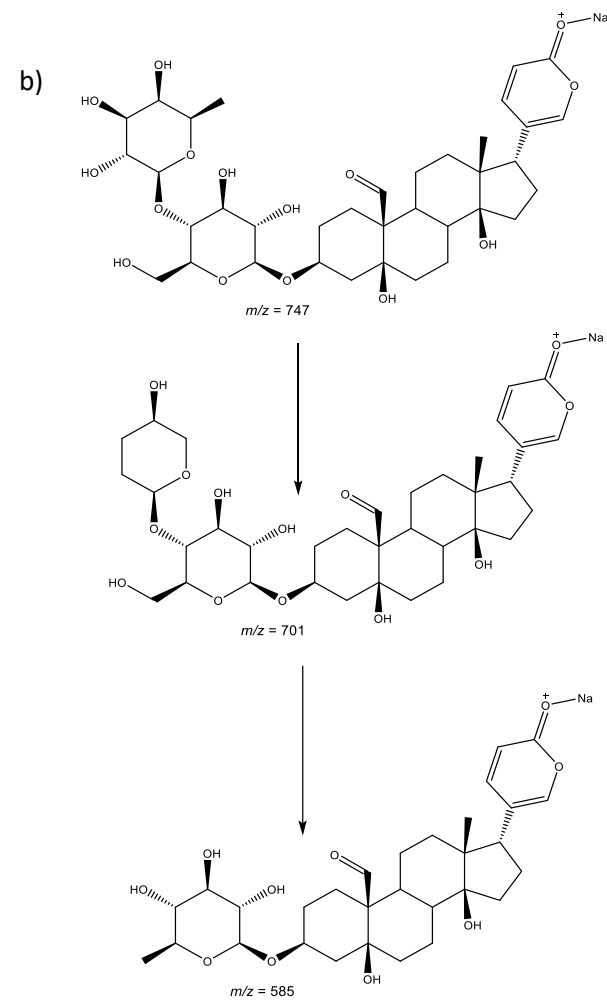
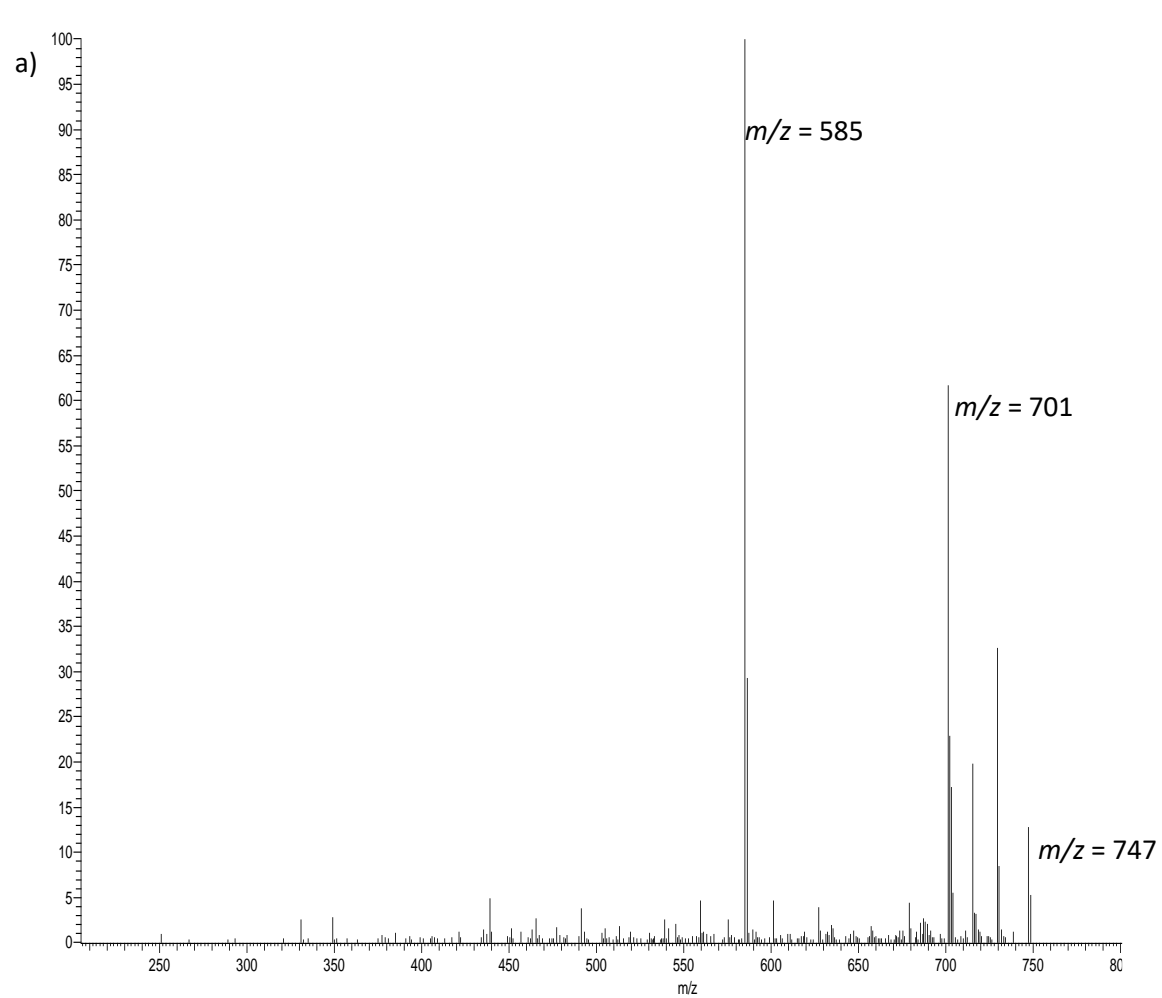


Figure 6.14: Full scan MS/MS spectrum for a) hellebrin and b) compound fragmentation.

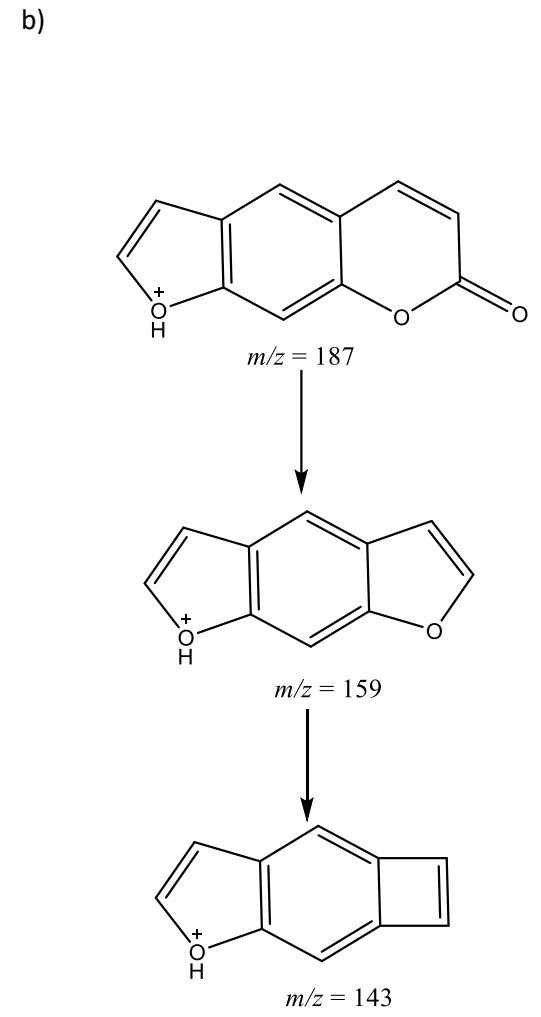
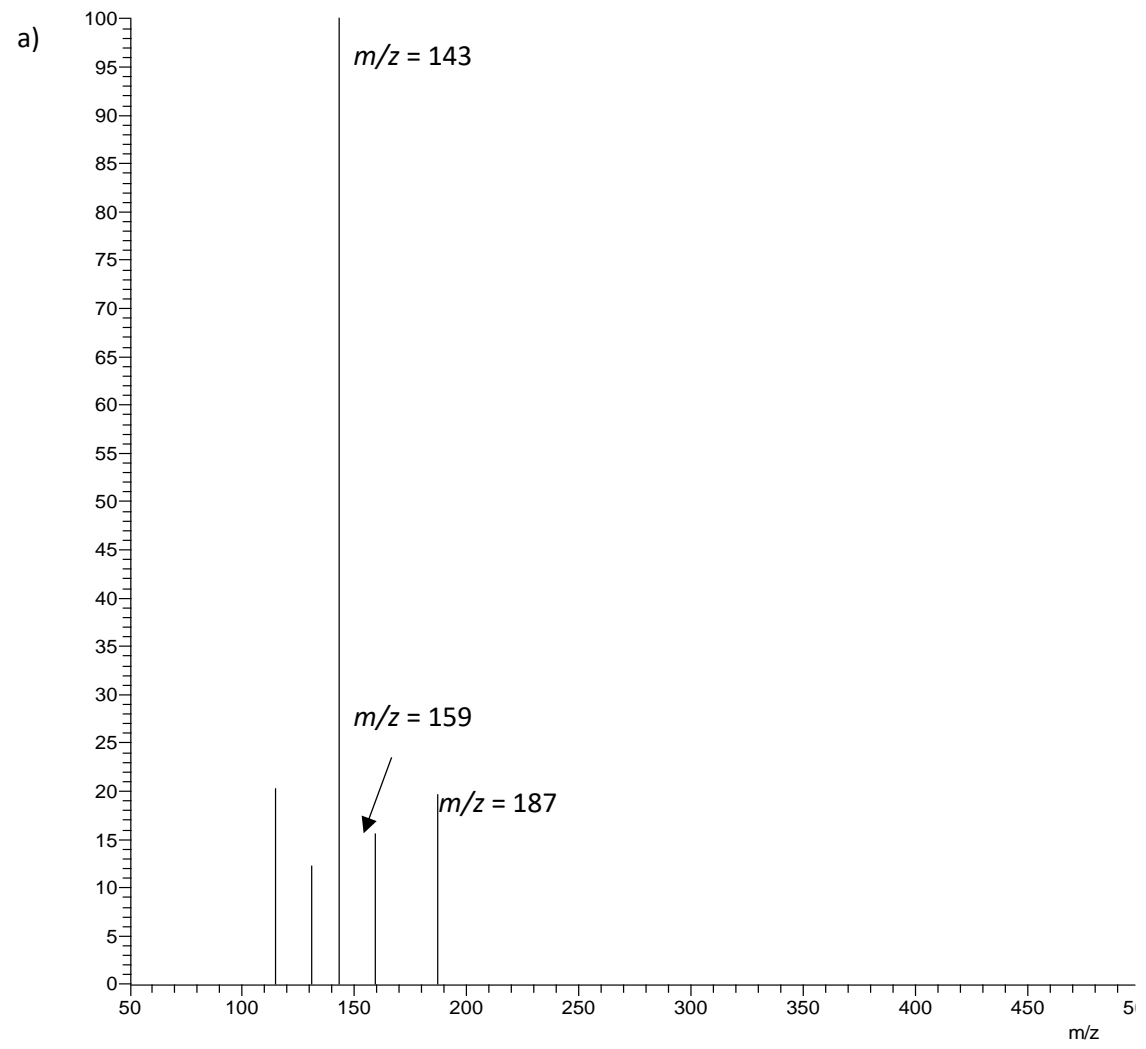


Figure 6.15: Full scan MS/MS spectrum for a) psoralen and b) compound fragmentation.<sup>392</sup>

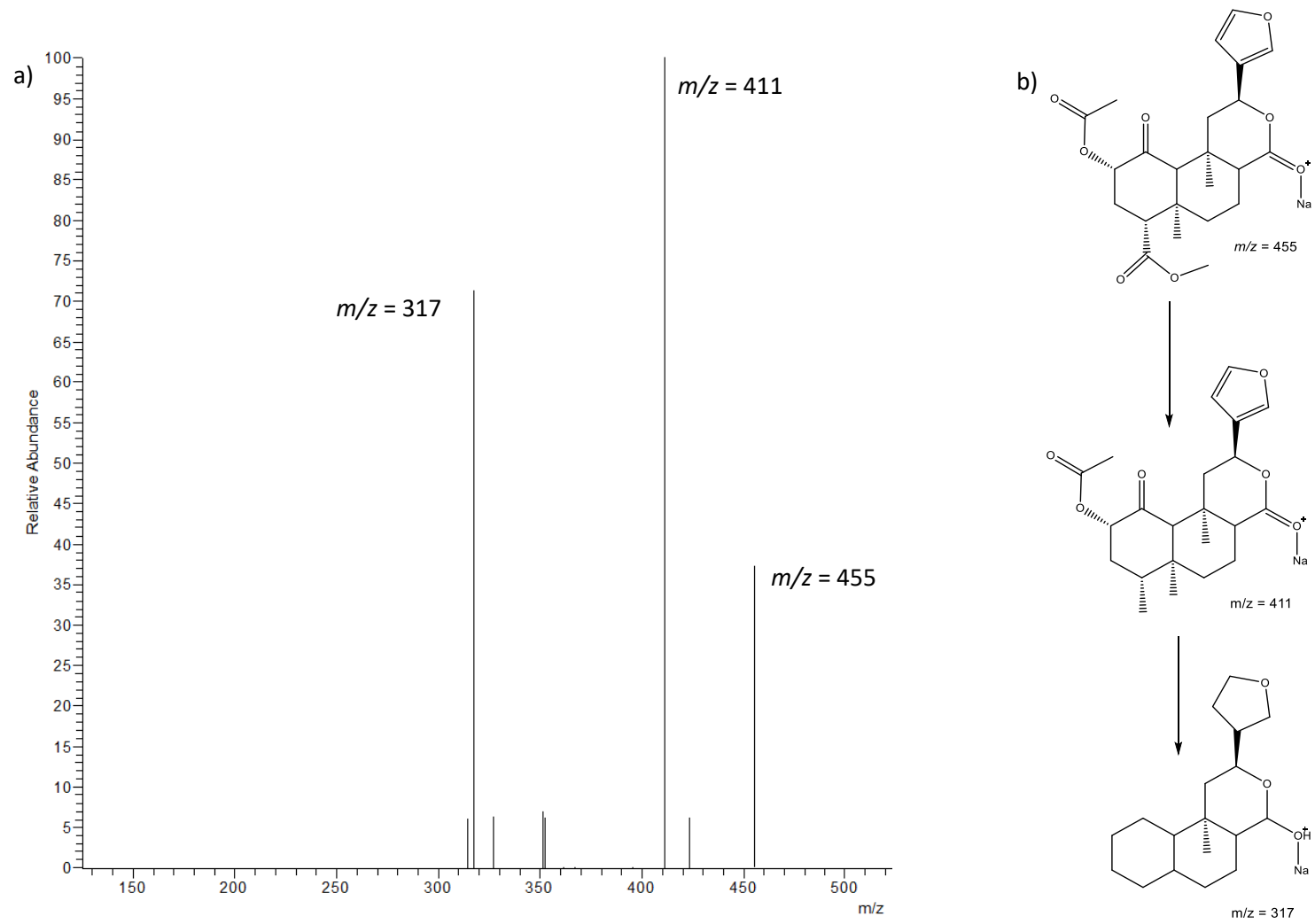


Figure 6.16: Full scan MS/MS spectrum for a) salvinorin A and b) compound fragmentation

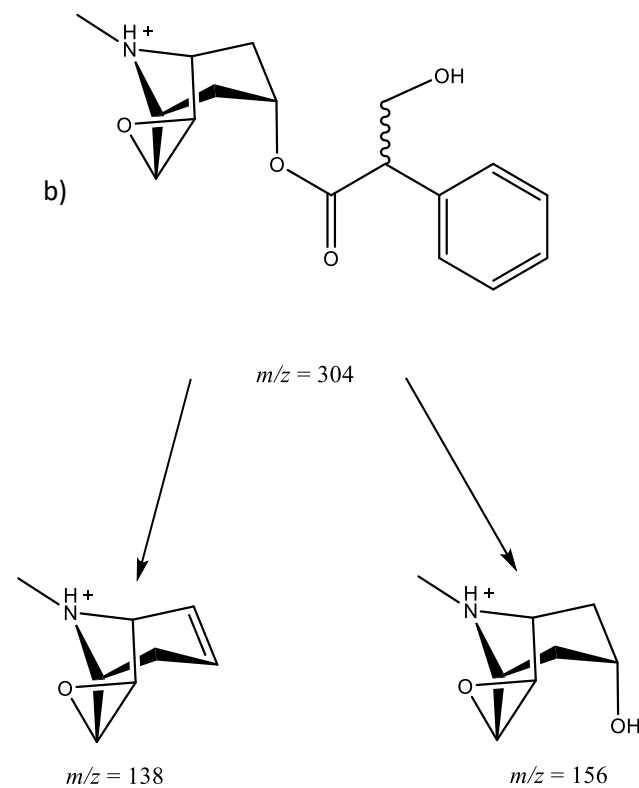
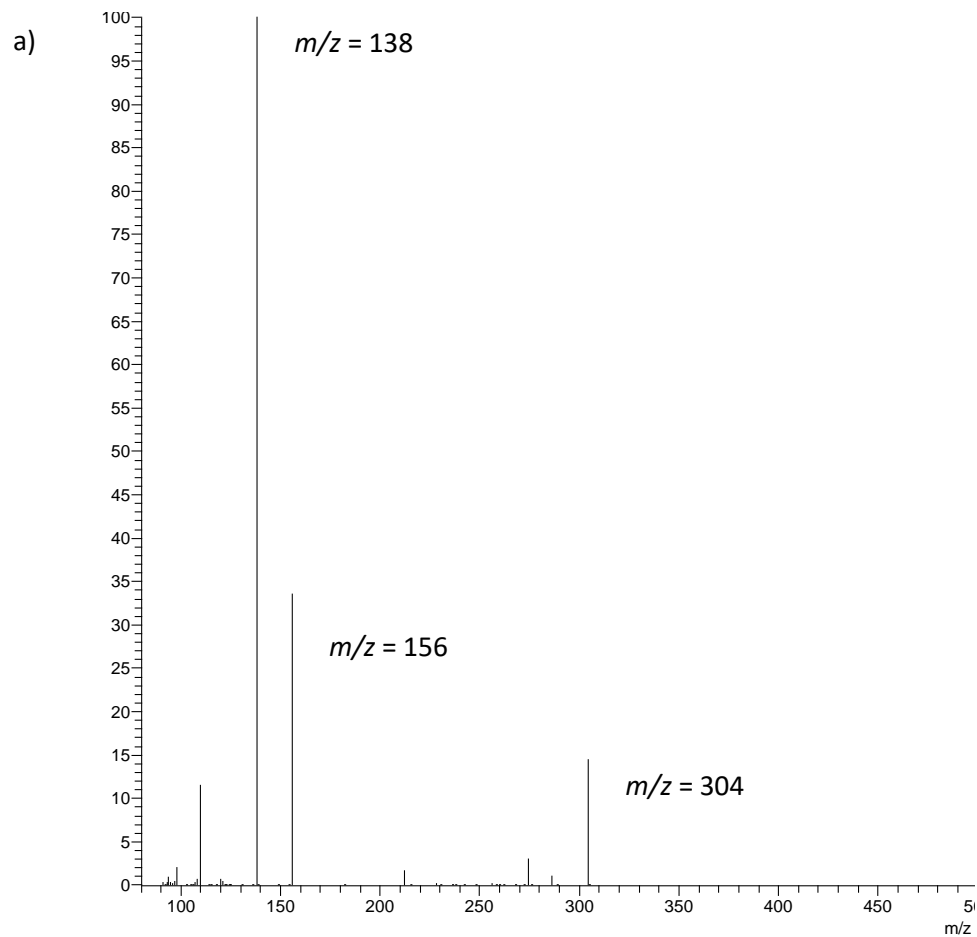


Figure 6.17: Full scan MS/MS spectrum for a) scopolamine and b) compound fragmentation.<sup>397</sup>

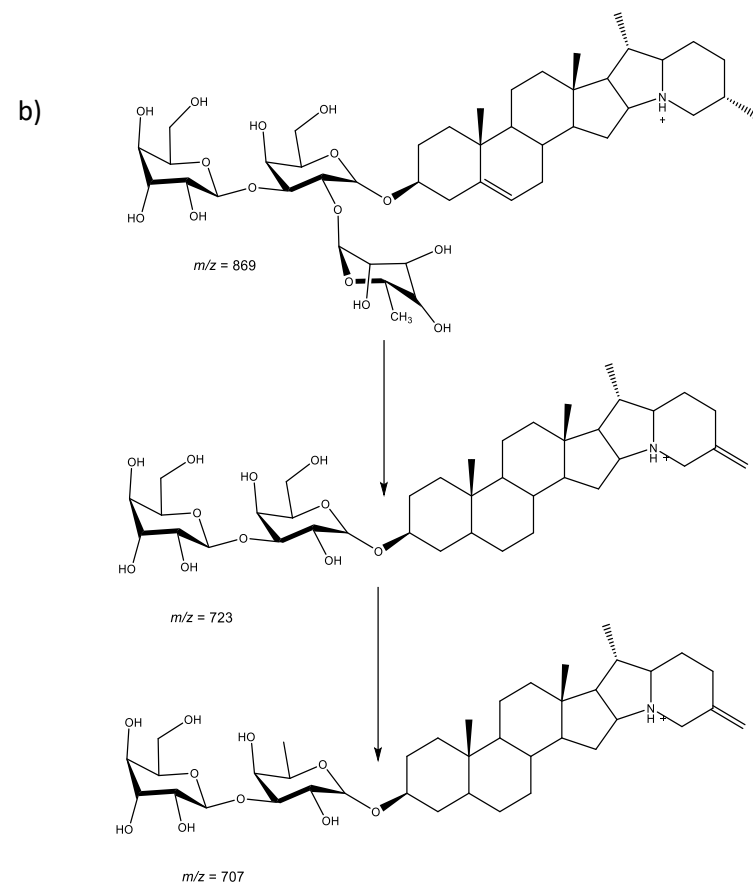
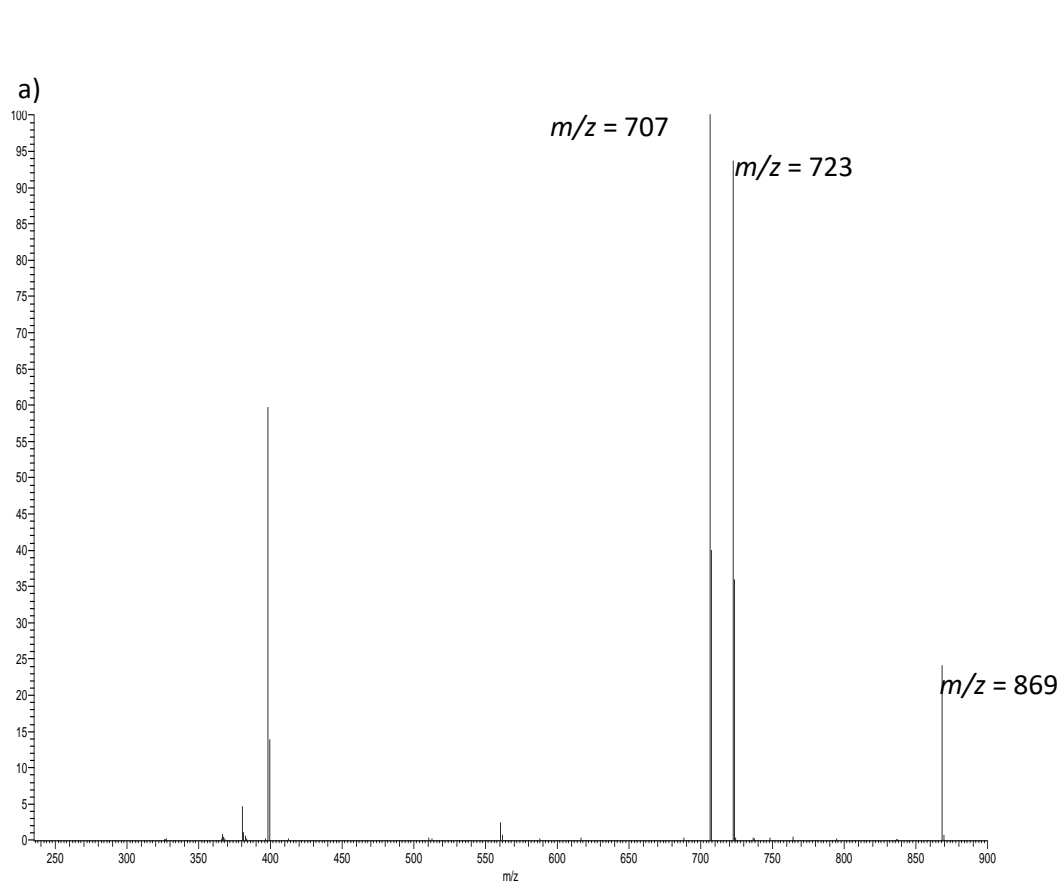


Figure 6.18: Full scan MS/MS spectrum for a)  $\alpha$ -solanine and b) compound fragmentation.<sup>398</sup>

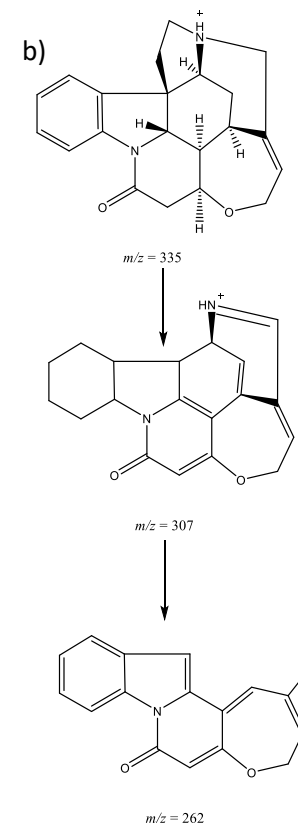
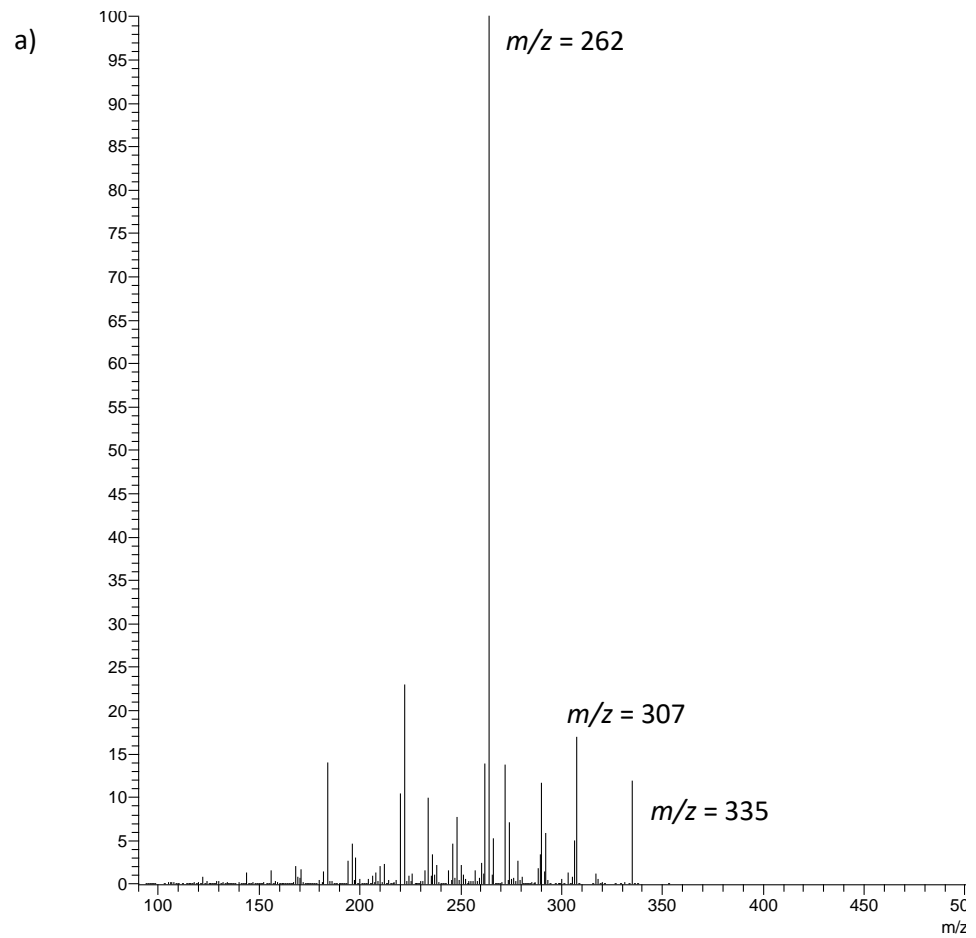


Figure 6.19: Full scan MS/MS spectrum for a) strychnine and b) compound fragmentation.<sup>399</sup>

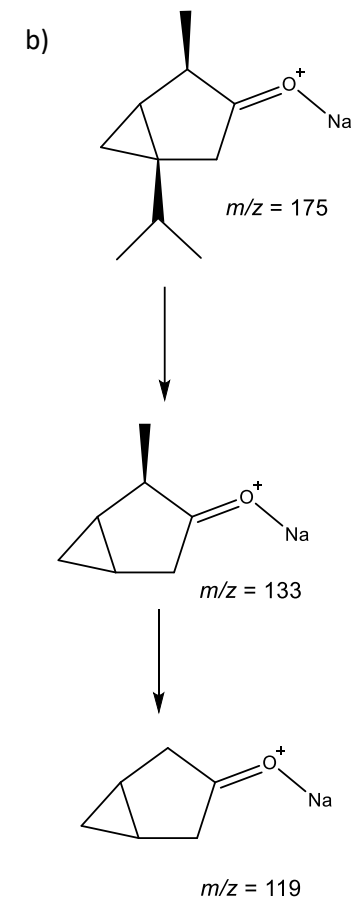
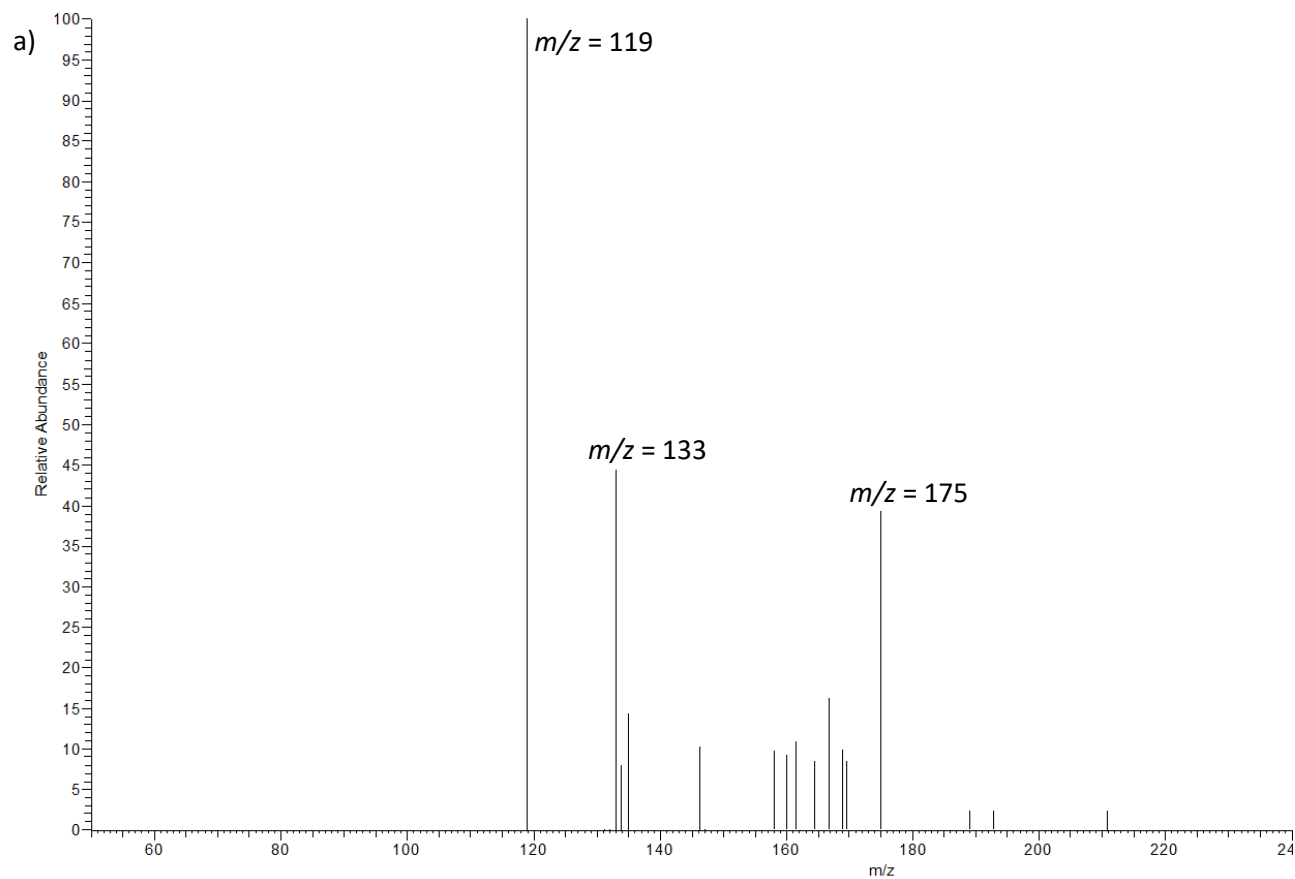


Figure 6.20: Full scan MS/MS spectrum for a)  $\alpha$ -thujone and b) compound fragmentation.

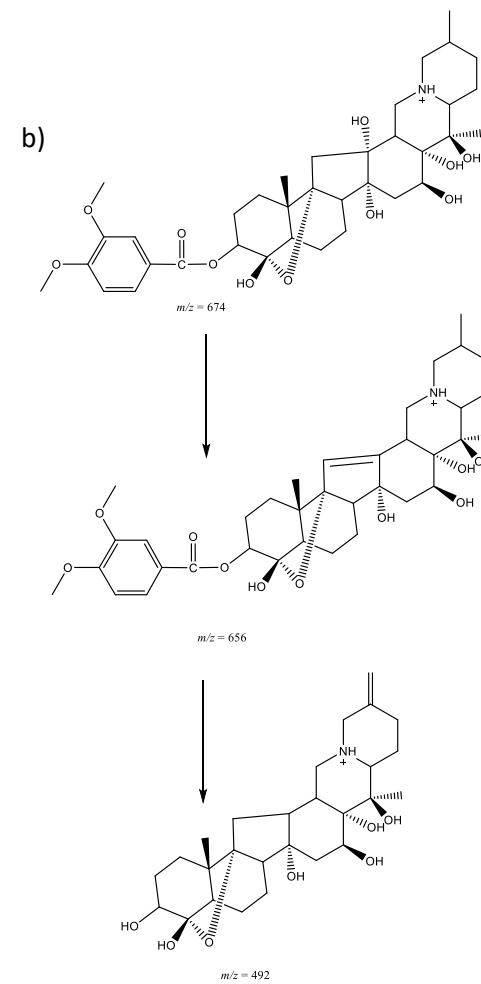
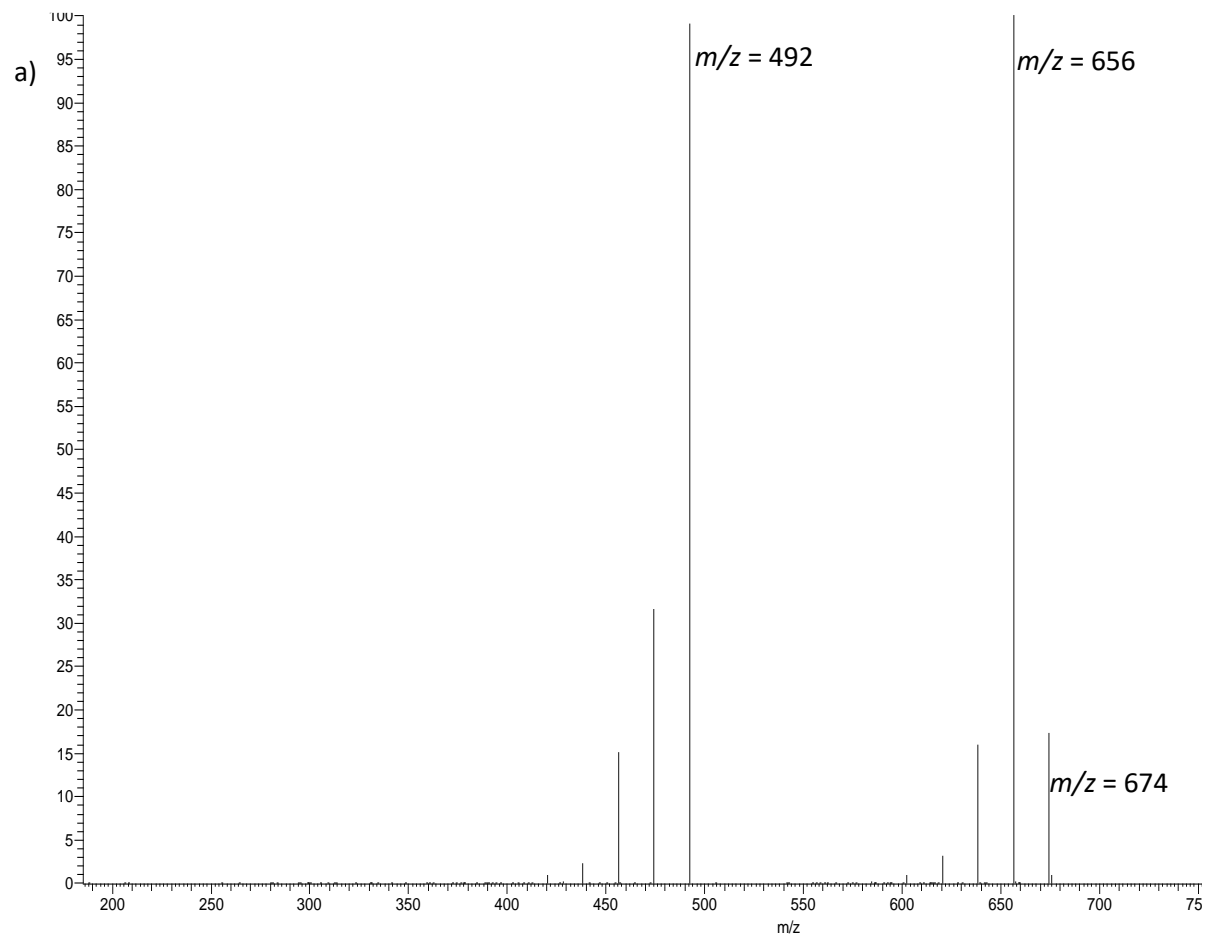


Figure 6.21: Full scan MS/MS spectrum for a) veratridine and b) compound fragmentation.

### **1.1.2. Use of internal standard**

As discussed in section 5.1.3 the use of internal standards can greatly improve the accuracy and precision of an analytical method and correct for any inaccuracies observed. For this study there were a number of isotope labelled standards available such as D3-atropine, D3-scopolamine and D6-colchicine. However due to supply issues these could not be included in this study.

### **1.1.3. Sample extraction**

In order to analyse the compounds present they must first be extracted from the plant material. Therefore solid-liquid extraction was investigated via sonication and accelerated solvent extraction (ASE) to assess the most suitable technique and solvent used. The initial extraction study was to determine the most appropriate extraction solvent using dandelion plants spiked with the compounds. Based on the LogP of the compounds as shown in Table 1 it would be expected that the compounds would extract into a polar solvent. The dandelion plant was separated into components of flower, stem, leaf and root, and approximately 0.1 g of material was accurately weighted out in triplicate for each solvent and extraction method and then crushed using a pestle and mortar. The compounds were then spiked onto the material at a concentration within the calibration range and left to dry. For sonication, the material was then transferred to a sample tubes and 10 mL of either methanol (m), acetonitrile (a), isopropanol (i) or chloroform (c) was added and the samples were sonicated for 30 minutes in an ultrasonic bath. Water was not included in the extraction study as it was unsuitable for use with the ASE equipment.

An additional method for solid-liquid extraction is the use of accelerated solvent extraction which utilises temperature and pressure in an automated system to efficiently extract compounds from a matrix. Therefore, ASE was assessed for suitability to allow for a more automated process. Due to the larger solvent volumes, 22 mL for large extraction tubes, used in ASE the amount of sample material was also increased. For ASE approximately 0.3 g of material was accurately weighted out in triplicate for ASE and then crushed using a pestle and

mortar. The compounds were then spiked onto the material at a concentration within the calibration range and left to dry. For accelerated solvent extraction a cellulose filter disc was placed in a 22 mL extraction cell and hydromatrix™ was added to fill approximately half the cell. The sample was then added to the cell and the cell topped up with hydromatrix™. The material was extracted with a 10 minute static extraction time at 100°C and 2000 psi and the extract was collected in 60 mL glass ASE collection vials. The extracts were then filtered through a 0.2 µm nylon syringe filter and 1 mL transferred to an autosampler vial and analysed via LC-MS/MS with calibration standards.

The ASE extraction showed lower recoveries for a number of compounds when compared with sonication which the most likely cause due to the efficiency of ASE to extract other plant components which caused matrix effects. As seen in Figure 6.22 a full scan chromatogram of the ASE extraction of unspiked plant material shows significant matrix peaks which could impact on ionisation and could lead to ion suppression within the ion trap. Therefore, ASE was not used for the plant extraction. The compounds extracted best in methanol with the highest extraction recoveries across all the compounds, Table 6.6, and plant materials with good % RSD of < 6.1 % across the replicates extracted with methanol. Therefore, methanol was chosen as the extraction solvent utilising sonication.

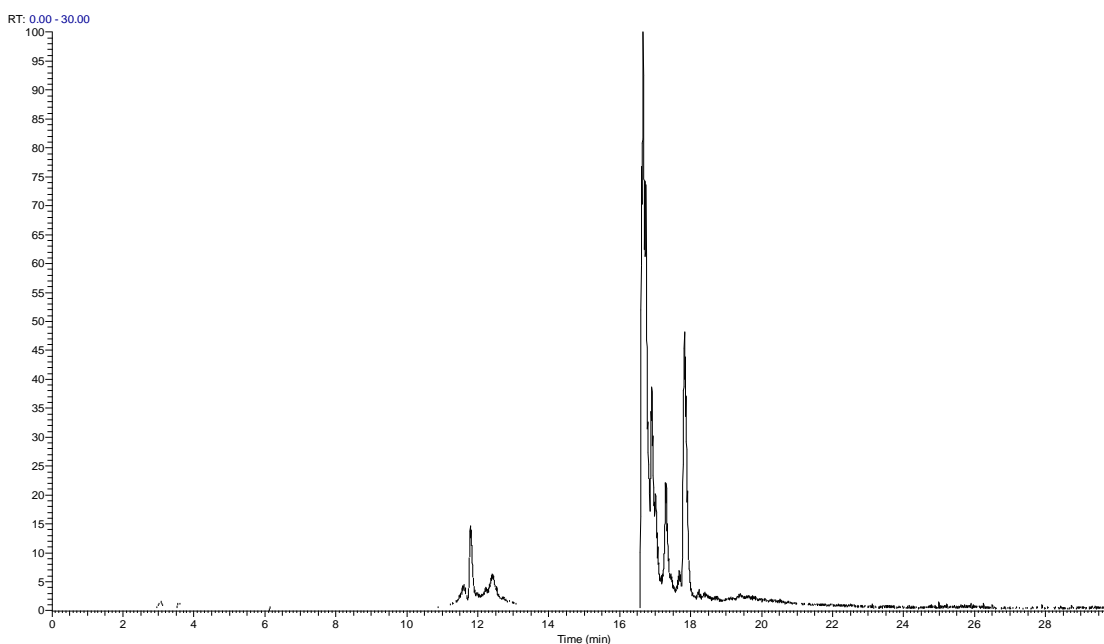


**Figure 6.22: Unspiked matrix TIC chromatogram following ASE**

The next stage in the sample preparation development was to optimise the sonication time. As there was minimal difference between the extraction efficiencies in the different plant component only the leaves were used for the remainder of the development due to the larger amount of material available. Approximately 0.1 g of material was accurately weighted out in triplicate for each duration and then crushed using a pestle and mortar. The compounds were then spiked onto the material at a concentration within the calibration range and left to dry. The material was then transferred to a sample tubes and 10 mL of methanol was added and the samples were sonicated for 0, 2.5, 5, 7.5, 10, 15, 20, 25 or 30 minutes in an ultrasonic bath. The extracts were then filtered through a 0.2 µm nylon syringe filter and 1 mL transferred to an autosampler vial and analysed via LC-MS/MS with calibration standards. From Figure 6.23 it can be seen that the optimal extract time is 15 mins and above which an extraction plateau is reached and therefore a longer extraction will have minimal impact on the recoveries obtained.

## **1.2. Method Validation**

### **1.2.1. Selectivity**

Blank samples of mobile phase and extracted nontoxic plant material (dandelion samples) were ran alongside the analysis at the beginning and end of each run. As no peaks were observed at the same retention time of the compounds of interest selectivity for the method was established. Dandelion samples were used as they were readily available and are a common plant found in gardens but contain none of the compounds of interest.<sup>16, 21, 400</sup>

### **1.2.2. Linearity**

Linearity was established by preparing mixed calibration standards of all 18 plant toxins. The calibration ranges were based upon compound response with ranges found in Table 6.7 for the 18 compounds analysed.

Using the ions identified in Table 6.4 for quantification, the average peak areas were used to construct calibration graphs for the plant toxins. The coefficient of

determination ( $R^2$ ) was greater than 0.995 so the method can be described as linear for all 18 compounds. (Table 6.7)

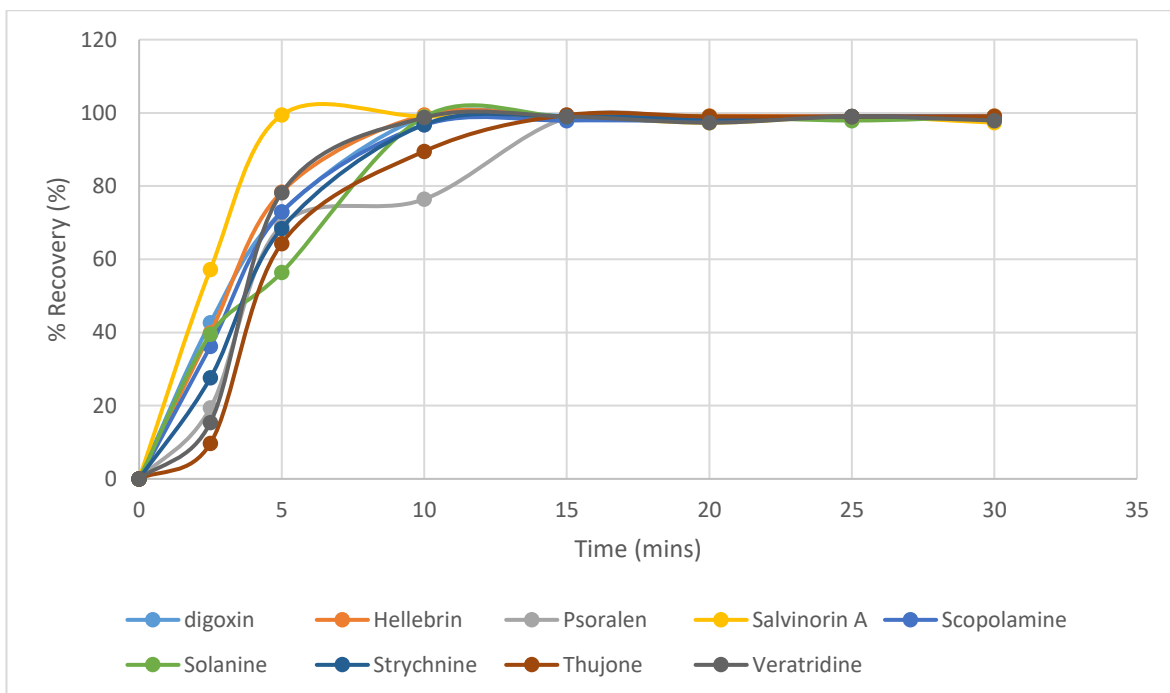
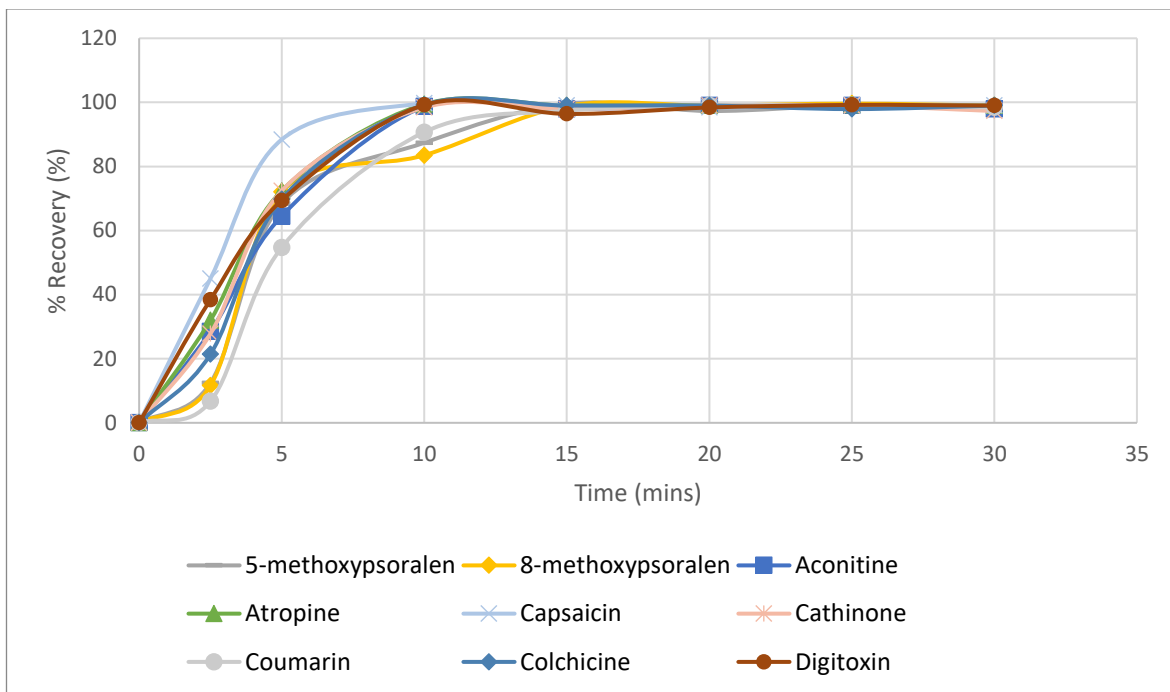


**Figure 6.23: Comparison of sonication time with compound recoveries**

**Table 6.6: Solvent extraction study results for sonication. m:methanol, a: acetonitrile, i: isopropanol and c: chloroform**

Compound	% Recovery (n=3)															
	Root				Leaf				Stem				Flower			
	m	a	i	c	m	a	i	c	m	a	i	c	m	a	i	c
5-methoxypsoralen	83.3	76.8	72.7	0.0	78.9	87.3	63.9	0.0	84.0	80.7	74.5	0.0	87.1	77.4	84.8	0.0
8-methoxypsoralen	93.2	54.5	52.9	0.0	89.7	41.2	61.8	0.0	91.2	52.4	52.7	0.0	90.2	48.7	64.5	0.0
Aconitine	96.5	50.9	61.1	34.3	96.0	53.6	61.3	35.3	80.6	50.8	63.2	36.9	71.2	48.7	65.3	32.2
Atropine	93.9	11.9	47.3	8.8	91.3	14.6	51.9	13.2	91.8	12.0	48.5	11.6	94.2	10.5	16.0	8.7
Capsaicin	98.0	73.8	79.3	57.2	91.7	70.1	78.9	55.9	96.3	74.0	80.1	69.9	83.0	74.5	75.3	44.9
Cathinone	91.1	8.7	15.4	20.7	94.0	8.0	15.8	10.2	84.9	5.9	16.1	23.3	97.4	9.9	12.9	10.2
Colchicine	94.9	26.2	22.9	16.2	83.9	22.9	24.4	15.9	97.6	17.3	23.2	15.2	89.4	22.1	26.1	16.7
Coumarin	97.9	5.4	7.2	1.5	97.4	5.3	7.2	1.7	97.5	6.4	6.9	1.3	98.8	6.6	7.0	1.8
Digitoxin	96.9	58.7	95.2	40.0	94.2	52.4	98.3	55.9	97.0	56.9	93.5	43.5	98.5	59.0	94.9	54.9
Digoxin	95.0	57.9	76.1	53.1	94.3	59.7	76.7	40.7	98.6	64.6	83.5	39.1	99.0	63.6	72.6	46.0
Hellebrin	99.0	20.6	21.6	16.4	98.9	17.4	21.4	15.0	99.4	22.6	20.7	17.7	98.7	21.6	20.4	18.2
Psoralen	97.7	67.4	73.0	0.0	99.4	69.9	77.7	0.0	97.9	67.2	71.3	0.0	98.2	66.6	76.0	0.0
Salvinorin A	97.7	32.8	6.7	20.9	95.3	35.9	0.0	18.7	96.4	16.7	16.2	17.1	99.6	32.3	4.5	31.5
Scopolamine	95.0	20.2	94.2	47.0	96.7	23.1	92.6	53.2	93.6	30.2	97.0	41.6	95.1	26.4	95.0	46.2
Solanine	95.4	65.5	67.8	14.2	96.8	61.6	89.0	28.9	96.2	62.3	55.3	29.3	96.6	57.3	52.0	26.8
Strychnine	99.2	90.4	43.5	47.6	94.3	76.8	38.5	41.6	96.5	83.0	57.8	52.4	93.7	80.9	36.1	50.7
Thujone	92.2	7.7	14.8	7.1	95.6	9.7	12.0	9.5	90.9	8.0	9.3	7.6	89.4	8.2	17.8	10.0
Veratridine	96.2	50.4	70.2	38.9	85.4	50.7	63.9	37.5	98.2	51.3	73.8	42.4	91.0	51.6	70.1	35.6

### **1.2.3. Precision**

Precision was established for both the standard and the extracted plant sample. For the standard precision low, medium and high calibration standards were prepared and injected in triplicate and the % coefficient of variance (%CV) calculated. Precision of between 0.3 and 10.7 was obtained across all compounds across the linear range.

### **1.2.4. Limits of detection and quantification**

The limit of quantification and limit of detection were calculated based on the standard deviation and response of the replicate calibration curve due to the method being operated in selected reaction monitoring mode (SRM). The LOD was calculated by multiplying the standards deviation for the y intercept by 3.3 then dividing by the average slope of the calibration curve and the LOQ was calculated by multiplying the standards deviation for the y intercept by 10 then dividing by the average slope of the calibration.<sup>105</sup> The calculated limit of detection was between 0.2 - 92 ng/mL and the calculated limit of quantification was between 0.8 – 308 ng/mL. The results for each compound can be seen in Table 6.7.

## **1.3. Standard Stability**

In order to assess the stability of the compound stored in solution in glass storage vials standard for access for against the calibration data on a weekly basis for 4 weeks then a 2-weekly basis for a further 8 weeks then on a 4-weekly basis for the remainder of the study when stored at 2-8 °C. From Figure 6.24 it can be seen that the majority of the compounds are stable when stored in methanol at 2-8°C. However, salvinorin A, cathinone and thujone were being impacted by the storage conditions more so than the other compounds as shown in Figure 6.24.

**Table 6.7. Linearity and LOQ/LOD results**

Compound	Calibration range (ng/mL)	No of data points	Linearity (y=)	R <sup>2</sup> Value	Precision (%CV) (low, mid, high)	LOD (ng/mL)	LOQ (ng/mL)
5-methoxypsoralen	0-100	7	1325.5x + 2893	0.9964	10, 4.6, 2.3	2.0	6.7
8-methoxypsoralen	0-100	7	1315.3x – 1107.7	0.9984	9.3, 2.2, 2.9	0.7	2.3
Aconitine	0-100	7	7001.2x -6390.8	0.9991	1.5, 0.9, 2.9	1.0	3.3
Atropine	0-100	7	4227.2x – 5294.6	0.9994	2.8, 2.6, 6.9	3.7	12
Capsaicin	0-100	7	6404.7x – 34412	0.9977	0.8, 2.2, 1.7	0.8	2.7
Cathinone	0-100	7	7116.8x – 36698	0.9957	1.4, 3.2, 2.4	6.3	20.1
Colchicine	0-100	7	267.94x + 115.8	0.9985	3.5, 4.1, 4.0	0.3	1.1
Coumarin	0-5000	10	4.1771x - 158.54	0.9990	0.6, 2.3, 1.7	92	308
Digitoxin	0-100	7	108.28x +258.93	0.9959	2.9, 5.0, 2.9	1.1	3.5
Digoxin	0-300	7	30.352x – 47.162	0.9988	2.8, 5.2, 4.1	5.5	18.2
Hellebrin	0-400	10	195.98x + 1686.6	0.9981	6.0, 6.7, 6.5	7.5	25
Psoralen	0-100	7	198.35x – 491.57	0.9952	10.7, 2.7, 3.3	1.2	4.1
Salvinorin A	0-300	8	33.69x – 124.93	0.9990	3.7, 1.4, 0.3	14	48
Scopolamine	0-100	7	720.56x + 142.49	0.9993	0.8, 5.5, 5.4	1.0	3.3
Solanine	0-100	7	2478.2x + 959.64	0.9996	1.8, 1.4, 1.6	2.4	7.9
Strychnine	0-100	7	2272.9x – 2670.2	0.9973	3.4, 2.4, 8.4	1.1	3.6
Thujone	0-100	7	73.474x + 180.44	0.9969	3.4, 2.8, 2.1	2.7	8.5
Veratridine	0-100	7	6533.4x – 814.27	0.9979	2.1, 1.0, 0.3	0.2	0.8

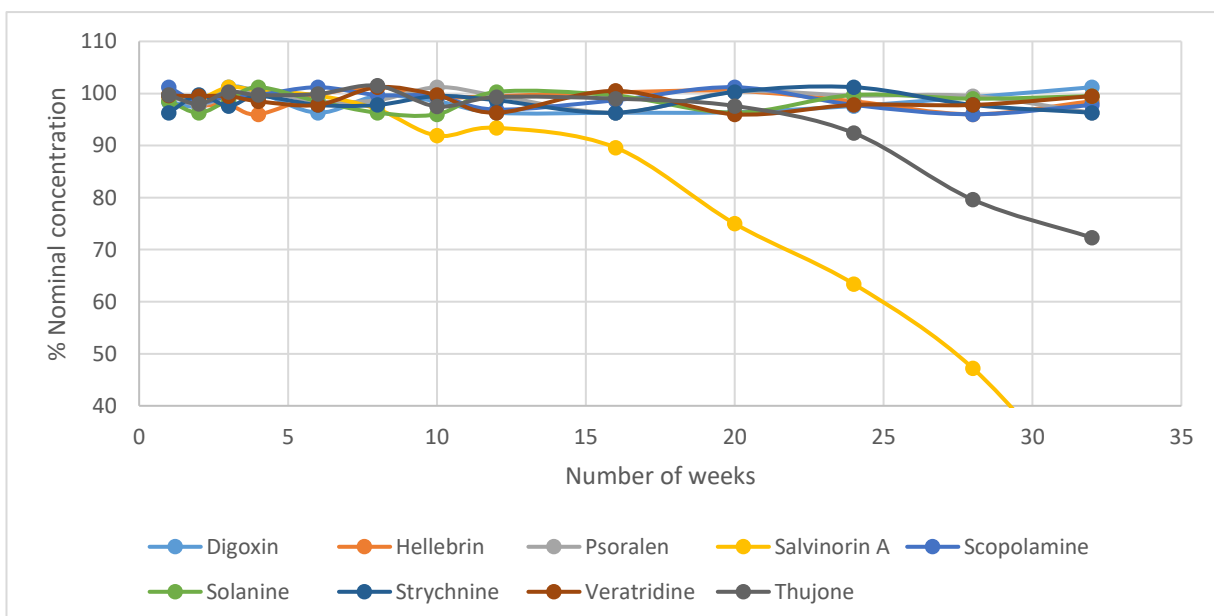
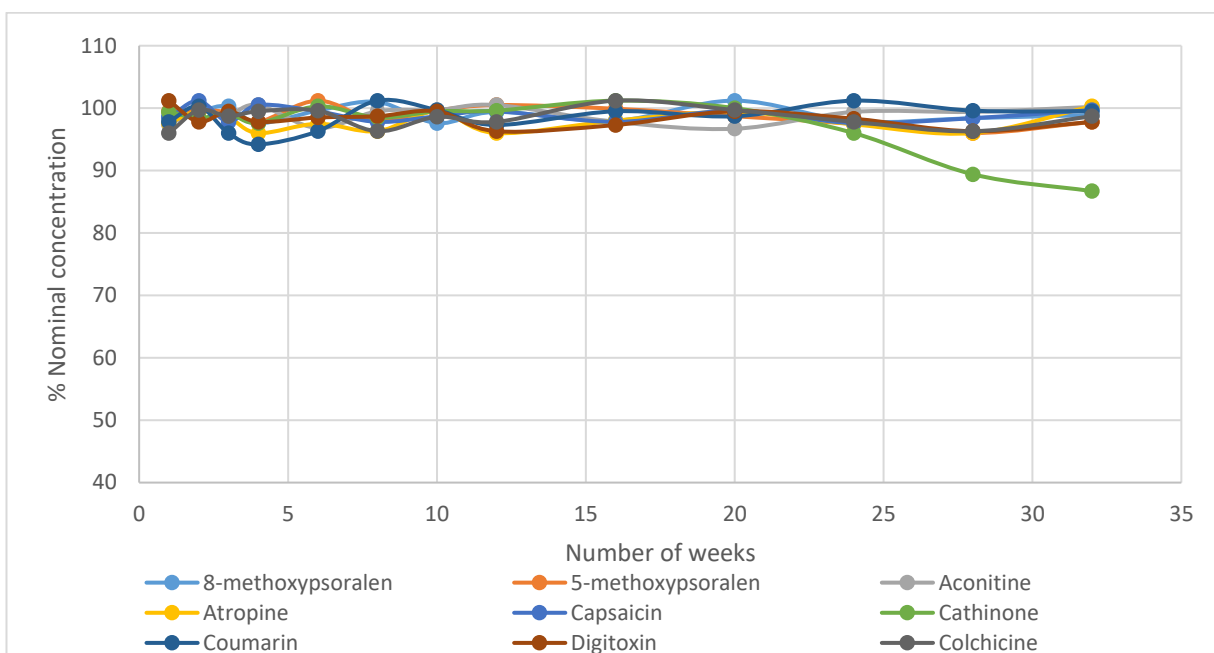


**Figure 6.24: Standard stability in methanol at 2-8 °C**

A reduction in % nominal concentration after a period of around 30 weeks, 15 weeks and 25 weeks for cathinone, salvinorin A and thujone respectively. The cause of the degradation of salvinorin is most likely due to the intermediate stock solution being stored in methanol, whereas the purchase stock of salvinorin was in acetonitrile. However, acetonitrile was not suitable for some of the compounds and therefore methanol was used meaning that in a mixed calibration solution and the limiting compound on storage would be salvinorin A.

## 1.4. Targeted plant analysis

### 1.4.1. Method

Samples obtained from Alnwick Gardens, private gardens and garden centre were analysed based on the areas of the plants believed to contain the compounds of interest based on communications with the head gardener at Alnwick.<sup>19</sup> The expected compounds and areas of plant believed to be present are found in Table 6.8. Where possible the parts included in Table 6.8 were collected, however due to varying growing patterns this was not always possible. There were also safety concerns when dealing with large plants, such as *Heracleum mantegazzianum* that lower parts of the plant and roots could not be safely accessed and were therefore not collected. Additionally, the bulbs of *Fritillaria L.* were not collected as only a small number of plants were present in Alnwick Gardens.

Approximately 0.1 g of material was taken from the plant using a clean scalpel and transferred to a vial and 10 mL of methanol was added. Samples were extracted using sonication for 15 minutes a 1 mL portion of the extract was filtered through 0.22 µm nylon syringe filters and transferred to autosampler vials for analysis via LC-MS. All samples were prepared and analysed in triplicate. Due to the unknown level of compound break down within the plant material once it had been collected all extractions were performed with 48 hrs of collection. Initial investigations found a number of extracted to be outside of the linear range for the compounds of interest and samples were therefore subsequently diluted with methanol to fall within the linear range of the method.

### 1.4.2. Results and discussion

The analysis of plant material seen in Table 6.9 showed some consistency with the information found in Table 6.8. *Atropa belladonna* is well reported in literature as showing high levels of toxins present in the berries in comparison with other areas of the plant which is in agreement with the data obtained in this study.<sup>217, 401</sup> However, there was some plants where the compounds were either present within other areas of the plant or not present in the areas expected. An example chromatogram from each of the compounds from various plants can be seen in Figures 6.25-6.28.

**Table 6.8: Types of plants and compounds present**

<b>Plant</b>	<b>Compound(s) believed to be present</b>	<b>Parts of plant</b>
<i>Aconitum lycoctonum</i>	Aconitine	Whole plant
<i>Aconitum napellus</i>	Aconitine	Whole plant
<i>Aquilegia alpina</i>	Aconitine	Seeds and root
<i>Aquilegia atrata</i>	Aconitine	Seeds and root
<i>Artemisia absinthium</i>	Thujone	Leaves
<i>Atropa belladonna</i>	Atropine, Scopolamine	Whole plant
<i>Catha edulis</i>	Cathinone	Leaves
<i>Colchicum autumnale</i>	Colchicine	Not reported
<i>Daphne laureola</i>	Coumarin	Whole plant
<i>Daphne mezereum</i>	Coumarin	Whole plant
<i>Brugmansia Suaveolens</i>	Atropine, Scopolamine	Whole plant
<i>Digitalis ferruginea</i>	Digoxin, Digitoxin	Whole plant
<i>Digitalis purpurea</i>	Digoxin, Digitoxin	Whole plant
<i>Fritillaria imperialis</i>	Veratridine	Bulbs
<i>Fritillaria meleagris</i>	Veratridine	Bulbs
<i>Helleborous argutifolis</i>	Hellebrin	Roots
<i>Helleborous foetidus</i>	Hellebrin	Roots
<i>Helleborous niger</i>	Hellebrin	Roots
<i>Helleborous odurus</i>	Hellebrin	Roots
<i>Helleborous orientalis</i>	Hellebrin	Roots
<i>Helleborous purpurascens</i>	Hellebrin	Roots
<i>Helleborous torquatus</i>	Hellebrin	Roots
<i>Helleborus cyclophyllus</i>	Hellebrin	Roots
<i>Helleborus early purple</i>	Hellebrin	Roots
<i>Helleborus viridis</i>	Hellebrin	Roots
<i>Heracleum mantegazzianum</i>	Psoralen, 5-Methoxypsoralen, 8-Methoxypsoralen	Whole plant
<i>Hyoscyamus niger</i>	Atropine, Scopolamine	Leaves and seeds
<i>Ruta graveolens</i>	Psoralen, 5-Methoxypsoralen, 8-Methoxypsoralen	Whole plant
<i>Salvia divinorum</i>	Salvinorin A	Leaves
<i>Solanum dulcamara</i>	Solanine	Whole plant
<i>Veratrum album</i>	Veratridine	Roots
<i>Veratrum nigrum</i>	Veratridine	Roots
<i>Capsicum chinense</i>	Capsaicin	Fruit
<i>Solanum tuberosum</i>	Solanine	Fruit and potato

There was also a large degree of variation between the genus of plants. For the 9 species of *Helleborus* the amount of hellebrin present within the root ranged from 0.83 – 55.36 µg/g there was also variation seen in the presence of hellebrin within the additional areas of the *Helleborus* plants analysed with some plant showing small amount of hellebrin presence, such as *Helleborous purpurascens* and *Helleborous argutifolis*, while others showed no presence, such as *Helleborous orientalis* and *Helleborous cyclophyllus*. There was also no correlation between a higher concentration of hellebrin found within the root and the presence in the above ground parts of the plant as can be seen in Figure 6.29.

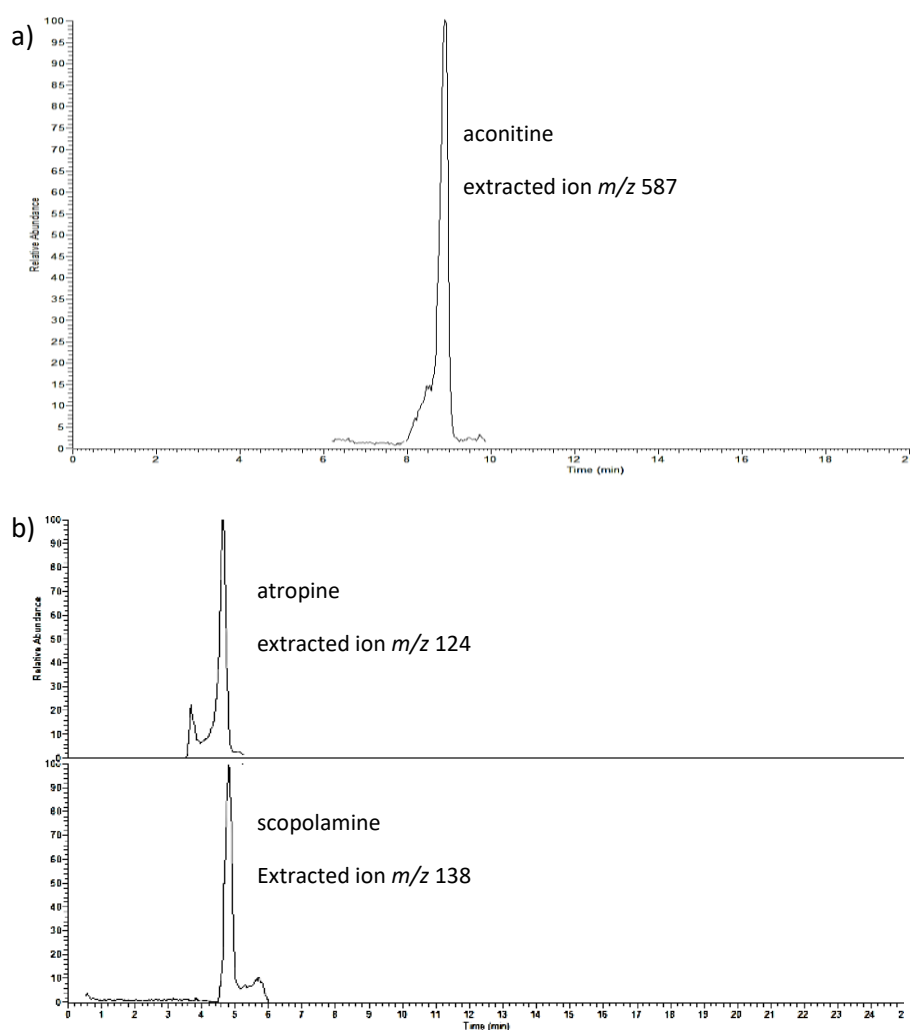


**Figure 6.25: Example extraction positive ion ESI SRM chromatogram of a) aconitine from *Aconitum lycoctonum* stem and b) atropine and scopolamine from *Brugmansia suaveolens* petal**

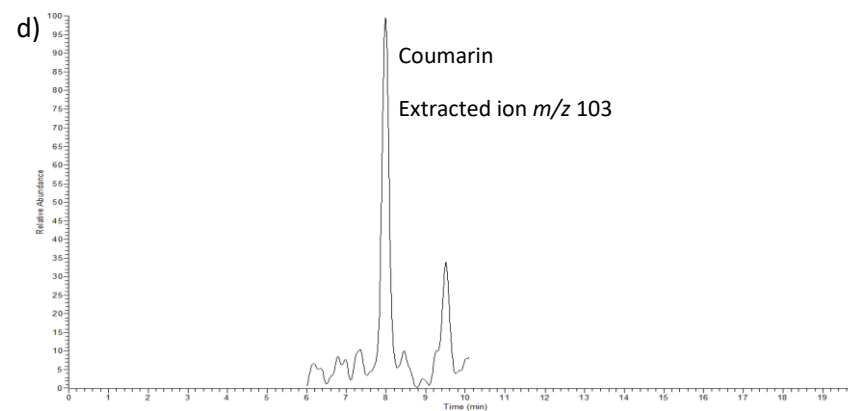
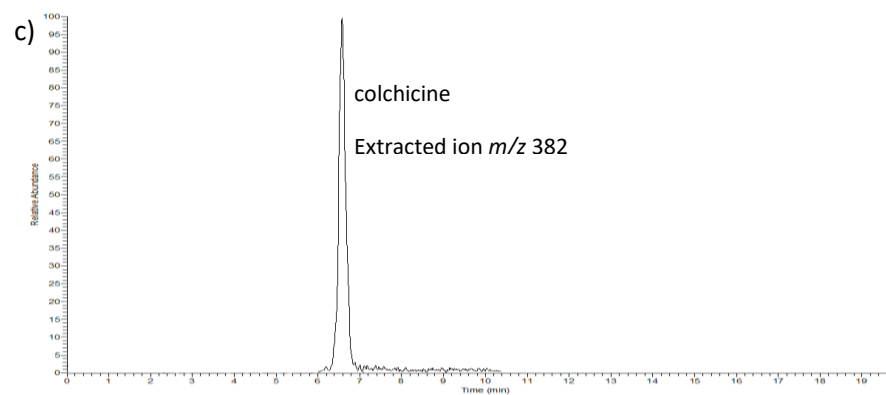
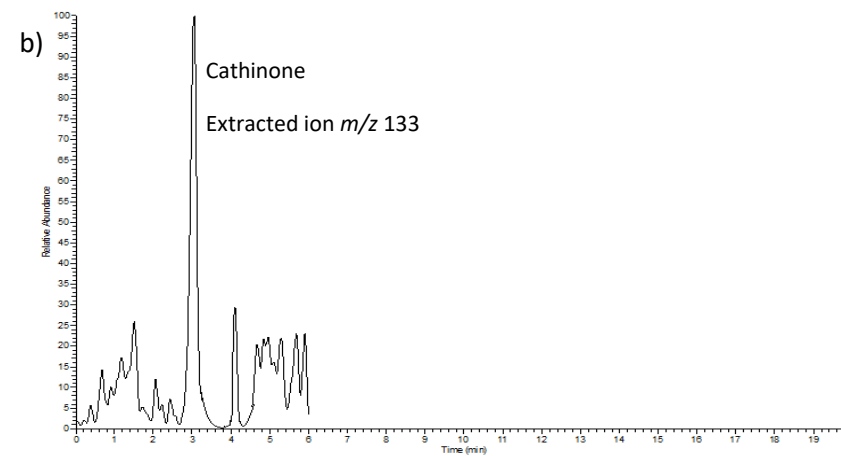
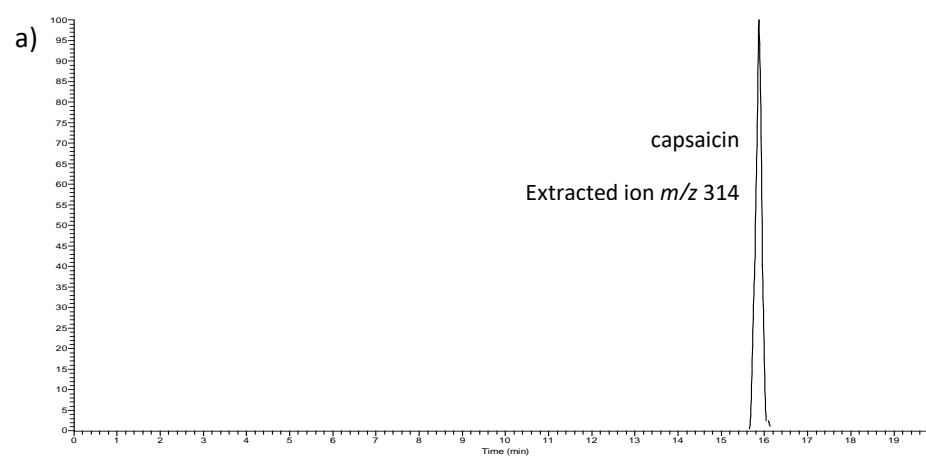


**Figure 6.26: Example extracted positive ion ESI SRM chromatogram of a) capsaicin from *Capsicum chinense* chilli, b) cathinone from *Catha edulis* leaf, c) colchicine from *Colchicum autumnale* bulb and d) coumarin from *Daphne laureola* leaf**

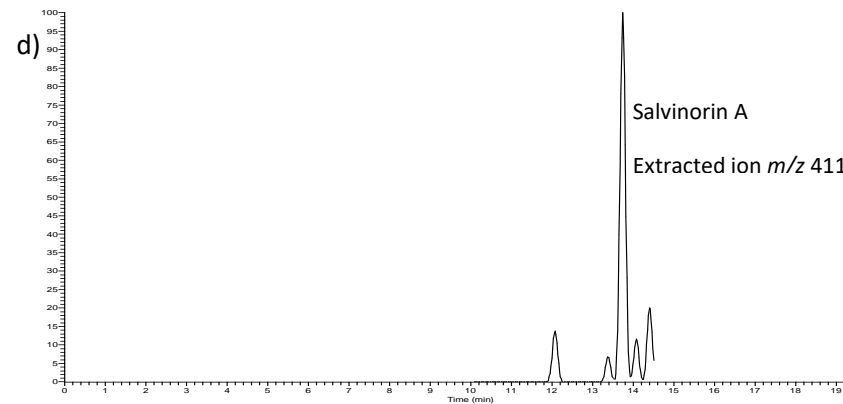
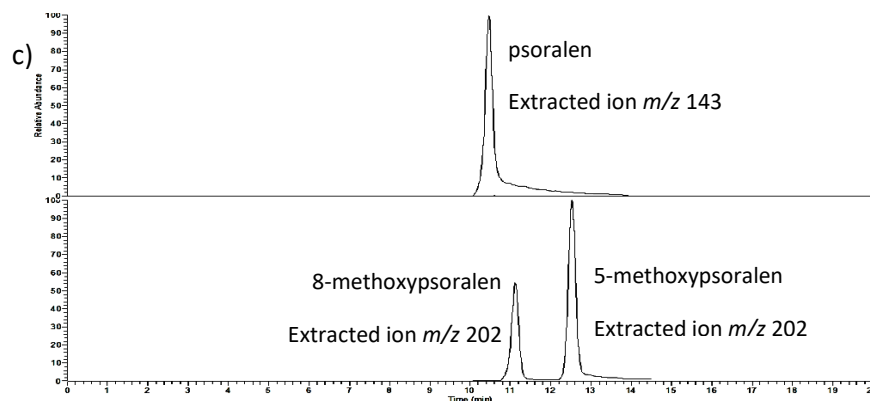
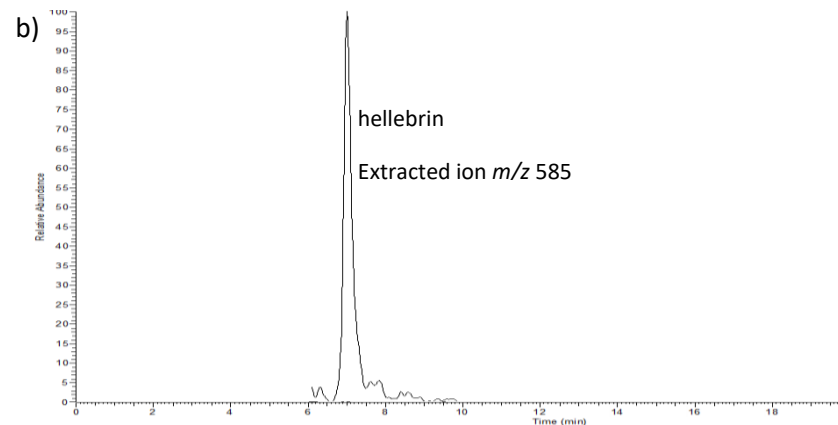
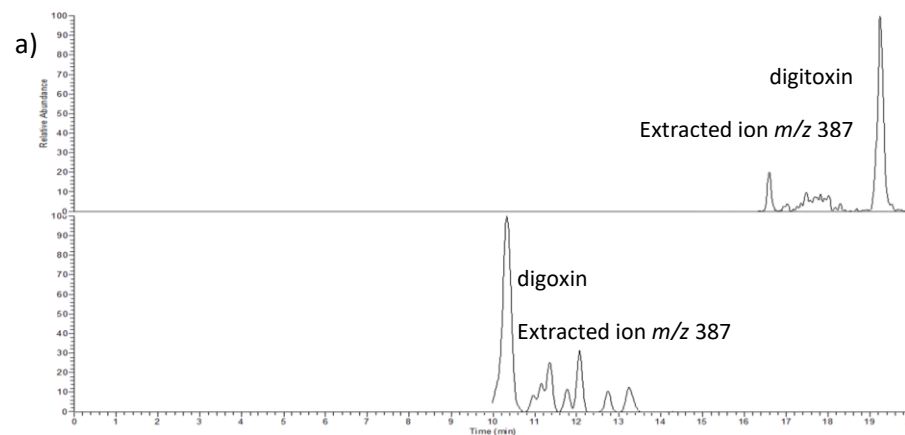
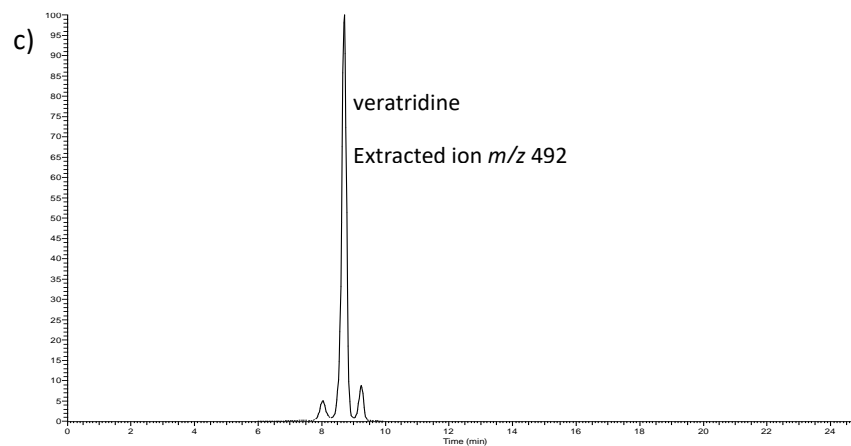
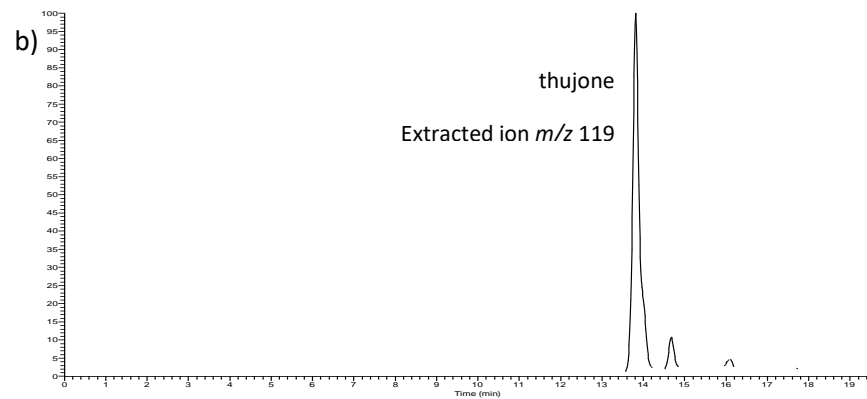
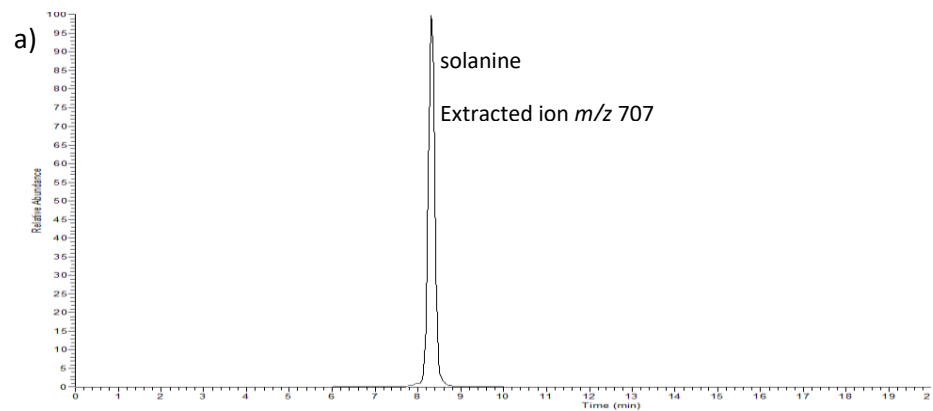


Figure 6.27: Example extracted positive ion ESI SRM chromatogram of a) digitoxin and digoxin from *Digitalis ferruginea* flower and d) hellebrin from *Helleborus cyclophyllus* root c) psoralen, 5- and 8-methoxypsoralen from *Ruta graveolens* foliage and d) salvinorin A from *Salvia divinorum*



**Figure 6.28: Example extracted positive ion ESI SRM chromatogram of a) solanine from *Solanum tuberosum*, b) thujone from *Artemisia absinthium* leaf and c) veratridine from *Veratrum album* flower**

In order to assess the risk of exposure to the plants analysed to adults and children the exposure factors were calculated, which is commonly used in environmental analysis to assess the risk of exposure to compounds such as PAHs and bisphenols. The exposure factors via inhalation, dermal absorption and ingestion can be calculated using the following equations.<sup>402-404</sup>

$$\text{Inhalation exposure risk (C}_{\text{air-adj}}) = C_{\text{air}} \times \text{ET} \times 1\text{day}/24\text{ hours} \times \text{EF} \times \text{ED}/\text{AT}$$

Where:       $C_{\text{air}}$  = Concentration of contaminant in air (mg/m<sup>3</sup>)  
                   $\text{ET}$  = Exposure time (hours/day)  
                   $\text{EF}$  = Exposure frequency (days/year)  
                   $\text{ED}$  = Exposure duration (years)  
                   $\text{AT}$  = Averaging time (days)

$$\text{Ingestion exposure risk (ADD)} = C_{\text{medium}} \times \text{IngR} \times \text{EF} \times \text{ED} / \text{BW} \times \text{AT}$$

Where:       $\text{ADD}$  = Average daily potential dose (mg/kg-day)  
                   $C_{\text{medium}}$  = Concentration of contaminant in medium (mg/g)  
                   $\text{IngR}$  = Ingestion rate (mg/day)  
                   $\text{EF}$  = Exposure frequency (days/year)  
                   $\text{ED}$  = Exposure duration (years)  
                   $\text{BW}$  = Body Weight (kg)  
                   $\text{AT}$  = Averaging time (days)

$$\text{Dermal exposure risk (ADD}_{\text{abs}}) = \text{DA}_{\text{event}} \times \text{SA} \times \text{EF} \times \text{ED} / \text{BW} \times \text{AT}$$

$$\text{DA}_{\text{event}} = K_p \times C \times t$$

Where:       $\text{ADD}_{\text{abs}}$  = Average daily dose (mg/kg-day)  
                   $\text{DA}_{\text{event}}$  = Absorbed dose (mg/cm<sup>2</sup>-event)  
                   $\text{SA}$  = Skin surface area available for contact (cm<sup>2</sup>)  
                   $\text{EF}$  = Exposure frequency (days/year)  
                   $\text{ED}$  = Exposure duration (years)  
                   $\text{BW}$  = Body Weight (kg)  
                   $\text{AT}$  = Averaging time (days)  
                   $K_p$  = Permeability coefficient (cm/hr)

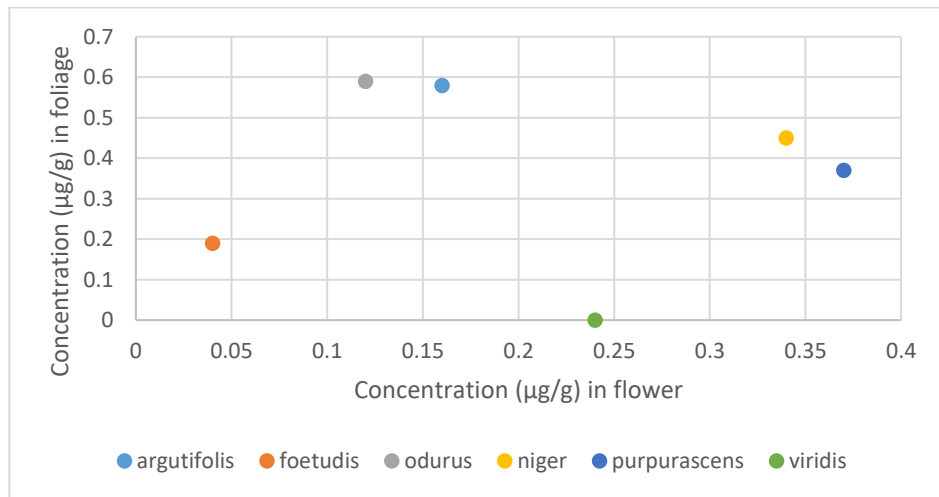
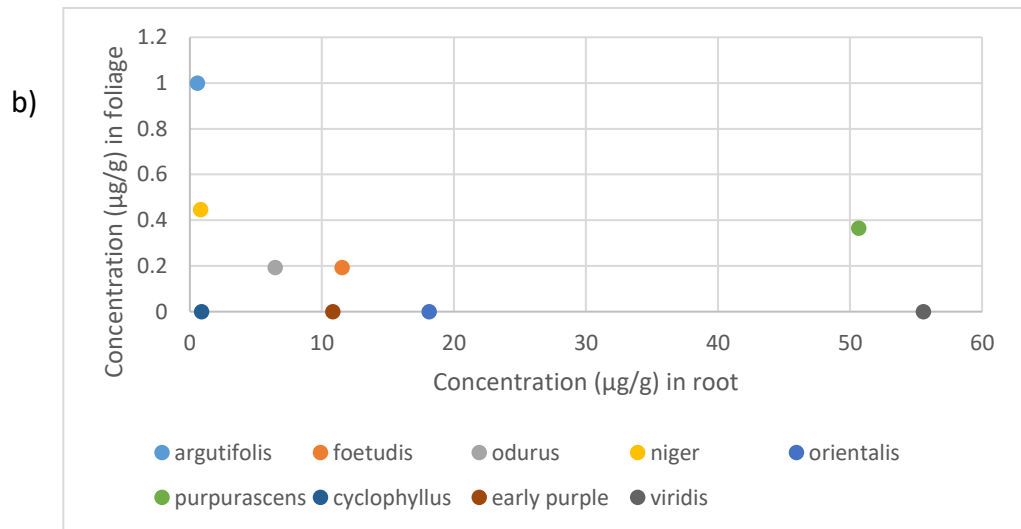
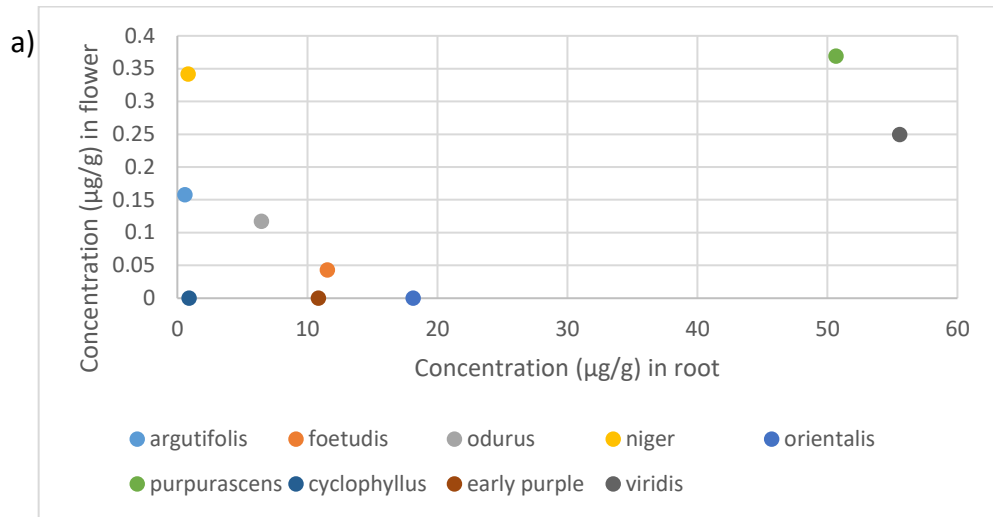


**Figure 6.29: Correlation graphs for hellebrin in a) root and flower concentration, b) root and foliage concentration and c) flower and foliage concentration**

**Table 6.9: Concentration of toxins found in plants sampled**

Plant	Part of plant	Compound	Concentration (µg/g)	Error (± µg/g) (n=3)	Dilution Factor
<i>Aconitum lycoctonum</i>	Foliage	Aconitine	0.00	N/A	N/A
	Stem	Aconitine	1.2	0.05	N/A
<i>Aconitum napellus</i>	Foliage	Aconitine	1.7	0.02	N/A
	Stem	Aconitine	0.90	0.02	N/A
<i>Aquilegia alpina</i>	Flower	Aconitine	0.16	0.01	N/A
	Seed	Aconitine	0.15	0.0006	N/A
	Stem	Aconitine	0.00	N/A	N/A
<i>Aquilegia atrata</i>	Flower	Aconitine	0.24	0.004	N/A
	Foliage	Aconitine	0.05	0.0006	N/A
	Stem	Aconitine	0.00	N/A	N/A
	Seed	Aconitine	0.56	0.02	N/A
<i>Artemisia absinthium</i>	Foliage	Thujone	322	9.7	10
	Stem	Thujone	110	3.5	10
<i>Atropa belladonna</i>	Berry	Atropine	63146	126	1000
		Scopolamine	44498	1201	1000
	Foliage	Atropine	2117	176	200
		Scopolamine	388	2.3	200
<i>Catha edulis</i>	Leaf	Cathinone	0.98	0.02	N/A
<i>Colchicum autumnale</i>	Bulb	Colchicine	578	2.9	100
	Leaf	Colchicine	127	0.9	100
<i>Daphne laureola</i>	Leaf	Coumarin	98	0.2	N/A
<i>Daphne mezereum</i>	Leaf	Coumarin	22	1.0	N/A
<i>Brugmansia suaveolens</i>	Petal	Atropine	31	0.8	N/A
		Scopolamine	29	2.5	N/A
	Pollen	Atropine	79	1.4	N/A
		Scopolamine	69	0.5	N/A
	Stem	Atropine	100	1.7	100
		Scopolamine	5257	37	100
<i>Digitalis ferruginea</i>	Flower	Digitoxin	184	2.2	N/A
		Digoxin	81	1.0	N/A
	Foliage	Digitoxin	70	0.6	N/A
		Digoxin	0.00	N/A	N/A
	Seed	Digitoxin	244	2.9	10
		Digoxin	26	0.6	10
<i>Digitalis purpurea</i>	Foliage	Digitoxin	256	3.6	10
		Digoxin	1.1	0.1	10
<i>Fritillaria imperialis</i>	Foliage	Veratridine	0.44	0.01	N/A
	Stem	Veratridine	0.00	N/A	N/A
<i>Fritillaria meleagris</i>	Foliage	Veratridine	0.04	0.001	N/A
	Stem	Veratridine	0.00	N/A	N/A
<i>Helleborous argutifolis</i>	Flower	Hellebrin	0.16	0.01	N/A
	Foliage	Hellebrin	0.58	0.02	N/A
	Root	Hellebrin	1.6	0.03	N/A
<i>Helleborous foetudis</i>	Flower	Hellebrin	0.04	0.004	N/A
	Foliage	Hellebrin	0.19	0.01	N/A
	Root	Hellebrin	2.2	0.1	N/A
<i>Helleborous odurus</i>	Flower	Hellebrin	0.12	0.007	N/A
	Foliage	Hellebrin	0.59	0.008	N/A
	Root	Hellebrin	6.5	0.4	N/A

**Table 6.9 (continued): Concentration of toxins found in plants sampled**

Plant	Part of plant	Compound	Concentration (µg/g)	Error (± µg/g) (n=3)	Dilution Factor
<i>Helleborous niger</i>	Flower	Hellebrin	0.34	0.02	N/A
	Foliage	Hellebrin	0.45	0.04	N/A
	Root	Hellebrin	0.83	0.05	N/A
<i>Helleborous orientalis</i>	Flower	Hellebrin	0.00	N/A	N/A
	Foliage	Hellebrin	0.00	N/A	N/A
	Root	Hellebrin	18.1	1.2	N/A
<i>Helleborous purpurascens</i>	Flower	Hellebrin	0.37	0.01	N/A
	Foliage	Hellebrin	0.37	0.04	N/A
	Root	Hellebrin	50.7	2.8	N/A
<i>Helleborous cyclophyllus</i>	Flower	Hellebrin	0.00	N/A	N/A
	Foliage	Hellebrin	0.00	N/A	N/A
	Root	Hellebrin	0.89	0.08	N/A
<i>Helleborous early purple</i>	Flower	Hellebrin	0.00	N/A	N/A
	Foliage	Hellebrin	0.00	N/A	N/A
	Root	Hellebrin	10.8	1.0	N/A
<i>Helleborous viridis</i>	Flower	Hellebrin	0.24	0.02	N/A
	Foliage	Hellebrin	0.00	N/A	N/A
	Root	Hellebrin	55.6	2.9	N/A
<i>Heracleum mantegazzianum</i>	Flower	Psoralen	1428	30	50
		5-Methoxypsoralen	920	15	50
		8-Methoxypsoralen	672	10	50
	Foliage	Psoralen	1703	14	50
		5-Methoxypsoralen	1298	17	50
		8-Methoxypsoralen	499	21	50
<i>Hyoscyamus niger</i>	Flower	Atropine	61	1.2	N/A
		Scopolamine	2755	58	100
	Root	Atropine	6.9	0.2	N/A
		Scopolamine	36	1.0	N/A
Seed	Atropine	91	6.2	N/A	
	Scopolamine	3907	176	100	
<i>Ruta graveolens</i>	Foliage	Psoralen	343	5.1	10
		5-Methoxypsoralen	335	5.0	10
		8-Methoxypsoralen	139	4.0	10
	Berry	Psoralen	42	0.5	N/A
		5-Methoxypsoralen	0.00	N/A	N/A
		8-Methoxypsoralen	4.1	0.04	N/A
<i>Veratrum album</i>	Flower	Veratridine	1.3	0.02	N/A
	Seed	Veratridine	0.00	N/A	N/A
<i>Capsicum chinense</i>	Stem	Capsaicin	3.1	0.09	N/A
	Foliage	Capsaicin	1.5	0.02	N/A
	Chilli	Capsaicin	53	0.2	N/A
<i>Solanum dulcamara</i>	Flower	Solanine	0.3	0.001	N/A
	Leaf	Solanine	0.73	0.01	N/A
	Stem	Solanine	0.93	0.01	N/A
	Root	Solanine	0.02	0.0002	N/A
<i>Solanum tuberosum</i>	Potato	Solanine	35	0.1	N/A
	Fruit	Solanine	30	0.5	N/A

C = Concentration of chemical in vehicle contacting skin (mg/cm<sup>3</sup>)

t = Time of contact (hours/event)

For this study the exposure factors via ingestion and dermal absorption were calculated. The exposure factors via inhalation were not calculated due to the fact that the concentration in air of the compounds is unknown. From the Environmental Protection Agency (EPA) website the following information can be obtained for different age ranges; BW, IngR and SA. The BW obtained were 80 kg, 11.4 kg, 13.8 kg, 18.6 kg and 31.8 kg for adults, children ages 1-<2 years, children ages 2-<3 years, children ages 3-<6 years and children ages 6-<11 years, respectively. For the IngR for the plant material located below the ground the ingestion rate via soil was used as it is unlikely that roots would be accidentally eaten and the ingestion rate for fruit and vegetables was used for the above ground parts of the plants. For this study the SA of the hands alone was used as this is the area most commonly in contact with plants. Based on the information on the EPA website the AT is equal to the exposure duration for non-carcinogens. Presumptions must be made in order to determine the EF, ED, K<sub>p</sub> and t for this study the presumptions as followed were used:

EF = 8 days per month over a period of four month while the plant is actively growing

ED = An exposure duration of 5 years based on perennial plants staying in the garden for this duration

t = 1 hour per event to tend to plants

K<sub>p</sub> = Reported as 0.000133 for digitoxin which was applied to all compounds within the study for consistency

All the numerical values used in the calculations are shown in Table 6.10.

The calculated exposure factors were then compared with the LD<sub>50</sub> to determine the number of days exposure are required to reach the LD<sub>50</sub> value. The results for the ingestion exposure factor can be seen in Appendix 1 and for the dermal exposure factor in Appendix 3 which has then been compared to the LD<sub>50</sub> the results of which can be seen in Appendix 2 for ingestion and Appendix 4 for dermal absorption.

**Table 6.10: Numerical values used in risk factor calculations**

Parameter	Numerical value	Comment	Reference
EF	0.087671	Fixed for all ages	N/A
ED	5	Fixed for all ages	N/A
AT	5	Fixed for all ages	N/A
BW	11.4	Child (1-<2 years)	402-404
	13.8	Child (2-<3 years)	
	18.6	Child (3-<6 years)	
	31.8	Child (6-<11 years)	
	80	Adult	
SA	6.9	Child (1-<2 years)	403
	8.8	Child (2-<3 years)	
	10.6	Child (3-<6 years)	
	15.1	Child (6-<11 years)	
	27.55	Adult	
IngR (above ground parts)	106.48	Child (1-<2 years)	404
	103.36	Child (2-<3 years)	
	103.79	Child (3-<6 years)	
	96.672	Child (6-<11 years)	
	84	Adult	
IngR (below ground parts)	30	Child (1-<2 years)	
	30	Child (2-<3 years)	
	30	Child (3-<6 years)	
	30	Child (6-<11 years)	
	10	Adult	
Kp	0.000133	Fixed for all compounds	N/A
t	1	Fixed for all ages	N/A

From the results obtained for the risk associated with the exposure to colchicine from the ingestion of *Colchicum autumnale* poses the greatest risk with the LD<sub>50</sub> surpassed with a single exposure event which reflect the reports in fatal poisoning following the ingestion of *Colchicum autumnale* following miss identification as wild garlic.<sup>247, 249, 405</sup> Colchicine has the third lowest LD<sub>50</sub> of all the compound analysed but when compared to the other three compounds; aconitine, colchicine and veratridine, it is present at the highest concentrations within the plant therefore accounting for the greater risk observed. *Atropa belladonna* berries also pose the large risk despite atropine not having a higher LD<sub>50</sub> than many of the compounds analysed. The amounts of days required to reach the LD<sub>50</sub> increases from 1.45 days through to 12.9 days with the movement through the age group from

youngest children through to adults for atropine. This is due to the high presence of atropine within the berries resulting in the LD<sub>50</sub> being reached by a much smaller degree of exposure. For all the remaining compounds the risk is far less and would require a large consumption of the plant material to reach the LD<sub>50</sub> level. However adverse effects have been reported for a number of compounds following accident ingestion or miss identification. From the results obtained for the dermal risk it would suggest that the risk is minimal. That being said it should be noted that some of the compounds produce effects which would not necessarily lead to death such as *Heracleum mantegazzianum* with the sap of the plant producing burns when exposed to UV radiation, with psoralen and 5-methoxypsoralen having the highest LD<sub>50</sub> of all the compounds used in this study.

## **1.5. Helleborous root extract and determination**

### **1.5.1. Method**

The whole root of *Helleborus purpurascens* was freeze dried using liquid nitrogen and then blitzed into a fine powder using a spice grinder. Approximately 2 g was weighed and placed in a Soxhlet thimble and placed in the Soxhlet extraction apparatus. The root material was extracted using 250 mL of methanol in order to ensure hellebrin would be extracted to use as an extraction check compound over a period of 5 days. The resulting extract was then concentrated to approximately 20 mL using a rotary evaporator prior to 1 mL portions being filtered using a 0.22 µm nylon syringe filter into an autosampler vial and analysed via preparative HPLC-UV.

### **1.5.2. Results and discussion**

Plants have been found to not only contain toxic compounds but also compounds of medical importance, including those which at certain levels are classified as toxic. There has been a limited number of studies on the compounds found within the Helleborous plant and their effects on the human body. Due to the highest concentration of hellebrin being found in the rhizomes of the Helleborous plant this study focuses on the use of Helleborous root allowing for hellebrin to be used as an extraction marker.

Preparative HPLC showed hellebrin extraction consistent with concentrations found in the LC-MS analysis based on comparison to a known standard as well as the addition of a number of other compounds as shown in Figure 6.30. Each fraction was then analysed via direct injection mass spectrometry to ensure single component fraction prior to be concentrated to dryness using a sample concentration then reconstitute in DMSO for analysis by NMR for structural elucidation.

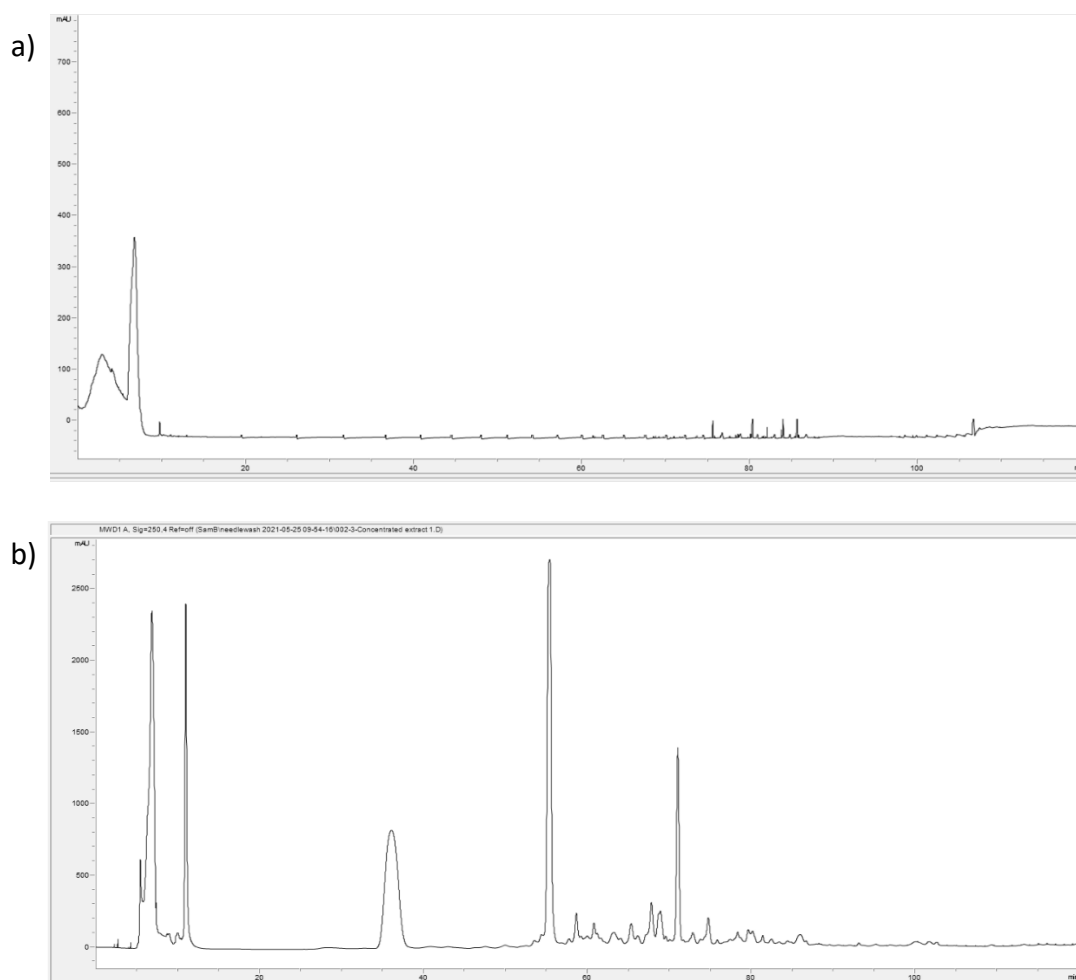


**Figure 6.30: Chromatogram of preparative HPLC-UV for a) hellebrin standard and b) plant extract**

The fractions obtained from the preparative HPLC system were initially analysed by direct injection ion trap mass spectrometry and it was found that the later fractions, >30 mins, had multiple components present and therefore would not be suitable for NMR analysis. In order to achieve single component fractions the

gradient profile was adjusted as per Table 6.11 and the samples re-injected with the resulting chromatogram shown in Figure 6.31.

**Table 6.11: Preparative LC gradient profile**

Initial gradient profile			Adjusted gradient profile		
Time (mins)	% A	% B	Time (mins)	% A	% B
0.00	95	5	0.00	90	10
120.00	50	50	100.00	90	10
			200.00	70	30
			240.00	70	30

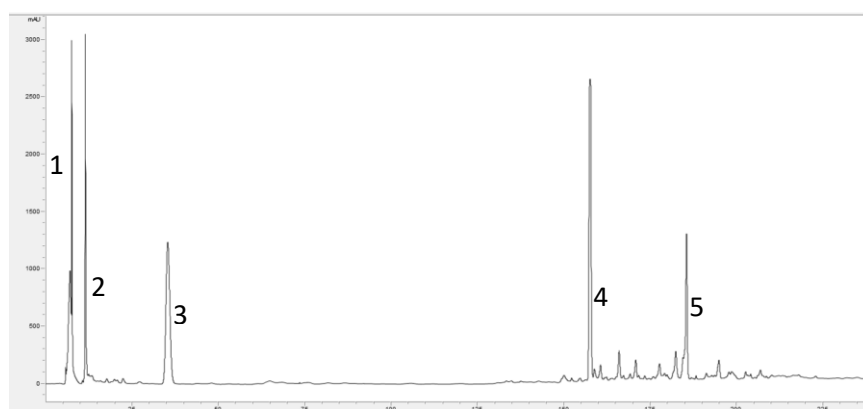


**Figure 6.31: Preparative HPLC-UV chromatogram following gradient adjustment**

The resulting fraction were then analysed by direct injection mass spectrometry to ensure single component fractions and to exclude fraction accounting for general plant compounds such as cholesterol, amino acids and fatty acids. Fraction not attributed to hellebrin or general plant compounds were subjected to further analysis via direct infusion MS/MS and NMR spectroscopy for structural elucidation.

Initial investigations found that the NMR instrumentation available was not able to detect compounds within any of the fractions, therefore the extraction was repeated with a larger weight of root material and the preparative HPLC was performed on two replicates of the extract and the fractions combined prior to

evaporating and reconstitution for NMR analysis. The combination of two replicate fraction allowed for proton NMR to be obtained however, it was still not possible to achieve carbon or HSQC data even when the number of scans was increased. The preparative HPLC step was then repeated using 10 portions of the sample extract totally 40 hours of analysis and the fractions again combined prior to evaporation and reconstitution. For each of the carbon and HSQC analysis the number of scans was increased giving an analysis from each carbon NMR of 5 hours and of 1 hour for HSQC. The combination of a higher number of fractions and the increase analysis on NMR was unable to achieve carbon or HSQC NMR as can be seen in Figure 6.32. The lack of sensitivity observed is potential due to a combination of two factors; the Hz of the NMR available, only 400 Hz, and that many of the fractions contained high molecular weight compound as therefore more material is required in order to gain suitable NMR data.

Prior to evaporating to dryness and reconstitution fractions were also analysed via direct infusion MS/MS at low (10 eV), medium (20 eV) and high (40 eV) collision energy and the resulting fragments were used for structural prediction using freely available competitive fragmentation modelling software available at <https://cfmid.wishartlab.com/identify>. The modelling software uses a similarity index between 0 – 1 to determine the accuracy of the match obtained. The software accuracy was assessed based on fraction 1 which based on the analysis of a standard solution is known to contain hellebrin. Table 6.12 shows the suggested structures based on the MS/MS spectrum and the match probability. From Table 6.12 it can be seen that the software is capable of matching the spectrum obtained for fraction 1 to the compound hellebrin with a high similarity. However, the similarity obtained for the remaining fraction is such that there is limited confidence in the match obtained. Therefore, structural elucidation of the compounds present in the remaining fractions was not possible.

From the information obtained, fractions 2 and 3 can be attributed to general plant compounds. However, fractions 4 and 5 contain high molecular weight compounds and due to the fragmentation observed are unlikely to be amino acid chains and are therefore compounds of interest.

Table 6.12: Tentative compound identification

Fraction	Precursor ion ( $m/z$ )	Compound	Similarity
1	747	Hellebrin	0.9982
2	349	2-[1-(2-hydroxyethyl)-2-undecyl-4,5-dihydroimidazol-1-ium-1-yl]acetate	0.3343
3	481	BIS(2,2,6,6-Tetramethyl-4-piperidinyl)sebacate	0.3473
4	1463	Not Found	N/A
5	1407	Not Found	N/A

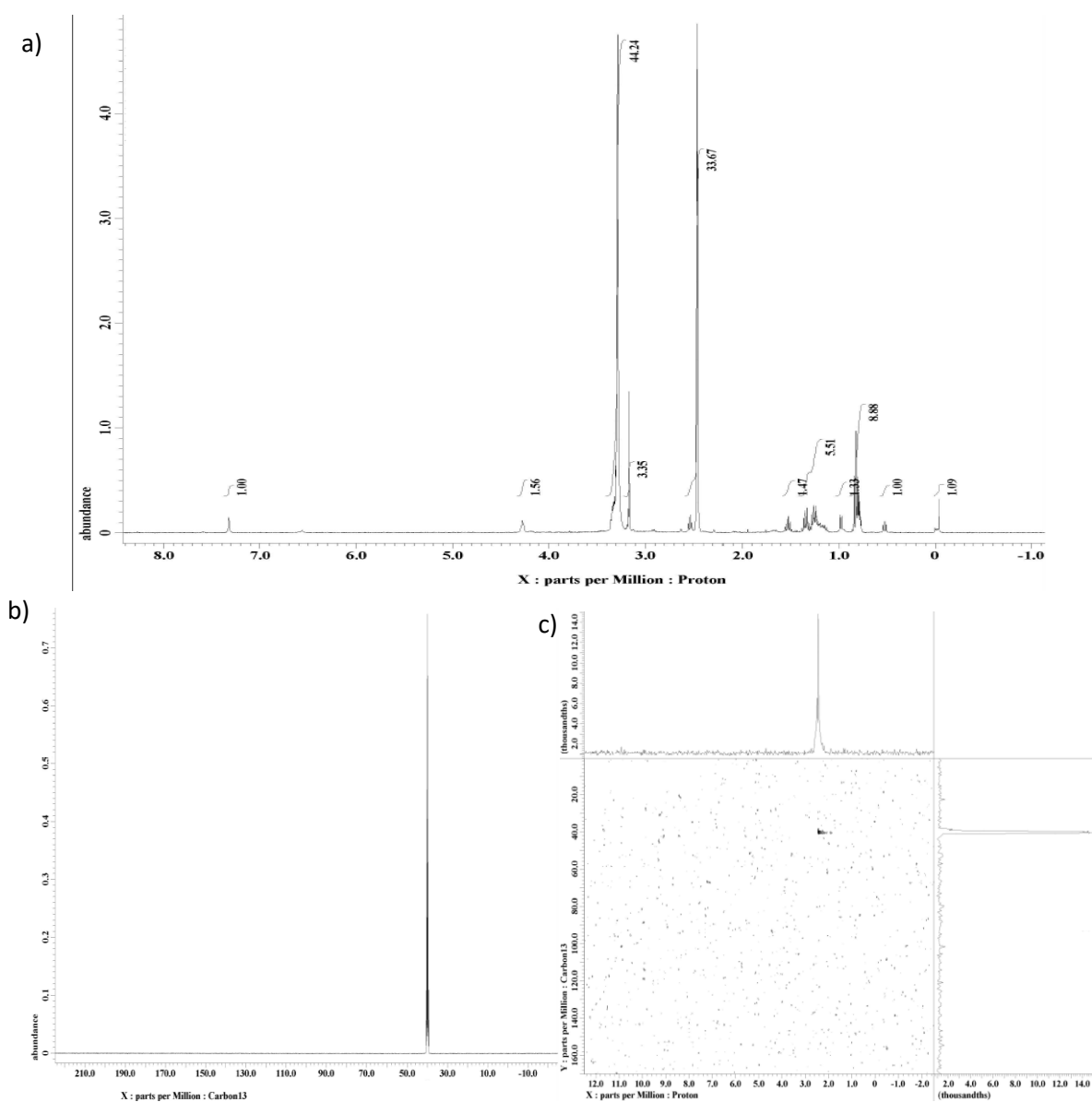


Figure 6.31: Example a) proton, b) carbon and c) HSQC NMR spectrum obtained from hellebrin root fractions.

## 1.6. Conclusion

A method has been developed and validated for the analysis of 18 known plant toxin found within plants common to the UK using an Eclipse Plus™ C18, 3.5 µm, 100 x 4.6 mm column and a gradient method of water + 0.1% formic acid (A) and methanol + 0.1% formic acid (B) at a flow rate of 0.3 mL/min. The developed method shows a high degree of linearity (>0.995), precision (<11 %) and sensitivity capable of detecting compounds within various parts of the plants investigated with minimal sample clean up and preparation. In a collaboration with Alnwick Garden, a variety of plants were analysed which are common to the UK including those which are commonly found growing wild or are available to purchase as ornamental plants from garden centres. Due to the ability to misidentify or ease of contact, these plants pose a significant risk to human health and therefore greater understanding is required. The resulting application of the developed LC-MS method allowed for the identification of the key plants and parts of those plants which pose the highest risks. The results obtained for the plant analysis showed good repeatability with %RSD of < 10.5 %. The data obtained allowed for the calculation of risk factors based upon the environmental protection agency calculations which are commonly used to assess the risk of environmental contaminants. From the risk factor calculations, the greatest risks of fatal poisoning are due to atropine from *Atropa belladonna* and colchicine from *Colchicum autumnale* with the risks decrease as the age range increases, as anticipated. However, the risk factors are based upon the LD<sub>50</sub> meaning care should be taken when reviewing the risk as many of the plants analysis can cause ill effects well below the LD<sub>50</sub> values and therefore all plants within the study should be handled with caution. One particular species which falls into this category is *Heracleum mantegazzianum*, commonly known as Giants hogweed, which is commonplace on riverbanks in the UK and can cause severe burns on exposure to UV radiation.

In addition to the plants obtained from Alnwick Gardens it was discovered that a number of these plants were available for purchase, such as *Helleborus orientalis*, *Digitalis purpurea* and *Aconitum carmichaelii* with no warning

information being given. Therefore, posing a potential risk to gardeners. The treatment of certain plants by native culture as medicines and the use of specific preparation techniques indicates that the knowledge of plants and their toxin is an aspect that more developed countries may have lost over the years. Therefore, better public awareness and information is required into the potential impact of plants available to the public to prevent the misidentification, mis-use and potentially fatal consequences associated with plants. As part of the collaborative project a number of activities are taking place at Alnwick Gardens including evening seminars and activity days in order to highlight the risks associated with these plants. Culminating in the installation of permanent information boards which will be placed in the poison garden for which visitors can partake in guided tours while visiting the garden.

As previously discussed there has been a number of publications relating to compounds present within *Helleborus* species which suggest numerous medical benefits, include anti-tumour treatments, with studies mainly focusing on the above ground plant parts. Due to the high levels of hellebrin present within the roots of the plant further extraction was performed on roots of *Helleborus purpurascens*. The extraction was subjected to preparative HPLC followed by MS/MS and NMR analysis in order to identify the compounds present. However due to the limitations of the NMR instrumentation available due to the Hz and the molecular weight of the compounds full structural elucidation could not be performed and therefore the structures could not be determined during this study.

## **Chapter 7: Conclusion and further work**

## 2. Conclusion and further work

### 2.1. Conclusion

The use of LC-MS has seen significant advancements over recent years due to the increase in operation simplicity, lower cost and the incorporation of libraries; leading to an increase in applications for LC-MS. In addition, LC-MS has been incorporated into refurbished hospital testing capacities within the North East NHS trust, namely the Queen Elizabeth hospital in Gateshead.<sup>406</sup> The inclusion of such techniques within testing environments poses both challenges and opportunities. The challenges faced includes the development of new methods and transfer of existing method onto new instrumentation while having the skills within the department to perform such a task. However, the advantages are that for a degree of capital cost the use of LC-MS is capable of being used for multiple assays and delivering higher levels of sensitivity and selectivity. Subsequently two LC-MS/MS methods have been developed and validated for the analysis of compounds in complex matrices, a method for the analysis of thyroid hormones and a method for the analysis of plant toxins.

For thyroid hormone analysis a method was developed for both low-resolution LC-MS/MS and high-resolution LC-MS/MS. In order to remove any matrix effects, a sample clean up method was required; for low-resolution LC-MS/MS a solid phase extraction method was developed and for high-resolution LC-MS/MS, due to the higher level of sensitivity, a dilution method was developed. The use of both low and high resolution LC-MS/MS within this study highlights consideration which should be considered when purchasing an instrument and the ways in which the impact a reduced level of instrument sensitivity can be addressed. The developed method gave good linearity, sensitivity and precision with  $r^2$  values of  $> 0.990$ , LOQs of  $< 5.9$  pmol/L and precision of  $< 3.9$  %. When compared with the information available for the current clinical method this greatly improves on both sensitivity and accuracy which could be of significant importance when a clinician is presented with a hypothyroid patient. Due to the high linear range,  $10^3 - 10^6$  pg/mL, of the method the quantification of both T3 and T4 can be performed within a single run, which in turn increases the sample through put capacity, as the currently method requires each hormone to be analysed separately. The method developed for the analysis of thyroid hormones provides an alternative

methodology for the analysis of clinical samples for the diagnosis and management of hypo and hyper thyroidism.

The method was also applied to the analysis of thyroid hormone supplements as well as the more fundamental dissolution testing. This allows for content uniformity and a dissolution profile to be obtained without preconcentration. This is important as the levels present in supplements may be below traditional quality control techniques, such as when using HPLC-UV/Vis. This highlights the ability of a newly developed single instrument method which is capable of being applied to a variety of pharmaceutical and clinical applications.

For the analysis of plant toxins, a method was developed for LC-MS/MS for the separation of 18 plant toxins found in plants grown in the UK. The developed method gave good linearity, sensitivity and precision with  $r^2$  values of  $> 0.995$ , LOQs of  $< 25$  ng/mL with the exception of coumarin which has an LOQ of 308 ng/mL and precision of  $< 10.7$  % for all 18 compounds. An extraction method was developed utilising sonication in methanol with extraction recoveries of  $> 71$  % for all the compounds analysed. The developed method was applied to the analysis of plants obtained from Alnwick Garden, private gardens and garden centres. The analysis showed that toxins were not only found within the parts of plant as per the head gardener at Alnwick Garden's information but also within additional areas. The identification of plant toxins is of significant importance as there is limited public knowledge as to the risks involved when coming into contact with these plant. Whether that be as a keen gardener or coming across them in the wild, such as hikers and walkers. Risk analysis showed that the greatest risk of fatal poisoning was due to the consumption of *Colchicum autumnale* which is often mistaken for wild garlic and *Atropa belladonna*, particularly the berry, which are often mistaken for edible berries, particularly by children. Due to the availability to purchase many of these plants as ornamental flowering plants there is a duty of care to garden centres to ensure this information is readily available. In addition to this a number of plants pose risks due to their abundance in nature such as *Heracleum mantegazzianum* which is an invasive species within the UK, often growing in areas frequented by walkers, which is responsible for burns on exposure to sunlight and as such is included on Schedule 9, Section 14 of The

Wildlife and Countryside Act 1981 and suspected sightings should be reported to local councils.<sup>407</sup>

An additional study was performed utilising *Helleborus purpurascens* to determine the present of additional toxins or compounds of interest. Tentative analysis found the presence of general plant compounds but was unable to provide data for the larger compounds present in the later fraction. However, NMR analysis was deemed unsuccessful due to the sensitivity of the instrumentation available and the large molecular size of the compounds of interest.

The development of the LC-MS methods and related application methods highlight the ability for the technique to be used for a number of different application and the benefits that can be gained. The ability to analyse a large number of compounds within one analytical method offer a significant advantage in terms of throughput. While the development of multiple applications for the method for the analysis of thyroid hormones demonstrated how the techniques is able to be applied to a range of industries and/or sample types with a relatively small amount of development. Allowing for both methods to be applied to a variety of setting and potentially streamlining future analysis. For example, the identification of potential toxins in a medical emergency, where time can often be the different between life and dead.

## **2.2. Further work**

The development of the plant toxin method allowed for the analysis of a variety of plants which contain compounds which are harmful in a number of ways. However, there is limited knowledge on the variations in concentrations of these compound over the course of the plants life cycle. One key part of this study was to investigate the seasonal differences in the toxin produces by plants however due to covid restrictions this could not take place. In order to determine the seasonal variation between the toxins found within the plant and the growing stages plants would be collected over the entire growing period over a duration of 1 year as well as in dormant bulb form. The samples would then be analysed via

the developed method to determine any variation present. Allowing for the season difference within the plant and possibly the areas of the plant to be better understood.

In addition to the analysis of plant material the method could also be applied to the analysis of toxicological matrices such as blood, serum, plasma and urine. In order to apply the method to these matrices and extraction technique would need to be developed which would be suited for all the compounds present. The development of such a method would allow for the simultaneous detection of the compounds from suspected poisoning. This would be of particular benefit for individuals who have been hospitalised with suspected poisoning as the swift determination of any toxins present would greatly improve the speed at which suitable treatment could be given and therefore, increase likelihood of survival. However, the main challenges with developing an extraction method for all 18 compounds would be in obtaining a method that was suitable for the compounds given the large variation in compounds structures and chemical properties. As such the method would need to be sufficiently robust to accommodate all the compounds present with minimal impact on the recoveries obtained. The work carried out in this study will form part of a number of events at Alnwick Garden in order to raise awareness of the potential risks of plants which are commonplace across the UK.

As previously discussed the available NMR instrumentation was unable to provide adequate information to allow for structural elucidation for the two fractions of interest. Therefore, further work is required to obtain a sample which is suitable for NMR analysis, via the processing of additional material over a longer period of time or via the use of a more sensitive NMR by outsourcing the analysis. In addition, further work could be completed into the preparative HPLC method with the investigation of alternative columns to allow for the separation to take place over a shorter run time. Once structural elucidation has been performed any compounds of interest would be submitted for toxicological analysis to determine the effects on cell lines.

### 3. References

1. M. Rodriguez-Aller, Gurny, R., Veuthey, J. L., Guillarme, D., "Coupling ultra high-pressure liquid chromatography with mass spectrometry: constraints and possible applications", *Journal of Chromatography A*, 2013, **1292**, 2-18.
2. P. Marquet, Lachatre, G., "Liquid chromatography - mass spectrometry. Potential in forensic and clinical toxicology", *Journal of Chromatography B*, 1999, **733**, 93-118.
3. S. Görög, "The changing face of pharmaceutical analysis", *Trends in Analytical Chemistry*, 2007, **26**, 12-17.
4. T. Zhang and D. G. Watson, "High performance liquid chromatographic approaches to mass spectrometry based metabolomics", *Current Metabolomics*, 2013, **1**, 58-83.
5. A. H. Wu and D. French, "Implementation of liquid chromatography/mass spectrometry into the clinical laboratory", *Clinica Chimica Acta*, 2013, **420**, 4-10.
6. J. M. van den Ouweland and I. P. Kema, "The role of liquid chromatography-tandem mass spectrometry in the clinical laboratory", *Journal of Chromatography B*, 2012, **883-884**, 18-32.
7. W. M. A. Niessen, "Advances in instrumentation in liquid chromatography-mass spectrometry and related liquid-introduction techniques", *Journal of Chromatography A*, 1998, **794**, 407-435.
8. M. M. Moein, A. El Beqqali and M. Abdel-Rehim, "Bioanalytical method development and validation: Critical concepts and strategies", *Journal of Chromatography B*, 2017, **1043**, 3-11.
9. H. H. Maurer, "Current role of liquid chromatography-mass spectrometry in clinical and forensic toxicology", *Analytical and Bioanalytical Chemistry*, 2007, **388**, 1315-1325.
10. P. J. Taylor, "Matrix effects: the Achilles heel of quantitative high-performance liquid chromatography-electrospray-tandem mass spectrometry", *Clinical Biochemistry*, 2005, **38**, 328-334.
11. C. L. CS Ho, MHM Chan, RCK Cheung, LK Law, LCW Lit, KF Ng, MWM Suen, and HL Tai, "Electrospray Ionisation Mass Spectrometry. Principles and Clinical Applications", *Clinical Biochemistry Reviews*, 2003, **24**, 1-12.
12. A. Kessler, "Mass spectrometry – a key technique for traceability in clinical chemistry", *Trends in Analytical Chemistry*, 2016, **84**, 74-79.

13. A. C. Bianco and B. W. Kim, "Deiodinases: implications of the local control of thyroid hormone action", *The Journal of Clinical Investigation*, 2006, **116**, 2571-2579.
14. S. K. Vashist and J. H. T. Luong, *Handbook of Immunoassay Technologies*, Academic Press, London, UK, 1<sup>st</sup> edn., 2018.
15. The Association of Clinical Biochemistry, "Guidelines for the use of thyroid function tests", [https://www.british-thyroid-association.org/sandbox/bta2016/uk\\_guidelines\\_for\\_the\\_use\\_of\\_thyroid\\_function\\_tests.pdf](https://www.british-thyroid-association.org/sandbox/bta2016/uk_guidelines_for_the_use_of_thyroid_function_tests.pdf), (accessed 05<sup>th</sup> April 2021).
16. K. Díaz, L. Espinoza, A. Madrid, L. Pizarro and R. Chamy, "Isolation and Identification of Compounds from Bioactive Extracts of *Taraxacum officinale* Weber ex F. H. Wigg. (Dandelion) as a Potential Source of Antibacterial Agents", *Evidence-Based Complementary and Alternative Medicine*, 2018, **2018**, 2706417.
17. Cobas, "FT3 III method sheet", [http://labogids.sintmaria.be/sites/default/files/files/ft3\\_iii\\_2017-03\\_v2.pdf](http://labogids.sintmaria.be/sites/default/files/files/ft3_iii_2017-03_v2.pdf), (accessed 03<sup>rd</sup> July 2018, 2018).
18. Cobas, "FT4 II method sheet", [http://labogids.sintmaria.be/sites/default/files/files/ft4\\_ii\\_2013-05\\_v2.pdf](http://labogids.sintmaria.be/sites/default/files/files/ft4_ii_2013-05_v2.pdf), (accessed 03<sup>rd</sup> July 2018, 2018).
19. T. Jones, Communication with Alnwick Garden's poison garden head gardener, personal communication.
20. "The Poison Garden", <https://www.alnwickgarden.com/the-garden/poison-garden/>, (accessed 30<sup>th</sup> March 2020, 2020).
21. F. E. Wirngo, M. N. Lambert and P. B. Jeppesen, "The Physiological Effects of Dandelion (*Taraxacum Officinale*) in Type 2 Diabetes", *The review of diabetic studies*, 2016, **13**, 113-131.
22. K. Skalicka-Wozniak, A. Grzegorzcyk, L. Swiatek, M. Walasek, J. Widelski, B. Rajtar, M. Polz-Dacewicz, A. Malm and H. O. Elansary, "Biological activity and safety profile of the essential oil from fruits of *Heracleum mantegazzianum* Sommier & Levier (Apiaceae).", *Food and Chemical Toxicology*, 2017, **109**, 820-826.

23. F. F. C. Giroud , M. Augsburger , B. Horisberger L. Rivier , P. Mangin, "Salvia divinorum: an hallucinogenic mint which might become a new recreational drug in Switzerland.", *Forensic Science International*, 2000, **112**, 143-150.
24. R. Hernandez-Bello, R. V. Garcia-Rodriguez, K. Garcia-Sosa, L. M. Pena-Rodriguez, M. Vazquez-Hernandez, F. R. Ramos-Morales, O. Corcoran and A. Sanchez-Medina, "Salvinorin A content in legal high products of *Salvia divinorum* sold in Mexico.", *Forensic Science International*, 2015, **249**, 197-201.
25. J. Płotka-Wasyłka, N. Szczepańska, M. de la Guardia and J. Namieśnik, "Modern trends in solid phase extraction: New sorbent media", *Trends in Analytical Chemistry*, 2016, **77**, 23-43.
26. C. F. Poole, "New trends in solid phase extraction", *Trends in Analytical Chemistry*, 2003, **22**, 362-373.
27. R. A. Trenholm, B. J. Vanderford and S. A. Snyder, "On-line solid phase extraction LC-MS/MS analysis of pharmaceutical indicators in water: a green alternative to conventional methods", *Talanta*, 2009, **79**, 1425-1432.
28. H. Scientific, "The basic principles of Soxhlet extraction", <https://www.hawachextractionthimble.com/the-basic-principle-of-soxhlet-extraction/>).
29. Daniel Dabbs, Norbert Mulders and I. A. Aksay, "Solvothermal removal of the organic template from L 3 ("sponge") templated silica monoliths", *Journal of Nanoparticle Research*, 2006, **8**, 603-614.
30. Lab Society, "Hydrocarbon Extraction [THE COMPLETE GUIDE]", <https://labsociety.com/hydrocarbon-extraction/>, (accessed 19<sup>th</sup> May 2021).
31. Chromacademy, "HPLC method development", <https://www.chromacademy.com/channels/hplc-training-courses/method-development/hplc-method-development-video-training-course/>, (accessed 19<sup>th</sup> May 2021).
32. Thermo Fisher, "Microscale SPE", <https://www.fishersci.co.uk/shop/products/hypersep-microscale-solid-phase-extraction-spe-tips/p-4524454>, (accessed 19<sup>th</sup> May 2021).
33. "Solid-Phase Extraction", <https://chem.libretexts.org/@go/page/155906>, (accessed 13<sup>th</sup> May 2021).

34. "Serum components", <https://rockland-inc.com/Serum-Protein-Components.aspx>, (accessed 13<sup>th</sup> May 2021).
35. K. Pyper, J. Brouwers, P. Augustijns, I. Khadra, C. Dunn, C. G. Wilson and G. W. Halbert, "Multidimensional analysis of human intestinal fluid composition", *European Journal of Pharmaceutics and Biopharmaceutics*, 2020, **153**, 226-240.
36. I. Kögel-Knabner, "The macromolecular organic composition of plant and microbial residues as inputs to soil organic matter", *Soil Biology and Biochemistry*, 2002, **34**, 139-162.
37. S. Bayne and M. Carlin, *Forensic applications of high performance liquid chromatography*, CRC Press, Boca Raton, 2010.
38. Chromatography Today, "The Role of Martin and Synge in the Birth of Modern Chromatography", <https://www.chromatographytoday.com/news/industrial-news/39/breaking-news/the-role-of-martin-and-synge-in-the-birth-of-modern-chromatography/33267>, (accessed 07<sup>th</sup> Mar 2022).
39. V. R. Meyer, *Practical High-Performance Liquid Chromatography*, Wiley, West Sussex, UK, 5<sup>th</sup> edn., 2010.
40. D. Remane, D. K. Wissenbach and F. T. Peters, "Recent advances of liquid chromatography-(tandem) mass spectrometry in clinical and forensic toxicology - An update", *Clinical Biochemistry*, 2016, **49**, 1051-1071.
41. H. H. Maurer, "Multi-analyte procedures for screening for and quantification of drugs in blood, plasma, or serum by liquid chromatography-single stage or tandem mass spectrometry (LC-MS or LC-MS/MS) relevant to clinical and forensic toxicology", *Clinical Biochemistry*, 2005, **38**, 310-318.
42. Waters, "How Does High Performance Liquid Chromatography Work?", [https://www.waters.com/waters/en\\_US/How-Does-High-Performance-Liquid-Chromatography-Work%3F/nav.htm?cid=10049055&locale=en\\_US](https://www.waters.com/waters/en_US/How-Does-High-Performance-Liquid-Chromatography-Work%3F/nav.htm?cid=10049055&locale=en_US), (accessed 17<sup>th</sup> May 2021).
43. LCGC, "Modern HPLC Pumps: Perspectives, Principles, and Practices", <https://www.chromatographyonline.com/view/modern-hplc-pumps-perspectives-principles-and-practices>, (accessed 17<sup>th</sup> May 2021).

44. J.J. van Deemter, F.J. Zuiderweg and A. Klinkenberg, "Longitudinal diffusion and resistance to mass transfer as causes of nonideality in chromatography", *Chemical Engineering Science*, 1956, **5**, 271-289.
45. H. G. Barth, "Chromatography Fundamentals, Part V: Theoretical Plates: Significance, Properties, and Uses",  
<https://www.chromatographyonline.com/view/chromatography-fundamentals-part-v-theoretical-plates-significance-properties-and-uses>, (accessed 19<sup>th</sup> Jan 2022).
46. R. Lake, "How do small particle size columns increase sample throughput?", <https://www.restek.com/row/technical-literature-library/articles/how-do-small-particle-size-columns-increase-sample-throughput/>, (accessed 19<sup>th</sup> Jan 2022).
47. R. E. Majors, "Developments in HPLC Column Packing Design", *LCGC LC column Technology Supplement*, 2006, **1**, 8-15.
48. Chromedia, "Reversed phase LC: Theory",  
<http://www.chromedia.org/chromedia?waxtrapp=nvlhIDsHiemBpdmBIIecCX&subNav=wrsmrDsHiemBpdmBIIecCXhB>, (accessed 18<sup>th</sup> May 2021).
49. P. Zuvela, M. Skoczylas, J. Jay Liu, T. Ba Czek, R. Kaliszan, M. W. Wong, B. Buszewski and K. Heberger, "Column Characterization and Selection Systems in Reversed-Phase High-Performance Liquid Chromatography", *Chemical Reviews*, 2019, **119**, 3674-3729.
50. C. Today, "Using Different HPLC Column Chemistries to Maximise Selectivity for Method Development", *Chromatography Today*, 2018, 26-27.
51. K. B. Sentell and J. G. Dorsey, "Retention mechanism in reversed phase liquid chromatography stationary phase bonding density and solute selectivity", *Journal of Chromatography*, 1989, **4610**, 193-207.
52. L. Z. Jake L. Rafferty, J. Ilja Siepmann and Mark R. Schure, "Retention Mechanism in Reversed-Phase Liquid Chromatography: A Molecular Perspective", *Analytical Chemistry*, 2007, **79**, 6551-6558.
53. M. Yang, Fazio, S., Munch, D., Drumm, P., "Impact of methanol and acetonitrile on separations based on pi-pi interactions with a reversed-phase phenyl column", *Journal of Chromatography A*, 2005, **1097**, 124-129.

54. B. Smidova, D. Satinsky, K. Dostalova and P. Solich, "The pentafluorophenyl stationary phase shows a unique separation efficiency for performing fast chromatography determination of highbush blueberry anthocyanins", *Talanta*, 2017, **166**, 249-254.
55. D. S. Bell, "Retention and selectivity of stationary phases used in HILIC.", *LC GC North America*, 2015, **33**.
56. D. S. Bell and C. T. Santasania, "Alternative Retention and Selectivity Using Fluorinated Stationary Phases", <https://www.sigmaaldrich.com/technical-documents/articles/reporter-us/alt-retention-selectivity-fl-stationary-phases.html>, (accessed 20<sup>th</sup> Mar 2021).
57. C. S. David S Bell, "Mechanisms of interaction responsible for alternative selectivity of fluorinated stationary phases.", *LC GC North America*, 2016, **34**, 2-6.
58. Chromacademy, "Buffer choice for HPLC separations", <https://www.chromacademy.com/channels/hplc-training-courses/principles/buffer-choice-for-hplc-separations/>, (accessed 19<sup>th</sup> May 2021).
59. Crawford Scientific, "Buffer choice for HPLC separations", <https://www.crawfordscientific.com/chromatography-blog/post/buffer-choice-for-hplc-separations>, (accessed 19<sup>th</sup> May 2021).
60. M. W. Dong and J. Wysocki, "Ultraviolet Detectors: Perspectives, Principles, and Practices", <https://www.chromatographyonline.com/view/ultraviolet-detectors-perspectives-principles-and-practices>, (accessed 6<sup>th</sup> May 2021).
61. LCGC, "How Does It Work? Part V: Fluorescence Detectors", <https://www.chromatographyonline.com/view/how-does-it-work-part-v-fluorescence-detectors>, (accessed 17<sup>th</sup> May 2021).
62. Shodex, "Detectors for HPLC", <https://www.shodexhplc.com/lessons/lesson-6-detectors-for-hplc/>, (accessed 17<sup>th</sup> May 2021).
63. J. H. Wade and R. C. Bailey, "Refractive index-based detection of gradient elution liquid chromatography using chip-integrated microring resonator arrays", *Analytical chemistry*, 2014, **86**, 913-919.

64. LCGC, "Avoiding Refractive Index Detector Problems", <https://www.chromatographyonline.com/view/avoiding-refractive-index-detector-problems-0>, (accessed 17<sup>th</sup> May 2021).
65. E. d. Hoffmann and V. Stroobant, *Mass Spectrometry: Principles and Applications*, Wiley, West Sussex, UK, 3<sup>rd</sup> edn., 2008.
66. R. Kostianen and T. J. Kauppila, "Effect of eluent on the ionization process in liquid chromatography-mass spectrometry", *Journal of Chromatography A*, 2009, **1216**, 685-699.
67. R. Kostianen, T. Kotiaho, T. Kuuranne and S. Auriola, "Liquid chromatography/atmospheric pressure ionization-mass spectrometry in drug metabolism studies", *Journal of Mass Spectrometry*, 2003, **38**, 357-372.
68. T. R. C. Andries P. Bruins, and Jack D. Henion, "Ion Spray Interface for Combined Liquid Chromatography/Atmospheric Pressure Ionization Mass Spectrometry", *Analytical Chemistry*, 1987, **59**, 2642-2646.
69. N. Arabzadeh and T. Khayamian, "Pneumatically assisted electrospray-ion mobility spectrometry for quantitative analysis of intact proteins", *Talanta*, 2012, **99**, 29-35.
70. A. P. Bruins, "Mechanistic aspects of electrospray ionisation", *Journal of Chromatography A*, **794**, 345-357.
71. T. Chen, Q. Yao, R. R. Nasaruddin and J. Xie, "Electrospray Ionization Mass Spectrometry: A Powerful Platform for Noble-Metal Nanocluster Analysis", *Angewandte Chemie International Edition*, 2019, **58**, 11967-11977.
72. L. Konermann, E. Ahadi, A. D. Rodriguez and S. Vahidi, "Unraveling the mechanism of electrospray ionization", *Analytical Chemistry*, 2013, **85**, 2-9.
73. C. Gu, D. Russell and P. Yehl, "Application of LCMS in small-molecule drug development", <https://www.europeanpharmaceuticalreview.com/article/43628/application-lcms-small-molecule-drug-development/>, (accessed 18<sup>th</sup> May 2021).
74. A. R. Johnson and E. E. Carlson, "Collision-Induced Dissociation Mass Spectrometry: A Powerful Tool for Natural Product Structure Elucidation", *Anal Chem*, 2015, **87**, 10668-10678.

75. R. Rodriguez-Fernandez, S. A. Vazquez and E. Martinez-Nunez, "Collision-induced dissociation mechanisms of [Li(uracil)]+", *Phys Chem Chem Phys*, 2013, **15**, 7628-7637.
76. D. J. Douglas, "Mechanism of the Collision-Induced Dissociation of Polyatomic Ions Studied by Triple Quadrupole Mass Spectrometry.", *Journal of Physical Chemistry*, 1982, **86**, 185-191.
77. Thermo. Scientific, "Pulsed Q Collision Induced Dissociation on Linear Ion Trap Mass Spectrometers", [https://assets.thermofisher.com/TFS-Assets/CMD/Product-Bulletins/PSB124-Pulsed-Q-Collision-Induced-Dissociation\(PQD\)-EN.pdf](https://assets.thermofisher.com/TFS-Assets/CMD/Product-Bulletins/PSB124-Pulsed-Q-Collision-Induced-Dissociation(PQD)-EN.pdf), (accessed 17<sup>th</sup> May 2021).
78. T. Guo, C. S. Gan, H. Zhang, Y. Zhu, O. L. Kon and S. K. Sze, "Hybridization of Pulsed-Q Dissociation and Collision-Activated Dissociation in Linear Ion Trap Mass Spectrometer for iTRAQ Quantitation", *Journal of Proteome Research*, 2008, **7**, 4831-4840.
79. W. W. Wu, G. Wang, P. A. Insel, C.-T. Hsiao, S. Zou, S. Maudsley, B. Martin and R.-F. Shen, "Identification of proteins and phosphoproteins using pulsed Q collision induced dissociation (PQD)", *Journal of the American Society for Mass Spectrometry*, 2011, **22**, 1753-1762.
80. M. Sargent, "Guide to achieving reliable quantitative LC-MS measurements", *RSC Analytical Methods Committee*, 2013.
81. C. G. Herbert, *Mass spectrometry basics*, CRC Press, Boca Raton, 2003.
82. E. d. Hoffmann, *Mass spectrometry : principles and applications*, Wiley, Hoboken, New Jersey, 3rd edn., 2007.
83. J. E. Campana, "Elementary theory of the quadrupole mass filter", *International Journal of Mass Spectrometry and Ion Physics*, 1980, **33**, 101-117.
84. N. V. Konenkov, M. Sudakov and D. J. Douglas, "Matrix methods for the calculation of stability diagrams in quadrupole mass spectrometry", *Journal of the American Society for Mass Spectrometry*, 2002, **13**, 597-613.
85. P. H. Dawson and D. J. Douglas, in *Encyclopedia of Spectroscopy and Spectrometry*, ed. J. C. Lindon, Elsevier, Oxford, 1999, DOI: <https://doi.org/10.1006/rwsp.2000.0249>, pp. 1921-1930.

86. C. Extrel, "Using Graphical Tools to Understand Quadrupole Theory", <https://www.azom.com/article.aspx?ArticleID=10996>, (accessed 07<sup>th</sup> Mar 2022).
87. J.-P. Schermann, in *Spectroscopy and Modeling of Biomolecular Building Blocks*, ed. J.-P. Schermann, Elsevier, Amsterdam, 1<sup>st</sup> edn., 2008, pp. 129-207.
88. D. J. Douglas, A. J. Frank and D. Mao, "Linear ion traps in mass spectrometry", *Mass Spectrometry Reviews*, 2005, **24**, 1-29.
89. M. S. Raymond E. March, Eric J. Reiner, Roger S. Mercer, Jeffry B. Plomley, David S. Waddell, Karen A MacPherson, "Ion trap mass spectrometry", *International Journal of Mass Spectrometry and Ion Processes*, 1992, **118**, 71-135.
90. C. L. H. Bruce E. Wilcox, and Alan G. Marshall, "Improved ion extraction from a linear octopole ion trap", *Journal of American Society for Mass Spectrometry*, 2002, **13**, 1304-1312.
91. X. Li, X. Zhang, R. Yao, Y. He, Y. Zhu and J. Qian, "Design and performance evaluation of a linear ion trap mass analyzer featuring half round rod electrodes", *Journal of American Society for Mass Spectrometry*, 2015, **26**, 734-740.
92. Thermo Scientific, "WideBand Activation Technology", <https://assets.thermofisher.com/TFS-Assets/CMD/Product-Bulletins/PSB102-WideBand-Activation-Technology-EN.pdf>, (accessed 17<sup>th</sup> Jan 2022).
93. Thermo Scientific, "Planet Orbitrap - Q Exactive plus", <https://planetorbitrap.com/q-exactive-plus#tab:schematic>, (accessed 18<sup>th</sup> Mar 2021).
94. Thermo Scientific, "Planet Orbitrap - ID-X", <https://planetorbitrap.com/orbitrap-id-x>, (accessed 18<sup>th</sup> Mar 2021).
95. A. Makarov, Denisov, E., Kholomeev, A., Balschun, W., Lange, O., Strupat, K., Horning, S., "Performance Evaluation of a Hybrid Linear Ion Trap/Orbitrap Mass Spectrometer", *Analytical chemistry*, 2006, **78**, 2113-2120.
96. Q. Hu, R. J. Noll, H. Li, A. Makarov, M. Hardman and R. Graham Cooks, "The Orbitrap: a new mass spectrometer", *Journal of Mass Spectrometry*, 2005, **40**, 430-443.

97. W. Xu, J. Zhang, D. Zhu, J. Huang, Z. Huang, J. Bai and X. Qiu, "Rapid separation and characterization of diterpenoid alkaloids in processed roots of *Aconitum carmichaeli* using ultra high performance liquid chromatography coupled with hybrid linear ion trap-Orbitrap tandem mass spectrometry", *Journal of Separation Science*, 2014, **37**, 2864-2873.
98. H. Oberacher, Arnhard, K., "Current status of non-targeted liquid chromatography-tandem mass spectrometry in forensic toxicology", *Trends in Analytical Chemistry*, 2016, **84**, 94-105.
99. E. S. Hecht, M. Scigelova, S. Eliuk and A. Makarov, in *Encyclopedia of Analytical Chemistry*, 2019, DOI: 10.1002/9780470027318.a9309.pub2, pp. 1-40.
100. R. H. Perry, R. G. Cooks and R. J. Noll, "Orbitrap mass spectrometry: instrumentation, ion motion and applications", *Mass Spectrometry Reviews*, 2008, **27**, 661-699.
101. R. A. Zubarev and A. Makarov, "Orbitrap mass spectrometry", *Analytical Chemistry*, 2013, **85**, 5288-5296.
102. D. Ryan, "Chapter 11: Atomic Mass Spectrometry (Inorganic MS)", [http://faculty.uml.edu/david\\_ryan/84.314/Instrumental%20Lecture%2011.pdf](http://faculty.uml.edu/david_ryan/84.314/Instrumental%20Lecture%2011.pdf), (accessed 18<sup>th</sup> May 2021).
103. European Medicines Agency, "Guideline on bioanalytical method validation", London, United Kingdom, 2011
104. A. Van Eeckhaut, K. Lanckmans, S. Sarre, I. Smolders and Y. Michotte, "Validation of bioanalytical LC-MS/MS assays: evaluation of matrix effects", *Journal of Chromatography B*, 2009, **877**, 2198-2207.
105. International conference on harmonisation, "ICH guideline Validation of analytical procedures - test and methodology", <http://www.ich.org/products/guidelines/quality/quality-single/article/validation-of-analytical-procedures-text-and-methodology.html>, (accessed 11th Feb 2019).
106. A. Okorie, J. Entwistle and J. R. Dean, "The application of in vitro gastrointestinal extraction to assess oral bioaccessibility of potentially toxic elements from an urban recreational site", *Applied Geochemistry*, 2011, **26**, 789-796.

107. Perkin Elmer, "<https://www.perkinelmer.com/uk/lab-products-and-services/application-support-knowledgebase/alphalisa-alphascreen-no-wash-assays/alpha-serum.html>", (accessed 29th Dec 2021, 2021).
108. R. Wayne, in *Plant Cell Biology*, ed. R. Wayne, Academic Press, San Diego, 2010, DOI: <https://doi.org/10.1016/B978-0-12-374233-9.00020-9>, pp. 339-356.
109. L. Stavalone and V. Lionetti, "Extracellular Matrix in Plants and Animals: Hooks and Locks for Viruses", *Frontiers in Microbiology*, 2017, **8**.
110. E. Frohlich and R. Wahl, "The forgotten effects of thyrotropin-releasing hormone: Metabolic functions and medical applications", *Frontiers in Neuroendocrinology*, 2019, **52**, 29-43.
111. A. Ben-Shlomo and S. Melmed, in *The Pituitary*, ed. S. Melmed, Academic Press, San Diego, 3<sup>rd</sup> edn., 2011, pp. 21-45.
112. H. M. Goodman, *Basic medical endocrinology*, Academic Press, Amsterdam, 4th edn., 2009.
113. R. S. Ahima and M. B. Jackson, in *Neurology and Clinical Neuroscience*, eds. A. H. V. Schapira, E. Byrne, S. DiMauro, R. S. J. Frackowiak, R. T. Johnson, Y. Mizuno, M. A. Samuels, S. D. Silberstein and Z. K. Wszolek, Mosby, Philadelphia, 2007, pp. 1545-1556.
114. V. D. Sarapura, D. F. Gordon and M. H. Samuels, in *The Pituitary*, ed. S. Melmed, Academic Press, San Diego, 3<sup>rd</sup> edn., 2011, pp. 167-203.
115. R. Mihai, "Physiology of the pituitary, thyroid, parathyroid and adrenal glands", *Surgery (Oxford)*, 2014, **32**, 504-512.
116. M. E. Hadley, *Endocrinology*, Prentice Hall, New Jersey, 6th ed.. edn., 2006.
117. J. L. Nath, F. H. Martini and E. F. Bartholomew, *Fundamentals of Anatomy & Physiology*, Pearson Education, Harlow, 2018.
118. A. Christianson and H. Bender, *The Complete Idiot's Guide to Thyroid Disease*, Penguin Random House LLC, New York, 1 edn., 2011.
119. V. A. Galton, "The ups and downs of the thyroxine pro-hormone hypothesis", *Molecular and Cellular Endocrinology*, 2017, **458**, 105-111.

120. Sara Danzi and I. Klein, "Potential uses of T3 in the treatment of human disease.", *Clinical Cornerstone*, 2005, **7**, 9-15.
121. Thyroid Clinic, "Multinodular goitre", <https://www.thyroid.com.au/thyroid-disorders/multinodular-goitre/>, (accessed 19<sup>th</sup> Apr 2021).
122. R. Summers and R. Macnab, "Thyroid, parathyroid hormones and calcium homeostasis", *Anaesthesia & Intensive Care Medicine*, 2017, **18**, 522-526.
123. Y.A. Ma and C.J. Sih, "Mechanism of thyroid hormone biosynthesis. Enzymatic oxidative coupling of 3,5-diiodo-L-tyrosine derivatives", *Tetrahedron Letters*, 1999, **40**, 9211-9214.
124. A.D. Dunn and J.T. Dunn, "The importance of thyroglobulin structure for thyroid hormone biosynthesis", *Biochimie*, 1999, **81**, 505-509.
125. D. W. Scoville, H. S. Kang and A. M. Jetten, "Transcription factor GLIS3: Critical roles in thyroid hormone biosynthesis, hypothyroidism, pancreatic beta cells and diabetes", *Pharmacology and Therapeutics*, 2020, **215**, 107632.
126. M. A. Crook, *Clinical Biochemistry and Metabolic Medicine*, CRC Press LLC, London, GBR, 2013.
127. T. F. Pirahanchi Y, Jialal I., *Physiology, Thyroid Stimulating Hormone.*, StatPearls, Treasure Island, Florida, 2020.
128. H. F. Escobar-Morreale, M. J. Obregon, A. Hernandez, F. Escobar del Rey and G. Morreale de Escobar, "Regulation of iodothyronine deiodinase activity as studied in thyroidectomized rats infused with thyroxine or triiodothyronine", *Endocrinology*, 1997, **138**, 2559-2568.
129. A. L. Maia, I. M. Goemann, E. L. Meyer and S. M. Wajner, "Deiodinases: the balance of thyroid hormone: type 1 iodothyronine deiodinase in human physiology and disease", *Journal of Endocrinology*, 2011, **209**, 283-297.
130. A. Lombardi, M. Moreno, P. de Lange, S. Iossa, R. A. Busiello and F. Goglia, "Regulation of skeletal muscle mitochondrial activity by thyroid hormones: focus on the "old" triiodothyronine and the "emerging" 3,5-diiodothyronine", *Frontiers in Physiology*, 2015, **6**, 237.

131. M. Moleti, M. Di Mauro, G. Sturniolo, M. Russo and F. Vermiglio, "Hyperthyroidism in the pregnant woman: Maternal and fetal aspects", *Journal of Clinical and Translational Endocrinology*, 2019, **16**, 100190.
132. J. Strawson, Q. Zhao and M. Dourson, "Reference dose for perchlorate based on thyroid hormone change in pregnant women as the critical effect", *Regulatory Toxicology and Pharmacology*, 2004, **39**, 44-65.
133. The National Health Service, "Hypothyroidism", <https://www.nhs.uk/conditions/underactive-thyroid-hypothyroidism/>, (accessed 24th Oct 2018, 2018).
134. The Newcastle upon Tyne Hospitals NHS, "Free T3, serum", <https://secure.newcastlelaboratories.com/test-directory/test/free-t3-serum/>, (accessed 24th July 2018, 2018).
135. The Newcastle upon Tyne Hospitals NHS, "Free T4, serum", <https://secure.newcastlelaboratories.com/test-directory/test/free-t4-serum/>, (accessed 24th July 2018, 2018).
136. The National Health Service, "Hyperthyroidism", <https://www.nhs.uk/conditions/overactive-thyroid-hyperthyroidism/causes/>, (accessed 04<sup>th</sup> April 2021).
137. I. D. Bobanga and C. R. McHenry, "Treatment of patients with Graves' disease and the appropriate extent of thyroidectomy", *Best Practice & Research Clinical Endocrinology & Metabolism*, 2019, **33**, 101319.
138. A. Antonelli, P. Fallahi, G. Elia, F. Ragusa, S. R. Paparo, I. Ruffilli, A. Patrizio, D. Gonnella, C. Giusti, C. Virili, M. Centanni, Y. Shoenfeld and S. M. Ferrari, "Graves' disease: Clinical manifestations, immune pathogenesis (cytokines and chemokines) and therapy", *Best Practice & Research Clinical Endocrinology & Metabolism*, 2020, **34**, 101388.
139. D. Taïeb, "Management of hyperthyroid patients following radioactive iodine therapy, with a specific emphasis on Graves' disease", *Médecine Nucléaire*, 2020, **44**, 284-286.
140. A. Asban, A. Anue, R. Xie and H. Chen, "Increasing Use of Thyroidectomy as Definitive Treatment for Hyperthyroidism", *Journal of Surgical Research*, 2020, **246**, 435-441.

141. K. Karndumri, Y. Thewjitcharoen, W. Chatchomchuan, S. Porramatikul, S. Krittiyawong, E. Wanothayaroj, S. Butadej, S. Nakasatien, R. Rajatanavin and T. Himathongkam, "Impact of first-line treatment choice on long-term outcomes of hyperthyroid Graves' disease patients with thyrotoxic periodic paralysis", *Journal of Clinical and Translational Endocrinology*, 2020, **21**, 100235.
142. T. Cheetham and R. Boal, "Graves' disease", *Paediatrics and Child Health*, 2019, **29**, 316-320.
143. A. Asban, S. Dream and B. Lindeman, "Is Hyperthyroidism Diagnosed and Treated Appropriately in the United States?", *Advances in Surgery*, 2019, **53**, 117-129.
144. S. M. Ferrari, I. Ruffilli, G. Elia, F. Ragusa, S. R. Paparo, A. Patrizio, V. Mazzi, A. Antonelli and P. Fallahi, "Chemokines in hyperthyroidism", *Journal of Clinical and Translational Endocrinology*, 2019, **16**, 100196.
145. S. Danzi and I. Klein, "Thyroid disease and the cardiovascular system", *Endocrinology & Metabolism Clinics of North America*, 2014, **43**, 517-528.
146. D. Dunn and C. Turner, "Hypothyroidism in Women", *Nursing for Women's Health*, 2016, **20**, 93-98.
147. L. Chaker, A. C. Bianco, J. Jonklaas and R. P. Peeters, "Hypothyroidism", *The Lancet*, 2017, DOI: 10.1016/s0140-6736(17)30703-1.
148. A. P. Delitala, G. Fanciulli, M. Maioli and G. Delitala, "Subclinical hypothyroidism, lipid metabolism and cardiovascular disease", *European Journal of International Medicine*, 2017, **38**, 17-24.
149. J. Gilbert, "Hypothyroidism", *Medicine*, 2017, **45**, 506-509.
150. C. G. P. Roberts, Ladenson, P. W., "Hypothyroidism", *The Lancet*, 2004, **363**, 793-803.
151. A. Aminorroaya, R. Meamar, M. Amini, A. Feizi, M. Nasri, A. Tabatabaei and E. Faghihimani, "The TSH levels and risk of hypothyroidism: Results from a population based prospective cohort study in an Iranian adult's population", *European Journal of International Medicine*, 2017, **41**, 55-61.

152. V. Gounden, J. Jonklaas and S. J. Soldin, "A pilot study: subclinical hypothyroidism and free thyroid hormone measurement by immunoassay and mass spectrometry", *Clinica Chimica Acta*, 2014, **430**, 121-124.
153. Plat4om, "Goitre: Causes, Symptoms, Diagnosis And Treatment", <https://www.plat4om.com/goitre-causes-symptoms-diagnosis-and-treatment/>, (accessed 19<sup>th</sup> Apr 2021).
154. A. Grossman, I. Feldhamer and J. Meyerovitch, "Treatment with levothyroxin in subclinical hypothyroidism is associated with increased mortality in the elderly", *European Journal of International Medicine*, 2017, DOI: 10.1016/j.ejim.2017.11.010.
155. H. F. Escobar-Morreale, J. I. Botella-Carretero and G. Morreale de Escobar, "Treatment of hypothyroidism with levothyroxine or a combination of levothyroxine plus L-triiodothyronine", *Best Practice & Research Clinical Endocrinology & Metabolism*, 2015, **29**, 57-75.
156. M. J. O. n. Hector F. Escobar-Morreale, Francisco Escobar del Rey, and Gabriella Morreale de Escobar, "Replacement therapy for hypothyroidism with thyroxine alone does not ensure euthyroidism in all tissues, as studied in thyroidectomized rats", *The Journal of Clinical Investigation*, 1995, **96**, 2828-2838.
157. J. S. Bolton, S. Chaudhury, S. Dutta, S. Gregory, E. Locke, T. Pierson and E. S. Bergmann-Leitner, "Comparison of ELISA with electro-chemiluminescence technology for the qualitative and quantitative assessment of serological responses to vaccination", *Malaria Journal*, 2020, **19**, 159.
158. J. Li and N. Wu, *Biosensors Based on Nanomaterials and Nanodevices*, CRC Press, 1<sup>st</sup> edn., 2017.
159. X. Zhu and T. Gao, in *Nano-Inspired Biosensors for Protein Assay with Clinical Applications*, ed. G. Li, Elsevier, Amsterdam, 2019, pp. 237-264.
160. J. Wu and H. X. Ju, in *Comprehensive Sampling and Sample Preparation*, ed. J. Pawliszyn, Academic Press, Oxford, 2012, pp. 143-167.
161. C. A. Marquette and L. J. Blum, "Electro-chemiluminescent biosensing", *Analytical and Bioanalytical Chemistry*, 2008, **390**, 155-168.
162. M. Sanchez-Carbayo, M. Mauri, R. Alfayate, C. Miralles and F. Soria, "Analytical and Clinical Evaluation of TSH and Thyroid hormones by

- Electrochemiluminescent Immunoassays", *Clinical Biochemistry*, 1999, **32**, 395-403.
163. PerkinElmer, "A Comparison of AlphaLISA Bead-Based Luminescence and Electrochemiluminescence Immunoassay Technologies for Detection of Human EPO, Amyloid Beta 42 and VEGF in Complex Sample Matrices", [https://www.perkinelmer.com/lab-solutions/resources/docs/PST\\_AlphaLISAECLComparisonPoster.pdf](https://www.perkinelmer.com/lab-solutions/resources/docs/PST_AlphaLISAECLComparisonPoster.pdf), (accessed 27<sup>th</sup> Apr 2021).
164. O. P. Soldin, L. Hilakivi-Clarke, E. Weiderpass and S. J. Soldin, "Trimester-specific reference intervals for thyroxine and triiodothyronine in pregnancy in iodine-sufficient women using isotope dilution tandem mass spectrometry and immunoassays", *Clinica Chimica Acta*, 2004, **349**, 181-189.
165. A. H. Kazerouni F., "Performance characteristics of three automated immunoassays for thyroid hormones", *Caspian Journal of Internal Medicine*, 2012, **3**, 400-404.
166. K. J. Welsh and S. J. Soldin, "How reliable are free thyroid and total T3 hormone assays?", *European Journal of Endocrinology*, 2016, **175**, 255-263.
167. L. S. Masika, Z. Zhao and S. J. Soldin, "Is measurement of TT3 by immunoassay reliable at low concentrations? A comparison of the Roche Cobas 6000 vs. LC-MSMS", *Clinical Biochemistry*, 2016, **49**, 846-849.
168. S. Aydin, "A short history, principles, and types of ELISA, and our laboratory experience with peptide/protein analyses using ELISA", *Peptides*, 2015, **72**, 4-15.
169. B. Asghar, R. Rahim and N. Jafar, "Comparison of routine diagnostic thyrotropin assays: ELISA and Chemiluminescence assay", *Clinical Biochemistry*, 2011, **44**, S51.
170. M. Banasik and T. Stedeford, in *Encyclopedia of Toxicology*, ed. P. Wexler, Academic Press, Oxford, 3<sup>rd</sup> edn., 2014, pp. 970-978.
171. O. Akama Friday, "Plant Toxins", *American Journal of Biomedical Science & Research*, 2019, **4**, 173-175.
172. G. N. Teke and V. Kuete, in *Toxicological Survey of African Medicinal Plants*, ed. V. Kuete, Elsevier, Amsterdam, 1<sup>st</sup> edn., 2014, pp. 63-98.

173. C. Hansch, J. P. Björkroth and A. Leo, "Hydrophobicity and central nervous system agents: on the principle of minimal hydrophobicity in drug design", *Journal of Pharmaceutical Sciences*, 1987, **76**, 663-687.
174. L. Z. Benet, C. M. Hosey, O. Ursu and T. I. Oprea, "BDDCS, the Rule of 5 and drugability", *Advanced drug delivery reviews*, 2016, **101**, 89-98.
175. Chemistry World, "Simple calculations for clinical trial success failed to find a winning formula", <https://www.chemistryworld.com/opinion/ruling-out-the-rule-of-five/4013074.article>, (accessed 26<sup>th</sup> Apr 2021).
176. D. Zhao, Y. Shen, Y. Shi, X. Shi, Q. Qiao, S. Zi, E. Zhao, D. Yu and E. J. Kennelly, "Probing the transcriptome of *Aconitum carmichaelii* reveals the candidate genes associated with the biosynthesis of the toxic aconitine-type C19-diterpenoid alkaloids", *Phytochemistry*, 2018, **152**, 113-124.
177. M. Rai, A. Rai, N. Kawano, K. Yoshimatsu, H. Takahashi, H. Suzuki, N. Kawahara, K. Saito and M. Yamazaki, "De Novo RNA Sequencing and Expression Analysis of *Aconitum carmichaelii* to Analyze Key Genes Involved in the Biosynthesis of Diterpene Alkaloids", *Molecules*, 2017, **22**.
178. Y. Shen, W. J. Liang, Y. N. Shi, E. J. Kennelly and D. K. Zhao, "Structural diversity, bioactivities, and biosynthesis of natural diterpenoid alkaloids", *Natural Product Reports*, 2020, **37**, 763-796.
179. M. Z. Judith Singhubera, b, Sonja Prinza, Brigitte Koppa,, "Aconitum in Traditional Chinese Medicine—A valuable drug or an unpredictable risk?", *Journal of Ethnopharmacology*, 2009, **126**, 18-30.
180. H. Niitsu, Y. Fujita, S. Fujita, R. Kumagai, M. Takamiya, Y. Aoki and K. Dewa, "Distribution of *Aconitum* alkaloids in autopsy cases of aconite poisoning", *Forensic Science International*, 2013, **227**, 111-117.
181. H. Li, L. Liu, S. Zhu and Q. Liu, "Case reports of aconite poisoning in mainland China from 2004 to 2015: A retrospective analysis", *Journal of Forensic and Legal Medicine*, 2016, **42**, 68-73.
182. J.-L. C. Zi-Dong Qiu, Wen Zeng, Ying Ma, Tong Chen, and C.-J.-S. L. Jin-Fu Tang, Lu-Qi Huang,, "Real-time toxicity prediction of *Aconitum* stewing system using extractive electrospray ionization mass spectrometry", *Acta Pharmaceutica Sinica B*, 2010, **10**, 903-912.

183. Drug Bank, "Drug Bank online database", <https://go.drugbank.com>, (accessed 18<sup>th</sup> Apr 2021).
184. Sigma Aldrich, "Aconitine Safety Data Sheet", <https://www.sigmaaldrich.com/MSDS/MSDS/DisplayMSDSPage.do?country=GB&language=en&productNumber=A8001&brand=SIGMA&PageToGoToURL=https%3A%2F%2Fwww.sigmaaldrich.com%2Fcatalog%2Fsearch%3Fterm%3DAconitine%26interface%3DAI%26N%3D0%26mode%3Dmatch%2520partialmax%26lang%3Den%26region%3DGGB%26focus%3Dproduct>, (accessed 18<sup>th</sup> Apr 2021).
185. Drug Bank, "Atropine", <https://go.drugbank.com/drugs/DB00572>, (accessed 18<sup>th</sup> Apr 2021).
186. Sigma Aldrich, "Capsaicin Safety Data Sheet", <https://www.sigmaaldrich.com/MSDS/MSDS/DisplayMSDSPage.do?country=GB&language=en&productNumber=M2028&brand=SIGMA&PageToGoToURL=https%3A%2F%2Fwww.sigmaaldrich.com%2Fcatalog%2Fsearch%3Fterm%3Dcapsaicin%26interface%3DAI%26N%3D0%26mode%3Dmatch%2520partialmax%26lang%3Den%26region%3DGGB%26focus%3Dproduct>, (accessed 18<sup>th</sup> Apr 2021).
187. Drug Bank, "Cathinone", <https://go.drugbank.com/drugs/DB01560>, (accessed 18<sup>th</sup> Apr 2021).
188. Drug Bank, "Colchicine", <https://go.drugbank.com/drugs/DB01394>, (accessed 18<sup>th</sup> Apr 2021).
189. Drug Bank, "Coumarin", <https://go.drugbank.com/drugs/DB04665>, (accessed 18<sup>th</sup> Apr 2021).
190. Drug Bank, "Digitoxin", <https://go.drugbank.com/drugs/DB01396>, (accessed 18<sup>th</sup> Apr 2021).
191. Drug Bank, "Digoxin", <https://go.drugbank.com/drugs/DB00390>, (accessed 18<sup>th</sup> Apr 2021).
192. Enzo Life Sciences, "Hellebrin Safety Data Sheet", [https://www.enzolifesciences.com/fileadmin/files/msds/MSDS\\_ALX-350-105\\_EU\\_EN.pdf](https://www.enzolifesciences.com/fileadmin/files/msds/MSDS_ALX-350-105_EU_EN.pdf), (accessed 18<sup>th</sup> Apr 2021).
193. W. Zhou, X. Chen, G. Zhao, D. Xu, Z. Jiang, L. Zhang and T. Wang, "Psoralen Induced Liver Injury by Attenuating Liver Regenerative Capability", *Frontiers in Pharmacology*, 2018, **9**, 1179.

194. Sigma Aldrich, "5-methoxypsoralen Safety Data Sheet", <https://www.sigmaaldrich.com/MSDS/MSDS/DisplayMSDSPage.do?country=GB&language=en&productNumber=275727&brand=ALDRICH&PageToGoToURL=https%3A%2F%2Fwww.sigmaaldrich.com%2Fcatalog%2Fsearch%3Fterm%3D5-methoxypsoralen%26interface%3DAI%26N%3D0%26mode%3Dmatch%2520partialmax%26lang%3Den%26region%3DGB%26focus%3Dproduct>, (accessed 18<sup>th</sup> Apr 2021).

195. Sigma Aldrich, "8-methoxypsoralen Safety Data Sheet", <https://www.sigmaaldrich.com/MSDS/MSDS/DisplayMSDSPage.do?country=GB&language=en&productNumber=M3501&brand=SIAL&PageToGoToURL=https%3A%2F%2Fwww.sigmaaldrich.com%2Fcatalog%2Fsearch%3Fterm%3D8-methoxypsoralen%26interface%3DAI%26N%3D0%26mode%3Dmatch%2520partialmax%26lang%3Den%26region%3DGB%26focus%3Dproduct>, (accessed 18<sup>th</sup> Apr 2021).

196. A. M. Brito-da-Costa, D. Dias-da-Silva, N. G. M. Gomes, R. J. Dinis-Oliveira and A. Madureira-Carvalho, "Pharmacokinetics and Pharmacodynamics of Salvinorin A and Salvia divinorum: Clinical and Forensic Aspects", *Pharmaceuticals*, 2021, **14**.

197. Sigma Aldrich, "Scopolamine Safety Data Sheet", <https://www.sigmaaldrich.com/MSDS/MSDS/DisplayMSDSPage.do?country=GB&language=en&productNumber=S1875&brand=SIGMA&PageToGoToURL=https%3A%2F%2Fwww.sigmaaldrich.com%2Fcatalog%2Fsearch%3Fterm%3DScopolamine%26interface%3DAI%26N%3D0%26mode%3Dmatch%2520partialmax%26lang%3Den%26region%3DGB%26focus%3Dproduct>, (accessed 18<sup>th</sup> Apr 2021).

198. Sigma Aldrich, "α-solanine Safety Data Sheet", <https://www.sigmaaldrich.com/MSDS/MSDS/DisplayMSDSPage.do?country=GB&language=en&productNumber=S3757&brand=ALDRICH&PageToGoToURL=https%3A%2F%2Fwww.sigmaaldrich.com%2Fcatalog%2Fsearch%3Fterm%3Dsolanine%26interface%3DAI%26N%3D0%26mode%3Dmatch%2520partialmax%26lang%3Den%26region%3DGB%26focus%3Dproduct>, (accessed 18<sup>th</sup> Apr 2021).

199. Sigma Aldrich, "Strychnine Safety Data Sheet", <https://www.sigmaaldrich.com/MSDS/MSDS/DisplayMSDSPage.do?country=GB&language=en&productNumber=S0532&brand=SIGMA&PageToGoToURL=https%3A%2F%2Fwww.sigmaaldrich.com%2Fcatalog%2Fsearch%3Fterm%3Dstrychnine>

%26interface%3DAI%26N%3D0%26mode%3Dmatch%2520partialmax%26lang%3Den%26region%3DGB%26focus%3Dproduct, (accessed 18<sup>th</sup> Apr 2021).

200. Sigma Aldrich, " $\alpha$ -thujone Safety Data Sheet",  
<https://www.sigmaaldrich.com/MSDS/MSDS/DisplayMSDSPage.do?country=GB&language=en&productNumber=89231&brand=ALDRICH&PageToGoToURL=https%3A%2F%2Fwww.sigmaaldrich.com%2Fcatalog%2Fsearch%3Fterm%3Dthujone%26interface%3DAI%26N%3D0%26mode%3Dmatch%2520partialmax%26lang%3Den%26region%3DGB%26focus%3Dproduct>, (accessed 18<sup>th</sup> Apr 2021).

201. Sigma Aldrich, "Veratridine product information sheet",  
[https://www.sigmaaldrich.com/content/dam/sigmaaldrich/docs/Sigma/Product\\_Information\\_Sheet/1/v5754pis.pdf](https://www.sigmaaldrich.com/content/dam/sigmaaldrich/docs/Sigma/Product_Information_Sheet/1/v5754pis.pdf), (accessed 18<sup>th</sup> Apr 2021).

202. Royal Society of Chemistry, "Hellebrin",  
<http://www.chemspider.com/Chemical-Structure.390435.html>, (accessed 18<sup>th</sup> Apr 2021).

203. FooDB, " $\alpha$ -solanine compound properties",  
<https://foodb.ca/compounds/FDB012500>, (accessed 18<sup>th</sup> Apr 2021).

204. FooDB, " $\alpha$ -thujone compound properties",  
<https://foodb.ca/compounds/FDB014960>, (accessed 18<sup>th</sup> Apr 2021).

205. L. C. McKinney, S. Chakraverty and P. De Weer, "Purification, solubility, and pKa of veratridine", *Analytical Biochemistry*, 1986, **153**, 33-38.

206. T. Y. Chan, "Aconitum alkaloid content and the high toxicity of aconite tincture", *Forensic Science International*, 2012, **222**, 1-3.

207. Q. B. Yinglan Zhao, Yan Zhou, Lei Lv, Guangyan Yan, Bo Chen, Li Wang, Xiaobo Cen, "Mechanism study of Aconitum-induced neurotoxicity in PC12 cells: Involvement of dopamine release and oxidative damage", *NeuroToxicology*, 2010, **31**, 752-757.

208. Ethno Plants, "Ruta graveolens",  
<https://www.ethnoplants.com/gb/aromatics-plants-seeds/288-ruta-graveolens-common-rue-seeds.html>, (accessed 08<sup>th</sup> June 2021).

209. Artemisia Annua, "Artemisia Absinthium", <https://www.artemisiaannua.net/en/artemisia-absinthium-absinthe-properties-uses-and-where-to-buy-it/>, (accessed 08<sup>th</sup> June 2021).
210. Plant world seeds, "Aquilegia atrata", [https://www.plant-world-seeds.com/store/view\\_seed\\_item/3120](https://www.plant-world-seeds.com/store/view_seed_item/3120), (accessed 08<sup>th</sup> June 2021).
211. Ethno Botanik, "Capsaicum chinense", <https://www.ethno2.ethnobotanik.org/Capsicum/Avenir/Avenir-Capsicum-chinense-en.html>, (accessed 08<sup>th</sup> June 2021).
212. T. Y. Chan, "Aconite poisoning following the percutaneous absorption of Aconitum alkaloids", *Forensic Science International*, 2012, **223**, 25-27.
213. Press Association, "Curry poisoner Lakhvir Singh found guilty of murder", *The Guardian*, <https://www.theguardian.com/uk/2010/feb/10/curry-poisoner-guilty-murder>, London, UK, 2010.
214. R. Camber, "Guilty of murder: Jilted woman who left ex-lover to die in agony after poisoning him with curry laced with deadly herb", *The Daily Mail*, <https://www.dailymail.co.uk/news/article-1249913/Lakhvir-Singh-guilty-killing-ex-lover-poisoned-curry.html>, London, UK, 2010.
215. The BBC News, "Curry poison killer Lakhvir Singh jailed for life", <http://news.bbc.co.uk/1/hi/england/london/8509798.stm>, (accessed 18<sup>th</sup> Apr 2021).
216. M. Taylor, "Poison curry killer jailed for 23 years", *The Guardian*, <https://www.theguardian.com/uk/2010/feb/11/poison-curry-killer-sentenced>, London, UK, 2010.
217. G. F. Kwakye, J. Jimenez, J. A. Jimenez and M. Aschner, "*Atropa belladonna* neurotoxicity: Implications to neurological disorders", *Food and Chemical Toxicology*, 2018, **116**, 346-353.
218. K. L. Kohnen-Johannsen and O. Kayser, "Tropane Alkaloids: Chemistry, Pharmacology, Biosynthesis and Production", *Molecules*, 2019, **24**.
219. K. M. Oksman-Caldentey, "Tropane and nicotine alkaloid biosynthesis-novel approaches towards biotechnological production of plant-derived pharmaceuticals", *Current Pharmaceutical Biotechnology*, 2007, **8**, 203-210.

220. S. Carnicella, L. Pain and P. Oberling, "Cholinergic effects on fear conditioning II: nicotinic and muscarinic modulations of atropine-induced disruption of the degraded contingency effect", *Psychopharmacology*, 2005, **178**, 533-541.
221. L. M. Sibylle Scholtz, Frank Krogmann, Gerd U Auffarth, "Poisons, Drugs and Medicine: On the Use of Atropine and Scopolamine in Medicine and Ophthalmology: An Historical Review of their Applications", *Journal of Eye Study and Treatment*, 2019, **2019**.
222. B. Al, "The Source-Synthesis- History and Use of Atropine", *Journal of Academic Emergency Medicine*, 2014, **13**, 2-3.
223. D. J. Bennett and G. W. Kirby, "Constitution and Biosynthesis of Capsaicin", *Journal of the Chemical Society*, 1968, 442-446.
224. B. C. N. Prasad, Vinod Kumar, H. B. Gururaj, R. Parimalan, P. Giridhar and G. A. Ravishankar, "Characterization of capsaicin synthase and identification of its gene (csy1) for pungency factor capsaicin in pepper (*Capsicum* sp.)", *Proceedings of the National Academy of Sciences of the United States of America*, 2006, **103**, 13315-13320.
225. C. Aza-Gonzalez, H. G. Nunez-Palenius and N. Ochoa-Alejo, "Molecular biology of capsaicinoid biosynthesis in chili pepper (*Capsicum* spp.)", *Plant Cell Rep*, 2011, **30**, 695-706.
226. M. Pasiński and B. Szulczyk, "Capsaicin inhibits sodium currents and epileptiform activity in prefrontal cortex pyramidal neurons", *Neurochemistry International*, 2020, **135**, 104709.
227. V. Arora, J. N. Campbell and M. K. Chung, "Fight fire with fire: Neurobiology of capsaicin-induced analgesia for chronic pain", *Pharmacology and Therapeutics*, 2020, DOI: 10.1016/j.pharmthera.2020.107743, 107743.
228. P. Supchocksoonthorn, N. Thongsai, W. Wei, P. Gopalan and P. Paoprasert, "Highly sensitive and stable sensor for the detection of capsaicin using electrocatalytic carbon dots grafted onto indium tin oxide", *Sensors and Actuators: B. Chemical*, 2021, **329**.
229. M. Du, X. Liu, D. Wang, Q. Yang, A. Duan, H. Chen, Y. Liu, Q. Wang and B. J. Ni, "Understanding the fate and impact of capsaicin in anaerobic co-digestion of food waste and waste activated sludge", *Water Research*, 2021, **188**, 116539.

230. G. W. R. Limited, "Guinness World Record: Hottest Chilli Pepper", <https://www.guinnessworldrecords.com/world-records/hottest-chili>, (accessed 18<sup>th</sup> Feb 2021, 2021).
231. L. Adaszek, D. Gadomska, L. Mazurek, P. Lyp, J. Madany and S. Winiarczyk, "Properties of capsaicin and its utility in veterinary and human medicine", *Research in Veterinary Science*, 2019, **123**, 14-19.
232. A. Pourmand, G. Esmailian, M. Mazer-Amirshahi, O. Lee-Park and Q. K. Tran, "Topical capsaicin for the treatment of cannabinoid hyperemesis syndrome, a systematic review and meta-analysis", *American Journal of Emergency Medicine*, 2021, **43**, 35-40.
233. S. Jones, E. L. Fileccia, M. Murphy, M. J. Fowler, M. V. King, S. E. Shortall, P. M. Wigmore, A. R. Green, K. C. Fone and F. J. Ebling, "Cathinone increases body temperature, enhances locomotor activity, and induces striatal c-fos expression in the Siberian hamster.", *Neuroscience Letters*, 2014, **559**, 34-38.
234. Jillian M. Hagel, Raz Krizevski, Korey Kilpatrick, Yaron Sitrit, Frédéric Marsolais, E. Lewinsohn and P. J. Facchini, "Expressed sequence tag analysis of khat (*Catha edulis*) provides a putative molecular biochemical basis for the biosynthesis of phenylpropylamino alkaloids", *Genetics and molecular biology*, 2011, **34**, 640-646.
235. R. A. Groves, J. M. Hagel, Y. Zhang, K. Kilpatrick, A. Levy, F. Marsolais, E. Lewinsohn, C. W. Sensen and P. J. Facchini, "Transcriptome profiling of khat (*Catha edulis*) and *Ephedra sinica* reveals gene candidates potentially involved in amphetamine-type alkaloid biosynthesis", *PLoS One*, 2015, **10**, e0119701.
236. J. M. Hagel, R. Krizevski, F. Marsolais, E. Lewinsohn and P. J. Facchini, "Biosynthesis of amphetamine analogs in plants", *Trends in Plant Science*, 2012, **17**, 404-412.
237. A. M. Feyissa and J. P. Kelly, "A review of the neuropharmacological properties of khat.", *Progress in Neuro-psychopharmacol and Biological Psychiatry*, 2008, **32**, 1147-1166.
238. T. Nichols, P. Khondkar and S. Gibbons, "The psychostimulant drug khat (*Catha edulis*): A mini-review.", *Phytochemistry Letters*, 2015, **13**, 127-133.

239. E. Gebissa, "Khat in the Horn of Africa: historical perspectives and current trends", *Journal of Ethnopharmacology*, 2010, **132**, 607-614.
240. L. Iversen, "acmd cathinodes report 2010.", A. C. o. t. M. o. Drugs, London, UK, 2010
241. U. H. Maier and M. H. Zenk, "Colchicine is formed by para-para phenol coupling from autumnaline.", *Tetrahedron Letters*, 1997, **38**, 7357-7360.
242. Richard B. Herbert, Abdullah E. Kattah and E. Knagg, "The biosynthesis of the phenethylisoquinoline alkaloid colchicine. Early and intermediate stages.", *Tetrahedron*, 1990, **46**, 7119-7138.
243. R. S. Nett, W. Lau and E. S. Sattely, "Discovery and engineering of colchicine alkaloid biosynthesis", *Nature*, 2020, **584**, 148-153.
244. R. B. Herbert, R. B. Kattah and E. Knagg, "The biosynthesis of the phenethylisoquinoline alkaloid colchicine. Early and intermediate stages.", *Tetrahedron*, 1990, **46**, 7119-7138.
245. A. I. Scott, "Biosynthesis of Colchicine", *Nature*, 1960, **186**, 556-556.
246. L. S. Jung, S. Winter, R. L. Eckstein, M. Kriechbaum, G. Karrer, E. Welk, M. Elsässer, T. W. Donath and A. Otte, "*Colchicum autumnale* L.", *Perspectives in Plant Ecology, Evolution and Systematics*, 2011, **13**, 227-244.
247. K. R. Nagesh, R. G. Menezes, P. Rastogi, N. R. Naik, J. M. Rasquinha, S. Senthilkumaran and A. Fazil, "Suicidal plant poisoning with *Colchicum autumnale*.", *Journal of Forensic and Legal Medicine*, 2011, **18**, 285-287.
248. C. B.-S. Michael Klintschar , Herbert Radner , and P. R. Gerald Henning "Colchicine poisoning by accidental ingestion of meadow saffron (*colchicum autumnale*): Pathological and medicolegal aspects.", *Forensic Science International*, 1999, **106**, 191-200.
249. Z. Sundov, Z. Nincevic, M. Definis-Gojanovic, M. Glavina-Durdov, I. Jukic, N. Hulina and A. Tonkic, "Fatal colchicine poisoning by accidental ingestion of meadow saffron-case report.", *Forensic Science International*, 2005, **149**, 253-256.
250. The National Health Service, "Colchicine",  
<https://www.nhs.uk/medicines/colchicine/#:~:text=Colchicine%20is%20a%20medic>

ine%20for,manage%20your%20condition%20long%20term, (accessed 07th Mar 2021, 2021).

251. F. Araniti, M. Scognamiglio, A. Chambery, R. Russo, A. Esposito, B. D'Abrosca, A. Fiorentino, A. Lupini, F. Sunseri and M. R. Abenavoli, "Highlighting the effects of coumarin on adult plants of *Arabidopsis thaliana* (L.) Heynh. by an integrated -omic approach", *Journal of Plant Physiology*, 2017, **213**, 30-41.
252. S. S. Garg, J. Gupta, S. Sharma and D. Sahu, "An insight into the therapeutic applications of coumarin compounds and their mechanisms of action", *European Journal of Pharmaceutical Sciences*, 2020, **152**, 105424.
253. H. Murat Bilgin, M. Atmaca, B. Deniz Obay, S. Ozekinci, E. Tasdemir and A. Ketani, "Protective effects of coumarin and coumarin derivatives against carbon tetrachloride-induced acute hepatotoxicity in rats", *Experimental and Toxicological Pathology*, 2011, **63**, 325-330.
254. E. Niro, R. Marzaioli, S. De Crescenzo, B. D'Abrosca, S. Castaldi, A. Esposito, A. Fiorentino and F. A. Rutigliano, "Effects of the allelochemical coumarin on plants and soil microbial community", *Soil Biology and Biochemistry*, 2016, **95**, 30-39.
255. A. Witaicenis, L. N. Seito, A. da Silveira Chagas, L. D. de Almeida, Jr., A. C. Luchini, P. Rodrigues-Orsi, S. H. Cestari and L. C. Di Stasi, "Antioxidant and intestinal anti-inflammatory effects of plant-derived coumarin derivatives", *Phytomedicine*, 2014, **21**, 240-246.
256. K. Rohini and P. S. Srikumar, "Therapeutic Role of Coumarins and Coumarin-Related Compounds", *Journal of Biofertilizers & Biopesticides*, 2014, **5**.
257. B. Shimizu, "2-Oxoglutarate-dependent dioxygenases in the biosynthesis of simple coumarins", *Frontiers in Plant Science*, 2014, **5**, 549.
258. F. Bourgaud, A. Hehn, R. Larbat, S. Doerper, E. Gontier, S. Kellner and U. Matern, "Biosynthesis of coumarins in plants: a major pathway still to be unravelled for cytochrome P450 enzymes", *Phytochemistry Reviews*, 2006, **5**, 293-308.
259. J. L. Rodrigues and L. R. Rodrigues, "Biosynthesis and heterologous production of furanocoumarins: perspectives and current challenges", *Natural Product Reports*, 2020, DOI: 10.1039/d0np00074d.

260. "Plants of the Parsley or Carrot Family", [https://www.wildflowers-and-weeds.com/Plant\\_Families/Apiaceae.htm](https://www.wildflowers-and-weeds.com/Plant_Families/Apiaceae.htm), (accessed 30th March 2020, 2020).
261. "Plants of the Honeysuckle and Adoxa Families", [https://www.wildflowers-and-weeds.com/Plant\\_Families/Caprifoliaceae.htm](https://www.wildflowers-and-weeds.com/Plant_Families/Caprifoliaceae.htm), (accessed 30 Mar 2020, 2020).
262. A. Messer, N. Raquet, C. Lohr and D. Schrenk, "Major furocoumarins in grapefruit juice II: phototoxicity, photogenotoxicity, and inhibitory potency vs. cytochrome P450 3A4 activity", *Food and Chemical Toxicology*, 2012, **50**, 756-760.
263. M. M. Melough, E. Cho and O. K. Chun, "Furocoumarins: A review of biochemical activities, dietary sources and intake, and potential health risks.", *Food and Chemical Toxicology*, 2018, **113**, 99-107.
264. J. Bartosova, K. Kuzelova, M. Pluskalova, I. Marinov, P. Halada and Z. Gasova, "UVA-activated 8-methoxypsoralen (PUVA) causes G2/M cell cycle arrest in Karpas 299 T-lymphoma cells", *Journal of Photochemistry and Photobiology B*, 2006, **85**, 39-48.
265. J. M. Carrascosa, A. Plana and C. Ferrandiz, "Effectiveness and safety of psoralen-UVA (PUVA) topical therapy in palmoplantar psoriasis: a report on 48 patients", *Actas Dermo-sifiliograficas (English edition)*, 2013, **104**, 418-425.
266. S. Doppalapudi, A. Jain, D. K. Chopra and W. Khan, "Psoralen loaded liposomal nanocarriers for improved skin penetration and efficacy of topical PUVA in psoriasis", *European Journal of Pharmaceutical Science*, 2017, **96**, 515-529.
267. H. Kato, C. Saito, E. Ito, T. Furuhashi, E. Nishida, T. Ishida, R. Ueda, H. Inagaki and A. Morita, "Bath-PUVA therapy decreases infiltrating CCR4-expressing tumor cells and regulatory T cells in patients with mycosis Fungoides", *Clinical Lymphoma Myeloma & Leukemia*, 2013, **13**, 273-280.
268. S. Tippisetty, D. Goudi, A. W. Mohammed and P. Jahan, "Repair efficiency and PUVA therapeutic response variation in patients with vitiligo", *Toxicology In Vitro*, 2013, **27**, 438-440.
269. R. Vongthongsri, R. Konschitzky, A. Seeber, C. Treitl, H. Honigsmann and A. Tanew, "Randomized, double-blind comparison of 1 mg/L versus 5 mg/L

- methoxsalen bath-PUVA therapy for chronic plaque-type psoriasis", *Journal of the American Academy of Dermatology*, 2006, **55**, 627-631.
270. A. F. M. Botelho, F. Pierezan, B. Soto-Blanco and M. M. Melo, "A review of cardiac glycosides: Structure, toxicokinetics, clinical signs, diagnosis and antineoplastic potential", *Toxicon*, 2019, **158**, 63-68.
271. H. A. Elbaz, T. A. Stueckle, H. Y. Wang, G. A. O'Doherty, D. T. Lowry, L. M. Sargent, L. Wang, C. Z. Dinu and Y. Rojanasakul, "Digitoxin and a synthetic monosaccharide analog inhibit cell viability in lung cancer cells", *Toxicology and Applied Pharmacology*, 2012, **258**, 51-60.
272. B. A. K. Kevin L. Kelly, John J. Johnston, "Quantitation of digitoxin, digoxin, and their metabolites by high-performance liquid chromatography using pulsed amperometric detection", *Journal of Chromatography A*, 1995, 289-295.
273. M. E. Deluca, A. M. Seldes and E. G. Gros, "Biosynthesis of digitoxin in *Digitalis purpurea*.", *Phytochemistry*, 1989, **28**, 109-111.
274. J. Jagielska, G. Salguero, B. Schieffer and U. Bavendiek, "Digitoxin elicits anti-inflammatory and vasoprotective properties in endothelial cells: Therapeutic implications for the treatment of atherosclerosis?", *Atherosclerosis*, 2009, **206**, 390-396.
275. A. Trenti, C. Boscaro, S. Tedesco, A. Cignarella, L. Trevisi and C. Bolego, "Effects of digitoxin on cell migration in ovarian cancer inflammatory microenvironment", *Biochemical Pharmacology*, 2018, **154**, 414-423.
276. J. P. Morth, B. P. Pedersen, M. J. Buch-Pedersen, J. P. Andersen, B. Vilsen, M. G. Palmgren and P. Nissen, "A structural overview of the plasma membrane Na<sup>+</sup>,K<sup>+</sup>-ATPase and H<sup>+</sup>-ATPase ion pumps", *Nature Reviews Molecular Cell Biology*, 2011, **12**, 60-70.
277. T. F. Wayne, Jr., "Clinical Use of Digitalis: A State of the Art Review", *American Journal of Cardiovascular Drugs*, 2018, **18**, 427-440.
278. T. W. Smith, "Digitalis. Mechanisms of Action and Clinical Use", *The New England Journal of Medicine*, 1988, 358-365.
279. M. V. Clausen, F. Hilbers and H. Poulsen, "The Structure and Function of the Na,K-ATPase Isoforms in Health and Disease", *Frontiers in Physiology*, 2017, **8**, 371.

280. J. Kumari and M. S. Rathore, "Na(+)/K(+)-ATPase a Primary Membrane Transporter: An Overview and Recent Advances with Special Reference to Algae", *The Journal of Membrane Biology*, 2020, **253**, 191-204.
281. D. S. P. M. B. Jograna, S.V. Kotwal, "Digitalis Species a Potent Herbal Drug", *Current Pharma Research*, 2010, **10**, 3821-3831.
282. J. Ramirez-Muroz, "Determination of digitoxin in pharmaceutical oral dosages by automatic discrete-sample analysis", *Analytica Chimica Acta*, 1974, **73**, 167-172.
283. S. Bremer-Streck, M. Kiehntopf, S. Ihle and K. Boeer, "Evaluation of a straightforward and rapid method for the therapeutic drug monitoring of digitoxin by LC-MS/MS", *Clinical Biochemistry*, 2013, **46**, 1728-1733.
284. T. Brillatz, M. Jacmin, K. Vougiannopoulou, E. A. Petrakis, E. Kalpoutzakis, J. Houriet, L. Pellissier, A. Rutz, L. Marcourt, E. F. Queiroz, A. D. Crawford, A. L. Skaltsounis and J. L. Wolfender, "Antiseizure potential of the ancient Greek medicinal plant *Helleborus odorus* subsp. *cyclophyllus* and identification of its main active principles", *Journal of Ethnopharmacology*, 2020, **259**, 1129-1143.
285. T. Iguchi, A. Yokosuka, N. Tamura, S. Takano and Y. Mimaki, "Bufadienolide glycosides and bufadienolides from the whole plants of *Helleborus lividus*, and their cytotoxic activity", *Phytochemistry*, 2020, **176**, 112415-112424.
286. F.-Y. Yang, Y.-F. Su, Y. Wang, X. Chai, X. Han, Z.-H. Wu and X.-M. Gao, "Bufadienolides and phytoecdystones from the rhizomes of *Helleborus thibetanus* (Ranunculaceae)", *Biochemical Systematics and Ecology*, 2010, **38**, 759-763.
287. O. S. Tsiftoglou, M. K. Stefanakis and D. M. Lazari, "Chemical constituents isolated from the rhizomes of *Helleborus odorus* subsp. *cyclophyllus* (Ranunculaceae)", *Biochemical Systematics and Ecology*, 2018, **79**, 8-11.
288. C. Bassarello, T. Muzashvili, A. Skhirtladze, E. Kemertelidze, C. Pizza and S. Piacente, "Steroidal glycosides from the underground parts of *Helleborus caucasicus*", *Phytochemistry*, 2008, **69**, 1227-1233.
289. T. Iguchi, A. Yokosuka, R. Kawahata, M. Andou and Y. Mimaki, "Bufadienolides from the whole plants of *Helleborus foetidus* and their cytotoxicity", *Phytochemistry*, 2020, **172**, 112277-112285.

290. Z. Liu, Y. Liu, B. Xue, W. Chen, W. Xu and R.-W. Jiang, "The co-occurrence of bufadienolides and podophyllotoxins from *Helleborus thibetanus*", *Biochemical Systematics and Ecology*, 2020, **90**.
291. K. Li, J. Feng, Y. Kuang, W. Song, M. Zhang, S. Ji, X. Qiao and M. Ye, "Enzymatic Synthesis of Bufadienolide O-Glycosides as Potent Antitumor Agents Using a Microbial Glycosyltransferase", *Advanced Synthesis & Catalysis*, 2017, **359**, 3765-3772.
292. L. M. Y. Banuls, A. Katz, W. Miklos, A. Cimmino, D. M. Tal, E. Ainbinder, M. Zehl, E. Urban, A. Evidente, B. Kopp, W. Berger, O. Feron, S. Karlish and R. Kiss, "Hellebrin and its aglycone form hellebrigenin display similar in vitro growth inhibitory effects in cancer cells and binding profiles to the alpha subunits of the Na<sup>+</sup>/K<sup>+</sup>-ATPase", *Molecular Cancer*, 2013, **12**, 1-14.
293. M. H. Franz, R. Birzoi, C. V. Maftei, E. Maftei, G. Kelter, H. H. Fiebig and I. Neda, "Studies on the constituents of *Helleborus purpurascens*: analysis and biological activity of the aqueous and organic extracts", *Amino Acids*, 2018, **50**, 163-188.
294. A. K. Laetitia Moreno Y Banuls, Walter Miklos, Alessio Cimmino, Daniel M Tal, Elena Ainbinder, Martin Zehl, Ernst Urban, Antonio Evidente, Brigitte Kopp, Walter Berger, Olivier Feron, Steven Karlish and Robert Kiss, "Hellebrin and its aglycone form hellebrigenin", *Molecular Cancer*, 2013, **33**, 1-14.
295. X. Wei, J. He, B. Gao, L. Han, Y. Mao, H. Zhao, N. Si, H. Wang, J. Yang and B. Bian, "Hellebrigenin anti-pancreatic cancer effects based on apoptosis and autophagy", *PeerJ*, 2020, **8**, e9011.
296. P. W. Yanhui Meng, Vladimir Sik, Huw H. Rees, Laurence Dinan, "Ecdysteroids and bufadienolides from *Helleborus torquatus* (Ranunculaceae)", *Phytochemistry*, 2001, **57**, 401-407.
297. X. Chen, A. Berim, F. E. Dayan and D. R. Gang, "A (-)-kolavenyl diphosphate synthase catalyzes the first step of salvinorin A biosynthesis in *Salvia divinorum*", *Journal of Experimental Botany*, 2017, **68**, 1109-1122.
298. L. Kutrzeba, F. E. Dayan, J. Howell, J. Feng, J. L. Giner and J. K. Zjawiony, "Biosynthesis of salvinorin A proceeds via the deoxyxylulose phosphate pathway.", *Phytochemistry*, 2007, **68**, 1872-1881.

299. K. A. Pelot, R. Mitchell, M. Kwon, L. M. Hagelthorn, J. F. Wardman, A. Chiang, J. Bohlmann, D. K. Ro and P. Zerbe, "Biosynthesis of the psychotropic plant diterpene salvinorin A: Discovery and characterization of the *Salvia divinorum* clerodienyl diphosphate synthase", *The Plant Journal*, 2017, **89**, 885-897.
300. R. Vohra, A. Seefeld, F. L. Cantrell and R. F. Clark, "*Salvia divinorum*: Exposures reported to a statewide poison control system over 10 years.", *The Journal of Emergency Medicine*, 2011, **40**, 643-650.
301. J. M. Hooker, Y. Xu, W. Schiffer, C. Shea, P. Carter and J. S. Fowler, "Pharmacokinetics of the potent hallucinogen, salvinorin A in primates parallels the rapid onset and short duration of effects in humans.", *Neuroimage*, 2008, **41**, 1044-1050.
302. M. W. Johnson, K. A. MacLean, C. J. Reissig, T. E. Prisinzano and R. R. Griffiths, "Human psychopharmacology and dose-effects of salvinorin A, a kappa opioid agonist hallucinogen present in the plant *Salvia divinorum*.", *Drug and Alcohol Dependence*, 2011, **115**, 150-155.
303. T. E. Prisinzano, "Psychopharmacology of the hallucinogenic sage *Salvia divinorum*", *Life Sciences*, 2005, **78**, 527-531.
304. J. H. Halpern, "Hallucinogens and dissociative agents naturally growing in the United States.", *Pharmacology and Therapeutics*, 2004, **102**, 131-138.
305. M. A. H. M.S.Y. Haddadin, F.A. Qaroot, R.K. Robinson "Effects of exposure to light on the solanine content of two varieties of potato (*Solanum tuberosum*) popular in Jordan.", *Food Chemistry*, 2001, **73**, 205-208.
306. V. Romanucci, G. Di Fabio, C. Di Marino, S. Davinelli, G. Scapagnini and A. Zarrelli, "Evaluation of new strategies to reduce the total content of  $\alpha$ -solanine and  $\alpha$ -chaconine in potatoes", *Phytochemistry Letters*, 2018, **23**, 116-119.
307. C. A. H. Louise Vida Traill Shepherd, Colin James Alexander,, J. A. S. James William McNicol, Diane McRae, Kent Frank McCue, and H. V. D. William Richardson Belknap, "Impact of light-exposure on the metabolite balance of transgenic potato tubers with modified glycoalkaloid biosynthesis", *Food Chemistry*, 2016, **200**, 263-273.

308. M. W. Klaus, Judith Wessels, Rudolf Geyer, "Metabolism of the potato saponins alpha-chaconine and alpha-solanine by gibberella pilicaris", *Phytochemistry*, 1997, **46**, 1005-1009.
309. D. G. Barceloux, "Potatoes, Tomatoes, and Solanine Toxicity (Solanum tuberosum L., Solanum lycopersicum L.)", *Medical Toxicology of Natural Substances*, 2008, 77-83.
310. I. Ginzberg, M. Thippeswamy, E. Fogelman, U. Demirel, A. M. Mweetwa, J. Tokuhisa and R. E. Veilleux, "Induction of potato steroidal glycoalkaloid biosynthetic pathway by overexpression of cDNA encoding primary metabolism HMG-CoA reductase and squalene synthase", *Planta*, 2012, **235**, 1341-1353.
311. K. Ohyama, A. Okawa, Y. Moriuchi and Y. Fujimoto, "Biosynthesis of steroidal alkaloids in Solanaceae plants: involvement of an aldehyde intermediate during C-26 amination", *Phytochemistry*, 2013, **89**, 26-31.
312. R. Akiyama, B. Watanabe, M. Nakayasu, H. J. Lee, J. Kato, N. Umemoto, T. Muranaka, K. Saito, Y. Sugimoto and M. Mizutani, "The biosynthetic pathway of potato solanidanes diverged from that of spirosolanes due to evolution of a dioxygenase", *Nature Communications*, 2021, **12**, 1300.
313. PubChem, "Solanine",  
<https://pubchem.ncbi.nlm.nih.gov/compound/262500>, (accessed 07th Mar 2021, 2021).
314. T. Singhapricha and A. C. Pomerleau, "A Case of Strychnine Poisoning from a Southeast Asian Herbal Remedy", *The Journal of Emergency Medicine*, 2017, **52**, 493-495.
315. F. Liu, X. Wang, X. Han, X. Tan and W. Kang, "Cytotoxicity and DNA interaction of brucine and strychnine-Two alkaloids of semen strychni", *International Journal of Biological Macromolecules*, 2015, **77**, 92-98.
316. X. F. Yin, Z. Li, S. H. Zhang, C. X. Wu, C. Wang and Z. Wang, "Determination of strychnine and brucine in traditional Chinese medicine preparations by capillary zone electrophoresis with micelle to solvent stacking", *Chinese Chemical Letters*, 2011, **22**, 330-333.
317. A. M. A. Adam, M. S. Refat, H. A. Saad and M. S. Hegab, "An environmentally friendly method to remove and utilize the highly toxic strychnine in

- other products based on proton-transfer complexation", *Journal of Molecular Structure*, 2015, **1102**, 170-185.
318. C. Yuan, L. Sun, M. Zhang, S. Li, X. Wang, T. Gao and X. Zhu, "Inhibition of human Nav1.5 sodium channels by strychnine and its analogs", *Biochemical Pharmacology*, 2011, **82**, 350-357.
319. C. Duverneuil, G. L. de la Grandmaison, P. de Mazancourt and J. C. Alvarez, "Liquid chromatography/photodiode array detection for determination of strychnine in blood: a fatal case report", *Forensic Science International*, 2004, **141**, 17-21.
320. Y. Li, X. Qi, Y.-W. Yang, Y. Pan and H.-M. Bian, "Toxic effects of strychnine and strychnine N-oxide on zebrafish embryos", *Chinese Journal of Natural Medicines*, 2014, **12**, 760-767.
321. A. Lin, X. Su, D. She, K. Qiu, Q. He and Y. Liu, "LC-MS/MS determination and comparative pharmacokinetics of strychnine, brucine and their metabolites in rat plasma after intragastric administration of each monomer and the total alkaloids from Semen Strychni", *Journal of Chromatography B* 2016, **1008**, 65-73.
322. G. Philippe, L. Nguyen, L. Angenot, M. Frederich, G. Moonen, M. Tits and J. M. Rigo, "Study of the interaction of antiplasmodial strychnine derivatives with the glycine receptor", *European Journal of Pharmacology*, 2006, **530**, 15-22.
323. S. Saraswati and S. S. Agarwal, "Strychnine inhibits inflammatory angiogenesis in mice via down regulation of VEGF, TNF-alpha and TGF-beta", *Microvascular Research*, 2013, **87**, 7-13.
324. A. A. Jensen, P. Gharagozloo, N. J. Birdsall and D. P. Zlotos, "Pharmacological characterisation of strychnine and brucine analogues at glycine and alpha7 nicotinic acetylcholine receptors", *European Journal of Pharmacology*, 2006, **539**, 27-33.
325. T. M. Kutchan, "Alkaloid Biosynthesis -The Basis for Metabolic Engineering of Medicinal Plants", *The Plant Cell*, 1995, **7**, 1059-1070.
326. E. C. Tatsis, I. Carqueijeiro, T. Duge de Bernonville, J. Franke, T. T. Dang, A. Oudin, A. Lanoue, F. Lafontaine, A. K. Stavrinides, M. Clastre, V. Courdavault and S. E. O'Connor, "A three enzyme system to generate the Strychnos alkaloid

- scaffold from a central biosynthetic intermediate", *Nature Communications*, 2017, **8**, 316.
327. S. I. Heimberger and A. I. Scott, "Biosynthesis of strychnine", *Chemical Communications*, 1973, 217-218.
328. "Plants of the Aster or Sunflower Family", [https://www.wildflowers-and-weeds.com/Plant\\_Families/Asteraceae.htm](https://www.wildflowers-and-weeds.com/Plant_Families/Asteraceae.htm), (accessed 30 Mar 2020, 2020).
329. P. M. C. Gambelunghea, "Absinthe. enjoying a new popularity among young people.", *Forensic Science International*, 2002, **130**, 183-186.
330. É. Zámoriné Németh and H. Thi Nguyen, "Thujone, a widely debated volatile compound: What do we know about it?", *Phytochemistry Reviews*, 2020, **19**, 405-423.
331. C. Schmiderer, S. Grausgruber-Groger, P. Grassi, R. Steinborn and J. Novak, "Influence of gibberellin and daminozide on the expression of terpene synthases and on monoterpenes in common sage (*Salvia officinalis*)", *Journal of Plant Physiology*, 2010, **167**, 779-786.
332. D. W. Lachenmeier, "Wormwood (*Artemisia absinthium* L.)-A curious plant with both neurotoxic and neuroprotective properties?", *Journal of Ethnopharmacology*, 2010, **131**, 224-227.
333. N. S. S. Karin M. Hold, Tomoko Ikeda, Toshio Narahashi, and John E. Casida, "alpha-Thujone (the active component of absinthe): gamma-Aminobutyric acid type A receptor modulation and metabolic detoxification", *Proceedings of the Natural Academy of Sciences of the United States of America*, 2000, **97**, 3826-3831.
334. M. J. Eadie, "Absinthe, epileptic seizures and Valentin Magnan", *The Journal of the Royal College of Physicians Edinburgh*, 2009, **39**, 73-78.
335. D. W. Lachenmeier, J. Emmert, T. Kuballa and G. Sartor, "Thujone - Cause of absinthism?", *Forensic Science International*, 2006, **158**, 1-8.
336. P. G. Cliftpm, "Veratridine as an amnestic agent in the domestic chick<sup>1</sup>", *Behavioural and Neural biology*, 1981, **32**, 295-307.
337. E. M. Silva Freitas, M. M. Fagian and M. A. da Cruz Hofling, "Effects of veratrine and veratridine on oxygen consumption and electrical membrane

- potential of isolated rat skeletal muscle and liver mitochondria", *Toxicol*, 2006, **47**, 780-787.
338. M. M. Augustin, D. R. Ruzicka, A. K. Shukla, J. M. Augustin, C. M. Starks, M. O'Neil-Johnson, M. R. McKain, B. S. Evans, M. D. Barrett, A. Smithson, G. K. Wong, M. K. Deyholos, P. P. Edger, J. C. Pires, J. H. Leebens-Mack, D. A. Mann and T. M. Kutchan, "Elucidating steroid alkaloid biosynthesis in *Veratrum californicum*: production of verazine in Sf9 cells", *The Plant Journal*, 2015, **82**, 991-1003.
339. M. Szeliga, J. Ciura and M. Tyrka, "Representational Difference Analysis of Transcripts Involved in Jervine Biosynthesis", *Life*, 2020, **10**.
340. A. G. Gyorgy Halmos, Balazs Lendvai, Gabor Repassy, Laszlo Z. Szabo, E. Sylvester Vizi, "Veratridine-evoked release of dopamine from guinea pig isolated cochlea", *Hearing Research*, 2000, **144**, 89-96.
341. B. E. B. a. S. B. Sheila A. Doggrel, "The effects of veratridine and BDF 9148 on the action potentials and contractility of the rat right ventricle", *General Pharmacology*, 1995, **26**, 593-601.
342. T. T. S. Matsumoto, T. Tanimoto, C. Saiki, M. Takeda and K. Ojima, "Excitatory mechanism of veratridine on slowly adapting pulmonary stretch receptors in anesthetized rabbits", *Life Sciences*, 1998, **63**, 1431-1437.
343. M. S. Shinichi Takahashi, Yasuo Fukuuchi, "Role of sodium ion influx in depolarization-induced neuronal cell death by high KCl or veratridine", *European Journal of Pharmacology*, 1999, **372**, 297-304.
344. Biorelevant, "Biorelevant Instructions V1.1", biorelevant.com, (accessed 27 Apr 2020, 2020).
345. J. Gu, O. P. Soldin and S. J. Soldin, "Simultaneous quantification of free triiodothyronine and free thyroxine by isotope dilution tandem mass spectrometry", *Clinical Biochemistry*, 2007, **40**, 1386-1391.
346. J. Svanfelt, J. Eriksson and L. Kronberg, "Analysis of thyroid hormones in raw and treated waste water", *Journal of Chromatography A*, 2010, **1217**, 6469-6474.

347. S. Yong, Y. Chen, T. K. Lee and H. K. Lee, "Determination of total thyroxine in human serum by hollow fiber liquid-phase microextraction and liquid chromatography-tandem mass spectrometry", *Talanta*, 2014, **126**, 163-169.
348. R. Tanoue, I. Kume, Y. Yamamoto, K. Takaguchi, K. Nomiya, S. Tanabe and T. Kunisue, "Determination of free thyroid hormones in animal serum/plasma using ultrafiltration in combination with ultra-fast liquid chromatography-tandem mass spectrometry", *Journal of Chromatography A*, 2018, **1539**, 30-40.
349. V. Neu, C. Bielow, K. Reinert and C. G. Huber, "Ultrahigh-performance liquid chromatography-ultraviolet absorbance detection-high-resolution-mass spectrometry combined with automated data processing for studying the kinetics of oxidative thermal degradation of thyroxine in the solid state", *Journal of Chromatography A*, 2014, **1371**, 196-203.
350. G. De Pergola, A. Ciampolillo, S. Paolotti, P. Trerotoli and R. Giorgino, "Free triiodothyronine and thyroid stimulating hormone are directly associated with waist circumference, independently of insulin resistance, metabolic parameters and blood pressure in overweight and obese women", *Clinical Endocrinology*, 2007, **67**, 265-269.
351. Sigma Aldrich, "LC/MS with Online Solid Phase Extraction (SPE-LC/MS) of Thyroid Hormones in Plasma on Ascentis® Express Phenyl-Hexyl using RP-Amide Traps", <https://www.sigmaaldrich.com/technical-documents/articles/analytical-applications/hplc/lc-ms-with-online-solid-phase-extraction-spe-lc-ms-of-thyroid-hormones-in-plasma-g006223.html>, (accessed 27th April 2020).
352. Sigma Aldrich, "LC/MS Analysis of Thyroid Hormones on Ascentis® Express F5", <https://www.sigmaaldrich.com/technical-documents/articles/analytical-applications/hplc/lc-ms-analysis-of-thyroid-hormones-g1006793.html>, (accessed 20<sup>th</sup> Mar 2021).
353. P. C. Shun-Hsin Liang, and Ty Kahler, *A Rapid and sensitive LC-MSMS method for the analysis of three forms of thyroid hormones using Raptor biphenyl LC columns.*, Thames Restek.
354. L. Shao, X. Chen, J. Lyu, M. Zhao, Q. Li, S. Ji, S. Qiang, D.-q. Tang, G. Houfa and M. Guo, "Enrichment and Quantitative Determination of Free 3,5-Diiodothyronine, 3',5'-Diiodothyronine, and 3,5-Diiodothyronamine in Human

Serum of Thyroid Cancer by Covalent Organic Hyper Cross-linked Poly-ionic Liquid", *Journal of Chromatography A*, 2021, **1637**, 461821.

355. E. Fröhlich and R. Wahl, "Physiological Role and Use of Thyroid Hormone Metabolites - Potential Utility in COVID-19 Patients", *Frontiers in Endocrinology*, 2021, **12**.

356. R. A. Louzada, A. S. Padron, S. R. Marques-Neto, L. Maciel, J. P. Werneck-de-Castro, A. C. F. Ferreira, J. H. M. Nascimento and D. P. Carvalho, "3,5-Diiodothyronine protects against cardiac ischaemia–reperfusion injury in male rats", *Experimental Physiology*, 2021, **106**, 2185-2197.

357. E. Silvestri, R. Senese, F. Cioffi, R. De Matteis, D. Lattanzi, A. Lombardi, A. Giacco, A. M. Salzano, A. Scaloni, M. Ceccarelli, M. Moreno, F. Goglia, A. Lanni and P. de Lange, "3,5-Diiodo-L-Thyronine Exerts Metabolically Favorable Effects on Visceral Adipose Tissue of Rats Receiving a High-Fat Diet", *Nutrients*, 2019, **11**, 278.

358. A. M. Couldwell, M. C. Thomas, T. W. Mitchell, A. J. Hulbert and S. J. Blanksby, "Tandem mass spectrometry of deprotonated iodothyronines", *Rapid Communications in Mass Spectrometry*, 2005, **19**, 2295-2304.

359. A. Bergeron, M. Furtado and F. Garofolo, "Importance of using highly pure internal standards for successful liquid chromatography/tandem mass spectrometric bioanalytical assays", *Rapid Commun Mass Spectrom*, 2009, **23**, 1287-1297.

360. M. Wang, C. Wang and X. Han, "Selection of internal standards for accurate quantification of complex lipid species in biological extracts by electrospray ionization mass spectrometry-What, how and why?", *Mass Spectrom Rev*, 2017, **36**, 693-714.

361. T. Kunisue, J. W. Fisher, B. Fatuyi and K. Kannan, "A method for the analysis of six thyroid hormones in thyroid gland by liquid chromatography-tandem mass spectrometry", *Journal of Chromatography B* 2010, **878**, 1725-1730.

362. J. Hillebrand, A. Heijboer and E. Endert, "Effects of repeated freeze–thaw cycles on endocrine parameters in plasma and serum", *Annals of Clinical Biochemistry*, 2017, **54**, 289-292.

363. G. D. Villanger, E. Learner, M. P. Longnecker, H. Ask, H. Aase, R. T. Zoeller, G. P. Knudsen, T. Reichborn-Kjennerud, P. Zeiner and S. M. Engel, "Effects of Sample Handling and Analytical Procedures on Thyroid Hormone Concentrations in Pregnant Women's Plasma", *Epidemiology*, 2017, **28**, 365-369.
364. The European Pharmacopeia Commission, *European Pharmacopeia 4*, the Council of Europe, Strasbourg, France, 2001.
365. United States Pharmacopeia convention, *United States Pharmacopeia 36*, Maryland, USA, 2013.
366. United States Pharmacopeia convention, "USP Pharmacopoeia", Rockville, 2005
367. The National Health Service, "Health Research Authority ", <https://www.hra.nhs.uk/planning-and-improving-research/application-summaries/research-summaries/cepa-biobank-newcastle/>, (accessed 17th Jan 2022).
368. J. Beike, L. Frommherz, M. Wood, B. Brinkmann and H. Köhler, "Determination of aconitine in body fluids by LC-MS-MS", *International Journal of Legal Medicine*, 2004, **118**, 289-293.
369. Y. Fujita, K. Terui, M. Fujita, A. Kakizaki, N. Sato, K. Oikawa, H. Aoki, K. Takahashi and S. Endo, "Five cases of aconite poisoning: toxicokinetics of aconitines", *Journal of Analytical Toxicology*, 2007, **31**, 132-137.
370. H. Ohta, Y. Seto and N. Tsunoda, "Determination of Aconitum alkaloids in blood and urine samples. I. High-performance liquid chromatographic separation, solid-phase extraction and mass spectrometric confirmation", *Journal of chromatography B*, 1997, **691**, 351-356.
371. R. Kaneko, S. Hattori, S. Furuta, M. Hamajima, Y. Hirata, K. Watanabe, H. Seno and A. Ishii, "Sensitive analysis of aconitine, hypaconitine, mesaconitine and jesaconitine in human body fluids and Aconitum tubers by LC/ESI-TOF-MS", *Journal of Mass Spectrometry*, 2006, **41**, 810-814.
372. J. Beyer, F. T. Peters, T. Kraemer and H. H. Maurer, "Detection and validated quantification of toxic alkaloids in human blood plasma--comparison of LC-APCI-MS with LC-ESI-MS/MS", *Journal of Mass Spectrometry*, 2007, **42**, 621-633.

373. P. Kintz, M. Villain, Y. Barguil, J. Y. Charlot and V. Cirimele, "Testing for atropine and scopolamine in hair by LC-MS-MS after *Datura innoxia* abuse", *Journal of Analytical Toxicology*, 2006, **30**, 454-457.
374. A. Xu, J. Havel, K. Linderholm and J. Hulse, "Development and validation of an LC/MS/MS method for the determination of L-hyoscyamine in human plasma", *Journal of Pharmaceutical and Biomedical Analysis*, 1995, **14**, 33-42.
375. G. R. Jones, P. P. Singer and B. Bannach, "Application of LC-MS analysis to a colchicine fatality", *Journal of Analytical Toxicology*, 2002, **26**, 365-369.
376. M. Chèze, M. Deveaux and G. Pépin, "Liquid chromatography-tandem mass spectrometry for the determination of colchicine in postmortem body fluids. Case report of two fatalities and review of the literature", *Journal of Analytical Toxicology*, 2006, **30**, 593-598.
377. A. Tracqui, P. Kintz, B. Ludes, C. Rougé, H. Douibi and P. Mangin, "High-performance liquid chromatography coupled to ion spray mass spectrometry for the determination of colchicine at ppb levels in human biofluids", *Journal of chromatography B*, 1996, **675**, 235-242.
378. J. Beyer, F. T. Peters, T. Kraemer and H. H. Maurer, "Detection and validated quantification of nine herbal phenalkylamines and methcathinone in human blood plasma by LC-MS/MS with electrospray ionization", *Journal of Mass Spectrometry*, 2007, **42**, 150-160.
379. Y. You, C. E. Uboh, L. R. Soma, F. Guan, D. Taylor, X. Li, Y. Liu and J. Chen, "Validated UHPLC–MS-MS Method for Rapid Analysis of Capsaicin and Dihydrocapsaicin in Equine Plasma for Doping Control", *Journal of Analytical Toxicology*, 2013, **37**, 122-132.
380. Christopher A. Reilly, Dennis J. Crouch, Garold S. Yost and A. A. Fatah, "Determination of Capsaicin, Nonivamide, and Dihydrocapsaicin in Blood and Tissue by Liquid Chromatography-Tandem Mass Spectrometry", *Journal of Analytical Toxicology*, 2002, **26**, 313-319.
381. Y. Tine, F. Renucci, J. Costa, A. Wélé and J. Paolini, "A Method for LC-MS/MS Profiling of Coumarins in *Zanthoxylum zanthoxyloides* (Lam.) B. Zepernich and Timler Extracts and Essential Oils", *Molecules*, 2017, **22**.

382. J. Carlier, J. Guitton, L. Romeuf, F. Bevalot, B. Boyer, L. Fanton and Y. Gaillard, "Screening approach by ultra-high performance liquid chromatography-tandem mass spectrometry for the blood quantification of thirty-four toxic principles of plant origin. Application to forensic toxicology", *Journal of Chromatography B*, 2015, **975**, 65-76.
383. M. J. Caspers, T. D. Williams, K. M. Lovell, A. Lozama, E. R. Butelman, M. J. Kreek, M. Johnson, R. Griffiths, K. Maclean and T. E. Prisinzano, "LC-MS/MS quantification of salvinorin A from biological fluids", *Analytical Methods*, 2013, **5**, 10.1039/C1033AY40810H.
384. Andrew J. Aubin and M. Waite, "UPLC MS/MS analysis of Salvinorin A from *Salvia Divinorum*", <https://www.waters.com/webassets/cms/library/docs/720002571en.pdf>, (accessed 20<sup>th</sup> May 2021).
385. S. D. Nielsen, J. M. Schmidt, G. H. Kristiansen, T. K. Dalsgaard and L. B. Larsen, "Liquid Chromatography Mass Spectrometry Quantification of  $\alpha$ -solanine,  $\alpha$ -chaconine, and Solanidine in Potato Protein Isolates", *Foods*, 2020, **9**, 416.
386. M. P. Dzakovich, J. L. Hartman and J. L. Cooperstone, "A High-Throughput Extraction and Analysis Method for Steroidal Glycoalkaloids in Tomato", *Frontiers in Plant Science*, 2019, DOI: 10.1101/2019.12.23.878223, 2019.2012.2023.878223.
387. S. W. Ng, C. K. Ching, A. Y. Chan and T. W. Mak, "Simultaneous detection of 22 toxic plant alkaloids (aconitum alkaloids, solanaceous tropane alkaloids, sophora alkaloids, strychnos alkaloids and colchicine) in human urine and herbal samples using liquid chromatography-tandem mass spectrometry", *Journal of Chromatography B*, 2013, **942-943**, 63-69.
388. B. Bach, M. Cleroux, M. Saillen, P. Schonenberger, S. Burgos, J. Ducruet and A. Vallat, "A new chemical tool for absinthe producers, quantification of alpha/beta-thujone and the bitter components in *Artemisia absinthium*", *Food Chemistry*, 2016, **213**, 813-817.
389. X. Zang, E. K. Fukuda and J. D. Rosen, "Method for the Determination of Veratridine and Cevadine, Major Components of the Natural Insecticide Sabadilla, in Lettuce and Cucumbers", *Journal of Agricultural and Food Chemistry*, 1997, **45**, 1758-1761.

390. Y. Gaillard and G. Pepin, "LC-EI-MS determination of veratridine and cevadine in two fatal cases of *Veratrum album* poisoning", *Journal of Analytical Toxicology*, 2001, **25**, 481-485.
391. ACE, "A guide to HPLC and LC-MS buffer selection", [https://www.hplc.eu/Downloads/ACE\\_Guide\\_BufferSelection.pdf](https://www.hplc.eu/Downloads/ACE_Guide_BufferSelection.pdf), (accessed 16<sup>th</sup> June 2021).
392. Y. Tian, R. Shi, M. Gao, H. Wang, Y. Du, L. Zhang, Q. Wang and M. Zhang, "Differentiation of Furanocoumarin Isomers with Ratio of Relative Abundance of Characteristic Fragment Ions and Application in *Angelicae dahuricae Radix*", *Chromatographia*, 2017, **80**.
393. J.-M. Zhang, C.-M. Fu, Y. Hu, Y. Li, S.-h. Qing and F. Gao, "Screening out Potential Cardio-Toxic Components of Chinese Herb *Radix Aconiti Lateralis* in Rat Dosed Plasma by High Performance Liquid Chromatography/Electrospray Ionization Quadrupole Time-Of-Flight Mass Spectrometry", *Analytical Letters - ANAL LETT*, 2012, **45**.
394. H. X. Chen, Y. Chen, P. Du and F. M. Han, "LC-MS for Identification and Elucidation of the Structure of In-Vivo and In-Vitro Metabolites of Atropine", *Chromatographia*, 2007, **65**, 413-418.
395. W. Li, Y. Sun, J. F. Fitzloff and R. B. van Breemen, "Evaluation of Commercial Ginkgo and Echinacea Dietary Supplements for Colchicine Using Liquid Chromatography-Tandem Mass Spectrometry", *Chemical Research in Toxicology*, 2002, **15**, 1174-1178.
396. C. Sun, Y. Wang, S. Sun, X. Chen, X. Shi, H. Fang, Y. Zhang and Z. Fang, "Fragmentation pathways of protonated coumarin by ESI-QE-Orbitrap-MS/MS coupled with DFT calculations", *Journal of Mass Spectrometry*, 2020, **55**, e4496.
397. Y. C. Huaixia Chen, Peng Du, and Fengmei Han, "Liquid Chromatography-Electrospray Ionization Ion Trap Mass Spectrometry for Analysis of in Vivo and in Vitro Metabolites of Scopolamine in Rats", *Journal of Chromatographic Science*, 2008, **46**, 74-80.
398. M. Cahill, G. Caprioli, S. Vittori and K. James, "Elucidation of the mass fragmentation pathways of potato glycoalkaloids and aglycons using Orbitrap mass spectrometry", *Journal of mass spectrometry : JMS*, 2010, **45**, 1019-1025.

399. J. Yan, Z. Liu, C. Yan, J. Xing and S. Liu, "Analysis of strychnos alkaloids using electrospray ionization Fourier transform ion cyclotron resonance multi-stage tandem mass spectrometry", *Rapid Communications in Mass Spectrometry*, 2006, **20**, 1335-1344.
400. W. Biel, A. Jaroszewska, E. Łysoń, A. Telesiński and M. T. Charles, "The chemical composition and antioxidant properties of common dandelion leaves compared with sea buckthorn", *Canadian Journal of Plant Science*, 2017, **97**, 1165-1174.
401. K. Fatur and S. Kreft, "Common anticholinergic solanaceous plants of temperate Europe - A review of intoxications from the literature (1966-2018).", *Toxicon*, 2020, **177**, 52-88.
402. Environmental Protection Agency, "Exposure assessment tool - Inhalation", <https://www.epa.gov/expobox/exposure-assessment-tools-routes-inhalation>, (accessed 31<sup>st</sup> May 2021).
403. Environmental Protection Agency, "Exposure assessment tool - Dermal", <https://www.epa.gov/expobox/exposure-assessment-tools-routes-dermal>, (accessed 31<sup>st</sup> May 2021).
404. Environmental Protection Agency, "Exposure assessment tool - Ingestion", <https://www.epa.gov/expobox/exposure-assessment-tools-routes-ingestion>, (accessed 31<sup>st</sup> May 2021).
405. H. Wollersen, F. Erdmann, M. Risse and R. Dettmeyer, "Accidental fatal ingestion of colchicine-containing leaves--toxicological and histological findings.", *Legal Medicine*, 2009, **11**, S498-S499.
406. The Queen Elizabeth Hospital, "Clinical Biochemistry Laboratory", <https://www.qegateshead.nhs.uk/clinicalbiochemistry>, (accessed 10<sup>th</sup> June 2021).
407. The Royal Horticultural Society, "Giant Hogweed", <https://www.rhs.org.uk/advice/profile?pid=458>, (accessed 10<sup>th</sup> June 2021).



### Appendix 1: Ingestion exposure risk factors

Plant	Part of plant	Compound	Exposure factor (µg/kg-Day)				
			Child (1-<2 years)	Child (2-<3 years)	Child (3-<6 years)	Child (6-<11 years)	Adult
<i>Aconitum lycoctonum</i>	Stem	Aconitine	1.0	0.8	0.6	0.3	0.1
<i>Aconitum napellus</i>	Foliage	Aconitine	1.4	1.1	0.8	0.5	0.2
	Stem	Aconitine	0.7	0.6	0.4	0.2	0.1
<i>Aquilegia alpina</i>	Flower	Aconitine	0.1	0.1	0.1	0.04	0.02
	Seed	Aconitine	0.1	0.1	0.1	0.04	0.01
<i>Aquilegia atrata</i>	Flower	Aconitine	0.2	0.2	0.1	0.1	0.02
	Foliage	Aconitine	0.04	0.03	0.02	0.01	0.01
	Seed	Aconitine	0.5	0.4	0.3	0.1	0.1
<i>Artemisia absinthium</i>	Foliage	Thujone	264	212	158	86	30
	Stem	Thujone	90	72	54	29	10
<i>Atropa belladonna</i>	Berry	Atropine	52000	41000	31000	17000	5800
		Scopolamine	36000	29000	22000	12000	4100
	Foliage	Atropine	1700	1400	1000	564	194
		Scopolamine	318	255	190	103	36
<i>Catha edulis</i>	Leaf	Cathinone	0.8	0.6	0.5	0.13	0.1
<i>Colchicum autumnale</i>	Leaf	Colchicine	470000	380000	280000	150000	53000
	Bulb	Colchicine	100000	83000	62000	34000	12000
<i>Daphne laureola</i>	Leaf	Coumarin	80	64	48	26	9
<i>Daphne mezereum</i>	Leaf	Coumarin	18	14	11	6	2
<i>Brugmansia suaveolens</i>	Petal	Atropine	26	21	15	8	3
		Scopolamine	24	19	14	8	3
	Pollen	Atropine	64	52	39	21	7
		Scopolamine	57	45	34	18	6
	Stem	Atropine	82	65	49	27	9
		Scopolamine	4300	3500	2600	1400	484

**Appendix 1 (continued): Ingestion exposure risk factors**

Plant	Part of plant	Compound	Exposure factor (µg/kg-Day)				
			Child (1-<2 years)	Child (2-<3 years)	Child (3-<6 years)	Child (6-<11 years)	Adult
<i>Digitalis ferruginea</i>	Flower	Digitoxin	151	121	90	49	17
		Digoxin	66	53	39	21	7
	Seed	Digitoxin	57	46	34	19	6
		Digoxin	200	160	120	65	22
<i>Digitalis purpurea</i>	Foliage	Digitoxin	209	168	125	68	23
		Digoxin	0.9	0.7	0.5	0.3	0.1
<i>Fritillaria imperialis</i>	Foliage	Veratridine	0.4	0.3	0.2	0.1	0.04
<i>Fritillaria meleagris</i>	Foliage	Veratridine	0.03	0.03	0.02	0.01	0.004
<i>Helleborous argutifolius</i>	Flower	Hellebrin	0.1	0.1	0.1	0.04	0.02
	Foliage	Hellebrin	0.5	0.4	0.3	0.2	0.1
	Root	Hellebrin	0.4	0.3	0.2	0.1	0.02
<i>Helleborous foetidus</i>	Flower	Hellebrin	0.03	0.03	0.02	0.01	0.004
	Foliage	Hellebrin	0.2	0.1	0.1	0.1	0.02
	Root	Hellebrin	0.5	0.4	0.3	0.2	0.02
<i>Helleborous odurus</i>	Flower	Hellebrin	0.1	0.1	0.1	0.03	0.01
	Foliage	Hellebrin	0.5	0.4	0.3	0.2	0.1
	Root	Hellebrin	1.5	1.2	1.0	0.5	0.1
<i>Helleborous niger</i>	Flower	Hellebrin	0.3	0.2	0.2	0.1	0.03
	Foliage	Hellebrin	0.4	0.3	0.2	0.1	0.04
	Root	Hellebrin	0.2	0.2	0.1	0.1	0.01
<i>Helleborous orientalis</i>	Root	Hellebrin	4.2	3.5	2.6	1.5	0.2
<i>Helleborous purpurascens</i>	Flower	Hellebrin	0.3	0.2	0.2	0.1	0.03
	Foliage	Hellebrin	0.3	0.2	0.2	0.1	0.03
	Root	Hellebrin	12	9.7	7.1	4.2	0.6

**Appendix 1 (continued): Ingestion exposure risk factors**

Plant	Part of plant	Compound	Exposure factor (µg/kg-Day)				
			Child (1-<2 years)	Child (2-<3 years)	Child (3-<6 years)	Child (6-<11 years)	Adult
<i>Helleborous cyclophyllus</i>	Root	Hellebrin	0.2	0.2	0.1	0.1	0.01
<i>Helleborous early purples</i>	Root	Hellebrin	2.5	2.1	1.5	0.9	0.1
<i>Helleborous viridis</i>	Flower	Hellebrin	0.2	0.2	0.1	0.1	0.02
	Root	Hellebrin	13	11	7.9	4.6	0.6
<i>Heracleum mantegazzianum</i>	Flower	Psoralen	1200	938	699	381	131
		5-methoxypsoralen	754	604	450	245	85
		8-methoxypsoralen	550	441	328	179	62
	Foliage	Psoralen	1400	1100	833	453	157
		5-methoxypsoralen	1100	852	635	346	120
		8-methoxypsoralen	408	327	244	133	46
<i>Hyoscyamus niger</i>	Flower	Atropine	50	40	30	16	6
		Scopolamine	2300	1800	1300	734	254
	Root	Atropine	1.6	1.3	1.0	0.7	0.1
		Scopolamine	8.3	6.9	5.1	3.0	0.4
	Seed	Atropine	75	60	45	24	8.4
		Scopolamine	3200	2600	1900	1000	360
<i>Ruta graveolens</i>	Foliage	Psoralen	281	225	168	91	32
		5-methoxypsoralen	274	220	164	89	31
		8-methoxypsoralen	114	91	68	37	13
	Berry	Psoralen	35	28	21	11	3.9
		8-methoxypsoralen	3.3	2.7	2.0	1.1	0.4
<i>Veratrum album</i>	Flower	Veratridine	1.1	0.9	0.6	0.4	0.1

**Appendix 1 (continued): Ingestion exposure risk factors**

Plant	Part of plant	Compound	Exposure factor (µg/kg-Day)				
			Child (1-<2 years)	Child (2-<3 years)	Child (3-<6 years)	Child (6-<11 years)	Adult
<i>Capsicum chinense</i>	Stem	Capsaicin	2.4	2.0	1.5	0.8	0.3
	Foliage	Capsaicin	1.2	1.0	0.7	0.4	0.1
	Chilli	Capsaicin	44	35	26	14	4.9
<i>Solanum dulcamara</i>	Flower	Solanine	224	179	134	73	25
	Leaf	Solanine	595	477	355	194	67
	Stem	Solanine	760	609	454	247	85
	root	Solanine	17	14	10	5.6	1.9
<i>Solanum tuberosum</i>	Potato	Solanine	29	23	17	9.4	3.3
	Fruit	Solanine	24	19	15	7.9	2.7

**Appendix 2: Number of day exposure required for ingestion risk to hit LD<sub>50</sub>**

Plant	Part of plant	Compound	LD <sub>50</sub> (mg/kg)	Days to reach LD <sub>50</sub>				
				Child (1-<2 years)	Child (2-<3 years)	Child (3-<6 years)	Child (6-<11 years)	Adult
<i>Aconitum Lycoctonum</i>	Stem	Aconitine	1	1000	1300	1700	3100	9100
<i>Aconitum Napellus</i>	Foliage	Aconitine	1	706	880	1200	2200	6300
	Stem	Aconitine	1	1400	1700	2300	4200	12000
<i>Aquilegia Alpina</i>	Flower	Aconitine	1	7600	9500	13000	23000	68000
	Seed	Aconitine	1	8100	10000	14000	25000	72000
<i>Aquilegia Atrata</i>	Flower	Aconitine	1	5100	6300	8500	16000	45000
	Foliage	Aconitine	1	24000	30000	42000	77000	220000
	Seed	Aconitine	1	2200	2700	3600	6700	19000
<i>Artemisia Absinthium</i>	Foliage	Thujone	500	1900	2400	3200	5800	17000
	Stem	Thujone	500	5600	6900	9300	17000	50000
<i>Atropa Belladona</i>	Berry	Atropine	75	1.5	1.8	2.4	4.5	13
		Scopolamine	1300	36	44	60	110	317
	Foliage	Atropine	75	43	54	72	133	384
		Scopolamine	1300	4100	5100	6800	13000	36000
<i>Catha Edulis</i>	Leaf	Cathinone	379.7	470000	590000	790000	150000	420000
<i>Colchicum Autumnale</i>	Leaf	Colchicine	5.87	0.01	0.02	0.02	0.04	0.1
	Bulb	Colchicine	5.87	0.1	0.1	0.1	0.2	0.5
<i>Daphne Laureola</i>	Leaf	Coumarin	359.5	4500	5600	7500	14000	40000
<i>Daphne Mezereum</i>	Leaf	Coumarin	359.5	20000	25000	34000	62000	180000
<i>Brugmansia Suaveolens</i>	Petal	Atropine	75	2900	3600	4900	4900	26000
		Scopolamine	1300	24000	67000	90000	170000	480000
	Pollen	Atropine	75	1200	1500	1900	3600	10000
		Scopolamine	1300	23000	29000	39000	71000	200000
	Stem	Atropine	75	920	1100	1500	2800	8200
		Scopolamine	1300	302	377	505	923	2700

Appendix 2 (continued): Number of day exposure required for ingestion risk to hit LD<sub>50</sub>

Plant	Part of plant	Compound	LD <sub>50</sub> (mg/kg)	Days to reach LD <sub>50</sub>				
				Child (1-<2 years)	Child (2-<3 years)	Child (3-<6 years)	Child (6-<11 years)	Adult
<i>Digitalis Ferruginea</i>	Flower	Digitoxin	3527	23000	29000	39000	72000	210000
		Digoxin	28.27	428	534	717	1300	3800
	Seed	Digitoxin	3527	18000	22000	30000	54000	160000
		Digoxin	28.27	1300	1700	2300	41000	12000
<i>Digitalis Purpurea</i>	Foliage	Digitoxin	3527	17000	21000	28000	52000	150000
		Digoxin	28.27	32000	40000	54000	99000	290000
<i>Fritillaria Imperialis</i>	Foliage	Veratridine	1.35	3800	4700	6300	12000	33000
<i>Fritillaria Meleagris</i>	Foliage	Veratridine	1.35	41000	52000	68000	120000	370000
<i>Helleborous Argutifolis</i>	Flower	Hellebrin	8.4	64000	80000	110000	200000	570000
	Foliage	Hellebrin	8.4	18000	22000	30000	54000	160000
	Root	Hellebrin	8.4	23000	28000	38000	66000	490000
<i>Helleborous Foetidus</i>	Flower	Hellebrin	8.4	250000	320000	420000	760000	2300000
	Foliage	Hellebrin	8.4	54000	67000	90000	160000	480000
	Root	Hellebrin	8.4	17000	20000	27000	47000	350000
<i>Helleborous Odurus</i>	Flower	Hellebrin	8.4	86000	110000	140000	260000	760000
	Foliage	Hellebrin	8.4	17000	22000	29000	54000	150000
	Root	Hellebrin	8.4	5600	6800	9200	16000	120000
<i>Helleborous Niger</i>	Flower	Hellebrin	8.4	30000	38000	51000	92000	270000
	Foliage	Hellebrin	8.4	23000	28000	38000	70000	200000
	Root	Hellebrin	8.4	44000	53000	72000	120000	920000
<i>Helleborous orientalis</i>	Root	Hellebrin	8.4	2000	2400	3300	5600	42000
<i>Helleborous Purpurascens</i>	Flower	Hellebrin	8.4	28000	35000	46000	85000	250000
	Foliage	Hellebrin	8.4	28000	35000	46000	85000	25000
	Root	Hellebrin	8.4	719	870	1200	2000	15000

Appendix 2 (continued): Number of day exposure required for ingestion risk to hit LD<sub>50</sub>

Plant	Part of plant	Compound	LD <sub>50</sub> (mg/kg)	Days to reach LD <sub>50</sub>				
				Child (1-<2 years)	Child (2-<3 years)	Child (3-<6 years)	Child (6-<11 years)	Adult
<i>Helleborous Cyclophyllus</i>	Root	Hellebrin	8.4	41000	49000	67000	110000	860000
<i>Helleborous Early Purples</i>	Root	Hellebrin	8.4	3400	4100	5500	9400	71000
<i>Helleborous Viridis</i>	Flower	Hellebrin	8.4	43000	53000	72000	130000	380000
	Root	Hellebrin	8.4	655	793	1100	1800	14000
<i>Heracleum mantegazzianum</i>	Flower	Psoralen	1700	1500	1800	2400	4500	13000
		5-methoxypsoralen	>3000	4000	5000	6700	12000	35000
		8-methoxypsoralen	791	1400	1800	2400	4400	13000
	Foliage	Psoralen	1700	1200	1500	2000	3700	11000
		5-methoxypsoralen	>3000	2800	3500	4700	8700	25000
		8-methoxypsoralen	791	1900	2400	3200	6000	17000
<i>Hyoscyamus Niger</i>	Flower	Atropine	75	1500	1900	2500	4600	13000
		Scopolamine	1300	576	719	964	1800	5100
	Root	Atropine	75	47000	57000	77000	130000	990000
		Scopolamine	1300	160000	190000	250000	440000	3300000
	Seed	Atropine	75	1000	1200	1700	3100	8900
		Scopolamine	1300	406	507	680	1200	3600
<i>Ruta Graveolens</i>	Foliage	Psoralen	1700	6100	7600	10000	19000	54000
		5-methoxypsoralen	>3000	11000	14000	18000	34000	97000
		8-methoxypsoralen	791	6900	8700	12000	210000	620000
	Berry	Psoralen	1700	49000	61000	82000	150000	440000
		8-methoxypsoralen	791	240000	300000	400000	730000	2100000
<i>Veratrum Album</i>	Flower	Veratridine	1.35	1200	1600	2100	3800	11000
<i>Capsicum chinense</i>	Stem	Capsaicin	47.3	19000	24000	32000	58000	170000
	Foliage	Capsaicin	47.3	40000	49000	66000	120000	350000
	Chilli	Capsaicin	47.3	1100	1400	1800	3300	9600

Appendix 2 (continued): Number of day exposure required for ingestion risk to hit LD<sub>50</sub>

Plant	Part of plant	Compound	LD <sub>50</sub> (mg/kg)	Days to reach LD50				
				Child (1-<2 years)	Child (2-<3 years)	Child (3-<6 years)	Child (6-<11 years)	Adult
<i>Solanum dulcamara</i>	Flower	Solanine	590	2600	3300	4400	8100	23000
	Leaf	Solanine	590	992	1200	1700	3000	8800
	Stem	Solanine	590	776	968	1300	2400	6900
	root	Solanine	590	34000	43000	57000	110000	300000
<i>Solanum tuberosum</i>	Potato	Solanine	590	20000	25000	34000	63000	180000
	Fruit	Solanine	590	24000	30000	41000	75000	220000

**Appendix 3: Dermal absorption exposure factor**

Plant	Part of plant	Compound	Exposure factor (ng/kg-Day)				
			Child (1-<2 years)	Child (2-<3 years)	Child (3-<6 years)	Child (6-<11 years)	Adult
<i>Aconitum Lycoctonum</i>	Stem	Aconitine	0.1	0.1	0.1	0.1	0.1
<i>Aconitum Napellus</i>	Foliage	Aconitine	0.6	0.6	0.5	0.5	0.3
	Stem	Aconitine	0.3	0.3	0.3	0.3	0.2
<i>Aquilegia Alpina</i>	Flower	Aconitine	0.01	0.01	0.01	0.01	0.01
	Seed	Aconitine	0.01	0.01	0.01	0.01	0
<i>Aquilegia Atrata</i>	Flower	Aconitine	0.01	0.01	0.01	0.01	0.01
	Foliage	Aconitine	0.01	0.01	0.01	0.01	0
	Seed	Aconitine	0.02	0.02	0.02	0.01	0.01
<i>Artemisia Absinthium</i>	Foliage	Thujone	29	30	27	23	16
	Stem	Thujone	16	17	15	13	9
<i>Atropa Belladona</i>	Berry	Atropine	6200	6500	5800	4800	3500
		Scopolamine	3500	3700	3300	2700	2000
	Foliage	Atropine	211	222	199	166	120
		Scopolamine	279	294	263	219	159
<i>Catha Edulis</i>	Leaf	Cathinone	0.2	0.2	0.2	0.1	0.1
<i>Colchicum</i>	Bulb	Colchicine	4100	4300	13000	3200	2300
	Leaf	Colchicine	896	944	2900	703	510
<i>Daphne Laureola</i>	Leaf	Coumarin	8.5	8.9	8.0	6.6	4.8
<i>Daphne Mezereum</i>	Leaf	Coumarin	1.7	1.8	1.6	1.4	1.0
<i>Brugmansia Suaveolens</i>	Petal	Atropine	1.3	1.4	1.2	1.0	0.7
		Scopolamine	1.2	1.3	1.1	0.9	0.7
	Pollen	Atropine	18	19	17	14	10
		Scopolamine	16	17	15	13	9.2
	Stem	Atropine	0.02	0.02	0.02	0.02	0.01
		Scopolamine	0.7	0.8	0.7	0.6	0.4

**Appendix 3 (continued): Dermal absorption exposure factor**

Plant	Part of plant	Compound	Exposure factor (ng/kg-Day)				
			Child (1-<2 years)	Child (2-<3 years)	Child (3-<6 years)	Child (6-<11 years)	Adult
<i>Digitalis Ferruginea</i>	Flower	Digitoxin	26	28	25	21	15
		Digoxin	12	12	11	9	7
	Foliage	Digitoxin	26	28	25	21	15
		Digitoxin	31	32	29	24	17
		Digoxin	3.2	3.4	3.0	2.5	1.8
<i>Digitalis Purpurea</i>	Foliage	Digitoxin	98	103	92	77	56
		Digoxin	0.4	0.4	0.4	0.3	0.2
<i>Fritillaria Imperialis</i>	Foliage	Veratridine	0.04	0.05	0.04	0.04	0.03
<i>Fritillaria Meleagris</i>	Foliage	Veratridine	0	0	0	0	0
<i>Helleborous Argutifolis</i>	Flower	Hellebrin	0.02	0.02	0.02	0.02	0.01
	Foliage	Hellebrin	0.2	0.2	0.2	0.1	0.1
	Root	Hellebrin	0.1	0.1	0.04	0.04	0.03
<i>Helleborous Foetudis</i>	Flower	Hellebrin	0	0	0	0	0
	Foliage	Hellebrin	0.02	0.02	0.02	0.01	0.01
	Root	Hellebrin	0.8	0.9	0.8	0.7	0.5
<i>Helleborous Odurus</i>	Flower	Hellebrin	0.01	0.01	0.01	0.01	0.01
	Foliage	Hellebrin	0.04	0.04	0.04	0.03	0.02
	Root	Hellebrin	0.5	0.5	0.5	0.4	0.3
<i>Helleborous Niger</i>	Flower	Hellebrin	0.04	0.04	0.04	0.03	0.02
	Foliage	Hellebrin	0.03	0.04	0.03	0.03	0.02
	Root	Hellebrin	0.06	0.06	0.06	0.05	0.03
<i>Helleborous orientalis</i>	Root	Hellebrin	1.5	1.5	1.4	1.1	0.8
<i>Helleborous Purpurascens</i>	Flower	Hellebrin	0.03	0.03	0.03	0.02	0.02
	Foliage	Hellebrin	0.00003	0.00004	0.00003	0.00003	0.00002
	Root	Hellebrin	0.005	0.005	0.004	0.004	0.003

**Appendix 3 (continued): Dermal absorption exposure factor**

Plant	Part of plant	Compound	Exposure factor (ng/kg-Day)				
			Child (1-<2 years)	Child (2-<3 years)	Child (3-<6 years)	Child (6-<11 years)	Adult
<i>Helleborous Cyclophyllus</i>	Root	Hellebrin	0.1	0.1	0.1	0.1	0.04
<i>Helleborous Early Purples</i>	Root	Hellebrin	0.8	0.8	0.8	0.6	0.5
<i>Helleborous Viridis</i>	Flower	Hellebrin	0.03	0.03	0.02	0.02	0.01
	Root	Hellebrin	4.9	5.1	4.6	3.8	7.8
<i>Heracleum mantegazzianum</i>	Flower	Psoralen	10	11	33	8	6
		5-methoxypsoralen	6.5	6.8	21	5.1	3.7
		8-methoxypsoralen	4.7	5	16	3.7	2.7
	Foliage	Psoralen	12	13	40	9	7
		5-methoxypsoralen	9.2	9.7	30	7.2	5.2
		8-methoxypsoralen	3.5	3.7	12	2.8	2.0
<i>Hyoscyamus Niger</i>	Flower	Atropine	3.6	3.8	3.4	2.8	2.0
		Scopolamine	160	169	151	126	91
	Root	Atropine	0.2	0.2	0.2	0.2	0.1
		Scopolamine	1.1	1.1	1.0	0.8	0.6
	Seed	Atropine	4.0	4.2	3.7	3.1	2.3
		Scopolamine	169	178	159	132	96
<i>Ruta Graveolens</i>	Foliage	Psoralen	34	35	31	26	19
		5-methoxypsoralen	33	35	31	26	19
		8-methoxypsoralen	14	14	13	11	7.8
	Berry	Psoralen	5.1	5.3	4.8	4.0	2.9
		8-methoxypsoralen	0.5	0.5	1.6	0.4	0.3
<i>Veratrum Album</i>	Flower	Veratridine	0.5	0.5	1.6	0.4	0.3
<i>Capsicum chinense</i>	Stem	Capsaicin	0.1	0.1	0.4	0.1	0.1
	Foliage	Capsaicin	0.0001	0.0002	0.0005	0.0001	0.0001
	Chilli	Capsaicin	0.006	0.007	0.02	0.005	0.004

**Appendix 3 (continued): Dermal absorption exposure factor**

Plant	Part of plant	Compound	Exposure factor (ng/kg-Day)				
			Child (1-<2 years)	Child (2-<3 years)	Child (3-<6 years)	Child (6-<11 years)	Adult
<i>Solanum dulcamara</i>	flower	Solanine	1.9	2.0	6.3	1.5	1.1
	leaf	Solanine	5.1	5.4	17	4.0	2.9
	stem	Solanine	6.6	6.9	22	5.1	3.7
	root	Solanine	0.2	0.2	0.5	0.1	0.1
<i>Solanum tuberosum</i>	Potato	Solanine	13	14	44	10	7.5
	Fruit	Solanine	7.8	8.2	25	6.1	4.4

**Appendix 4: Number of years exposure required for dermal risk to hit LD<sub>50</sub>**

Plant	Part of plant	Compound	LD <sub>50</sub>	Years to reach LD <sub>50</sub>				
				Child (1-<2 years)	Child (2-<3 years)	Child (3-<6 years)	Child (6-<11 years)	Adult
<i>Aconitum Lycoctonum</i>	Stem	Aconitine	1	>100	>100	>100	>100	>100
<i>Aconitum Napellus</i>	Foliage	Aconitine	1	>100	>100	>100	>100	>100
	Stem	Aconitine	1	>100	>100	>100	>100	>100
<i>Aquilegia Alpina</i>	Flower	Aconitine	1	>100	>100	>100	>100	>100
	Seed	Aconitine	1	>100	>100	>100	>100	>100
<i>Aquilegia Atrata</i>	Flower	Aconitine	1	>100	>100	>100	>100	>100
	Foliage	Aconitine	1	>100	>100	>100	>100	>100
	Seed	Aconitine	1	>100	>100	>100	>100	>100
<i>Artemisia Absinthium</i>	Foliage	Thujone	500	>100	>100	>100	>100	>100
	Stem	Thujone	500	>100	>100	>100	>100	>100
<i>Atropa Belladona</i>	Berry	Atropine	75	33	32	35	42	59
		Scopolamine	1300	>100	>100	>100	>100	>100
	Foliage	Atropine	75	>100	>100	>100	>100	>100
		Scopolamine	1300	>100	>100	>100	>100	>100
<i>Catha Edulis</i>	Leaf	Cathinone	379.7	>100	>100	>100	>100	>100
<i>Colchicum autumnale</i>	Bulb	Colchicine	5.87	3.9	3.7	1.2	5.0	6.9
	Leaf	Colchicine	5.87	18	17	5.5	23	32
<i>Daphne Laureola</i>	Leaf	Coumarin	359.5	>100	>100	>100	>100	>100
<i>Daphne Mezereum</i>	Leaf	Coumarin	359.5	>100	>100	>100	>100	>100
<i>Brugmansia Suaveolens</i>	Petal	Atropine	75	>100	>100	>100	>100	>100
		Scopolamine	1300	>100	>100	>100	>100	>100
	Pollen	Atropine	75	>100	>100	>100	>100	>100
		Scopolamine	1300	>100	>100	>100	>100	>100
	Stem	Atropine	75	>100	>100	>100	>100	>100
		Scopolamine	1300	>100	>100	>100	>100	>100

Appendix 4 (continued): Number of years exposure required for dermal risk to hit LD<sub>50</sub>

Plant	Part of plant	Compound	LD <sub>50</sub>	Years to reach LD <sub>50</sub>				
				Child (1-<2 years)	Child (2-<3 years)	Child (3-<6 years)	Child (6-<11 years)	Adult
<i>Digitalis Ferruginea</i>	Flower	Digitoxin	3527	>100	>100	>100	>100	>100
		Digoxin	28.27	>100	>100	>100	>100	>100
	Seed	Digitoxin	3527	>100	>100	>100	>100	>100
		Digoxin	28.27	>100	>100	>100	>100	>100
<i>Digitalis Purpurea</i>	Foliage	Digitoxin	3527	>100	>100	>100	>100	>100
		Digoxin	28.27	>100	>100	>100	>100	>100
<i>Fritillaria Imperialis</i>	Foliage	Veratridine	1.35	>100	>100	>100	>100	>100
<i>Fritillaria Meleagris</i>	Foliage	Veratridine	1.35	>100	>100	>100	>100	>100
<i>Helleborous Argutifolis</i>	Flower	Hellebrin	8.4	>100	>100	>100	>100	>100
	Foliage	Hellebrin	8.4	>100	>100	>100	>100	>100
	Root	Hellebrin	8.4	>100	>100	>100	>100	>100
<i>Helleborous Foetidus</i>	Flower	Hellebrin	8.4	>100	>100	>100	>100	>100
	Foliage	Hellebrin	8.4	>100	>100	>100	>100	>100
	Root	Hellebrin	8.4	>100	>100	>100	>100	>100
<i>Helleborous Odurus</i>	Flower	Hellebrin	8.4	>100	>100	>100	>100	>100
	Foliage	Hellebrin	8.4	>100	>100	>100	>100	>100
	Root	Hellebrin	8.4	>100	>100	>100	>100	>100
<i>Helleborous Niger</i>	Flower	Hellebrin	8.4	>100	>100	>100	>100	>100
	Foliage	Hellebrin	8.4	>100	>100	>100	>100	>100
	Root	Hellebrin	8.4	>100	>100	>100	>100	>100
<i>Helleborous orientalis</i>	Root	Hellebrin	8.4	>100	>100	>100	>100	>100
<i>Helleborous Purpurascens</i>	Flower	Hellebrin	8.4	>100	>100	>100	>100	>100
	Foliage	Hellebrin	8.4	>100	>100	>100	>100	>100
	Root	Hellebrin	8.4	>100	>100	>100	>100	>100

Appendix 4 (continued): Number of years exposure required for dermal risk to hit LD<sub>50</sub>

Plant	Part of plant	Compound	LD <sub>50</sub>	Years to reach LD <sub>50</sub>				
				Child (1-<2 years)	Child (2-<3 years)	Child (3-<6 years)	Child (6-<11 years)	Adult
<i>Helleborous Cyclophyllus</i>	Root	Hellebrin	8.4	>100	>100	>100	>100	>100
<i>Helleborous Early Purples</i>	Root	Hellebrin	8.4	>100	>100	>100	>100	>100
<i>Helleborous Viridis</i>	Flower	Hellebrin	8.4	>100	>100	>100	>100	>100
	Root	Hellebrin	8.4	>100	>100	>100	>100	>100
<i>Heracleum mantegazzianum</i>	Flower	Psoralen	1700	>100	>100	>100	>100	>100
		5-methoxypsoralen	>3000	>100	>100	>100	>100	>100
		8-methoxypsoralen	791	>100	>100	>100	>100	>100
	Foliage	Psoralen	1700	>100	>100	>100	>100	>100
		5-methoxypsoralen	>3000	>100	>100	>100	>100	>100
		8-methoxypsoralen	791	>100	>100	>100	>100	>100
<i>Hyoscyamus Niger</i>	Flower	Atropine	75	>100	>100	>100	>100	>100
		Scopolamine	1300	>100	>100	>100	>100	>100
	Root	Atropine	75	>100	>100	>100	>100	>100
		Scopolamine	1300	>100	>100	>100	>100	>100
	Seed	Atropine	75	>100	>100	>100	>100	>100
		Scopolamine	1300	>100	>100	>100	>100	>100

Appendix 4 (continued): Number of years exposure required for dermal risk to hit LD<sub>50</sub>

Plant	Part of plant	Compound	LD <sub>50</sub>	Years to reach LD <sub>50</sub>				
				Child (1-<2 years)	Child (2-<3 years)	Child (3-<6 years)	Child (6-<11 years)	Adult
<i>Ruta Graveolens</i>	Foliage	Psoralen	75	>100	>100	>100	>100	>100
		5-methoxypsoralen	1300	>100	>100	>100	>100	>100
		8-methoxypsoralen	1700	>100	>100	>100	>100	>100
	Berry	Psoralen	>3000	>100	>100	>100	>100	>100
		8-methoxypsoralen	791	>100	>100	>100	>100	>100
<i>Veratrum Album</i>	Flower	Veratridine	1700	>100	>100	>100	>100	>100
<i>Capsicum chinense</i>	Stem	Capsaicin	791	>100	>100	>100	>100	>100
	Foliage	Capsaicin	1.35	>100	>100	>100	>100	>100
	Chilli	Capsaicin	47.3	>100	>100	>100	>100	>100
<i>Solanum dulcamara</i>	flower	solanine	590	>100	>100	>100	>100	>100
	leaf	Solanine	590	>100	>100	>100	>100	>100
	stem	Solanine	590	>100	>100	>100	>100	>100
	root	Solanine	590	>100	>100	>100	>100	>100
<i>Solanum tuberosum</i>	Potato	Solanine	590	>100	>100	>100	>100	>100
	Fruit	Solanine	590	>100	>100	>100	>100	>100